Fossil Record

26 (1) 2023

PENSOFT.

für Natur
MUSEUM FÜR NATURKUNDE
BERLIN

Fossil Record
An International Journal of Palaeontology

Editor-in-Chief

Florian Witzmann
Museum für Naturkunde Berlin
Invalidenstraße 43
10115 Berlin
E-Mail: florian.witzmann@mfn-berlin.de
Tel: +49 30 889140 - 8820
Fax: +49 30 889140 - 8565

Editorial Secretary

Boryana Ovcharova
Pensoft Publishers,
Prof. Georgi Zlatarski Street 12
1700 Sofia, Bulgaria
Tel: +359-2-8704281
Fax: +359-2-8704282
E-Mail: journals@pensoft.net

Editorial Board

Anne-Claire Fabre, Bern, Switzerland
Carolin Haug, Munich, Germany
Christian Klug, Zürich, Switzerland
Johannes Müller, Berlin, Germany
Torsten Scheyer, Zurich, Switzerland
Alexander Schmidt, Göttingen, Germany
Florian Witzmann, Berlin, Germany
Hui-ting Wu, Beijing, China

Fossil Record

2023. Volume 26. Issue 1

ISSN: 2193-0066 (print), 2193-0074 (online)

In Focus

The cover picture shows a neornithischian tooth from Khok Sanam locality in labial, lingual, and mesial/distal views.

See paper of **Manitkoon S, Deesri U, Warapeang P, Nonsrirach T, Chanthasit P** Ornithischian dinosaurs in Southeast Asia: a review with palaeobiogeographic implications.

Cover design

PENSOFT

Fossil Record
An International Journal of Palaeontology

Content of volume **26** (**1**) 2023

Manitkoon S, Deesri U, Warapeang P, Nonsrirach T, Chanthasit P
Ornithischian dinosaurs in Southeast Asia: a review with palaeobiogeographic implications 1

Yamada K, Yamamoto S, Takahashi Y
A new remarkable cimicoid genus and species (Hemiptera, Heteroptera, Cimicomorpha) from mid-Cretaceous Burmese amber, with implications for its aberrant male genitalia 27

Pazinato PG, Müller P, Haug JT
New species of Tanaidacea from Cretaceous Kachin amber, with a brief review of the fossil record of tanaidacean crustaceans 39

Loréal E, Syromyatnikova EV, Danilov IG, Čerňanský A
The easternmost record of the largest anguine lizard that has ever lived – *Pseudopus pannonicus* (Squamata, Anguidae): new fossils from the late Neogene of Eastern Europe 51

Araújo R, Smith AS
Recognising and quantifying the evolution of skeletal paedomorphosis in Plesiosauria 85

Toumoulin A, Decombeix A-L, Harper CJ, Serbet R
Early Jurassic silicified woods from Carapace Nunatak, South Victoria Land, Antarctica 103

Joyce WG, Evers SW, Ren S, Rollot Y, Schwermann AH
The helochelydrid turtle *Helochelydra nopcsai* from the Early Cretaceous (late Barremian – early Aptian) fissure fills of Balve, North Rhine-Westphalia, Germany, including a large sample of granicones 117

Voss M, Hampe O, Mahlow K, Vilanova JC
New findings of *Prototherium ausetanum* (Mammalia, Pan-Sirenia) from paving stones in Girona (Catalonia, Spain)? 135

Abstract & Indexing Information

Biological Abstracts® (Thompson ISI)
BIOSIS Previews® (Thompson ISI)
Camgridge Scientific Abstracts (CSA/CIG)
Web of Science® (Thompson ISI)
Zoological Record™ (Thompson ISI)

Fossil Record 26 (1) 2023, 1–25 | DOI 10.3897/fr.26.93456

Ornithischian dinosaurs in Southeast Asia: a review with palaeobiogeographic implications

Sita Manitkoon[1,2], Uthumporn Deesri[1,2], Prapasiri Warapeang[2], Thanit Nonsrirach[2], Phornphen Chanthasit[3]

1 *Faculty of Science, Mahasarakham University, Khamriang, Mahasarakham, 44150, Thailand*
2 *Palaeontological Research and Education Centre, Mahasarakham University, Khamriang, Mahasarakham, 44150, Thailand*
3 *Sirindhorn Museum, Department of Mineral Resources, Sahatsakhan, Kalasin, 46140, Thailand*

https://zoobank.org/F8C273F5-D7C5-4A5C-BF0A-56C7C3085D55

Corresponding author: Uthumporn Deesri (uthumporn_deesri@yahoo.com)

Academic editor: Torsten Scheyer ♦ **Received** 13 August 2022 ♦ **Accepted** 16 December 2022 ♦ **Published** 10 January 2023

Abstract

Ornithischian dinosaurs have been discovered in Thailand, Laos, and Malaysia. These bird-hipped herbivores remain relatively rare by comparison with saurischian dinosaurs. In the Late Jurassic, stegosaurs and basal neornithischians from Thailand showed similarities to Middle-Late Jurassic taxa from China. Ornithischians appeared in the fossil record again during the late Early Cretaceous (Aptian-Albian) of Thailand and Laos. They are represented by non-hadrosaurid iguanodontians and basal ceratopsians. A few specimens have been reported from poorly dated Early Cretaceous rocks of Malaysia. Here, we illustrate the diversity of ornithischian assemblages in Southeast Asia and discuss their palaeobiogeographical implications.

Key Words

Cretaceous, Jurassic, Ornithischia, palaeobiogeography, Southeast Asia

Introduction

Southeast Asia consists of a mosaic of microcontinents derived from the northern margin of eastern Gondwana which, after drifting northwards, collided with each other and with South China in the late Palaeozoic and Mesozoic (Metcalfe 1998). Numerous vertebrate fossils have been discovered from the non-marine Mesozoic formations of the Indochina block, from the Khorat Plateau of north-eastern Thailand, as well as from southern Laos (Buffetaut 1991; Buffetaut and Suteethorn 1998a). However, the record of non-marine Mesozoic vertebrates from other SE Asian terranes is far less well known (Buffetaut et al. 2005a). Southeast Asian dinosaur fossils have been discovered in Thailand, Laos, Myanmar, Malaysia, and Cambodia (Buffetaut et al. 1995, 2003, 2021; Allain et al. 1999; Sone et al. 2015; Xing et al. 2016). They are dominated by sauropods and theropods, based on the number of bones and diversity, whereas ornithischians have fewer fossil remains (Buffetaut et al. 2015). The temporal distribution of Southeast Asian non-avian dinosaurs ranges from the Late Triassic/Early Jurassic to the late Early Cretaceous (Buffetaut et al. 2000; Laojumpon et al. 2017; Manitkoon et al. 2022). However, body fossils of ornithischians reported from Southeast Asia have been limited to the Late Jurassic and the late Early Cretaceous (Aptian-Albian) formations (Fig. 1; Table 1).

Josué-Heilmann Hoffet was the first to describe dinosaur fossils from Southeast Asia (Brett-Surman et al. 2012). Various postcranial ornithischian remains were reported from the Grès Supérieurs Formation of Muong Phalane, near Savannakhet in southern Laos (Buffetaut 1991). Hoffet described the material as a new species of hadrosaurid (duck-billed dinosaur) "*Mandschurosaurus laosensis*" (Hoffet 1944). However, some palaeontologists consider "*M. laosensis*" a *nomen dubium* (Buffetaut 1991; Horner et al. 2004).

Copyright *Sita Manitkoon et al.* This is an open access article distributed under the terms of the Creative Commons Attribution License (CC BY 4.0), which permits unrestricted use, distribution, and reproduction in any medium, provided the original author and source are credited.

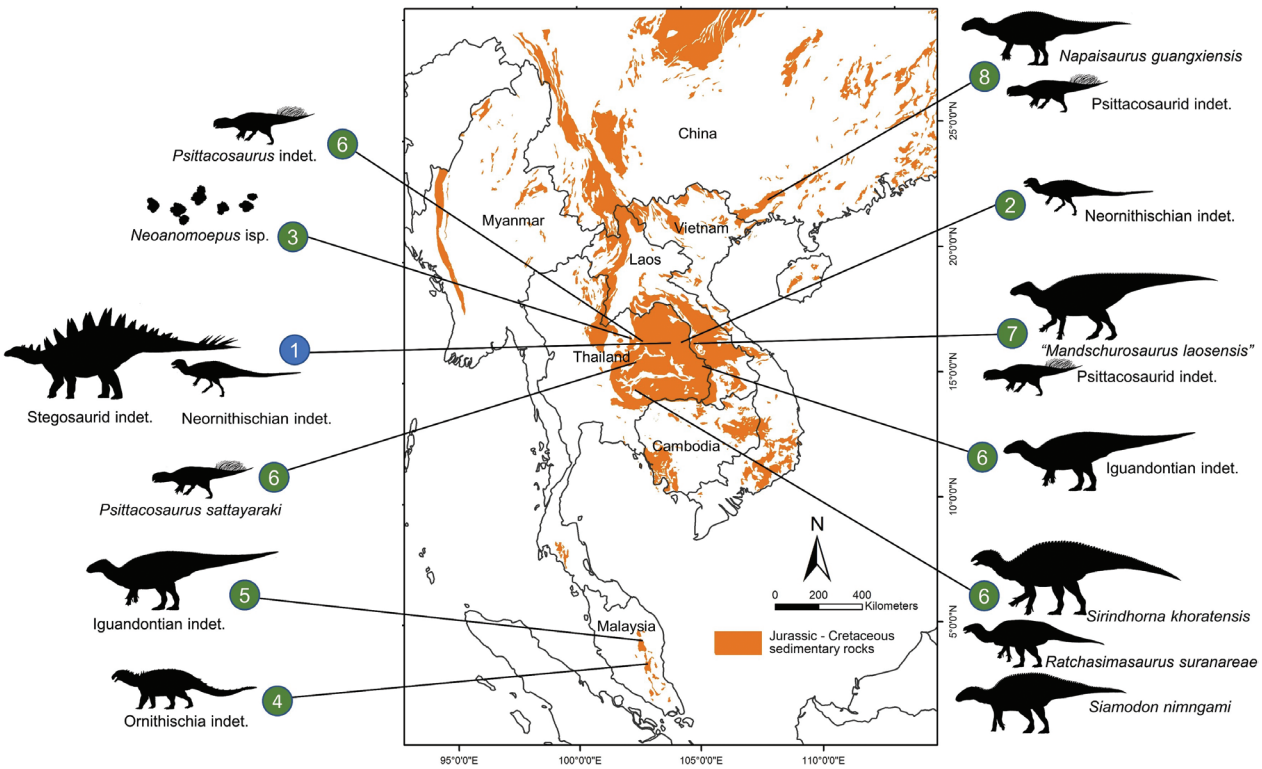

Figure 1. Southeast Asia map showing the distribution of Jurassic–Cretaceous non-marine sediments in Southeast Asia (modified from CCOP's 1:2 million Geologic map of East and Southeast Asia), Number in circles = rock formations: 1, Lower Phu Kradung; 2, Upper Phu Kradung; 3, Phra Wihan; 4, ?Tembling Group; 5, Gagau Group; 6, Khok Kruat; 7, Grès Supérieurs; 8, Xinlong (Thanh and Khuc 2006; Department of Mineral Resources 2014; Uchida et al. 2017; Teng et al. 2019; Yan et al. 2019).

Most ornithischians in Southeast Asia are known from the Khorat Group of Thailand. After the first discovery of a dinosaur bone in 1976 from Khon Kaen Province, north-eastern Thailand, a Thai-French team began excavations in 1981, and more dinosaur remains were found (Grote et al. 2009). Ornithischian bones were found in two formations, including the lowest Phu Kradung Formation and the top-most Khok Kruat Formation (Buffetaut et al. 2015). Although the exact genus or species has not yet been identified from the Late Jurassic Phu Kradung Formation, material of stegosaurids and basal neornithischians were excavated (Buffetaut et al. 2001, 2014; Manitkoon et al. 2019). By contrast, the late Early Cretaceous Khok Kruat Formation (Aptian-Albian) yields abundant neornithischian dinosaurs comprising three taxa of iguanodontians, *Siamodon nimngami* (Buffetaut and Suteethorn 2011), *Ratchasimasaurus suranareae* (Shibata et al. 2011), and *Sirindhorna khoratensis* (Shibata et al. 2015), plus one taxon of basal ceratopsian, *Psittacosaurus sattayaraki* (Buffetaut and Suteethorn 1992). The Khok Kruat Formation of Thailand is considered the lateral equivalent to the Grès Supérieurs Formation of southern Laos (Cappetta et al. 1990; Buffetaut et al. 2005b; Racey 2009; Allain et al. 2012).

The faunal assemblage from the Aptian Xinlong Formation of southern China shows many similarities to the Khok Kruat Formation of the Khorat Group of Thailand, especially the presence of the four endemic genera of hybodont sharks restricted to Southeast Asia and South China (Cuny 2012; Cuny et al. 2017). The Xinlong ornithischians include iguanodontian (*Napaisaurus guangxiensis*) and a possibly basal ceratopsian (Mo et al. 2016; Ji and Zhang 2022).

In Peninsular Malaysia, the Jurassic-Cretaceous rocks are mostly continental deposits, but the record of dinosaurs remains scanty (Rahman 2019). The first discovery was made by the University of Malaya's palaeontological team in 2014 from the State of Pahang, Malay Peninsula (Sone et al. 2015). This included teeth of spinosaurids and an indeterminate ornithischian, together with a fish assemblage that has strong affinities with the Early Cretaceous Sao Khua Formation of Thailand (Teng et al. 2019). Teeth of iguanodontians were found in the inland district of Terengganu in 2014 by a team from the Mineral and Geoscience Department Malaysia and the Malaysian Geological Heritage Group (Akhir et al. 2015).

The principal purpose of this study is to illustrate the diversity of ornithischian assemblages in Southeast Asia and southern China, focusing on Thailand where the majority of material has been reported, and to discuss their evolution and palaeobiogeography.

Institutional abbreviations

PRC Palaeontological Research and Education Centre, Mahasarakham University, Thailand.

SM Sirindhorn Museum, Kalasin Province, Thailand.

NRRU Northeastern Research Institute of Petrified Wood and Mineral Resources (In Honor of His Majesty the King) Nakhon Ratchasima Rajabhat University.

WNM Wittaya Nimngam Museum, Surin Province, Thailand.

Thailand

Thailand comprises two major tectonic terranes: the Shan-Thai (or Sibumasu) block in the western part and the Indochina block in the eastern part that is separated by the Nan-Uttaradit suture (Department of Mineral Resources 2014). The Mesozoic Khorat Group is a Thai stratigraphic group of non-marine rocks ranging from Late Jurassic to Early Cretaceous in north-eastern Thailand and consists of five formations: Phu Kradung, Phra Wihan, Sao Khua, Phu Phan, and Khok Kruat (Racey 2009) (Fig. 2). Three of the formations (Phu Kradung, Sao Khua, and Khok Kruat) have yielded rich deposits with vertebrate remains including selachians, actinopterygians, sarcopterygians, amphibians, turtles, crocodyliformes, pterosaurs, non-avian dinosaurs, and birds (Buffetaut and Suteethorn 1998a; Buffetaut et al. 2003, 2005b, 2006).

Phu Kradung Formation

The formation is considered as forming the base the Khorat Group which outcrops mostly on the Khorat Plateau in north-eastern Thailand (Racey 2009). The age of the Phu Kradung Formation is still uncertain, with contradictory signals coming from vertebrate palaeontology and palynology and it is conventionally considered as either Late Jurassic or Early Cretaceous in age (Racey et al. 1996). The presence of *Dicheiropollis etruscus* in the Phu Kradung Formation seems to confirm an Early Cretaceous age, although some of the lower part of the Phu Kradung Formation could still be Late Jurassic (?Tithonian) (Racey and Goodall 2009). The rich vertebrate site Phu Noi and the nearby Ban Khok Sanam localities, which are in the lower part of the Phu Kradung Formation have yielded fossil assemblages similar to those found in the Middle-Late Jurassic of China (Buffetaut et al. 2003; Cuny et al. 2014; Chanthasit et al. 2019). Currently, no named ornithischian taxa have not been reported from the Phu Kradung Formation.

Stegosauridae indet. Buffetaut et al. 2001

Material. SM2011-1-001 (renumbered from KPS2-1 in Buffetaut et al. (2001)), a single posterior dorsal vertebra (Fig. 3A).

Locality and age. Ban Khok Sanam locality, Kham Muang District, Kalasin Province; the lower Phu Kradung Formation, Late Jurassic.

Previous study. This the first evidence of a thyreophoran dinosaur in Southeast Asia. The specimen is identified as belonging to the family Stegosauridae, which is more advanced than primitive taxa, such as huayangosaurid *Huayangosaurus* from the Middle Jurassic of China (Buffetaut et al. 2001). The specimen has a much higher neural arch and more upright transverse processes, indicating that it should be referred to the Stegosauridae (Buffetaut et al. 2001).

Comments. The anterior part of the centrum and the neural arch of SM2011-1-001 has been destroyed, but likely to possess centra of the dorsal vertebrae longer than wide as most stegosaurians, except for *Miragaia longicollum* (Maidment et al. 2008; Mateus et al. 2009).

Table 1. Ornithischian taxa in Southeast Asia plus southern China.

Formation	Age	Taxa	Country	References
Xinlong	late Early Cretaceous (Aptian-Albian)	*Napaisaurus guangxiensis*	China	Ji and Zhang (2022)
		Iguanodontian indet.		Mo et al. (2016)
		?Psittacosaurid		Mo et al. (2016); Cuny et al. (2017)
Grès Supérieurs	late Early Cretaceous (Aptian-Albian)	"*Mandschurosaurus laosensis*"	Laos	Hoffet (1944)
		Iguanodontian indet.		Hoffet (1944); Buffetaut (1991)
		?Psittacosaurid		Allain et al. (1999)
Khok Kruat	late Early Cretaceous (Aptian-Albian)	*Siamodon nimngami*	Thailand	Buffetaut and Suteethorn (2011)
		Ratchasimasaurus suranareae		Shibata et al. (2011)
		Sirindhorna khoratensis		Shibata et al. (2015)
		Iguanodontian indet.		Manitkoon et al. (2022)
		Psittacosaurus sattayaraki		Buffetaut and Suteethorn (1992)
		Psittacosaurus sp.		Buffetaut et al. (2007)
Gagau Group	?Early Cretaceous (?Aptian)	Iguanodontian indet.	Malaysia	Akhir et al. (2015)
?Tembeling Group	Early Cretaceous (?late Valanginian -early Hauterivian)	Ornithischian indet.	Malaysia	Sone et al. (2015, 2022)
Phra Wihan	?Berriasian-Valanginian	*Neoanomoepus* isp. (footprint)	Thailand	Lockley et al. (2009)
Upper Phu Kradung	Early Cretaceous (?Berriasian)	Basal neornithischian indet.	Thailand	Buffetaut et al. (2001); Buffetaut et al. (2014)
Lower Phu Kradung	Late Jurassic	Stegosaurid indet.	Thailand	Buffetaut et al. (2001)
		Basal neornithischian indet.		Buffetaut et al. (2014); Manitkoon et al. (2019)

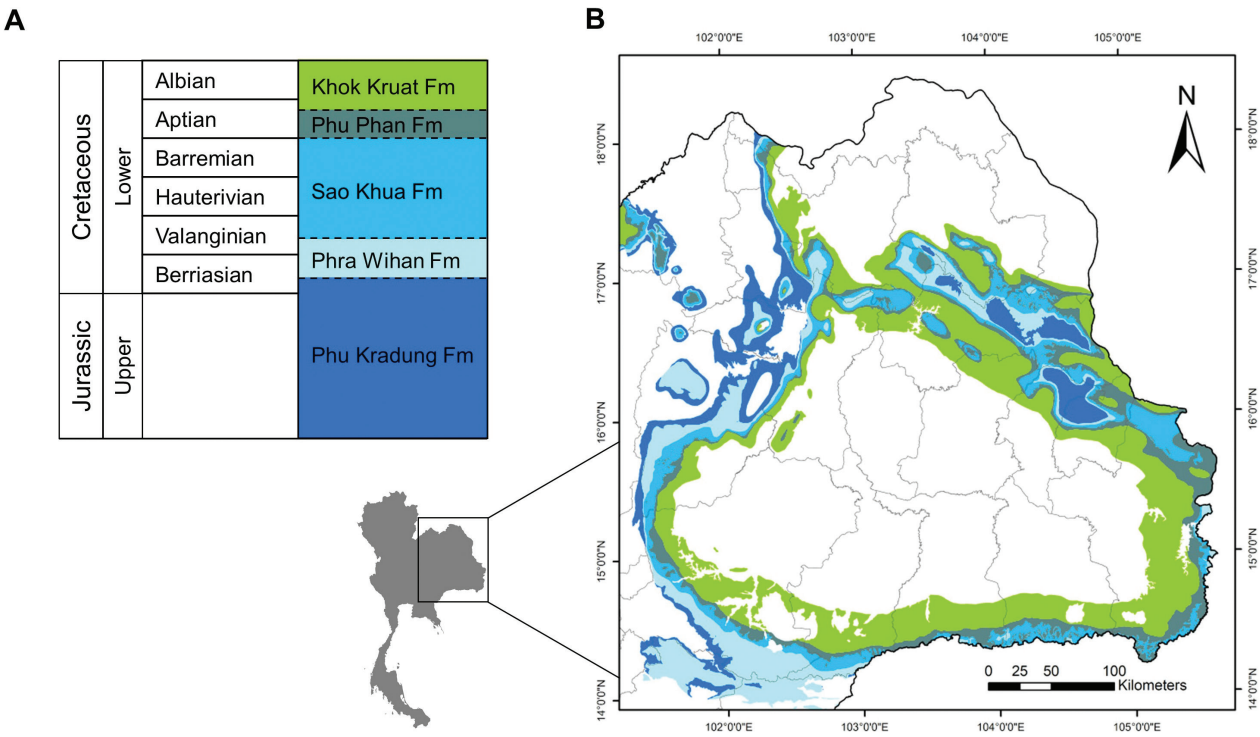

Figure 2. Stratigraphy of Khorat Group (modified from Tucker et al. (2022)) **A.** Location map showing the formations of the Khorat Group on the Khorat Plateau of north-eastern Thailand (**B**).

Basal neornithischian indet. ('Phu Noi neornithischian')

References. Buffetaut et al. 2014; Manitkoon et al. 2019.

Material. PRC 149 (renumbered from PN 13-09 in Buffetaut et al. (2014)), a lower jaw (Figs 3B, 4A, B); PRC 150, an articulated postcranial skeleton (Manitkoon et al. 2019) (Fig. 3C).

Locality and age. Phu Noi locality, Kham Muang District, Kalasin Province; the lower Phu Kradung Formation, Late Jurassic.

Previous study. Buffetaut and his team reported a lower jaw (PRC 149) from the Phu Noi locality. The fan-shaped teeth with a strongly ridged crown and an asymmetric enamel distribution suggests that the specimen belongs to a small ornithopod dinosaur (Buffetaut et al. 2014). A well-preserved articulated small ornithischian skeleton without skull (PRC 150) was reported from the same locality (Manitkoon et al. 2019). The pre-acetabular process of the ilium is narrow, long with a perfectly rounded termination and slightly ventrally curved. The post-acetabular process is short and high. A combination of characters resembles those Jurassic basal neornithischians from China, such as *Agilisaurus louderbacki* and *Hexinlusaurus multidens* (Manitkoon et al. 2019).

Comments. Many taxa of basal neornithischians, once considered as early members of ornithopods, have been reclassified as the basal neornithischians (Boyd 2015; Madzia et al. 2018, 2021; Dieudonné et al. 2020). The similarities to the Chinese taxa, for example, the axial skeleton, is composed of 15 dorsal and five sacrals; the Brevis shelf of the ilium is visible in lateral view along the entire length; a distinct supra-acetabular flange on the pubic peduncle of the ilium; prepubis tip extends beyond the distal end of the pre-acetabular process of ilium, suggesting PRC 149 is a basal neornithischian outside the clade Ornithopoda. Numerous limb bones of various sizes from basal neornithischians were also found at the Phu Noi site, indicating that these dinosaurs were abundant in this area. It is the oldest neornithischian known, so far, from southeast Asia. *Agilisaurus louderbacki* and *Hexinlusaurus multidens* exhibit symmetrically distributed enamel (Peng 1992; Barrett et al. 2005), but the dentary teeth of PRC 149 and other isolated teeth from Phu Noi are different in having asymmetrically distributed enamel on the teeth as in *Yandusaurus hongheensis* from the upper Shaximiao Formation, *Nanosaurus agilis* (= *Drinker*, *Othnielia*, *Othnielosaurus*) from the Late Jurassic Morrison Formation, and a variety of more derived neornithischians (Barrett et al. 2005; Butler et al. 2008; Galton 2009; Carpenter and Galton 2018). Preliminary comparisons seem to indicate that it is a new taxon (Buffetaut et al. 2014; Manitkoon et al. 2019).

Basal neornithischian indet. ('Khok Sanam neornithischian')

Material. WNM-Ks-001, an isolated tooth (Fig. 4C–E).

Locality and age. Khok Sanam locality, Kham Muang District, Kalasin Province; the lower Phu Kradung Formation, Late Jurassic.

Comments. A dentary tooth shows the fan-shaped crown, and has the characters of the posterior teeth present in the dentary teeth of PRC 149 (Buffetaut et al. 2014) and of *Nanosaurus agilis* (Carpenter and Galton 2018). Although

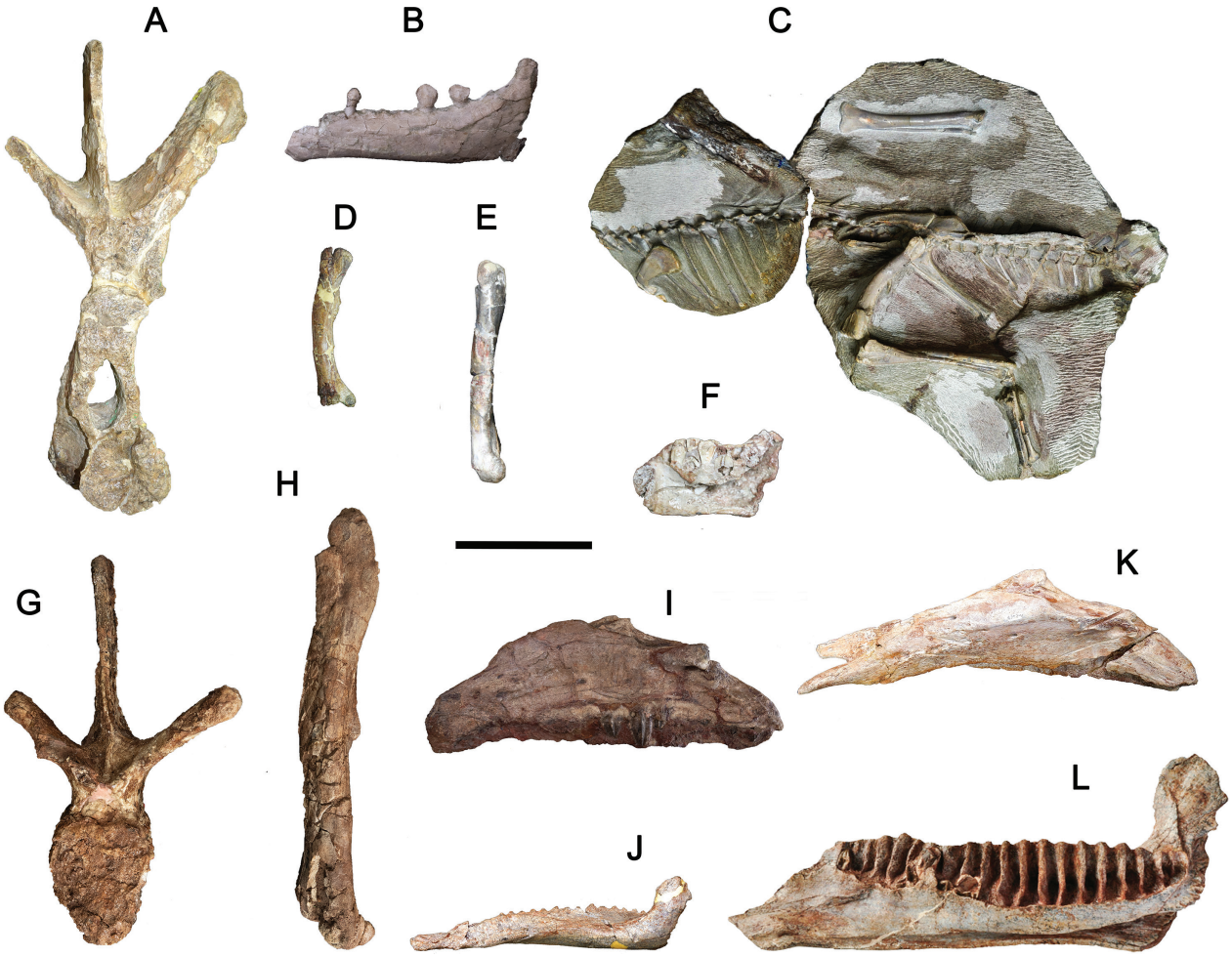

Figure 3. Exceptional specimen of ornithischian dinosaurs from Thailand. Stegosaurid vertebra (**A.** SM2011-1-001), Phu Noi neornithischian left dentary (**B.** PRC149), Phu Noi neornithischian articulated skeleton (**C.** PRC150), Dan Luang neornithischian left femur (**D.** SM2016-1-081), *Psitacosaurus* indet. Right femur (**E.** SM2016-1-080), *Psitacosaurus sattayaraki* right dentary (**F.** SM2016-1-163), Khok Pha Suam iguanodontian dorsal vertebra (**G.** SM2021-1-113), Khok Pha Suam iguanodontian left femur (**H.** SM2021-1-118), *Siamodon nimngami* left maxilla (**I.** PRC-4), *Ratchasimasaurus suranareae* left dentary (**J.** NRRU-A2064), *Sirindhorna khoratensis* left maxilla (**K.** NRRU-A2048), *Sirindhorna khoratensis* right dentary (**L.** NRRU3001-167); **A** and **G** in anterior view; **B–D**, and **H–J** in lateral view; **E, F** and **L** in medial view. Scale bars: 10 cm (**A, C–E**, **G–L**); 5 cm (**B, F**).

the enamelled surface is thin, a well-developed ornamentation of ridges is still noticeable on the lingual side as the enamel is asymmetrically distributed. The margin of the laterally compressed crowns bears distinct denticles. The labial side of the tooth bears no enamel and shows worn facets. The ornamented lingual side does not show a prominent median ridge, contrasting with the European Early Cretaceous *Hypsilophodon foxii* (Galton 2009) and other derived neornithischians. There is moderately developed labiolingual expansion ('cingulum') at the base of the crown, as seen in basal neornithischians (Barrett et al. 2005). The cylindrical root has been preserved and curves to the labial side.

Basal neornithischian indet. ('Dan Luang neornithischian')

Material. SM2016-1-081, a left femur (Buffetaut et al. 2003, 2006, 2014) (Fig. 5).

Locality and age. Dan Luang locality, Kamcha-I District, Mukdahan Province; upper Phu Kradung Formation, ?Early Cretaceous.

Previous study. This is the first basal neornithischian specimen to have been discovered in Thailand, excavated in 1996, but it has not yet been described (Buffetaut and Suteethorn 1998a; Buffetaut et al. 2001, 2002, 2003, 2006). Buffetaut and Suteethorn considered that it is generally similar to *Yandusaurus* (= *Hexinlusaurus multidens*) from China (Buffetaut and Suteethorn 1998a).

Description. The left femur is robust and almost complete, except the distal end is eroded. It is 12.08 cm in length, and has a transverse mid-shaft diameter of 1.57 cm. The shaft of the femur is bowed in the lateral view resembling that of those early ornithopods and basal neornithischians, such as *Hexinlusaurus multidens* (He and Cai 1984), *Agilisaurus louderbacki* (Peng 1992), *Hypsilophodon foxii* (Galton 2009) and the Phu Noi neornithischian (Manitkoon et al. 2019). The femoral

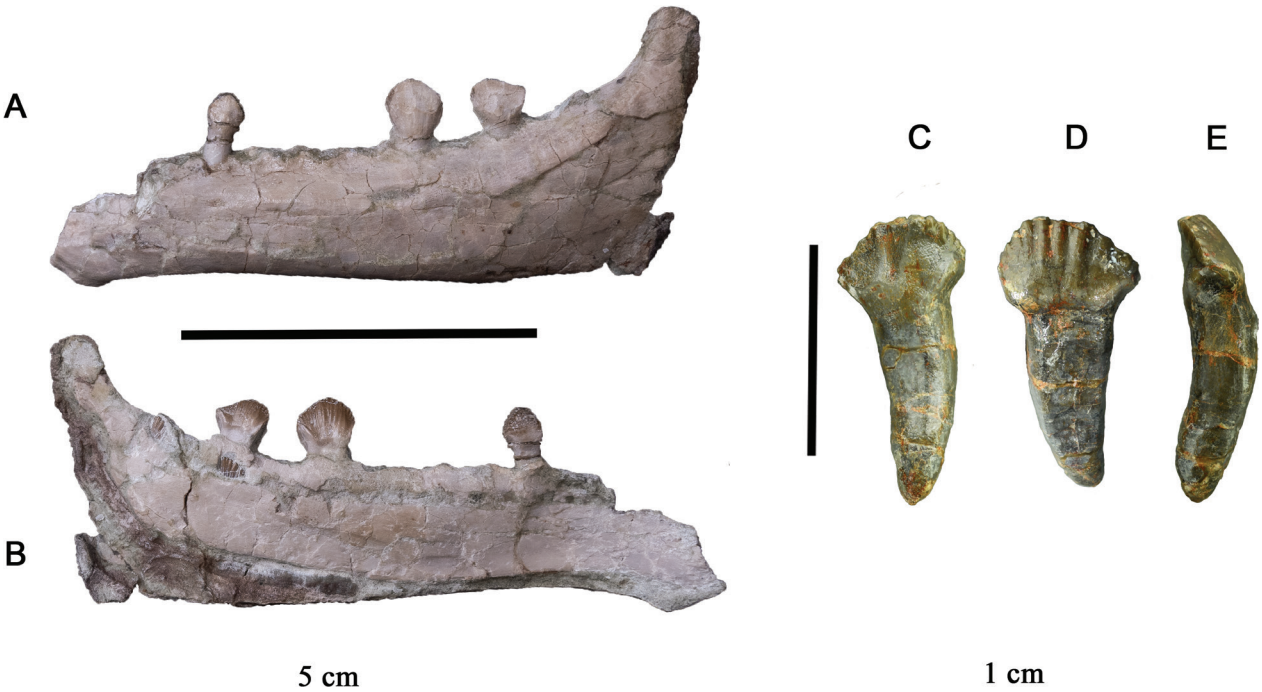

Figure 4. Basal neornithischian specimens from the lower Phu Kradung Formation. (left) Left dentary (PRC 149) from Phu Noi locality, in lateral (**A**) and medial (**B**) views; (right) isolated tooth (WNM-Ks-001) from Khok Sanam locality, in labial (if dentary) (**C**), lingual (**D**) and mesial/distal (**E**) views. Scale bars: 5 cm (**A, B**); 1 cm (**C–E**).

head is mostly intact, but the finished, articular surface is unpreserved. The anterior end of the greater trochanter is slightly convex, while the posterior end is strongly convex. The greater trochanter lies upon the same plane as the femoral head. The lesser trochanter is distinguished from the greater trochanter by a deep groove. The fourth trochanter, located on the medial margin, is incomplete, its position being in the proximal half of the femur as in PRC 150. An oval fossa occurs between the base of the fourth trochanter and the femoral shaft for muscle insertion. The distal portion of the femoral shaft shows mediolaterally expansion towards the distal condyles and, although it was damaged, posteriorly the distal condyles are separated by a caudal intercondylar groove.

Comments. The Dan Luang locality has yielded mamenchisaurid teeth (Suteethorn et al. 2013), a possible mamenchisaurid rib, theropod teeth, crocodyliform osteoderms and large teeth resembling the pholidosaurid *Chalawan thailandicus* (Buffetaut and Ingavat 1980; Martin et al. 2014), shell fragments of the basal trionychoid turtle *Basilochelys macrobios* (Tong et al. 2009), petrified wood, and amber. The site belongs to the upper part of the Phu Kradung Formation (?basal Cretaceous), based on the appearance of large pholidosaurid crocodylomorphs and large trionychoid turtles. This contrasts with the semi-aquatic fauna, such as the small xinjiangchelyid turtles *Phunoichelys thirakhupti*, and *Kalasinemys prasarttongosothi* (Tong et al. 2015, 2019b), and teleosaurid *Indosinosuchus potamosiamensis* (Martin et al. 2019), from the lower Phu Kradung localities, such as Phu Noi. We suggest that SM2016-1-081 belongs in a basal position in Neornithischia, as with the older Phu Noi taxon, but more specimens are needed to increase our understanding of the basal neornithischians from the upper Phu Kradung Formation.

Phra Wihan Formation

The Phra Wihan Formation underlies the Sao Khua Formation, is underlain by the Phu Kradung Formation and is dated as Early Cretaceous (Berriasian to early Barremian) by a rich palynological assemblage (Racey 2009; Racey and Goodall 2009). Lithology and stratigraphy indicate a depositional environment of braided streams and occasional meandering rivers in a humid climate. The formation has not yielded skeletal material, but the biodiversity of dinosaurs can be assessed by study of its footprint faunas. The site of Hin Lat Pa Chad is located at Phu Wiang, Khon Kaen Province. Dinosaur footprints are present on the upper surface of the Phra Wihan Formation's sandstone (Buffetaut and Suteethorn 1993) and the palaeoenvironment is thought to be brackish water or fluvial shallow (Kozu 2017). At least one trackway was made by a small-sized theropod. Others belonged to a small quadrupedal or bipedal ornithischian (Fig. 6), as the pes tracks are tetradactyl, and that at least one manus track is also tetradactyl, and may be interpreted as pentadactyl (Lockley et al. 2009; Kozu 2017). The pes axis is inwardly rotated and the pes digit I is short and anteromedially directed, while manus is outwardly rotated and situated lateral to pes digit III or IV (Lockley et al. 2009). It was classified in the ichnogenus *Neoanomoepus* isp. on the basis of the type material from Canada, and heteropody

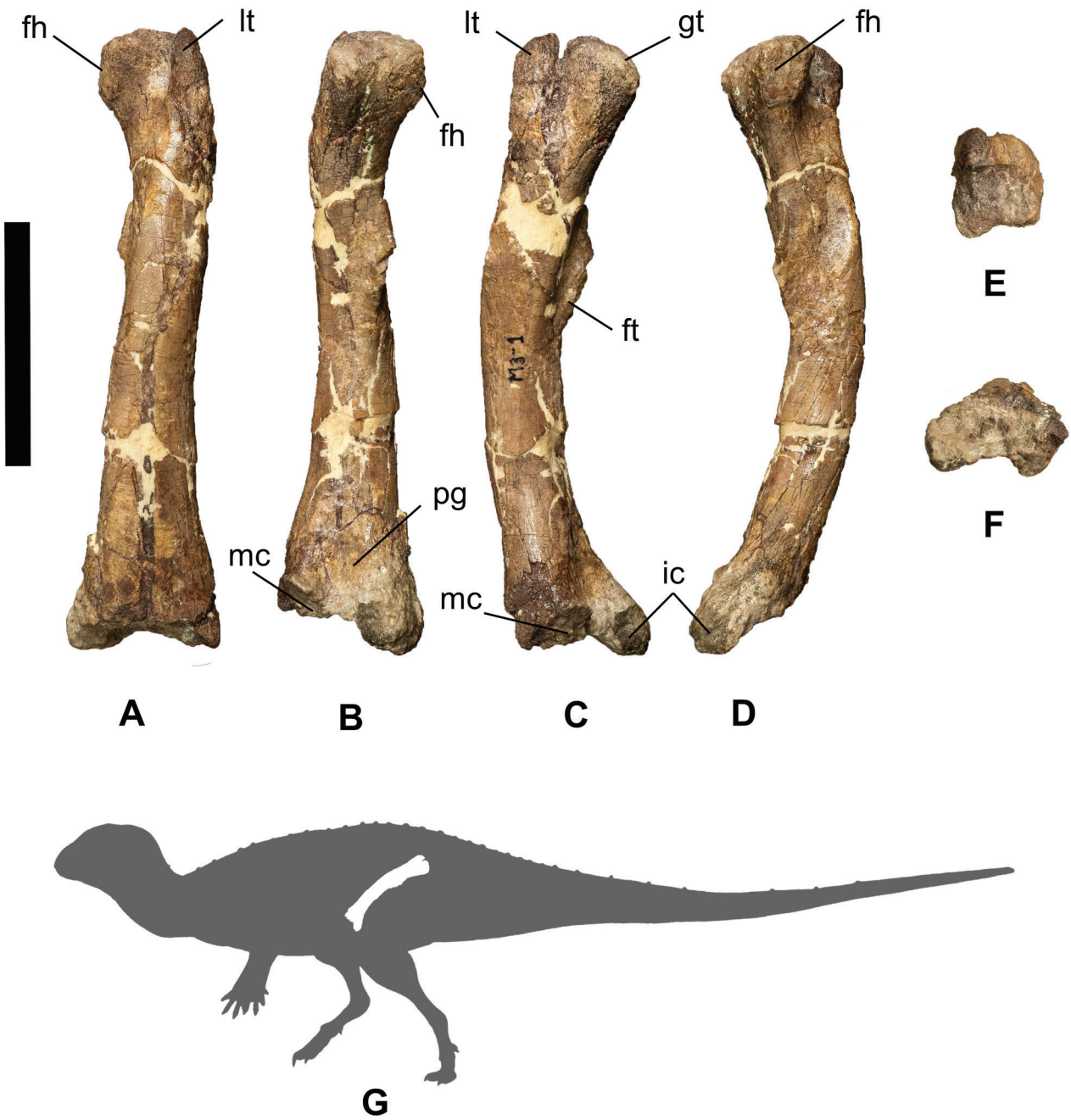

Figure 5. Left femur of the 'Dan Luang neornithischian' (SM2016-1-081) in anterior (**A**), posterior (**B**), lateral (**C**) medial (**D**) proximal (**E**) and distal (**F**) views; Reconstruction showing the bone in left lateral view (**G**); Abbreviations: fh, femoral head; ft, fourth trochanter; gt, greater trochanter; mc, medial condyle; lc, lateral condyle; lt, lesser trochanter; pg, posterior intercondyle groove. Scale bar: 5 cm.

was noted (pes much larger than manus). *Neoanomoepus* is attributed to basal ornithischians and ornithopods, suggesting that these hitherto unknown earliest Cretaceous ichnofaunas may represent a radiation of ornithopods (Le Loeuff et al. 2002; Lockley et al. 2009; Kozu 2017).

Khok Kruat Formation

The formation is composed of reddish-brown, reddish-purple sandstone, siltstone and mudstone, with some conglomerate beds (Department of Mineral Resources 2014). The Khok Kruat Formation conformably overlies the Phu Phan Formation and is widespread in the outer parts of the Phu Phan Range. The Khok Kruat Formation of Thailand is equivalent to the upper part of the Grès Supérieurs Formation of southern Laos (Weishampel et al. 2004) and is considered as Aptian-Albian in age on the basis of its vertebrate fauna and palynology (Cappetta et al. 1990; Buffetaut et al. 2005b; Racey and Goodall 2009). By contrast with other formations in the Khorat Group, the ornithischian dinosaur remains are fairly abundant at various localities in north-eastern Thailand. An ornithopod track was previously mentioned in the

Figure 6. The trackway *Neoanomoepus* isp. from the Hin Lat Pra Chad locality, Scale bar: 10 cm (Photograph by Krishna Sutcha).

Khok Kruat Formation at Huai Dan Chum (Tha Uthen) track-site, Nakhon Phanom Province (Buffetaut et al. 2005a). From hundreds of footprints and dozens of trails on reddish-brown sandstone, it is assumed that there were dinosaurs similar to ornithomimosaurs and small-sized crocodylomorphs (Buffetaut et al. 2005a; Le Loeuff et

al. 2009). Le Loeuff et al. (2009) remarked that the Tha Uthen specimen (T23) is remarkably similar to ornithopod tracks. However, Kozu and his team suggested that it belongs to a small-sized theropod (Kozu et al. 2017).

Ratchasimasaurus suranareae Shibata et al., 2011

Material. holotype NRRU-A2064, a left dentary (Fig. 3J).

Locality and age. Ban Pong Malaengwan, Khok Kruat Subdistrict, Nakhon Ratchasima Province; late Early Cretaceous Khok Kruat Formation (Aptian).

Previous study. *R. suranareae* is a hadrosauroid (Madzia et al. 2020; Shibata et al. 2015) and the material comprises a complete toothless left dentary with 18 alveoli (Shibata et al. 2011). One autapomorphy of *R. suranareae* is its elongated and dorsoventrally shallow dentary ramus, with a ratio of length (from the rostral to the caudal margin)/height (at the middle of the dentary) of 6.9 (Shibata et al. 2011). It shows both primitive and derived characters for iguanodontians, such as a caudally inclined coronoid process and alveolar trough with a primitive crown impression, and a derived buccal shelf between the tooth row and the coronoid process (Shibata et al. 2011).

Comment. The length of *R. suranareae* dentary is 19.81 cm, which is relatively small when compared to other skull material of iguanodontians from Thailand. It is not possible to determine if it is an immature or mature individual (Shibata et al. 2011). This compares with the nearly complete right dentary of *Sirindhorna khoratensis* (NRRU3001-167), which is about 38 cm in length with 20 alveoli (Shibata et al. 2015). In iguanodontians, tooth number increases during growth and single teeth also becoming relatively wider, as in *Dysalotosaurus lettowvorbecki* and *Zalmoxes robustus*, and there is a slight ontogenetic increase of dentary tooth positions from 10 to 13 and 8 to 10, respectively (Weishampel et al. 2003; Hübner and Rauhut 2010). In hadrosauroids, there are many ontogenetic changes occurring in the skull and mandible, and the dentary experiences an elongation of the mandibular ramus during growth (Bell 2011; Campione and Evans 2011; Prieto-Marquez and Guenther 2018). However, the ratio of length/height of the dentary of *R. suranareae* is 6.9, and approximately 5 in *S. khoratensis* (NRRU3001-167), contradicting the ontogenetic tend of hadrosauroids mentioned above, if *R. suranareae* is a younger stage of *S. khoratensis*.

Siamodon nimngami Buffetaut & Suteethorn, 2011

Material. holotype PRC-4, a left maxilla (Fig. 3I) and the referred materials, an isolated maxillary tooth (PRC-5) and a braincase (PRC-6).

Locality and age. Ban Saphan Hin, Khok Kruat Subdistrict, Nakhon Ratchasima Province; late Early Cretaceous Khok Kruat Formation (Aptian) (Buffetaut and Suteethorn 2011).

Previous study. *S. nimngami* shows a combination of iguanodontian features: maxilla shaped like an isosceles triangle, with the dorsal process located at about mid-length of the bone; a strong longitudinal bulge on the medial surface of the maxilla; maxillary teeth bear a strong median primary ridge, one short weak subsidiary ridge or no subsidiary ridge; and mamillated denticles on the crown margins similar to *Gongpoquansaurus mazongshanensis* and *Probactrosaurus mongoliensis* from China (Buffetaut and Suteethorn 2011). There may have been as many as 25 tooth positions in the maxilla (Buffetaut and Suteethorn 2011). It differs from hadrosaurids in the jugal, which forms a tab-like process, whereas in hadrosaurids, the expanded anterior end of the jugal contacts and overlaps a large sutural area on the maxilla (Buffetaut and Suteethorn 2011). *S. nimngami* and *R. suranareae* were mentioned as members of hadrosauroids (Shibata et al. 2015), but the phylogenetic analysis recovered *S. nimngami* at the base of Hadrosauriformes (Madzia et al. 2020).

Additional material and description. WNM-Sp-001 (Fig. 8I, J), an isolated dentary tooth from the same locality is referred to *S. nimngami*. It is well preserved and apparently from a right dentary. It generally resembles a previously reported *S. khoratensis* dentary tooth (Shibata et al. 2015). The crown of the tooth is leaf-shaped with enamel covering only the lingual surface. The ratio of apicobasal length / mesiodistal width: 1.87. One prominent primary ridge situated slightly distal to the mid-line makes the crown asymmetric. The secondary ridge is positioned mesial and it is less prominent. In contrast to *S. khoratensis* dentary teeth, where the crowns appear to be apicobasally erect, whereas in *S. nimngami*, the dentary teeth appear to be curved apicobasally. Shibata et al. (2015) noted that there were no other accessory ridges on the crown of *S. khoratensis*, but WNM-KS-001 shows at least one very faint accessory ridge on the mesial side. Small denticles are present on the mesial and distal margins of the upper half of the crown.

Comment. Some palaeontologists consider *S. nimngami* a *nomen dubium* as its material does not show any autapomorphic characters, and it might be referable to some of the other taxa from the same area (Norman 2014). However, Shibata et al. (2015) showed the possibility of three iguanodontians in the Khok Kruat Formation. The holotype specimen of *S. nimngami* and *S. khoratensis* maxilla (NRRU-A2048) are similar in size. They likely to belong to same growth stage, but have distinct physical characteristics suggesting that they represent different animals, while comparisons to *R. suranareae* are not feasible as overlapping material has not been discovered.

There has been some disagreement about the type locality of *S. nimngami* given by Shibata and his team, and Buffetaut and Suteethorn; however, we would like to confirm that, after corroboration from the holotype collector, Mr. Witaya Nimngam, we now know that the type locality of *S. nimngami* is at Ban Saphan Hin. This is far from the type locality of *S. khoratensis* and definitely not from Ban Nong Rangka as previously suggested (Fig. 7).

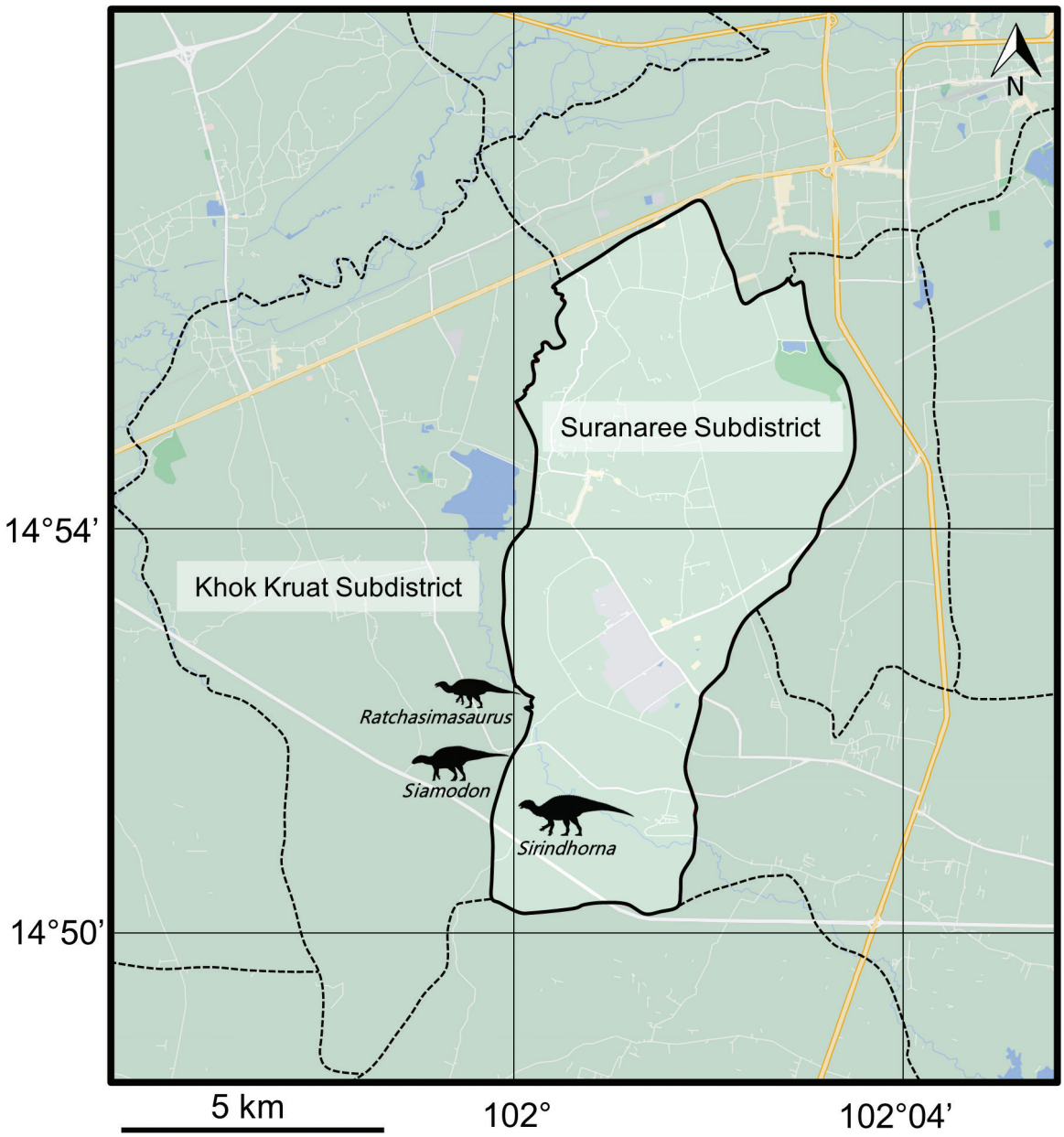

Figure 7. Locality map of Nakhon Ratchasima Province, showing localities of *Siamodon*, *Ratchasimasaurus* and *Sirindhorna*.

Sirindhorna khoratensis **Shibata et al., 2015**

Material. holotype NRRU3001-166, an articulated braincase including referred skull elements: a braincase articulating with a left postorbital (NRRU-A2035), dorsal half of a braincase (NRRU3001-65), caudal portion of a braincase (NRRU3001-179), a right premaxilla (NRRU-A3623), a left maxilla (NRRU-A2048) (Fig. 3K), a right maxilla (NRRU-A2047), a right jugal (NRRU3001-7), a right quadrate (NRRU3001-175), a predentary (NRRU3001-169), a left dentary (NRRU3001-14), a right dentary (NRRU3001-167) (Fig. 3L), a right surangular (NRRU3001-137), isolated maxillary teeth (NRRU-A1956, A3630, A3649, NRRU3001-157, 163), an isolated dentary tooth (NRRU3001-28).

Locality and age. Ban Saphan Hin (a different site from the *S. nimngami* was found), Suranaree Subdistrict, Nakhon Ratchasima Province; late Early Cretaceous Khok Kruat Formation (Aptian).

Previous study. It is known from the presence of several braincases and dentaries that at least four individuals are known. The holotype material, a braincase, shows an autapomorphy: a sagittal crest extending along the entire dorsal surface of the parietal and reaching the frontoparietal suture (Shibata et al. 2015). Referred materials display a unique combination of characters, such as antorbital fossa of the maxilla not visible, a slightly rostrally deepening dentary ramus, and dentary teeth with primary and secondary ridges, but no accessory ridges (Shibata et al. 2015). It was recovered in the basal position of non-hadrosaurid hadrosauroids (Shibata et al. 2015). However, later analysis recovered it near the base of Hadrosauromorpha, more advanced than *R. suranareae* (Madzia et al. 2020). The *S. khoratensis* maxilla (NRRU-A2048) has a low-angled triangular shape and the caudally positioned lacrimal

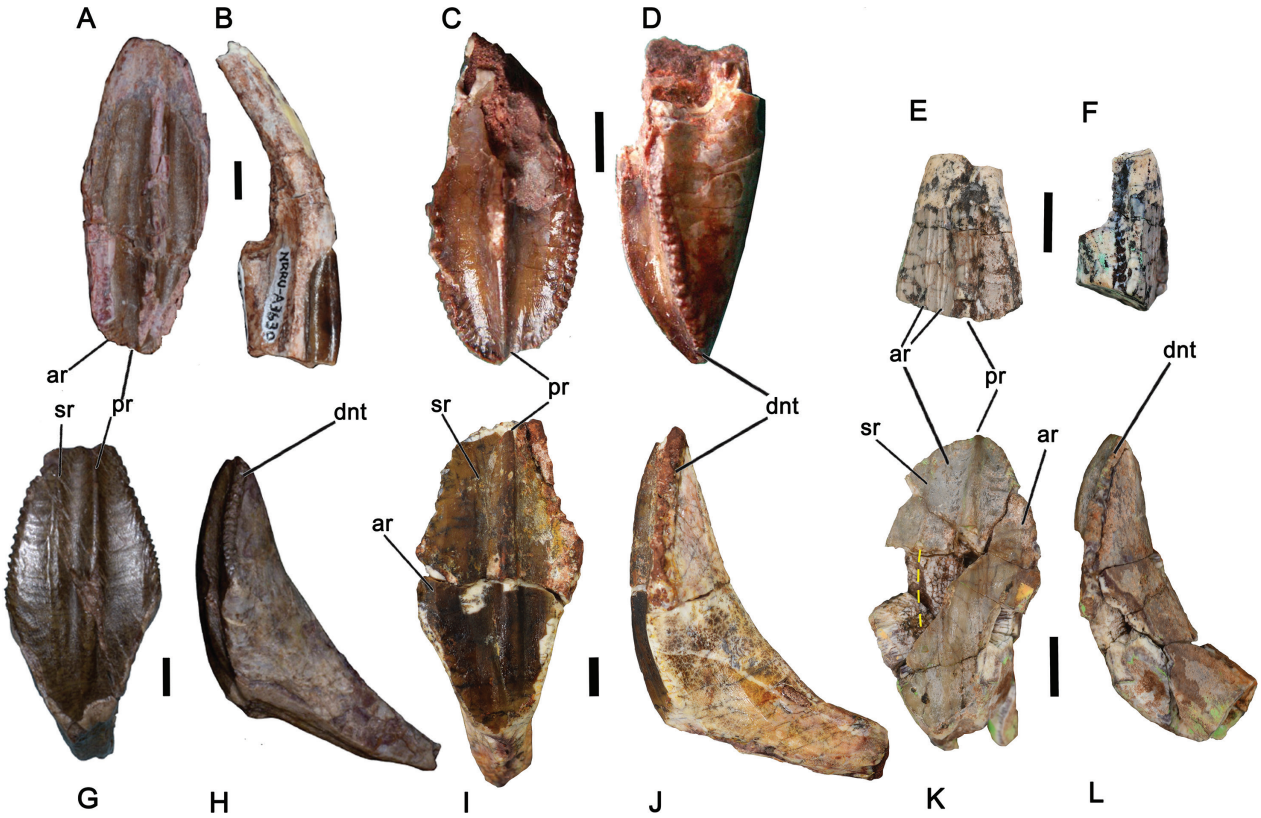

Figure 8. Isolated Thai iguanodontian teeth; *Sirindhorna khoratensis* maxillary tooth (**A, B.** NRRU-A1959) and dentary tooth (**G, H.** NRRU3001-28); *Siamodon nomngami* maxillary tooth (**C, D.** PRC-5) and dentary tooth (**I, J.** WNM-Sp-001); Khok Pha Suam iguanodontian maxillary tooth (**E, F.** SM2021-1-122) and dentary tooth (**K, L.** SM2021-1-121). In labial (**A, C, E**), mesial (**B, D, F**), lingual (**G, I, K**), and distal (**H, J, L**) views. Abbreviations: ar; accessory ridges, pr; primary ridge, sr; secondary ridge. Scale bars: 0.5 cm (Modified from Buffetaut and Suteethorn (2011); Shibata et al. (2015); Manitkoon et al. (2022)).

process, and its 24 alveoli are rostrocaudally arranged and slightly curved caudolaterally. It is different from the isosceles triangular shape with a dorsal process positioned at the middle of the maxilla in *S. nimngami* (Shibata et al. 2015). *R. suranareae* has a low and elongated dentary ramus and a robust coronoid process that differs from the robust and straight dentary ramus with a subvertical coronoid process seen in *S. khoratensis* (Shibata et al. 2015).

Comment. *S. khoratensis* is considered to be the best-preserved iguanodontian ornithopod in Southeast Asia (Shibata et al. 2015). In addition to the published cranial material, the Ban Saphan Hin locality has also yielded a postcranial skeleton that is assumed to belong to *S. khoratensis* because the five discovered braincases show no features to imply the presence of different taxa (Shibata et al. 2018). CT-scanning revealed the brain morphology of *S. khoratensis*, which has general endocast features resembling those of non-hadrosaurid hadrosauroids (Shibata et al. 2018).

Iguanodontian indet. ('Khok Pha Suam iguanodontian')

Material. Isolated teeth and postcranial material including: cervical vertebra (PRC 155); dorsal vertebra (SM2021-1-113) (Fig. 3G); proximal caudal vertebra (SM2021-1-114); distal caudal vertebrae (PRC 156 and SM2021-1-115); chevron (PRC 157); metacarpal (SM2021-1-116); left femur (SM2021-1-117) (Fig. 3H); right femur (SM2021-1-118); tibia (SM2021-1-119); fibula (PRC 158); and phalanx (SM2021-1-120).

Locality and age. Khok Pha Suam, Na Kham Subdistrict, Si Muang Mai District, Ubon Ratchathani Province; late Early Cretaceous Khok Kruat Formation (Aptian-Albian).

Previous study. Teeth of iguanodontians are common at Khok Pha Suam, but fragmentary (Manitkoon et al. 2022). Some isolated postcranial bones belonging to iguanodontians were discovered, including vertebrae and limb bones from different individuals, based on the great discrepancy in size of the left and right femur (Manitkoon et al. 2022; Samathi and Suteethorn 2022). Samathi and Suteethorn assumed that most of the Khok Pha Suam iguanodontian material belonged to a single taxon, and found its phylogenetic position to be a non-hadrosauriform styracosternan (Samathi and Suteethorn 2022).

Comment. The teeth of Thai iguanodontians exhibit a robust primary ridge displaced distally relative to the crown apicobasal axis, which is a derived feature of iguanodontians amongst ornithopods (Norman 2004, 2014). They also possess mammillate marginal denticles, which is a synapomorphy of taxa closer to hadrosaurids than basal ankylopollexians, such as *Camptosaurus* (Fanti et al. 2016).

The maxillary teeth of Thai forms, including *S. khoratensis* (Fig. 8A), *S. nimngami* (Fig. 8C), and the Khok Pha Suam taxon (Fig. 8E), are diagnostic of the level of ankylopollexian iguanodontian by displaying the prominent primary ridge, accessory ridges, and the vertical channels marking the positions occupied by successional tooth crowns (Norman 2014). The different maxillary teeth characteristics are as follows: *S. khoratensis*: lanceolate-shaped crown, primary ridge separates the labial surface unevenly, distal portion of the labial surface bears weak subsidiary ridges and is slightly broader than the mesial portion (Shibata et al. 2015); *S. nimngami*: diamond-shaped crown, primary ridge in a median position, no/one short weak accessory ridge is present in what is presumably the mesial half of the crown, in the apical part. (Buffetaut and Suteethorn 2011); Khok Pha Suam iguanodontian: possibly diamond-shaped crown, primary ridge divides the crown into two asymmetrical halves, at least four weak accessory ridges in what is presumably the mesial portion along the apicobasal axis. The more derived hadrosauroids usually lose the accessory ridges on the crowns of maxillary teeth, and show a shifting of the primary ridge on the maxillary tooth crown to the mid-line (You et al. 2003).

The dentary teeth of the Thai forms, including *S. khoratensis* (Fig. 8B), *S. nimngami* (Fig. 8D), and Khok Pha Suam taxon (Fig. 8F) (not preserved in *R. suranareae*) possess a prominent primary ridge. The crowns allowed the teeth to interlock, resulting in the more elaborate structure of the dental battery. The different characteristics are as follow: *S. khoratensis*: wide with leaf-shaped crown, the secondary ridge is positioned mesial to and is less prominent than the primary ridge, with no other accessory ridges (Shibata et al. 2015); *S. nimngami*: leaf-shaped crown, the secondary ridge is positioned mesial to and is less prominent than the primary ridge, at least one faint accessory ridge is present on the mesial side, crown appears to be curved apicobasally; Khok Pha Suam iguanodontian: leaf-shaped crown, the less prominent secondary ridge is positioned mesial to and is less prominent than the primary ridge and at least two weak accessory ridges are present on the mesial and the distal portion. The dentary teeth of *S. nimngami* and the Khok Pha Suam iguanodontian show accessory ridges, which are absent in *S. khoratensis*. This character appeared in basal hadrosauroids (Prieto-Márquez et al. 2016). In this respect, *S. khoratensis* is probably more advanced than *S. nimngami* and the Khok Pha Suam iguanodontian.

So far, three taxa of styracosternan iguanodontians, including *S. ninngami*, *R. suranareae*, and *S. khoratensis*, have been described from the Khok Kruat Formation in Nakhon Ratchasima Province plus one Laotian taxon "*M. laosensis*" from the Grès Supérieurs Formation of Laos. If Khok Pha Suam iguanodontian is one of the previously-named taxa from Nakhon Ratchasima, this would provide a geographic distribution of about 400 km to the far east (Fig. 1). However, the Khok Pha Suam locality is closer to Savannakhet than Nakhon Ratchasima. The comparison between them has to be very careful, and overlapping elements are required. It would be significant if the Khok Pha Suam iguanodont is a new taxon, as it would mean that there was a diversity of up to five to six species in the region. It is necessary to compare the postcranial material between the Khok Pha Suam taxon and *S. khoratensis*.

If a high diversity in iguanodontians is present in Southeast Asia, then careful consideration and more materials will be required. This may be similar to the case of *Edmontosaurus*, the duck-billed edmontosaurine that was widely distributed in the Late Cretaceous (Campanian-Maastrichtian) ranging from Colorado to Alaska of North America, where several genera were consolidated into two species under a single genus, based on ontogenetic variation, morphometrics and several other factors (Campione and Evans 2011; Takasaki et al. 2020).

Psittacosaurus sattayaraki Buffetaut & Suteethorn, 1992

Material. holotype SM2016-1-163 (renumbered from TF 2449a by Buffetaut and Suteethorn (1992)), right dentary (Fig. 3F); SM2016-1-164 (renumbered from TF 2449b by Buffetaut and Suteethorn (1992)) maxilla fragment.

Locality and age. Ban Dong Bang Noi, Lat Yai Subdistrict, Mueang District, Chaiyaphum Province; late Early Cretaceous Khok Kruat Formation (Aptian).

Previous study. Apart from the ornithopods mentioned above, another valid taxon from the Khok Kruat Formation is a small basal ceratopsian. *P. sattayaraki* was described from a well-preserved dentary (SM2016-1-163) and a maxilla fragment (SM2016-1-164), and it is the southernmost known occurrence of this genus (Buffetaut and Suteethorn 1992). However, the incompleteness of the material makes the validity of the taxa questionable (Sereno 2000; You and Dodson 2004). Buffetaut, Suteethorn, and Khansubha (2007) defended *P. satayaraki* as a species of *Psittacosaurus*, based on the tooth and dentary morphology clearly exhibiting fan-shaped tooth crowns bearing bulbous primary ridge, and a markedly convex alveolar border in lateral or medial view and an incipient ventral flange of the dentary. The taxon has been accepted as a valid species of *Psittacosaurus* in other reviews (Averianov et al. 2006; Lucas 2006).

Comment. Although *Psittacosaurus* was abundant in the Early Cretaceous of Eastern Asia (especially China, Mongolia, and Siberia), it is worth noting that material of *Psittacosaurus* seems to be scarce in Southeast Asia. In Thailand, only fragmentary materials were discovered in Chaiyaphum and Khon Kaen Provinces, and have not been found in other Khok Kruat localities (Manitkoon et al. 2022).

Psittacosaurus sp. Buffetaut et al., 2007

Material. SM2016-1-080, a right femur (Fig. 3E); unnumbered material including isolated tooth, a dentary fragment, a dorsal vertebra, and a fragmentary sacrum.

Locality and age. SM2016-1-080 was collected from the banks of the Nam Phong River, Ban Bueng Klang Village, Nam Phong District, Khon Kaen Province; other materials were collected from Phu Hin Rong, Mancha Khiri District, Khon Kaen Province; all specimens belong to late Early Cretaceous Khok Kruat Formation (Aptian-Albian).

Previous study. Additional postcranial specimens referred to as *Psittacosaurus* have been found in Khon Kaen Province (Buffetaut et al. 2007). The alveolar margin of the dentary fragment is markedly convex resembling the holotype of *P. sattayaraki*, but it is a larger individual (Buffetaut et al. 2007).

Comment. Only the femur is still kept in the Sirindhorn Museum.

Laos

Grès Supérieurs Formation (= Khok Kruat Formation)

All of the dinosaur-bearing beds in the Savannakhet Basin belong to the top of the Grès Supérieurs Formation (Racey 2009; Cavin et al. 2019). The age of dinosaurs in Savannakhet Province is Aptian–Albian, constrained by the non-marine Cretaceous bivalve *Trigonioides kobayashi-Plicatounio Suzuki* (Allain et al. 1999; Cavin et al. 2019). The Grès Supérieurs Formation is considered the lateral equivalent of the Khok Kruat Formation in neighbouring Thailand. Both are considered as Aptian-Albian in age, based on their vertebrate assemblages, bivalves, and palynomorphs (Cappetta et al. 1990; Buffetaut et al. 2005b; Racey 2009; Allain et al. 2012) . Laos has yielded not only skeletal materials, but possibly an ornithopod trackway from Muong Phalane (Allain et al. 1997; Le Loeuff et al. 2009).

"*Mandschurosaurus laosensis*" Hoffet, 1944

Material. unnumbered specimen consists of vertebrae, ilium, and femora.

Locality and age. Muong Phalane, Savannakhet Province of Laos; Grès Supérieurs Formation (≈ the Khok Kruat Formation), Aptian–Albian.

Previous study. *Mandschurosaurus* was the first dinosaur named from China, its material collected from the Late Cretaceous Yuliangze Formation (Maastrichtian) in Heilongjiang (Amur) River area between China and Russia (Godefroit et al. 2011). It was initially referred to the genus "*Trachodon*" *amurense* (Riabinin 1925), but was later re-assigned in 1930 to a new genus as *Mandschurosaurus amurensis* (Godefroit et al. 2011). *M. amurensis* is a large hadrosaurid (duck-billed dinosaurs), based on a poorly preserved and incomplete skeleton, and is often considered as a *nomen dubium* (Horner et al. 2004). Hoffet described the Laotian ornithopod material as "*Mandschurosaurus laosensis*" (Hoffet 1944), which was considered Late Cretaceous (Senonian) in age (Buffetaut 1991). However, some palaeontologists consider "*M. laosensis*" a *nomen dubium* (Buffetaut 1991; Horner et al. 2004). "*M. laosensis*" is potentially a non-hadrosaurid iguanodontian, such as *Siamodon*, *Ratchasimasaurus*, and *Sirindhorna* from rocks of the same age in Thailand. Hoffet also suggested that another ilium which is more robust than "*M. laosensis*", indicated the presence of a second taxon (Buffetaut 1991; Allain et al. 1999).

Iguanodontian indet. ('Savannakhet iguanodontian B')

Material. unnumbered specimen consists of series of dorsal vertebrae, rib, pubis, and ischium.

Locality and age. Ban Lamthouay, Tang Vay District, Savannakhet Province; The Grès Supérieurs Formation (≈ the Khok Kruat Formation), Aptian-Albian.

Comments. These unpublished materials are kept in the Dinosaur Museum of Savannakhet. It is necessary to compare these with the unpublished postcranial material of *S. khoratensis*.

Psittacosaurid indet. ('Savannakhet psittacosaurid')

Material. unnumbered specimen of left mandible.

Locality and age. Ban Lamthouay, Tang Vay District, Savannakhet Province; Grès Supérieurs Formation (≈ the Khok Kruat Formation), Aptian–Albian.

Comments. The unpublished specimen of psittacosaurid indet. was reported and the cast of this specimen is displayed in the Dinosaur Museum of Savannakhet (Allain et al. 1999; Buffetaut et al. 2007; Cavin et al. 2019). Detailed comparison with *Psittacosaurus sattayaraki* of Thailand is needed after a full description of this material has been completed.

Malaysia

The Tembeling Group

This non-marine fossil-bearing unit was informally referred to as 'the Pahang vertebrate bed' and is located in the interior of Pahang State, but the exact location of the site has been kept confidential. Hybodont sharks and ray-finned fish fishes were reported from this assemblage, which have strong affinities with fauna in the Early Cretaceous of Thailand (Teng et al. 2019). The four hybodont taxa, including *Heteroptychodus kokutensis*, *Isanodus paladeji*, *Lonchidion* aff. *khoratensis*, and *Mukdahanodus* aff. *trisivakulii*, were previously known only from the Sao Khua Formation (Khorat Group) and equivalent strata of Ko Kut (Kut Island) (Teng et al. 2019). Plants, bivalves, turtles and dinosaurs (teeth of a spinosaurid and an ornithischian) also reported from the

same bonebed (Sone et al. 2015; Teng et al. 2019). They considered this site is correlated to the Early Cretaceous part (Temus Shale) of the Tembeling Group, and is equal to the Sao Khua Formation of Thailand in age based on faunal composition and biostratigraphic correlation (Teng et al. 2019).

So far, the ornithischians from the Tembling Group have not been published, but some information was released in the Malaysian media (University of Malaya 2014). We are unable to provide further details currently.

The Gagau Group

Far northeast from the Pahang vertebrate bed, another dinosaur site was found in the Chichir River of Hulu Terengganu in the north-eastern part of the Mount Gagau Area (Rahman 2019). The fossil area is underlain by the Jurassic-Cretaceous Gagau Group, comprising footprints and teeth within the Lotong Sandstone (Akhir et al. 2015). The teeth were found in ex-situ conglomerate boulders, and identified as belonging to iguanodontian dinosaurs.

Southern China

Xinlong Formation

Material of ornithischians was reported from the Napai Basin in south-western Guangxi Zhuang Autonomous Region (Dong 1979). The assemblage belongs to the Early Cretaceous (Aptian) Xinlong Formation (sometimes called the Napai Formation), and shows resemblance to the Khok Kruat Formation Southeast Asia (Mo et al. 2016). The four species of hybodonts from the assemblage (*Acrorhizodus khoratensis*, "*Hybodus*" *aequitridentatus*, *Thaiodus ruchae* and *Khoratodus foreyi*) are endemic to Southeast Asia and South China, and restricted to the Aptian-Albian interval (Cuny 2012; Cuny et al. 2017). These vertebrate fossils support the Xinlong Formation as coeval with the Khok Kruat Formation of Thailand and the 'Grès Supérieurs' Formation of Laos (Mo et al. 2016).

Napaisaurus guangxiensis Ji & Zhang, 2022

Material. The holotype, FS-20-007 to 008, a right ischium and ilium.

Locality and age. Napai Basin, Fusui County; Xinlong Formation, Early Cretaceous (Aptian).

Previous study. This is the first named basal iguanodontian taxon from southern China, based on characteristics of the ilium and ischium which differ from other known iguanodontian taxa (Ji and Zhang 2022).

Comments. The authors did not perform a phylogenetic analysis of the taxon. It is necessary to compare with the unpublished ischium and ilium of *S. khoratensis*.

Iguanodontian indet. Mo et al., 2016

Material. Unnumbered specimens including cervical vertebra, dorsal vertebra, distal end of left humerus, distal end of left femur, and isolated teeth.

Locality and age. Napai Basin, Guangxi Zhuang Autonomous Region; Xinlong Formation, Early Cretaceous (Aptian).

Previous study. These poorly preserved specimens cannot be identified more precisely. However, some lower teeth bear a strong median primary ridge and at least one subsidiary ridge suggesting a relatively advanced iguanodontian (Mo et al. 2016).

Comments. There are many taxa of iguanodontians in Thailand and Laos, but it cannot be concluded whether these materials belong to *Napaisaurus guangxiensis* or not.

?Psittacosaurid indet. Mo et al., 2016

Material. Unnumbered specimens including distal end of a right femur.

Locality and age. Napai Basin, Guangxi Zhuang Autonomous Region; Xinlong Formation, Early Cretaceous (Aptian).

Previous study. Mo et al. (2016) reported an incomplete femur, which resembles a psittacosaurid. Although the condition of the specimen is poor, this group is widely distributed in the early Cretaceous of China, Mongolia, Siberia, Thailand, and Laos. It is possible that this basal ceratopsian could be present in the Xinlong Formation (Buffetaut and Suteethorn 1992; Buffetaut et al. 2007; Mo et al. 2016).

Discussion

Evolution of Southeast Asian ornithischians

The origin of ornithischians remains controversial (Baron and Barrett 2018). *Chilesaurus diegosuarezi* from the Late Jurassic (Tithonian) of Chile and *Pisanosaurus mertii* from the Early Late Triassic (Carnian) of Argentina, were considered to be the most basal ornithischians (Butler et al. 2008; Baron and Barrett 2017; Baron et al. 2017). However, some palaeontologists consider them as primitive dinosauriforms (Müller et al. 2018; Madzia et al. 2021). Other primitive true ornithischians were also discovered from the Early Jurassic in southern Gondwana, for example, *Eocursor parvus* (potentially Sinemurian) in South Africa (Butler et al. 2007), *Heterodontosaurus tucki* (potentially Sinemurian) in South Africa (Sereno 2012), *Lesothosaurus diagnosticus* (= *Stormbergia dangershoeki*) in Lesotho and South Africa (Baron et al. 2017), and *Laquintasaura venezuelae* (Hettangian) in Venezuela (Barrett et al. 2014). Ornithischians evolved later to become remarkably diverse in the Jurassic and one of the most successful groups of Cretaceous herbivores.

So far, Asian ornithischians have been found from five epochs as follows:

1) Early Jurassic

A few basal thyreophorans have been reported from Yunnan Province, China (Norman et al. 2007; Yao et al. 2022). During this epoch, basal thyreophorans are known from Africa, Europe and North America (Barrett et al. 2014). However, evidence of their existence is yet to be found in Southeast Asia. Although dinosaur remains have come from the Late Triassic-Early Jurassic Nam Phong Formation of north-eastern Thailand, the fossils discovered include only postcranial material of sauropodomorphs (Buffetaut et al. 2000; Laojumpon et al. 2017) and large theropod footprints (Liard et al. 2015). In the Mesozoic red beds of northern Thailand, an indeterminate sauropod from the Chiang Muan District, Phayao Province was found and dated as post-Toarcian in age, possibly at the boundary between the Early and Middle Jurassic (Chanthasit et al. 2018). However, ornithischian material has yet to be discovered.

2) Middle Jurassic

A few basal neornithischians (such as *Agilisaurus* and *Kulindadromeus*) were reported from China and Russia (Barrett et al. 2005; Godefroit et al. 2014). Heterodontosaurids, possibly ankylosaurians and stegosaurians appeared in China (Dong et al. 1983; Dong 1993; Zheng et al. 2009). Interestingly, filamentous integumentary structures in ornithischians have only been from Asian taxa so far (*Tianyulong* and *Kulindadromeus* and appeared again in *Psittacosaurus* in the Early Cretaceous). These provide evidence for protofeathers being basal to ornithischians, rather than just to theropods, as previously suspected (Godefroit et al. 2014). The Middle Jurassic dinosaurs in Southeast Asia are still obscure.

3) Late Jurassic

As in Africa, Europe, and the USA, Asian ornithischian faunas were dominated by stegosaurs during this time. Some basal neornithischians are reported from the USA, China, and Thailand. Basal iguanodontians (such as *Dryosaurus*, *Dysalotosaurus* and *Camptosaurus*) evolved in North America, Africa, and Europe, but there is no evidence for these taxa in Asia (Norman 2004; Xu et al. 2018). However, there were the earliest known marginocephalians, the Chaoyangsauridae, in China. The presence of Jurassic ceratopsians restricted to Asia indicates an Asian origin for the group (Zhao et al. 1999). In Thailand, the lower part of the Phu Kradung Formation yields stegosaurians and basal neornithischians. While the upper part, which is likely considered as Lower Cretaceous in age (Tong et al. 2015, 2019b), still includes basal neornithischians and other groups of dinosaurs (such as metricanthosaurids and mamenchisaurids) similar to those from the lower Phu Kradung Formation.

4) Early Cretaceous

By this time, the number of stegosaurids decreased and these were eventually lost (Tumanova and Alifanov 2018). In contrast, we observe an apparent increase of ankylosaurians and the appearance of jeholosaurids, considered to have been an endemic group in East Asia (Han et al. 2012). During the late Early Cretaceous, iguanodontians evolved larger body sizes and became the dominant herbivores in the ecosystem. Several non-hadrosaurid iguanodontians have been reported from China, Japan, Mongolia, Thailand, Laos, and possibly Malaysia (Norman 2004). Several species of *Psittacosaurus* and basal neoceratopsians have been found in China, Japan, Mongolia, Russia, South Korea, Thailand, Laos, and possibly Uzbekistan (You and Dodson 2004; Averianov et al. 2006).

5) Late Cretaceous

The Beringian land bridge between present-day Siberia and Alaska, which opened during the Aptian-Albian, served as a migration route for terrestrial vertebrates between Asia and North America during the Late Cretaceous (Russell 1993). Hence, we can see the similarities between the dinosaur fauna from these two continents. Many dinosaur groups (including ankylosaurids, hadrosaurids, neoceratopsians, pachycephalosaurians, tyrannosaurids and troodontids) supposedly originated in Asia (Bell 2011). Asian ornithischian dinosaurs diverged considerably in the Late Cretaceous. Non-hadrosaurid hadrosauroids were replaced with hadrosaurids, the medium to large-sized duck-billed dinosaurs (Tsogtbaatar et al. 2019; Kobayashi et al. 2021). Hadrosaurids became dominant, and extended across China, Japan, Kazakhstan, Mongolia, and Russia. There are two thescelosaurids known from Mongolia and South Korea (Huh et al. 2011; Makovicky et al. 2011). Several pachycephalosaurians, exclusively known from Laurasia, were found in China and Mongolia (Sullivan 2006). Several ankylosaurians are reported from China, Japan, Mongolia, and Uzbekistan (Park et al. 2021). Several neoceratopsians (such as leptoceratopsids and protoceratopsids) were reported from China, Mongolia, and Uzbekistan, but there is only one taxon of ceratopsid from China, contrary to their prevalence in North America (Xu et al. 2010). However, although the diversity of ornithischian dinosaurs during this epoch was highest, no dinosaur bones of this age have been reported in Southeast Asia.

Palaeobiogeographic implications

Southeast Asia consists of a mosaic of microcontinents. In the late Palaeozoic and Mesozoic, the northern margin of eastern Gondwana, after drifting northwards, collided with South China and other microcontinents (Metcalfe 1998). These terranes were united by the Late Triassic. Most of the dinosaur fossils in north-eastern Thailand, Laos, and Cambodia have been found on the Indochina Terrane.

Stage 1: Late Jurassic to Early Cretaceous

The oldest record of ornithischian dinosaurs in southeast Asia so far is from the Phu Kradung Formation of north-eastern Thailand, which is the basal unit of the Khorat Group (Racey et al. 1996; Racey 2009). Stegosaurids and small-bodied basal neornithischians have been unearthed, together with mamenchisaurid sauropods, and metricanthosaurid theropods, from the rich vertebrate assemblages of the Phu Noi locality and the nearby Khok Sanam locality, which is considered as the lowermost part of Phu Kradung Formation (Buffetaut et al. 2001; Cuny et al. 2014; Chanthasit et al. 2019; Manitkoon and Deesri 2019). Racey and Goodall (2009) supposed that the lower Phu Kradung Formation could be Late Jurassic (?Tithonian) in age, which was also supported by the evidence from vertebrate remains (Buffetaut et al. 2001; Buffetaut et al. 2006).

Interestingly, the vertebrate faunas from the lower Phu Kradung Formation share similarities with the those from the Middle-Late Jurassic (Bathonian-Callovian) Khlong Min Formation of the Thai southern peninsula from the Sibumasu Terrane (Buffetaut et al. 2005a; Cuny et al. 2014). Hybodont sharks (Cuny et al. 2014), brachyopoid temnospondyls (Buffetaut et al. 1994; Nonsrirach et al. 2021), teleosaurid crocodylomorphs (Buffetaut et al. 1994; Cuny et al. 2009; Martin et al. 2019), and mamenchisaurid sauropods (Buffetaut et al. 2005a; Suteethorn et al. 2013) from both the lower Phu Kradung and Khlong Min Formations indicate a wide distribution.

The upper part of Phu Kradung Formation is Early Cretaceous in age, based on the presence of *Dicheiropollis etruscus* (Racey and Goodall 2009) and a turnover of hybodont shark, turtle and crocodylomorph faunas (Tong et al. 2009, 2019b; Cuny et al. 2014; Martin et al. 2019). Microremains of the hybodont *Acrodus kalasinensis*, *Jaiodontus* sp. and related denticles from the Khlong Min Formation are found in the lower Phu Kradung (Cuny et al. 2014). The genus *Acrodus* is known from the Triassic and Jurassic (Rees and Underwood 2006), and *Jaiodontus* is restricted to the Oxfordian of China (Klug et al. 2010). In addition, the absence of the more common *Heteroptychodus* from the Early Cretaceous assemblages and its presence in the upper Phu Kradung Formation supports the age difference between the upper and lower parts of the Phu Kradung Formation (Cuny et al. 2014).

The xinjiangchelyid turtles (such as *Phunoichelys kalasinensis* and *Kalasinemys prasarttongosothi*) from Phu Noi can be correlated with those from the Late Jurassic of China as follows: the Late Jurassic Shangshaximiao (= upper Shaximiao) Formation of Sichuan Basin, the Middle-Late Jurassic Shishugou, Toutunhe and Qigu formations of the Junggar and Turpan Basins, and the Middle Jurassic Chuanjie Formation in Yunnan Basin. In contrast, records of this group in Early Cretaceous deposits are scarce in Asia (Tong et al. 2015, 2019b). The turtle fauna from the lower Phu Kradung are distinct from assemblages in the upper part, which include abundant remains of more advanced turtles, such as the trionychoid *Basilochelys macrobios* (Tong et al. 2009, 2015, 2019b).

The presence of teleosaurid crocodylomorphs (such as *Indosinosuchus potamsiamensis*) from Phu Noi suggest a Middle-Late Jurassic age contrary to crocodylomorphs from the upper part, which are characterised by pholidosaurids (such as *Chalawan thailandicus*) and atoposaurids (Lauprasert et al. 2011; Martin et al. 2014), indicating a faunal turnover in Southeast Asia through the Jurassic-Cretaceous (Martin et al. 2019).

The saurischian dinosaur faunas from both the lower and the upper Phu Kradung Formation consist of mamenchisaurids and metriacanthosaurids, which are well-known from the Middle-Late Jurassic/Early Cretaceous Formations in the Sichuan-Yunnan-Northern Junggar Basin of China. Mamenchisaurids (such as *Mamenchisaurus* and *Omeisaurus*) are eusauropods, and are also present in the Chuanjie Formation, Shishugou Formation, lower and upper Shaximiao Formation, Suining Formation, and Penglaizhen Formation (Buffetaut et al. 2006; Xing et al. 2015; Wang et al. 2019; Ren et al. 2021). Metriacanthosaurids (= sinraptorids) from Phu Noi show similar characteristics to *Sinraptor dongi* from the Upper Jurassic Shishugou Formation of the Junggar Basin in north-western China, and *Yangchuanosaurus* from the Middle-Late Jurassic Shaximiao Formation and possibly Late Jurassic-Early Cretaceous Suining Formation (Chanthasit et al. 2019). Both mamenchisaurids and metrianthosaurids were once thought to be endemic to east Asia. However, the report of isolated fossils from the Itat Formation of Russia and the taxon *Wamweracaudia* from Tendaguru extends the geographic distribution of mamenchisaurids into Siberia and Africa (Averianov et al. 2019; Mannion et al. 2019). Furthermore, *Metriacanthosaurus*, a close relative of *Sinraptor*, has been found in the upper Oxford Clay Formation of England.

The single stegosaur bone from the lower Phu Kradung Formation cannot provide definitive proof, except that it is more advanced than the Middle Jurassic *Huayangosaurus* and likely to be closer to those from the Late Jurassic taxa, such as *Tuojiangosaurus* (Buffetaut et al. 2001). Basal neornithischians from Phu Noi show characters that resemble taxa from the lower and upper Shaximiao Formation of China and the Late Jurassic Morrison Formation of US (Barrett et al. 2005; Carpenter and Galton 2018; Manitkoon et al. 2019).

As mentioned above, the dinosaur faunas including metriacanthosaurids and mamenchisaurids, and basal neornithischians have been found in both the lower and upper parts of the Phu Kradung Formation indicating that, despite the change in other groups of vertebrate faunas, dinosaurs remained the same and had long stratigraphic ranges. Another noteworthy point is the Phu Kradung Formation, and the Klong Min Formation show a remarkable biodiversity and reveal a close relationship with Chinese Jurassic vertebrate assemblages suggesting that the vertebrate faunas are more widespread than previously thought. This is probably not surprising as the vertebrate-bearing terranes of Southeast Asia and China were fused by the

Late Triassic and Mesozoic terrestrial sandstones are widespread from China south to Malaysia (Sone and Metcalfe 2008; Cai and Zhang 2009; Choong et al. 2022).

Stage 2: Early Cretaceous (?Berriasian to pre-Barremian)

The trackway of a small quadrupedal ornithopod is found in the Phra Wihan Formation of Thailand. This Formation was dated as Lower Cretaceous (Berriasian-Early Barremian) from a rich palynological assemblage (Racey 2009; Racey and Goodall 2009). However, a subsequent study using radiometric dating on detrital zircon grains suggested that the dates for the underlying Sao Khua Formation are much older than previously suspected (Tucker et al. 2022). The study restricted the upper part of the Sao Khua Formation to no earlier than early Hauterivian, which means that the Phra Wihan Formation is likely not younger than Valanginian in age (Tucker et al. 2022).

The Sao Khua Formation of Thailand was assigned to the Early Cretaceous on palynological evidence (Racey et al. 1996), and probably Valanginian-Barremian on the basis of dinosaurs and bivalves (Meesook 2000). In the most recent publications, Sao Khua vertebrate fauna, including turtles and theropod dinosaurs, are considered to be Barremian (Samathi et al. 2019b; Tong et al. 2019a), and following a more refined regional biostratigraphic correlation of the freshwater bivalves *Pseudohyria* (*Matsumotoina*) *matsumotoi* suggesting a late Barremian age (Tumpeesuwan et al. 2010). Lastly, the radiometric data on detrital zircon grains indicated a tightly restricted late Valanginian-early Hauterivian age (133.6–132.1 Ma) for the Sao Khua Formation, and establishes that the dinosaur fauna is ~ 5–9 million years older than currently known (Tucker et al. 2022).

The Sao Khua Formation is dominated by sauropods (somphospondylian titanosauriforms, other titanosauriforms and diplodocoids) and theropods (spinosaurids, megaraptorans and coelurosaurs) in terms of species-richness and overall abundance (Buffetaut and Suteethorn 1998a; Buffetaut et al. 2002; Samathi et al. 2019a) (Fig. 9). Amongst the thousands of saurischian bones that have been collected from north-eastern Thailand, no evidence of ornithischians has yet been found in this formation (Buffetaut et al. 2015). The lack of ornithischians in the Sao Khua Formation is possibly consistent with the ecological composition of Valanginian/Hauterivian aged assemblages from Gondwana, for example, the "wood beds" of the upper Kirkwood Formation of South Africa and the Bajada Colorado Formation of South America, which are dominated by various-sized theropods and multiple cohabiting species of sauropods (Tucker et al. 2022). This is in contrast to those pre-Barremian dinosaur assemblages of Laurasian landmasses from Europe and North America, which have a diverse ornithischian record including ankylosaurians and iguanodontians and which shared habitats with other sauropod and theropod dinosaurs (Norman 2010; Kirkland et al. 2016; Tucker et al. 2022). By comparison with contemporaneous formations in Asia, ornithischian remains are still somewhat limited (Tucker et al. 2022). Material of an indeterminate stegosaurian has been reported from the Mengyin Formation (Berriasian-Valanginian), Shandong Province of China (Tucker et al. 2022). A stegosaurine *Wuerhosaurus homheni* and probable basal ceratopsians have been reported from the Lianmuqin Formation (?Valanginian) of Tugulu Group, Xinjiang Region of China (Sereno and Shichin 1988; Maidment et al. 2008).

Although the late Valanginian-early Hauterivian seems to be a crucial period for the ornithischian dinosaurs in southeast Asia, it does not mean that they were completely absent, but possibly reflected niche overlap, competition between herbivores considerably, and/or different timing of biogeographic dispersal. However, the vertebrate assemblage from 'the Pahang vertebrate bed' of Malaysia shows strong affinities with faunas in the Sao Khua of Thailand (Teng et al. 2019). An ornithischian tooth from this site may help fill the gap in the disappearance of ornithischian dinosaurs from Southeast Asia during this time.

The Early Cretaceous Phu Phan Formation is unconformably underlain by the red siltstones of the Sao Khua Formation, whereas the contact with the overlying Khok Kruat Formation is conformable suggesting that the Phu Phan Formation must fall within the interval early Hauterivian to Aptian, based on the ages of the over- and underlying formations (Racey 2009; Tucker et al. 2022). Theropod tracks have been reported, while vertebrate bones are extremely rare. Only a large sauropod limb bone has been found in a cliff face at Phu Kum Kao locality, Kalasin Province (Buffetaut et al. 2002; Buffetaut et al. 2003). No evidence of ornithischians has hitherto been reported.

Stage 3: Middle Cretaceous (Aptian to Albian)

In contrast with the Sao Khua Formation, the younger Khok Kruat Formation contains abundant neornithischian dinosaurs remains including iguanodontians and basal ceratopsians, fewer theropods (spinosaurids and carcharodontosaurians) and titanosauriforms sauropods have been found (Buffetaut et al. 2005b; Chokchaloemwong et al. 2019; Manitkoon et al. 2022).

The Khok Kruat Formation of Thailand, together with the Grès Supérieurs Formation of Laos and the Xinlong Formation of southern China share the same palaeobiogeography, supported by vertebrate fossils (Buffetaut and Suteethorn 1998b; Mo et al. 2016; Cuny et al. 2017), and have yielded five iguanodontian taxa, and at least one taxon of *Psittacosaurus* (Buffetaut and Suteethorn 1992; Buffetaut and Suteethorn 2011; Shibata et al. 2015; Ji and Zhang 2022). This stage represents the highest diversity of ornithischians, and also refines the temporal shift from sauropod-dominated to iguanodontian-dominated ecosystems during the Cretaceous in southeast Asia. Both iguanodontians and ceratopsians possibly spread in this region during the Aptian. One hypothesis suggests Cerapoda (ornithopods+ceratopsians) dentitions are suited

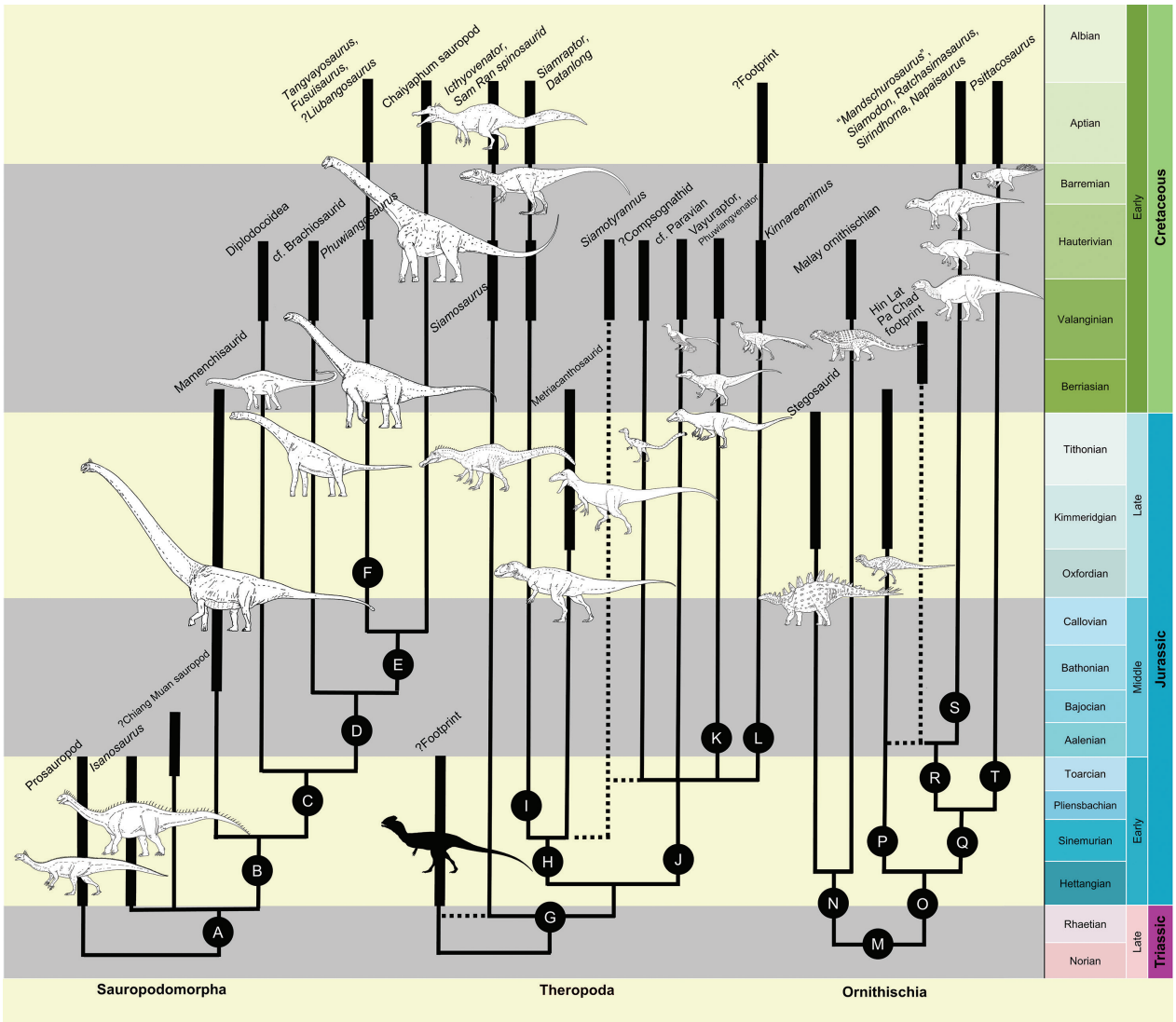

Figure 9. Phylogenetic relationships of non-avian dinosaurs in southeast Asia and southern China. Abbreviations: A, Sauropoda; B, Eusauropoda; C, Neosauropoda; D, Macronaria; E, Titanosauriformes; F, Somphospondyli; G, Tetanurae; H, Allosauroidea; I, Carcharodontosauria; J, Coelurosauria; K, Megaraptora; L, Ornithomimosauria; M, Genasauria; N, Thyreophora; O, Neornithischia; P, Basal neornithischian; Q, Cerapoda; R, Ornithopoda; S, Iguanodontia; T, Ceratopsia (Cuny et al. 2014; Mo et al. 2016; Laojumpon et al. 2017; Chanthasit et al. 2018; Samathi et al. 2019a; Rolando et al. 2022; Sone et al. 2022; Sriwisan et al. 2022).

for efficiently grinding vegetation as a reason for their successful competition with other herbivores in later Cretaceous time (Strickson et al. 2016).

Basal iguanodontians first appeared in North America, Africa, and Europe during the late Jurassic (possibly Kimmeridgian) (Norman 2004). Ankylopollexia, a derived clade of iguanodontian, is inferred to have immigrated to West Europe from North America prior to the Valanginian, and dispersed into East Asia from West Europe via the elongated archipelago around the Jurassic-Cretaceous boundary, probably associated with the coeval global marine regression (Xu et al. 2018). Asian basal ankylopollexians were diverse during the Early Cretaceous including taxa like *Fukuisaurus* and *Koshisaurus* (Barremian) from Japan (Shibata and Azuma 2015), *Lanzhousaurus* (Barremian) from China (You et al. 2005), and *Bayannurosaurus* (early Aptian) from Inner Mongolia, China (Xu et al. 2018). Later, the non-hadrosaurid hadrosauroids are mainly known from the middle Cretaceous (Aptian-Albian). For instance, *Altirhinus* and *Choyrodon* from Mongolia (Norman 1998; Gates et al. 2018); *Equijubus*, *Gongpoquansaurus*, *Jintasaurus*, and *Xuwulong* from Gansu Province, China (You et al. 2003, 2014; You and Li 2009); *Probactrosaurus* and *Penelopognathus* from Inner Mongolia, China (Rozhdestvenskiy 1967; Godefroit et al. 2005); *Ratchasimasaurus*, *Sirindhorna*, and possibly *Siamodon* from Thailand (Shibata et al. 2015).

The earliest known ceratopsians (or even marginocephalian dinosaurs) are in the family Chaoyangsauridae (*Chaoyangosaurus* and *Yinlong*), from the Late Jurassic of China (You and Dodson 2004). Until the Early Cretaceous (late Barremian-Aptian), the genus *Psittacosaurus* roamed across China, Mongolia, Russia, Thailand and possibly Laos (Buffetaut et al. 2007). Although as many as 19 species

have been referred to this genus, about 9–12 are currently considered valid (Napoli et al. 2019). Although psittacosaurids were abundant in the Early Cretaceous of Eastern Asia, they appear to be scarce in Southeast Asia (Buffetaut and Suteethorn 1992; Buffetaut et al. 2007). Specimens of *Psittacosaurus* are often found in lacustrine deposits (Averianov et al. 2006; Buffetaut et al. 2007), which differs from the fluvial deposits with an arid or semi-arid subtropical climate of the Khok Kruat Formation and the Grès Supérieurs Formation (Racey et al. 1996; Wongko 2018). Both factors, depositional environment and palaeoclimate, may provide an explanation for the scarcity of psittacosaurid materials in Thailand and Laos (Manitkoon et al. 2022).

After the Aptian-Albian stages, no further Mesozoic vertebrate fossils have been reported from Southeast Asia. The Khok Kruat Formation is unconformably overlain by the Maha Sarakham Formation (Albian-Cenomanian), which was deposited in a hypersaline, land-locked salt lake within an arid, continental desert, coinciding with worldwide high sea level in the Late Cretaceous and the flooding of marine-sourced water over what is now the Khorat Plateau (Racey et al. 1996).

Conclusions

So far, most southeast Asian ornithischian dinosaur fossils have been found in the Khorat Group of north-eastern Thailand. At least six taxa have been reported and dated from the Late Jurassic to the late Early Cretaceous. The oldest are known from the Late Jurassic Phu Kradung Formation represented by stegosaurids and basal neornithischians. There appears to be an absence of ornithischian dinosaurs during the pre-Barremian of the Sao Khua Formation. The Early Cretaceous Khok Kruat Formation (Aptian-Albian) contains abundant advanced iguanodontians plus basal ceratopsians, which reflects the shift from sauropod-dominated to ornithischian-dominated ecosystems. Iguanodontians and psittacosaurids are also found in the Grès Supérieurs Formation of Laos and the Xinlong Formation of southern China with many similarities to the Khok Kruat fauna of Thailand and these formations are considered equivalent in age. The rare dinosaur specimens from Malaysia are also an age anomaly. However, we propose that the ornithischian tooth from the Tembeling Group represents the existence of ornithischians that are missing from the time-equivalent Sao Khua Formation of Thailand. This study illustrates the diversity of ornithischian assemblages in Southeast Asia, providing an updated review and a discussion about their palaeobiogeographic implications.

Acknowledgements

We would like to thank many colleagues for useful suggestions and comments; Clive Burrett and Thitiwoot Sethapanichsakul for their help with the English language. Kamonlak Wongko, Sasa-On Khansubha, Wilailuck Naksri, and Kantanat Trakunweerayut for providing data on ornithischian specimen and map preparation. Witaya Nimgnam for material from Ban Khok Sanam and Ban Saphan Hin localities. We are grateful to the staff of the Palaeontological Research and Education Centre of Mahasarakham University, Sirindhorn Museum, and Northeastern Research Institute of Petrified Wood and Mineral Resources (In Honor of His Majesty the King) Nakhon Ratchasima Rajabhat University, who took part in our fieldwork and helped during visits to the collection. This research project was financially supported by Mahasarakham University.

References

Akhir AMM, Rahman MNBA, Jamaluddin MH (2015) The Discovery of dinosaur Fossils in Mount Gagau, Hulu Terengganu, Malaysia. In: The 2nd International Symposium Asian Dinosaurs in Thailand 2015, 57.

Allain R, Taquet P, Battail B, Dejax J, Richir P, Veran M, Sayarath P, Khenthavong B, Thamvirith P, Hom B (1997) Pistes de dinosaures dans les niveaux du Crétacé inférieur de Muong Phalane, province de Savannakhet (Laos). Comptes Rendus de l'Academie de Sciences - Serie IIa. Sciences de la Terre et des Planetes 325: 815–821. https://doi.org/10.1016/S1251-8050(97)82761-9

Allain R, Taquet P, Battail B, Dejax J, Richir P, Véran M, Limon-Duparcmeur F, Vacant R, Mateus O, Sayarath P, Khenthavong B, Phouyavong S (1999) Un nouveau genre de dinosaure sauropode de la formation des Gres superieurs (Aptien-Albien) du Laos. Comptes Rendus de l'Academie de Sciences - Serie IIa. Sciences de la Terre et des Planetes 329: 609–616. https://doi.org/10.1016/S1251-8050(00)87218-3

Allain R, Xaisanavong T, Richir P, Khentavong B (2012) The first definitive Asian spinosaurid (Dinosauria: Theropoda) from the early Cretaceous of Laos. Naturwissenschaften 99(5): 369–377. https://doi.org/10.1007/s00114-012-0911-7

Averianov AO, Voronkevich AV, Leshchinskiy SV, Fayngertz AV (2006) A ceratopsian dinosaur *Psittacosaurus sibiricus* from the early cretaceous of West Siberia, Russia and its phylogenetic relationships. Journal of Systematic Palaeontology 4(4): 359–395. https://doi.org/10.1017/S1477201906001933

Averianov A, Krasnolutskii S, Ivantsov S, Skutschas P, Schellhorn R, Schultz J, Martin T (2019) Sauropod remains from the Middle Jurassic Itat Formation of West Siberia, Russia. PalZ 93(4): 691–701. https://doi.org/10.1007/s12542-018-00445-8

Baron MG, Barrett PM (2017) A dinosaur missing-link? *Chilesaurus* and the early evolution of ornithischian dinosaurs. Biology Letters 13(8): 20170220. https://doi.org/10.1098/rsbl.2017.0220

Baron MG, Barrett PM (2018) Support for the placement of *Chilesaurus* within Ornithischia: A reply to Müller et al. Biology Letters 14(3): 20180002. https://doi.org/10.1098/rsbl.2018.0002

Baron MG, Norman DB, Barrett PM (2017) Postcranial anatomy of *Lesothosaurus diagnosticus* (Dinosauria: Ornithischia) from the Lower Jurassic of southern Africa: implications for basal ornithischian taxonomy and systematics. Zoological Journal of the Linnean Society 179: 125–168. https://doi.org/10.1111/zoj.12434

Barrett PM, Butler RJ, Knoll F (2005) Small-Bodied Ornithischian Dinosaurs from the Middle Jurassic of Sichuan, China. Source: Journal of Vertebrate Paleontology Journal of Vertebrate Paleontology 25: 823–834. https://doi.org/10.1671/0272-4634(2005)025[0823:SODFTM]2.0.CO;2

Barrett PM, Butler RJ, Mundil R, Scheyer TM, Irmis RB, Sánchez-Villagra MR (2014) A palaeoequatorial ornithischian and new constraints on early dinosaur diversification. Proceedings. Biological Sciences 281(1791): 2–7. https://doi.org/10.1098/rspb.2014.1147

Bell PR (2011) Cranial osteology and ontogeny of *Saurolophus angustirostris* from the late cretaceous of Mongolia with comments on *Saurolophus osborni* from Canada. Acta Palaeontologica Polonica 56(4): 703–722. https://doi.org/10.4202/app.2010.0061

Boyd CA (2015) The systematic relationships and biogeographic history of ornithischian dinosaurs. PeerJ 3: e1523. https://doi.org/10.7717/peerj.1523

Brett-Surman MK, Holtz TRJ, Farlow JO [Eds] (2012) The Complete Dinosaur. 2nd ed. Indiana University Press.

Buffetaut E (1991) On the age of the Cretaceous dinosaur-bearing beds of southern Laos. Newsletters on Stratigraphy 24(1–2): 59–73. https://doi.org/10.1127/nos/24/1991/59

Buffetaut E, Ingavat R (1980) A new crocodilian from the Jurassic of Thailand, *Sunosuchus thailandicus* n.sp. (Mesosuchia, Goniopholididae), and the palaeogeographical history of South-East Asia in the Mesozoic. Geobios 13(6): 879–889. https://doi.org/10.1016/S0016-6995(80)80042-8

Buffetaut E, Suteethorn V (1992) A New Species of the Ornithischian Dinosaur *Psittacosaurus* from the Early Cretaceous of Thailand. Palaeontology 35: 801–812. [Available from:] https://a1992ke44400004

Buffetaut E, Suteethorn V (1993) The dinosaurs of Thailand. Journal of Southeast Asian Earth Sciences 8(1–4): 77–82. https://doi.org/10.1016/0743-9547(93)90009-E

Buffetaut E, Suteethorn V (1998a) Early Cretaceous dinosaurs from Thailand and their bearing on the early evolution and biogeographical history of some groups of Cretaceous dinosaurs. In: Lucas SG, Kirkland JI, Estep JW (Eds) Lower and Middle Cretaceous Terrestrial Ecosystems. New Mexico Museum of Natural History and Science Bulletin No.14, New Mexico, 2005–2010.

Buffetaut E, Suteethorn V (1998b) The biogeographical significance of the Mesozoic vertebrates from Thailand. Biogeography and Geological Evolution of SE Asia: 83–90.

Buffetaut E, Suteethorn V (2011) A new iguanodontian dinosaur from the Khok Kruat Formation (Early Cretaceous, Aptian) of northeastern Thailand. Annales de Paléontologie 97(1–2): 51–62. https://doi.org/10.1016/j.annpal.2011.08.001

Buffetaut E, Tong H, Suteethorn V, Raksaskulwong L (1994) Jurassic vertebrates from the southern peninsula of Thailand and their implications. A preliminary report. In: The International Symposium on: Stratigraphic Correlation of Southeast Asia. Bangkok, Thailand, 253–256.

Buffetaut E, Suteethorn V, Martin V, Tong H, Chaimanee Y, Triamwichanon S (1995) New dinosaur discoveries in Thailand. Proceedings of the International Conference on Geology, Geotechnology and Mineral Resources of Indochina: 157–161.

Buffetaut E, Suteethorn V, Cuny G, Tong H, Le Loeuff J, Khansubha S, Jongautchariyakul S (2000) The earliest known sauropod dinosaur. Nature 407(6800): 72–74. https://doi.org/10.1038/35024060

Buffetaut E, Suteethorn V, Tong HY (2001) The first thyreophoran dinosaur from Southeast Asia: a stegosaur vertebra from the Late Jurassic Phu Kradung Formation of Thailand. Neues Jahrbuch Fur Geologie Und Palaontologie-Monatshefte: 95–102. https://doi.org/10.1127/njgpm/2001/2001/95

Buffetaut E, Suteethorn V, Le Loeuff J, Cuny G, Tong H, Khansubha S (2002) A review of the sauropod dinosaurs of Thailand. In: The Symposium on Geology of Thailand. Bangkok, Thailand, 95–101. https://www.academia.edu/397937/A_review_of_the_sauropod_dinosaurs_of_Thailand

Buffetaut E, Suteethorn V, Cuny G, Khansubha S, Tong H, Le Loeuff J, Cavin L (2003) Dinosaurs in Thailand. Maha Sarakham University Journal (Special Issue): 69–82.

Buffetaut E, Suteethorn V, Tong H, Košir A (2005a) First dinosaur from the Shan-Thai Block of SE Asia: A Jurassic sauropod from the southern peninsula of Thailand. Journal of the Geological Society 162(3): 481–484. https://doi.org/10.1144/0016-764904-053

Buffetaut E, Suteethorn V, Le Loeuff J, Khansubha S, Tong H, Wongko K (2005b) The Dinosaur Fauna from the Khok Kruat Formation (Early Cretaceous) of Thailand. International Conference on Geology, Geotechnology and Mineral Resources of Indochina (GEOINDO 2005): 575–581.

Buffetaut E, Suteethorn V, Tong H (2006) Dinosaur Assemblages from Thailand: a Comparison with Chinese Faunas. In: Lu JC, Kobayashi Y, Huang D, Lee Y-N (Eds) Papers from the 2005 Heyuan International Dinosaur Symposium. Geological Publishing House, Beijing, 19–37.

Buffetaut E, Suteethorn V, Khansubha S (2007) The ceratopsian dinosaur *Psittacosaurus* in the Early Cretaceous of Southeast Asia: a review of old and recent finds. In: GEOTHAI'07 International Conference on Geology of Thailand: Towards Sustainable Development and Sufficiency Economy, 338–343.

Buffetaut E, Suteethorn S, Suteethorn V, Deesri U, Tong H (2014) Preliminary note on a small ornithopod dinosaur from the Phu Kradung Formation (terminal Jurassic – basal Cretaceous) of Phu Noi, north-eastern Thailand. Journal of Science and Technology Mahasarakham University 33: 344–347.

Buffetaut E, Suteethorn V, Suteethorn S, Tong H (2015) The Ornithischian Dinosaurs of South-East Asia. In: The 2nd International Symposium Asian Dinosaurs in Thailand 2015, 12–13.

Buffetaut E, Vanchan L, Sophady H (2021) First dinosaur bone from Cambodia: a sauropod fibula from the Late Mesozoic of Koh Kong Province. In: Current Studies on Past Biodiversity in Southeast Asia 2021, 11.

Butler RJ, Smith RMH, Norman DB (2007) A primitive ornithischian dinosaur from the Late Triassic of South Africa, and the early evolution and diversification of Ornithischia. Proceedings. Biological Sciences 274(1621): 2041–2046. https://doi.org/10.1098/rspb.2007.0367

Butler RJ, Upchurch P, Norman DB (2008) The phylogeny of the ornithischian dinosaurs. Journal of Systematic Palaeontology 6(1): 1–40. https://doi.org/10.1017/S1477201907002271

Cai JX, Zhang KJ (2009) A new model for the Indochina and South China collision during the Late Permian to the Middle Triassic. Tectonophysics 467(1–4): 35–43. https://doi.org/10.1016/j.tecto.2008.12.003

Campione NE, Evans DC (2011) Cranial growth and variation in edmontosaurs (dinosauria: Hadrosauridae): Implications for latest cretaceous megaherbivore diversity in North America. PLoS ONE 6(9): e25186. https://doi.org/10.1371/journal.pone.0025186

Cappetta H, Buffetaut E, Suteethorn V (1990) A new hybodont shark from the Lower Cretaceous of Thailand. Neues Jahrbuch für Geologie und Paläontologie. Monatshefte 11(11): 659–666. https://doi.org/10.1127/njgpm/1990/1990/659

Carpenter K, Galton PM (2018) A photo documentation of bipedal ornithischian dinosaurs from the Upper Jurassic Morrison Formation, USA. Geology of the Intermountain West 5: 167–207. https://doi.org/10.31711/giw.v5.pp167-207

Cavin L, Deesri U, Veran M, Khentavong B, Jintasakul P, Chanthasit P, Allain R (2019) A new Lepisosteiformes (Actinopterygii: Ginglymodi) from the Early Cretaceous of Laos and Thailand, SE Asia. Journal of Systematic Palaeontology 17(5): 393–407. https://doi.org/10.1080/14772019.2018.1426060

Chanthasit P, Ditbanjong P, Munjai D, Varavudh S (2018) Study on reddish terrestrial sedimentary rocks in the Mesozoic Era from Chiang Muan District, Phayao Province of Thailand: Sedimentology, lithostratigraphy, and fossils. Kalasin, Thailand.

Chanthasit P, Suteethorn S, Manitkoon S, Nonsrirach T, Suteethorn V (2019) Biodiversity of the Late Jurassic/Early Cretaceous Phu Noi, Phu Kradung Formation, Kalasin, Thailand. In: Advancing Paleontological Research and Specimen Conservation in Southeast Asia, The International Symposium and Workshop, 14–16.

Chokchaloemwong D, Hattori S, Cuesta E, Jintasakul P, Shibata M, Azuma Y (2019) A new carcharodontosaurian theropod (Dinosauria: Saurischia) from the Lower Cretaceous of Thailand. PLoS ONE 14(10): 1–43. https://doi.org/10.1371/journal.pone.0222489

Choong C, Pubellier M, Sautter B, Gebretsadik HT (2022) Records of the oceanic propagator closure at the southern splay of the Palaeo-Tethys. Geological Journal 57(9): 1–35. https://doi.org/10.1002/gj.4520

Cuny G (2012) Freshwater hybodont sharks in Early Cretaceous ecosystems: A review. In: Godefroit P (Ed.) Bernissart Dinosaurs and Early Cretaceous Terrestrial Ecosystems. Indiania University Press, Bloomington, 518–529.

Cuny G, Srisuk P, Khamha S, Suteethorn V, Tong H (2009) A new elasmobranch fauna from the Middle Jurassic of southern Thailand. Geological Society Special Publication 315: 97–113. https://doi.org/10.1144/SP315.8

Cuny G, Liard R, Deesri U, Liard T, Khamha S, Suteethorn V (2014) Shark faunas from the Late Jurassic-Early Cretaceous of northeastern Thailand. Palaontologische Zeitschrift 88(3): 309–328. https://doi.org/10.1007/s12542-013-0206-0

Cuny G, Mo J, Amiot R, Buffetaut E, Suteethorn S, Suteethorn V, Tong H (2017) New data on Cretaceous freshwater hybodont sharks from Guangxi Province, South China. Research & Knowledge 3: 11–15.

Department of Mineral Resources (2014) Mesozoic era. In: Strokes RB, Raksaskulwong M (Eds) Geology of Thailand. Bureau of Geological Suevey Department of Mineral Resources, Bangkok, Thailand, 113–157.

Dieudonné PE, Cruzado-Caballero P, Godefroit P, Tortosa T (2020) A new phylogeny of cerapodan dinosaurs. Historical Biology 33(10): 2335–2355. https://doi.org/10.1080/08912963.2020.1793979

Dong Z (1979) Dinosaurs from the Cretaceous of South China. In: Cheng J, Qu Z (Eds) Mesozoic and Cenozoic Red Beds of South China. Science Press, Beijing, China, 342–350.

Dong Z (1993) An ankylosaur (ornithischian dinosaur) from the Middle Jurassic of the Junggar Basin, China. Vertebrata Palasiatica 10: 257–266. http://www.ivpp.cas.cn/cbw/gjzdwxb/xbwzxz/200812/W020090813370614393532.pdf

Dong Z-M, Zhou S, Zhang Y (1983) Dinosaurs from the Jurassic of Sichuan. Palaeontologica Sinica 162: 1–136.

Fanti F, Cau A, Panzarin L, Cantelli L (2016) Evidence of iguanodontian dinosaurs from the Lower Cretaceous of Tunisia. Cretaceous Research 60: 267–274. https://doi.org/10.1016/j.cretres.2015.12.008

Galton PM (2009) Notes on Neocomian (Lower Cretaceous) ornithopod dinosaurs from England - *Hypsilophodon*, *Valdosaurus*, "*Camptosaurus*", "*Iguanodon*" - and referred specimens from Romania and elsewhere. Genève 28: 211–273.

Gates TA, Tsogtbaatar K, Zanno LE, Chinzorig T, Watabe M (2018) A new iguanodontian (Dinosauria: Ornithopoda) from the Early Cretaceous of Mongolia. PeerJ 6: e5300. https://doi.org/10.7717/peerj.5300

Godefroit P, Li H, Shang CY (2005) A new primitive hadrosauroid dinosaur from the Early Cretaceous of Inner Mongolia (P.R. China). Comptes Rendus. Palévol 4(8): 697–705. https://doi.org/10.1016/j.crpv.2005.07.004

Godefroit P, Lauters P, Van Itterbeck J, Bolotsky YL, Dong Z, Jin L, Wu W, Bolotsky IY, Hai S, Yu T (2011) Recent advances on study of hadrosaurid dinosaurs in Heilongjiang (Amur) River area between China and Russia. Giornale di Geologia 14: 160–191.

Godefroit P, Sinitsa SM, Dhouailly D, Bolotsky YL, Sizov AV, McNamara ME, Benton MJ, Spagna P (2014) A Jurassic ornithischian dinosaur from Siberia with both feathers and scales. Science 345(6195): 451–455. https://doi.org/10.1126/science.1253351

Grote PJ, Boonchai N, Jintasakul P (2009) Paleontological parks and museums and prominent fossil sites in Thailand and their importance in the conservation of fossils. In: Lipps JH, Granier BRC (Eds) PaleoParks - The protection and conservation of fossil sites worldwide. Carnets de Géologie / Notebooks on Geology, 75–95.

Han F-L, Barrett PM, Butler RJ, Xu X (2012) Postcranial anatomy of *Jeholosaurus shangyuanensis* (Dinosauria, Ornithischia) from the Lower Cretaceous Yixian Formation of China. Journal of Vertebrate Paleontology 32(6): 1370–1395. https://doi.org/10.1080/02724634.2012.694385

He X, Cai K (1984) The Middle Jurassic Dinosaurian Fauna from Dashanpu, Zigong, Sichuan Vol. I The Ornithopod Dinosaurs. Sichuan Scientific and Technological Publishing House I: 1–66.

Hoffet JH (1944) Description des ossements les plus caractéristiques appartenant à des Avipelviens du Sénonien du Bas-Laos [Description of the most characteristic bones belonging to bird-hipped dinosaurs from the Senonian of Lower Laos]. Comptes Rendus des Séances du Conseil des Recherches Scientifiques de l'Indochine.

Horner JR, Weishampel BD, Forster CA (2004) Hadrosauridae. In: Weishampel DB, Dodson P, Osmólska H (Eds) The Dinosauria. University of California Press, 438–463. https://doi.org/10.1525/california/9780520242098.003.0023

Hübner TR, Rauhut OWM (2010) A juvenile skull of *Dysalotosaurus lettowvorbecki* (Ornithischia: Iguanodontia), and implications for cranial ontogeny, phylogeny, and taxonomy in ornithopod dinosaurs. Zoological Journal of the Linnean Society 160(2): 366–396. https://doi.org/10.1111/j.1096-3642.2010.00620.x

Huh M, Lee DG, Kim JK, Lim JD, Godefroit P (2011) A new basal ornithopod dinosaur from the Upper Cretaceous of South Korea. Neues Jahrbuch für Geologie und Paläontologie. Abhandlungen 259(1): 1–24. https://doi.org/10.1127/0077-7749/2010/0102

Ji SA, Zhang P (2022) First new genus and species of Basal Iguanodontian Dinosaur (Ornithischia: Ornithopoda) from Southern China. Acta Geoscientica Sinica 43: 1–10. https://doi.org/10.3975/cagsb.2021.090701

Kirkland JI, Simpson EL, Blieux DDDE, Madsen SK, Bogner E, Tibert NE (2016) Depositional Constraints on the Lower Cretaceous Stikes Quarry Dinosaur Site: Upper Yellow Cat Member, Cedar Mountain Formation, Utah. Palaios 31(9): 421–439. https://doi.org/10.2110/palo.2016.041

Klug S, Tütken T, Wings O, Pfretzschner HU, Martin T (2010) A Late Jurassic freshwater shark assemblage (Chondrichthyes, Hybodontiformes) from the southern Junggar Basin, Xinjiang, Northwest China. Palaeobiodiversity and Palaeoenvironments 90(3): 241–257. https://doi.org/10.1007/s12549-010-0032-2

Kobayashi Y, Takasaki R, Kubota K, Fiorillo AR (2021) A new basal hadrosaurid (Dinosauria: Ornithischia) from the latest Cretaceous Kita - ama Formation in Japan implies the origin of hadrosaurids. Scientific Reports 11(1): 1–15. https://doi.org/10.1038/s41598-021-87719-5

Kozu S (2017) Dinosaur Footprints from the Khorat Group, Northeastern Thailand. University of Tsukuba. http://doi.org/10.15068/00150050

Kozu S, Sardsud A, Saesaengseerung D, Pothichaiya C, Agematsu S, Sashida K (2017) Dinosaur footprint assemblage from the Lower Cretaceous Khok Kruat Formation, Khorat Group, northeastern Thailand. Geoscience Frontiers 8(6): 1479–1493. https://doi.org/10.1016/j.gsf.2017.02.003

Laojumpon C, Suteethorn V, Chanthasit P, Lauprasert K, Suteethorn S (2017) New evidence of sauropod dinosaurs from the Early Jurassic Period of Thailand. Acta Geologica Sinica 91(4): 1169–1178. https://doi.org/10.1111/1755-6724.13352

Lauprasert K, Laojumpon C, Saenphala W, Cuny G, Thirakhupt K, Suteethorn V (2011) Atoposaurid crocodyliforms from the Khorat Group of Thailand: First record of *Theriosuchus* from Southeast Asia. Palaontologische Zeitschrift 85(1): 37–47. https://doi.org/10.1007/s12542-010-0071-z

Le Loeuff J, Khansubha S, Buffetaut E, Suteethorn V, Tong H, Souillat C (2002) Dinosaur footprints from the Phra Wihan Formation (Early Cretaceous of Thailand). Comptes Rendus. Palévol 1(5): 287–292. https://doi.org/10.1016/S1631-0683(02)00037-4

Le Loeuff J, Saenyamoon T, Souillat C, Suteethorn V, Buffetaut E (2009) Mesozoic vertebrate footprints of Thailand and Laos. Geological Society Special Publication 315: 245–254. https://doi.org/10.1144/SP315.17

Liard T, Liard R, Le Loeuff J (2015) The Vertebrate Footprints from Ban Non Toom, Nong Bua Daeng District, Chaiyaphum Province, Thailand. In: The 2nd International Symposium on Asian Dinosaurs in Thailand. Bangkok, Thailand, 59.

Lockley MG, McCrea RT, Matsukawa M (2009) Ichnological evidence for small quadrupedal ornithischians from the basal Cretaceous of SE Asia and North America: Implications for a global radiation. Geological Society of London, Special Publications 315(1): 255–269. https://doi.org/10.1144/SP315.18

Lucas SG (2006) The *Psittacosaurus biochron*, Early Cretaceous of Asia. Cretaceous Research 27(2): 189–198. https://doi.org/10.1016/j.cretres.2005.11.011

Madzia D, Boyd CA, Mazuch M (2018) A basal ornithopod dinosaur from the Cenomanian of the Czech Republic. Journal of Systematic Palaeontology 16(11): 1–13. https://doi.org/10.1080/14772019.2017.1371258

Madzia D, Jagt JWM, Mulder EWA (2020) Osteology, phylogenetic affinities and taxonomic status of the enigmatic late Maastrichtian ornithopod taxon *Orthomerus dolloi* (Dinosauria, Ornithischia). Cretaceous Research 108: 104334. https://doi.org/10.1016/j.cretres.2019.104334

Madzia D, Arbour VM, Boyd CA, Farke AA, Cruzado-Caballero P, Evans DC (2021) The phylogenetic nomenclature of ornithischian dinosaurs. PeerJ 9: e12362. https://doi.org/10.7717/peerj.12362

Maidment SCR, Norman DB, Barrett PM, Upchurch P (2008) Systematics and phylogeny of Stegosauria (Dinosauria: Ornithischia). Journal of Systematic Palaeontology 6(4): 367–407. https://doi.org/10.1017/S1477201908002459

Makovicky PJ, Kilbourne BM, Sadleir RW, Norell MA, Makovicky PJ, Kilbourne BM, Sadleir RW, Norell MA (2011) A new basal ornithopod (Dinosauria, Ornithischia) from the Late Cretaceous of Mongolia. Journal of Vertebrate Paleontology 31(3): 626–640. https://doi.org/10.1080/02724634.2011.557114

Manitkoon S, Deesri U (2019) Evolutionary Stages of Ornithischian Dinosaurs in the Khorat Group of Thailand. In: The 1st Asian Palaeontological Congress. Beijing, China, 82.

Manitkoon S, Suteethorn S, Deesri U, Suteethorn V (2019) An Articulated Skeleton of the Neornithischian Dinosaur from the Late Jurassic – Early Cretaceous, Phu Kradung Formation of Thailand. In: The 4th International Symposium on Asian Dinosaur. Ulaanbaatar, Mongolia, 34.

Manitkoon S, Deesri U, Lauprasert K, Warapeang P, Nonsrirach T, Nilpanapan A, Wongko K, Chanthasit P (2022) Fossil assemblage from the Khok Pha Suam locality of northeastern, Thailand: An overview of vertebrate diversity from the Early Cretaceous Khok Kruat Formation (Aptian-Albian). Fossil Record (Weinheim) 25(1): 83–98. https://doi.org/10.3897/fr.25.83081

Mannion PD, Upchurch P, Schwarz D, Wings O (2019) Taxonomic affinities of the putative titanosaurs from the Late Jurassic Tendaguru Formation of Tanzania: Phylogenetic and biogeographic implications for eusauropod dinosaur evolution. Zoological Journal of the Linnean Society 185(3): 784–909. https://doi.org/10.1093/zoolinnean/zly068

Martin JE, Lauprasert K, Buffetaut E, Liard R, Suteethorn V (2014) A large pholidosaurid in the Phu Kradung Formation of north-eastern Thailand. Palaeontology 57(4): 757–769. https://doi.org/10.1111/pala.12086

Martin JE, Suteethorn S, Lauprasert K, Tong H, Buffetaut E, Liard R, Salaviale C, Deesri U, Claude J, Martin JE, Suteethorn S, Lauprasert K, Tong H, Buffetaut E, Liard R, Salaviale C, Deesri U, Suteethorn V, Suteethorn V, Claude J (2019) A new freshwater teleosaurid from the Jurassic of northeastern Thailand. Journal of Vertebrate Paleontology 38: 1–28. https://doi.org/10.1080/02724634.2018.1549059

Mateus O, Maidment SCR, Christiansen NA (2009) A new long-necked "sauropod-mimic" stegosaur and the evolution of the plated dinosaurs. Proceedings. Biological Sciences 276(1663): 1815–1821. https://doi.org/10.1098/rspb.2008.1909

Meesook A (2000) Cretaceous environments of North- eastern Thailand. In: Okada H, Mateer NJ (Eds) Cretaceous Environments of Asia. Elsevier, Amsterdam, 207–223. https://doi.org/10.1016/S0920-5446(00)80023-0

Metcalfe I (1998) Palaeozoic and Mesozoic geological evolution of the SE Asian region: multidisciplinary constraints and implications for biogeography. Biogeography and Geological Evolution of SE Asia: 25–41. https://doi.org/10.1186/1475-2891-11-45

Mo J, Buffetaut E, Tong H, Amiot R, Cavin L, Cuny G, Suteethorn V, Suteethorn S, Jiang S (2016) Early Cretaceous vertebrates from the Xinlong Formation of Guangxi (southern China): A review.

Geological Magazine 153(1): 143–159. https://doi.org/10.1017/S0016756815000394

Müller RT, Pretto FA, Kerber L, Silva-Neves E, Dias-da-Silva S (2018) Comment on 'A dinosaur missing-link? *Chilesaurus* and the early evolution of ornithischian dinosaurs.'. Biology Letters 14(3): 20170581. https://doi.org/10.1098/rsbl.2017.0581

Napoli JG, Hunt T, Erickson GM, Norell MA, Norell MA (2019) *Psittacosaurus amitabha*, a New Species of Ceratopsian Dinosaur from the Ondai Sayr Locality, Central Mongolia. American Museum Novitates 2019(3932): 1–36. https://doi.org/10.1206/3932.1

Nonsrirach T, Manitkoon S, Lauprasert K (2021) First occurrence of brachyopid temnospondyls in Southeast Asia and review of the Mesozoic amphibians from Thailand. Fossil Record (Weinheim) 24(1): 33–47. https://doi.org/10.5194/fr-24-33-2021

Norman DB (1998) On Asian ornithopods (Dinosauria: Ornithischia). 3. A new species of iguanodontid dinosaur. Zoological Journal of the Linnean Society 122(1–2): 291–348. https://doi.org/10.1111/j.1096-3642.1998.tb02533.x

Norman DB (2004) Basal Iguanodontia. In: The Dinosauria. University of California Press, 413–437. https://doi.org/10.1525/california/9780520242098.003.0022

Norman DB (2010) A taxonomy of iguanodontians (Dinosauria: Ornithopoda) from the lower Wealden Group (Cretaceous: Valanginian) of southern England. Zootaxa 2489(1): 47–66. https://doi.org/10.11646/zootaxa.2489.1.3

Norman DB (2014) On the history, osteology, and systematic position of the Wealden (Hastings group) dinosaur *Hypselospinus fittoni* (Iguanodontia: Styracosterna). Zoological Journal of the Linnean Society 173(1): 92–189. https://doi.org/10.1111/zoj.12193

Norman DB, Butler RJ, Maidment SCR (2007) Reconsidering the status and affinities of the ornithischian dinosaur *Tatisaurus oehleri* Simmons, 1965. Zoological Journal of the Linnean Society 150(4): 865–874. https://doi.org/10.1111/j.1096-3642.2007.00301.x

Park JY, Lee YN, Currie PJ, Ryan MJ, Bell P, Sissons R, Koppelhus EB, Barsbold R, Lee S, Kim SH (2021) A new ankylosaurid skeleton from the Upper Cretaceous Baruungoyot Formation of Mongolia: Its implications for ankylosaurid postcranial evolution. Scientific Reports 11: 1–10. https://doi.org/10.1038/s41598-021-02273-4

Peng G (1992) Jurassic Ornithopod *Agilisaurus louderbacki* (Ornithopoda: Fabrosauridae) from Zigong, Sichuan, China. Vertebrata PalAsiatica 30: 39–51.

Prieto-Marquez A, Guenther MF (2018) Perinatal specimens of *Maiasaura* from the Upper Cretaceous of Montana (USA): Insights into the early ontogeny of saurolophine hadrosaurid dinosaurs. PeerJ 6: e4734. https://doi.org/10.7717/peerj.4734

Prieto-Márquez A, Erickson GM, Ebersole JA (2016) Anatomy and Osteohistology of the basal hadrosaurid dinosaur *Eotrachodon* from the uppermost Santonian (Cretaceous) of southern appalachia. PeerJ 4: e1872. https://doi.org/10.7717/peerj.1872

Racey A (2009) Mesozoic red bed sequences from SE Asia and the significance of the Khorat Group of NE Thailand. Geological Society of London, Special Publications 315(1): 41–67. https://doi.org/10.1144/SP315.5

Racey A, Goodall JGS (2009) Palynology and stratigraphy of the Mesozoic Khorat Group red bed sequences from Thailand. Geological Society of London, Special Publications 315(1): 69–83. https://doi.org/10.1144/SP315.6

Racey A, Love MA, Canham AC, Goodall JGS, Polachan S, Jones PD (1996) Stratigraphy and reservoir potential of the Mesozoic Khorat group, NE Thailand Part 1: Stratigraphy and Sedimentary Evolution. Journal of Petroleum Geology 19(1): 5–40. https://doi.org/10.1111/j.1747-5457.1996.tb00511.x

Rahman MNBA (2019) Jurassic-Cretaceous Stratigraphy of Malaysia. Open Journal of Geology 09(10): 668–670. https://doi.org/10.4236/ojg.2019.910070

Rees J, Underwood CJ (2006) Hybodont sharks from the Middle Jurassic of the Inner Hebrides, Scotland. Transactions of the Royal Society of Edinburgh. Earth Sciences 96(4): 351–363. https://doi.org/10.1017/S0263593300001346

Ren XX, Sekiya T, Wang T, Yang ZW, You HL (2021) A revision of the referred specimen of *Chuanjiesaurus anaensis* Fang et al., 2000: A new early branching mamenchisaurid sauropod from the Middle Jurassic of China. Historical Biology 33(9): 1872–1887. https://doi.org/10.1080/08912963.2020.1747450

Riabinin AN (1925) A mounted skeleton of the gigantic reptile *Trachodon amurense* nov. sp. Izvestija Geologicheskogo Komiteta 44: 1–12.

Rolando AMA, Motta MJ, Agnolín FL, Manabe M, Tsuihiji T, Novas FE (2022) A large Megaraptoridae (Theropoda: Coelurosauria) from Upper Cretaceous (Maastrichtian) of Patagonia, Argentina. Scientific Reports 12: 1–29. https://doi.org/10.1038/s41598-022-09272-z

Rozhdestvenskiy AK (1967) New iguanodonts from central Asia. International Geology Review 9(4): 556–566. https://doi.org/10.1080/00206816709474485

Russell DA (1993) The role of Central Asia in dinosaurian biogeography. Canadian Journal of Earth Sciences 30(10): 2002–2012. https://doi.org/10.1139/e93-176

Samathi A, Suteethorn S (2022) New materials of iguanodontians (Dinosauria: Ornithopoda) from the Lower Cretaceous Khok Kruat Formation, Ubon Ratchathani, Thailand. Zootaxa 5094(2): 301–320. https://doi.org/10.11646/zootaxa.5094.2.5

Samathi A, Chanthasit P, Sander PM (2019a) A review of theropod dinosaurs from the Late Jurassic to mid-Cretaceous of Southeast Asia. Annales de Paléontologie 105(3): 1–15. https://doi.org/10.1016/j.annpal.2019.03.003

Samathi A, Chanthasit P, Sander PM (2019b) Two new basal coelurosaurian theropod dinosaurs from the Lower Cretaceous Sao Khua Formation of Thailand. Acta Palaeontologica Polonica 64: 239–260. https://doi.org/10.4202/app.00540.2018

Sereno PC (2000) The fossil record, systematics and evolution of pachycephalosaurs and ceratopsians from Asia. In: The Age of Dinosaurs in Russia and Mongolia. Cambridge University Press, 489–492.

Sereno PC (2012) Taxonomy, morphology, masticatory function and phylogeny of heterodontosaurid dinosaurs. ZooKeys 226: 1–225. https://doi.org/10.3897/zookeys.226.2840

Sereno PC, Shichin C (1988) *Psittacosaurus xinjiangensis* (Ornithischia: Ceratopsia), a New Psittacosaur from the Lower Cretaceous of Northwestern China. Journal of Vertebrate Paleontology 8(4): 353–365. https://doi.org/10.1080/02724634.1988.10011724

Shibata M, Azuma Y (2015) New basal hadrosauroid (Dinosauria: Ornithopoda) from the Lower Cretaceous Kitadani Formation, Fukui, central Japan. Zootaxa 3914(4): 421–440. https://doi.org/10.11646/zootaxa.3914.4.3

Shibata M, Jintasakul P, Azuma Y (2011) A new Iguanodontian dinosaur from the Lower Cretaceous Khok Kruat Formation, Nakhon

Ratchasima in Northeastern Thailand. Acta Geologica Sinica - English Edition 85(5): 969–976. https://doi.org/10.1111/j.1755-6724.2011.00530.x

Shibata M, Jintasakul P, Azuma Y, You H-L (2015) A New Basal Hadrosauroid Dinosaur from the Lower Cretaceous Khok Kruat Formation in Nakhon Ratchasima Province, Northeastern Thailand. PLoS ONE 10(12): e0145904. https://doi.org/10.1371/journal.pone.0145904

Shibata M, Jintasakul P, Azuma Y, Chokchaloemwong D, Kawabe S (2018) All about *Sirindhorna khoratensis* (Ornithopoda; Hadrosauroidea). In: Te 6th International Symposium of International Geoscience Programme IGCP Project 608, 4–5.

Sone M, Metcalfe I (2008) Parallel Tethyan sutures in mainland Southeast Asia: New insights for Palaeo-Tethys closure and implications for the Indosinian orogeny. Comptes Rendus Geoscience 340(2–3): 166–179. https://doi.org/10.1016/j.crte.2007.09.008

Sone M, Hirayama R, He YH, Yoshida M, Komatsu T (2015) First Dinosaur Fossils from Malaysia: Spinoaurid and Ornithischian Teeth. In: The 2nd International Symposium Asian Dinosaurs in Thailand 2015, 18.

Sone M, Cuny G, Hirayama R, Kocsis L, Buffetaut E, Deesri U (2022) New vertebrate fossils from the Cretaceous dinosaur-bearing deposit of Malaysia. In: The 6th International Palaeontological Congress. Khon Kaen, Thailand, 186.

Sriwisan A, Thasod Y, Manitkoon S, Warapeang P (2022) Preliminary study on a paravian-like ungual from the Early Cretaceous Sao Khua Formation of Thailand. In: The 6th International Palaeontological Congress. Khon Kaen, Thailand, 203.

Strickson E, Prieto-Márquez A, Benton MJ, Stubbs TL (2016) Dynamics of dental evolution in ornithopod dinosaurs. Scientific Reports 6(1): 28904. https://doi.org/10.1038/srep28904

Sullivan RM (2006) A taxonomic review of the Pachycephalosauridae (Dinosauria: Ornithischia). New Mexico Museum of Natural History and Science Bulletin: 347–365. http://0-apps.webofknowledge.com.cisne.sim.ucm.es/full_record.do?product=UA&search_mode=GeneralSearch&qid=21&SID=R2H4i6lD2cJGE66Kd6E&page=1&doc=1

Suteethorn S, Le Loeuff J, Buffetaut E, Suteethorn V, Wongko K (2013) First evidence of a mamenchisaurid dinosaur from the Late Jurassic/Early Cretaceous Phu Kradung Formation of Thailand. Acta Palaeontologica Polonica 58: 459–469. https://doi.org/10.4202/app.2009.0155

Takasaki R, Fiorillo AR, Tykoski RS, Kobayashi Y (2020) Re-examination of the cranial osteology of the Arctic Alaskan hadrosaurine with implications for its taxonomic status. PLoS ONE 15(5): e0232410. https://doi.org/10.1371/journal.pone.0232410

Teng YH, Sone M, Hirayama R, Yoshida M, Komatsu T, Khamha S, Cuny G (2019) First Cretaceous fish fauna from Malaysia. Journal of Vertebrate Paleontology 39(1): 1–14. https://doi.org/10.1080/02724634.2019.1573735

Thanh T-D, Khuc V (2006) Stratigraphic Units of Vietnam. Vietnam National University Publishing House, Hanoi, Vietnam, 526.

Tong H, Claude J, Naksri W, Suteethorn V, Buffetaut E, Khansubha S, Wongko K, Yuangdetkla P (2009) *Basilochelys macrobios* n. gen. and n. sp., a large cryptodiran turtle from the Phu Kradung Formation (later Jurassic-earliest Cretaceous) of the Khorat Plateau, NE Thailand. Geological Society Special Publication 315: 153–173. https://doi.org/10.1144/SP315.12

Tong H, Naksri W, Buffetaut E, Suteethorn V, Suteethorn S, Deesri U, Sila S, Chanthasit P, Claude J (2015) A new primitive eucryptodiran turtle from the Upper Jurassic Phu Kradung Formation of the Khorat Plateau, NE Thailand. Geological Magazine 152(1): 166–175. https://doi.org/10.1017/S0016756814000223

Tong H, Buffetaut E, Suteethorn V, Suteethorn S, Cuny G, Cavin L, Deesri U, Martin JE, Wongko K, Naksri W, Claude J (2019a) Phu Din Daeng, a new Early Cretaceous vertebrate locality on the Khorat Plateau, NE Thailand. Annales de Paléontologie 105(3): 223–237. https://doi.org/10.1016/j.annpal.2019.04.004

Tong H, Naksri W, Buffetaut E, Suteethorn S, Suteethorn V, Chanthasit P, Claude J (2019b) *Kalasinemys*, a new xinjiangchelyid turtle from the Late Jurassic of NE Thailand. Geological Magazine 156(10): 1–12. https://doi.org/10.1017/S0016756818000791

Tsogtbaatar K, Weishampel DB, Evans DC, Watabe M (2019) A new hadrosauroid (Dinosauria: Ornithopoda) from the Late Cretaceous Baynshire Formation of the Gobi Desert (Mongolia). PLoS ONE 14(4): 1–47. https://doi.org/10.1371/journal.pone.0208480

Tucker RT, Hyland EG, Gates TA, King MR, Roberts EM, Foley EK, Berndt D, Hanta R, Khansubha S, Aswasereelert W, Zanno LE (2022) Age, depositional history, and paleoclimatic setting of Early Cretaceous dinosaur assemblages from the Sao Khua Formation (Khorat Group), Thailand. Palaeogeography, Palaeoclimatology, Palaeoecology 601: 111107. https://doi.org/10.1016/j.palaeo.2022.111107

Tumanova TA, Alifanov VR (2018) First Record of Stegosaur (Ornithischia, Dinosauria) from the Aptian–Albian of Mongolia. Paleontological Journal 52(14): 1771–1779. https://doi.org/10.1134/S0031030118140186

Tumpeesuwan S, Sato Y, Nakhapadungrat S (2010) A new species of *Pseudohyria* (*Matsumotoina*) (Bivalvia: Trigonioidoidea) from the Early Cretaceous Sao Khua Formation, Khorat Group, Northeastern Thailand. Tropical Natural History 10: 93–106.

Uchida E, Mizoguchi A, Sato H, Shimoda I, Watanabe R (2017) Determining the construction sequence of the Preah Vihear monument in Cambodia from its sandstone block characteristics. Heritage Science 5(1): 1–15. https://doi.org/10.1186/s40494-017-0155-0

University of Malaya (2014) First herbivorous ornithischian dinosaur fossil from Malaysia. ScienceDaily. www.sciencedaily.com/releases/2014/11/141121121137.htm

Wang J, Norell MA, Pei R, Ye Y, Chang SC (2019) Surprisingly young age for the mamenchisaurid sauropods in South China. Cretaceous Research 104: 104176. https://doi.org/10.1016/j.cretres.2019.07.006

Weishampel DB, Jianu C, Csiki Z, Norman DB (2003) Osteology and phylogeny of *Zalmoxes* (n. g.), an unusual Euornithopod dinosaur from the latest Cretaceous of Romania. Journal of Systematic Palaeontology 1(2): 65–123. https://doi.org/10.1017/S1477201903001032

Weishampel DB, Barrett PM, Coria RA, Le Loeuff J, Xing X, Xijin Z, Sahni A, Gomani EMP, Noto CR (2004) Dinosaur Distribution. In: The Dinosauria. University of California Press, 517–606. https://doi.org/10.1525/california/9780520242098.003.0027

Wongko K (2018) Spinosaurid Diversity and Depositional Environment of the Khok Kruat Fomation from Northeastern Thailand. Mahasarakham University.

Xing L, Miyashita T, Zhang J, Li D, Ye Y, Sekiya T, Wang F, Currie PJ (2015) A new sauropod dinosaur from the late Jurassic of China and the diversity, distribution, and relationships of mamenchisaurids. Journal of Vertebrate Paleontology 35(1): 37–41. https://doi.org/10.1080/02724634.2014.889701

Xing L, McKellar RC, Xu X, Li G, Bai M, Persons WS IV, Miyashita T, Benton MJ, Zhang J, Wolfe AP, Yi Q, Tseng K, Ran H, Currie PJ (2016) A Feathered Dinosaur Tail with Primitive Plumage Trapped

in Mid-Cretaceous Amber. Current Biology 26(24): 3352–3360. https://doi.org/10.1016/j.cub.2016.10.008

Xu X, Wang KB, Zhao XJ, Li DJ (2010) First ceratopsid dinosaur from China and its biogeographical implications. Chinese Science Bulletin 55(16): 1631–1635. https://doi.org/10.1007/s11434-009-3614-5

Xu X, Tan Q, Gao Y, Bao Z, Yin Z, Guo B, Wang J, Tan L, Zhang Y, Xing H (2018) A large-sized basal ankylopollexian from East Asia, shedding light on early biogeographic history of Iguanodontia. Science Bulletin 63(9): 556–563. https://doi.org/10.1016/j.scib.2018.03.016

Yan L, Peng H, Zhang S, Zhang R, Kašanin-Grubin M, Lin K, Tu X (2019) The spatial patterns of red beds and Danxia Landforms: Implication for the formation factors–China. Scientific Reports 9(1): 1–10. https://doi.org/10.1038/s41598-018-37238-7

Yao X, Barrett PM, Yang L, Xu X, Bi S (2022) A new early branching armored dinosaur from the Lower Jurassic of southwestern China. eLife 11: 1–43. https://doi.org/10.7554/eLife.75248

You H, Dodson P (2004) Basal Ceratopsia. In: Weishampel DB, Osmolska H, Dodson P (Eds) The Dinosauria. University of California Press, Berkeley, 478–493. https://doi.org/10.1525/california/9780520242098.003.0025

You HL, Li DQ (2009) A new basal hadrosauriform dinosaur (Ornithischia: Iguanodontia) from the Early Cretaceous of northwestern China. Canadian Journal of Earth Sciences 46(12): 949–957. https://doi.org/10.1139/E09-067

You HL, Luo ZX, Shubin NH, Witmer LM, Tang ZL, Tang F (2003) The earliest-known duck-billed dinosaur from deposits of late Early Cretaceous age in northwest China and hadrosaur evolution. Cretaceous Research 24(3): 347–355. https://doi.org/10.1016/S0195-6671(03)00048-X

You HL, Ji Q, Li D (2005) *Lanzhousaurus magnidens* gen. et sp. nov. from Gansu Province, China: the largest-toothed herbivorous dinosaur in the world. Geological Bulletin of China 24: 785–794. http://www.chinasciencejournal.com/index.php/DZTB/article/view/248914

You HL, Li DQ, Dodson P (2014) *Gongpoquansaurus mazongshanensis* (Lü, 1997) comb. Nov. (ornithischia: Hadrosauroidea) from the early Cretaceous of Gansu Province, northwestern China. In: Eberth DA, Evans DC (Eds) Hadrosaurs. Indiana University Press, 73–76.

Zhao X, Cheng Z, Xu X (1999) The Earliest Ceratopsian from the Tuchengzi Formation of Liaoning, China. Journal of Vertebrate Paleontology 19(4): 681–691. https://doi.org/10.1080/02724634.1999.10011181

Zheng X-T, You H-L, Xu X, Dong Z-M (2009) An Early Cretaceous heterodontosaurid dinosaur with filamentous integumentary structures. Nature 458(7236): 333–336. https://doi.org/10.1038/nature07856

Fossil Record 26 (1) 2023, 27–38 | DOI 10.3897/fr.@.86784

A new remarkable cimicoid genus and species (Hemiptera, Heteroptera, Cimicomorpha) from mid-Cretaceous Burmese amber, with implications for its aberrant male genitalia

Kazutaka Yamada[1,2], Shûhei Yamamoto[3], Yui Takahashi[4]

1 *Institute of Natural and Environmental Sciences, University of Hyogo, Yayoigaoka 6-chome, Sanda-shi, Hyogo 669-1546, Japan*
2 *Museum of Nature and Human Activities, Hyogo, Yayoigaoka 6-chome, Sanda-shi, Hyogo 669-1546, Japan*
3 *The Hokkaido University Museum, Hokkaido University, Kita 10, Nishi 8, Kita-ku, Sapporo 060-0810, Japan*
4 *Keio Yochisha Elementary School, Ebisu 2-35-1, Shibuya, Tokyo 150-0013, Japan*

https://zoobank.org/6A3587A7-9E57-40AC-B9FD-753EDDBA73C5

Corresponding author: Kazutaka Yamada (yamada.kaz@gmail.com)

Academic editor: Carolin Haug ♦ **Received** 21 May 2022 ♦ **Accepted** 21 December 2022 ♦ **Published** 13 January 2023

Abstract

A new genus and species of cimicoid true bug, *Ecpaglocoris ditomeus* Yamada & Yamamoto, **gen. et sp. nov.**, is described and illustrated from mid-Cretaceous (Cenomanian–Albian) amber in the Kachin State of northern Myanmar (Burma). This new fossil genus and species is reminiscent of members of Anthocoridae by the strongly flattened and elongated body, four-segmented labium, distinct costal fracture and presence of fossula spongiosa on fore tibiae, but should not be ascribed to this family. The new taxon cannot be placed in any extant cimicoid families, based upon hemelytral, male genital and other morphological structures. Based on the hemelytral membrane venation and presence of dorsal laterotergites on abdominal segments I to VIII, it can be assumed that this new genus belongs to the extinct family Vetanthocoridae. *Ecpaglocoris ditomeus* **gen. et sp. nov.** has aberrant male genitalia characterised by sickle-shaped left and right parameres and grooves running throughout the paramere. This characteristic indicates that traumatic insemination occurred in this genus. The peculiar combination of male genital characteristics seen in *Ecpaglocoris* **gen. nov.** prevents its placement in any of the extant cimicoid families.

Key Words

Cenomanian, Cimicoidea, male genital morphology, Myanmar, traumatic insemination, Vetanthocoridae

Introduction

Cimicoidea, a morphologically and ecologically diverse group in the suborder Heteroptera, is currently represented by seven extant families based on the concepts of Ford (1979), Schuh and Štys (1991), Schuh et al. (2009), Weirauch et al. (2019) and Schuh and Weirauch (2020): Anthocoridae Fieber, 1836; Cimicidae Latreille, 1802; Curaliidae Schuh, Weirauch & Henry, 2008; Lasiochilidae Carayon, 1972; Lyctocoridae Reuter, 1884; Plokiophilidae China, 1953; and Polyctenidae Westwood, 1874. In addition, the extinct family Vetanthocoridae Yao, Cai & Ren, 2006 is treated as a member of this superfamily (Tang et al. 2016; Schuh and Weirauch 2020). Popov (2016) established a monotypic fossil family Taimyrocoridae to accommodate the new species *Taimyrocoris sukatshevae*, based on specimens from Late Cretaceous amber of the Taimyr Peninsula in Far North Russia and classified the taxon as belonging to Cimicoidea. However, this family has been overlooked by subsequent authors, including in a comprehensive review of the heteropteran classification and natural history by Schuh and Weirauch (2020). Based on Popov's description and figures, the superfamily placement of Taimyrocoridae may be agreed upon; however, this decision may be controversial because of the difficulty in interpreting morphological details.

Copyright *Kazutaka Yamada et al.* This is an open access article distributed under the terms of the Creative Commons Attribution License (CC BY 4.0), which permits unrestricted use, distribution, and reproduction in any medium, provided the original author and source are credited.

The fossil records of cimicoid true bugs currently extend from the Middle Jurassic to Oligocene for species found in China, Mongolia, Siberia, Myanmar (Burma), Ukraine, the Baltics and Germany (e.g. Statz and Wagner (1950); Yao et al. (2006); Shcherbakov (2007); Engel (2008); Popov (2016); Tang et al. (2016); Schuh and Weirauch (2020)). A total of 28 genera and 38 species from six families (Anthocoridae, Cimicidae, Lyctocoridae, Plokiophilidae, Taimyrocoridae and Vetanthocoridae) have been reported to date, with most described as members of Anthocoridae from Eocene Baltic amber (Popov 2003; Popov et al. 2011a, 2011b; Schuh and Weirauch 2020). In Vetanthocoridae, 12 genera and 16 species in two tribes are known from the Middle Jurassic to Lower Cretaceous in China (Tang et al. 2016) and they are represented only by compression fossils. Recently, *Pubivetanthocoris carnalis* Tang, Wang & Yao, 2022 was described from mid-Cretaceous Kachin amber of northern Myanmar — this was the first observation of amber inclusion of Vetanthocoridae (Tang et al. 2022).

Observations of the structure of male genitalia are crucial for diagnosing and placing specific groups of Cimicomorpha; however, these structures are not visible in most compression or impression fossils. Even in amber fossils, male genitalia are seldom visible at perfectly clear angles. In Cimicoidea, the details of male genitalic morphology remain unknown, except for those of *Lyctoferus* Popov, 2003 (Anthocoridae) from Eocene Baltic and Ukrainian ambers (Popov 2003) and *Quasicimex* Engel, 2008 (Cimicidae) from Kachin amber (Engel 2008).

The current study reports a well-preserved cimicoid true bug amber fossil from the Hukawng Valley in the Kachin State of northern Myanmar, which is herein described as a new genus and species, *Ecpaglocoris ditomeus* gen. et sp. nov. Although the external appearance of this cimicoid species mostly resembles that of Anthocoridae members, the hemelytral membrane venations and presence of dorsal laterotergites on abdominal segments I to VIII reasonably place it in the family Vetanthocoridae. Therefore, this amber inclusion represents the second discovery of the family Vetanthocoridae in mid-Cretaceous amber, revealing a new genus and species with novel morphological data on male genitalia. This well-preserved amber fossil enables a series of detailed morphological observations on the male genitalia in *E. ditomeus* gen. et sp. nov. and it provides new insights into male genital morphology and phylogenetic relationships within Cimicoidea.

Materials and methods

The amber specimen used in this study was obtained from the Noije Bum Hill of the Hukawng Valley in the State of Kachin, northern Myanmar (Burma). A variety of clastic sedimentary deposits, thin limestone beds and abundant coal and carbonaceous materials have been recognised at the mine and the occurrence of amber is associated with a narrow horizon in fine-grained facies (Cruickshank and Ko 2003). Burmese amber from the Kachin State or recently called "Kachin amber", had been previously considered as being of the Eocene age (Chhibber 1934), but Cruickshank and Ko (2003) suggested a much older Cretaceous age. Based on uranium-lead (U-Pb) dating of zircons of the surrounding sedimentary matrix, amber dates have recently been established as the earliest Cenomanian (98.79 ± 0.62 Ma) (Shi et al. 2012). However, the amber deposits of Kachin may possibly be slightly older (Balashov 2021) and, thus, we here adopted the mid-Cretaceous age (i.e. Cenomanian–Albian) for the amber from the Hukawng Valley.

Regarding recent conflicts in Myanmar (e.g. Sokol (2019); Poinar and Ellenberger (2020); Peretti (2021)), the Kachin amber piece used in this study has been collected before the control of the amber mining areas in the Kachin State started in November 2017 and that we follow the recommendations by Haug et al. (2020). The sole specimen used in this study was legally purchased from an Italian amber dealer on 2 January 2018; it was mined before 2017.

An amber piece containing an inclusion was prepared for cutting, grinding and polishing by the third author. The amber piece is a small, flattened, semicircular or sub-rectangular polished prism of approximately 12 × 7 × 4.5 mm in size. Observations were performed using a binocular microscope (stereoscopic zoom microscope SMZ1500; Nikon). Photographs (Figs 1, 2, 4A, B) were taken using a digital camera (EOS 80D; Canon) attached to an extreme macro-lens (MP-E 65 mm, F2.8, 1–5×; Canon) and a flash light (Macro Twin Lite MT-24 EX; Canon). Line drawings (Figs 3, 4C, D) were prepared principally using an eyepiece grid. The software Helicon Focus 7.7.5 was used for image stacking. All digital images were edited and assembled using Adobe Photoshop CC 2022. The type specimen is deposited the American Museum of Natural History, New York, USA (AMNH), under the registered number of AMNH Bu-SY33. The terminology generally follows Carayon (1972) and Schuh and Weirauch (2020). This publication is registered in ZooBank under: urn:lsid:zoobank.org:pub:6A3587A7-9E57-40AC-B9FD-753EDDBA73C5.

Systematic palaeontology

Superfamily Cimicoidea Latreille, 1802
Family Vetanthocoridae Yao, Cai & Ren, 2006

Genus *Ecpaglocoris* Yamada & Yamamoto, gen. nov.
https://zoobank.org/4846A233-F2BF-4083-A2DD-0DEEA05247FB

Type species. *Ecpaglocoris ditomeus* Yamada & Yamamoto, sp. nov., by original designation.

Etymology. The genus name is a combination of the Greek ekpaglos (= wondrous, astounding) and koris (= bug), referring to this new fossil bug possessing unique male genitalia amongst Cimicoidea; gender masculine.

Diagnosis. Body (Fig. 1) elongated, dorsoventrally flattened; head (Figs 1, 3A) porrect; labium (Figs 1D, 2B, C) reaching middle of mesosternum; pronotum (Figs 1A, C, 3A) with pair of long erect setae near antero-lateral and postero-lateral angles and a pair of similarly long setae behind anterior margin; pronotal callus flat, with longitudinal shallow groove on the mid-line; hemelytral membrane (Fig. 3D) with 10 or more long, slightly curved veins; a very long trichobothrium (Figs 2E, 3D, E) present on middle of corium-membrane boundary; ostiolar peritreme (Figs 2F, 3F) slightly curved forward at apex, distinctly continued to a fine carina which reaches anterior margin of metapleura; fore femur (Figs 2G, 3G) extremely enlarged; fore tibia (Figs 2G, 3G) strongly expanded towards apex, bearing 4–5 long, stout spines and 4–5 small teeth on ventral side and with greatly developed fossula spongiosa at apex; middle and hind tibiae (Figs 1B, D, 3H, I) with several long, stout spines, lacking fossula spongiosa; dorsal laterotergites (Fig. 2D) not fused with mediotergites on abdominal segments I to VIII; pygophore (Fig. 4A–C) symmetrical, longer than combined length of abdominal sterna VII and VIII in ventral view, very broadly connected to abdominal segment VIII; proctiger well-developed; parameres (Fig. 4) symmetrical, orientated anteriorly, very slender and long, moderately curved, acute towards apex, with groove running throughout the paramere.

Differential diagnosis. The new genus *Ecpaglocoris* differs from the genus *Pubivetanthocoris* Tang, Wang & Yao, 2022 by the head shorter than pronotum (in *Pubivetanthocoris*, slightly longer than pronotum); vertex wider than twice the width of an eye in dorsal view (in *Pubivetanthocoris*, narrower than the width of an eye); lateral margin of pronotum not membranous, only carinated at antero-lateral angle (in *Pubivetanthocoris*, membranous, flattened and widely carinated); hemelytra parallel-sided (in *Pubivetanthocoris*, strongly curved); PCu and R+M absent on hemelytra (in *Pubivetanthocoris*, present); and fore tibia strongly expanded towards apex (in *Pubivetanthocoris*, slender, not expanded).

Description. Male. Body elongated, dorsoventrally flattened.

Head (Figs 1, 3A) porrect, slightly shorter than width across eyes; three pairs of long, erect trichobothria (cephalic macrosetae) on each side of anterior clypeus, near front margin of each eye and each side of vertex between eye and ocellus; anteocular region slightly longer than length of eye in dorsal view; eyes prominent, exceeding level of dorsal and ventral surfaces of head in lateral view; ocelli situated between eyes in front of an imaginary line that passes through posterior margin of eyes; vertex wider than twice the width of an eye in dorsal view; postocular region constricted, demarcated by transverse shallow furrow; neck long, smooth, highly polished. Antennal segment I (Figs 1, 3A) stout, exceeding apex of head, with a few short setae; prepedicellite present between segments I and II; segment II (Figs 1, 2A, 3B) stout, slightly thickened towards apex, about as long as head width across eyes, covered with suberect setae that are much shorter than width of the segment, intermixed with long setae that are longer than width of the segment; segments III and IV (Figs 1, 2A, 3B) filiform, much narrower than maximum width of segment II, equal in length, about 0.7 times as long as segment II, sparsely covered with long erect setae intermixed with short procumbent setae, longest setae much longer than twice the width of the respective segment. Labrum short, rounded at apex, not wholly covering labial segment I. Labium (Figs 1D, 2B, C, 3C) long, reaching middle of mesosternum, weakly curving; segment I visible, much shorter than the other segments; segment II stout, basally narrowed, approximately eye length long; segment III extremely long, slightly thickened near base and gradually narrowed towards apex, approximately 3.6 times as long as segment II; segment IV much slender, half as long as segment III.

Pronotum (Figs 1A, C, 3A) nearly trapezoidal, shallowly depressed postero-medially, sparsely covered with tiny punctures, with pair of long erect setae near antero-lateral and postero-lateral angles and with pair of similarly long setae behind anterior margin; anterior margin slightly concave; lateral margin strongly angulate antero-laterally in dorsal view, densely covered with short setae; lateral carinae strongly expanded at antero-lateral angle; collar absent; callus flat, with longitudinal shallow groove on the mid-line; posterior margin deeply concave. Scutellum (Fig. 1A, B) large, sub-equilateral, mesal length longer than basal width, weakly depressed through middle, sparsely covered with short procumbent setae, with a pair of long erect setae near lateral margin base. Hemelytra (Figs 1A, B, 3D) parallel-sided, surpassing apex of abdomen, overall covered with short procumbent setae; claval suture, medial fracture and costal fracture clearly visible; distal end of medial fracture not contiguous with costal fracture; costal margin slightly sinuate. Membrane (Figs 1A, B, 3D) with a cross vein running along corium-membrane boundary and 10 or more long, slightly curved veins radiating posteriorly from it; stub (processus corial) present at distal end of a cross vein; a very long trichobothrium (Figs 2E, 3D, E) present on middle of corium-membrane boundary, the length much longer than three times that of other setae on hemelytron. Mesosternum wide, coarse, mesally with longitudinal carina. Metasternum extremely swollen, obtuse at apex. Metepisternum wide, overall occupied by evaporatorium surrounding the metathoracic scent gland. Metathoracic scent gland (Figs 2F, 3F) with a wide ostiolar peritreme; ostiolar peritreme curved slightly forward at apex, distinctly continued to a fine carina that reaches anterior margin of metapleura while gently curving; median furrow running throughout the ostiolar peritreme. Fore femur (Figs 2G, 3G) extremely enlarged, unarmed, much thicker than width of middle femur; fore tibia (Figs 2G, 3G) strongly expanded towards apex, bearing 4–5 long, stout spines and 4–5 small teeth on ventral side, with well-developed fossula spongiosa at apex; middle coxae widely separated from each other; middle tibia

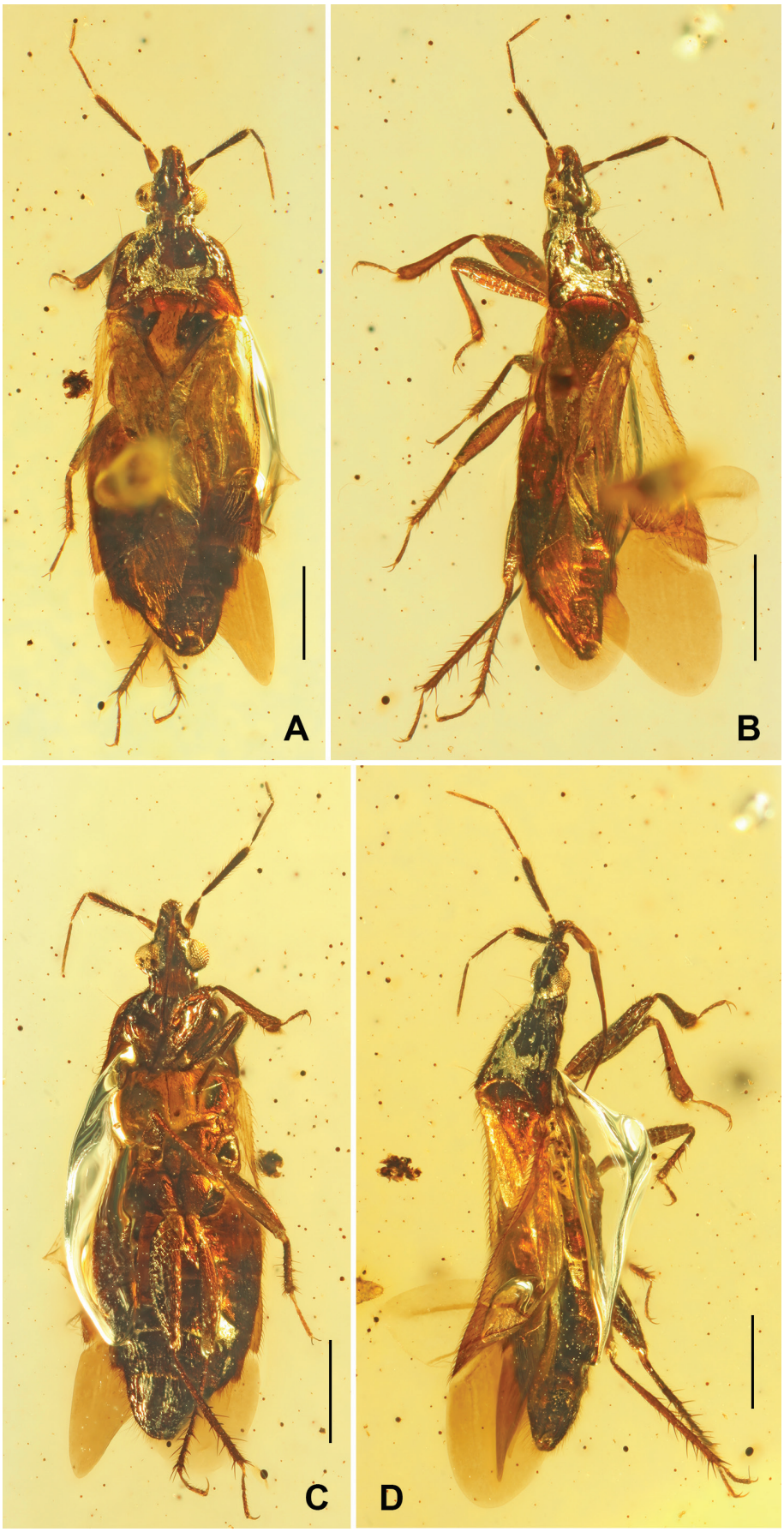

Figure 1. General habitus of *Ecpaglocoris ditomeus* gen. et sp. nov., male, holotype (AMNH Bu-SY33). **A.** Dorsal view; **B.** Left laterodorsal view; **C.** Ventral view; **D.** Right laterodorsal view. Scale bars: 0.5 mm.

(Figs 1B, 3H) expanded towards apex, covered with several long, stout spines on apical two-thirds and with tibial comb at apex, lacking fossula spongiosa; hind coxae proximate with each other; hind femur thickened, slightly narrower than width of fore femur, equal to hind tibia; hind tibia (Figs 1B–D, 3I) nearly cylindrical, densely covered with long, stout spines on apical three-fourths, with small tibial comb at apex, lacking fossula spongiosa. Tarsus three-segmented. Pretarsus of each leg with long, slender, symmetrical claws.

Abdomen (Figs 1C, D, 2D) lateroventrally covered with dense short setae; lateral margins of sterna VI–VIII densely covered with short, suberect setae intermixed with thickly setae; dorsal laterotergites (Fig. 2D) not fused with mediotergites on abdominal segments I to VIII; sterna II and III broad, and VIII very narrow.

Male genitalia (Fig. 4): Pygophore (Fig. 4A–C) symmetrical, large, longer than combined length of abdominal sterna VII and VIII in ventral view, very broadly connected to abdominal segment VIII, dorsally depressed, posteriorly narrowed and rounded in dorsal view, densely covered with short, erect setae along outer margin and on posteroventral surface, lacking long trichobothria; proctiger well-developed; parameres (Fig. 4) symmetrical, arising from near mid-line of dorsocaudal part of pygophore, orientated anteriorly, very slender and long, moderately curved, acute towards apex, with groove running throughout paramere.

Ecpaglocoris ditomeus **Yamada & Yamamoto, sp. nov.**
https://zoobank.org/77E88787-3A77-4B12-8D6E-2DFA4D6719D2
Figs 1–4

Type material. Holotype: male, a well-preserved adult in Kachin amber, with the registered number AMNH Bu-SY33 (deposited in AMNH).

Etymology. The species epithet is named for the Greek di (= two, double) and tomeus (= knife, cutter), referring to the slender, sickle-shaped left and right parameres in male genitalia.

Type locality and horizon. Noije Bum Hill, Hukawng Valley, Kachin State, northern Myanmar; mid-Cretaceous (Cenomanian–Albian).

Diagnosis. As in generic diagnosis.

Description. Male. Body 3.1 mm long, pale to dark brown (Fig. 1), sparsely covered with procumbent setae.

Head (Figs 1, 3A) uniformly dark brown, 0.35 mm in length excluding neck, 0.39 mm in width across eyes; eye length 0.15 mm, width 0.08 mm, in dorsal view. Antennae (Figs 1, 2A, 3B) dark brown, segments I and IV tinged pale brown; lengths of segments I–IV (mm): 0.18, 0.38, 0.28 and 0.28. Labium (Figs 1D, 2B, C) pale brown; lengths of segments II–IV (mm): 0.15, 0.54 and 0.27.

Pronotum (Figs 1A, C, 3A) uniformly dark brown; anterior width 0.25 mm, approximately 0.65 times as wide as mesal pronotal length; basal width 0.74 mm, approximately three times as wide as anterior width. Scutellum (Fig. 1A, B) somewhat paler than pronotum. Hemelytra (Figs 1A, B, 3D) generally pale brown, but cuneus apically tinged with dark brown; embolial margin 1.06 mm, about three times as long as cuneal margin; embolium approximately 0.6 times as wide as maximum width of endocorium; cuneal margin 0.34 mm; membrane semi-transparent. Venter of thorax (Fig. 1C) uniformly dark brown. Legs (Figs 1B–D, 2G, 3G–I) generally pale brown, femora tinged dark brown; lengths of femur, tibia and tarsus of fore leg (in mm): 0.6, 0.5 and 0.28; middle leg: 0.5, 0.44 and 0.25; hind leg: 0.8, 0.8 and 0.46, respectively.

Abdomen (Figs 1C, D, 2D) brown to dark brown.

Female. Unknown.

Discussion

Family placement of *Ecpaglocoris*

This new genus and species is reminiscent of members of Anthocoridae and can be unambiguously placed in Cimicoidea (Heteroptera: Cimicomorpha), based on the following characters: labium with four segmented; costal fracture distinct, delimiting cuneus; hemelytral membrane without closed cell; fossula spongiosa present at least on fore tibiae; absent ventral laterotergites; and insertion of paramere shifted to near mid-line of pygophore (Schuh et al. 2009; Weirauch et al. 2019; Schuh and Weirauch 2020).

However, the new genus *Ecpaglocoris* has the following unusual characteristics in membrane venation, dorsal laterotergites on abdomen and male genitalia, which are not observed in either Anthocoridae or other families of Cimicoidea: membrane with a cross vein running along the corium-membrane boundary and 10 or more long veins radiating from it (Fig. 3D) (in Cimicoidea, 4–5 free veins, rarely with one long closed cell without emanating veins); dorsal laterotergites not fused with mediotergites on abdominal segments I to VIII (Fig. 2D) (in Cimicoidea, on abdominal segments I to III or I and II); pygophore symmetrical (Fig. 4A–C) (in Cimicoidea, except for Plokiophilidae, asymmetrical); left and right parameres symmetrical, with groove (Fig. 4C, D) (in most Cimicoidea, asymmetrical; in a part, non-grooved).

Excepting the unusual membrane venation and male genitalia features, some morphological features of *Ecpaglocoris* gen. nov. are observed in the anthocorid genera *Scoloposcelis* Fieber, 1864 (Tribe Scolopini), *Xylocoris* Dufour, 1831 (Xylocorini) and *Blaptostethus* Fieber, 1860 (Blaptostethini). The characteristics shared by *Ecpaglocoris* gen. nov. and *Scoloposcelis* include: body elongated and dorsoventrally flattened; pronotum shallowly depressed postero-medially, with flat callus; hemelytra parallel-sided; and fore- and hind femora enlarged. However, *Scoloposcelis* is also characterised by femora with small teeth on the ventral side, ostiolar peritreme not continuing to a fine carina and males with

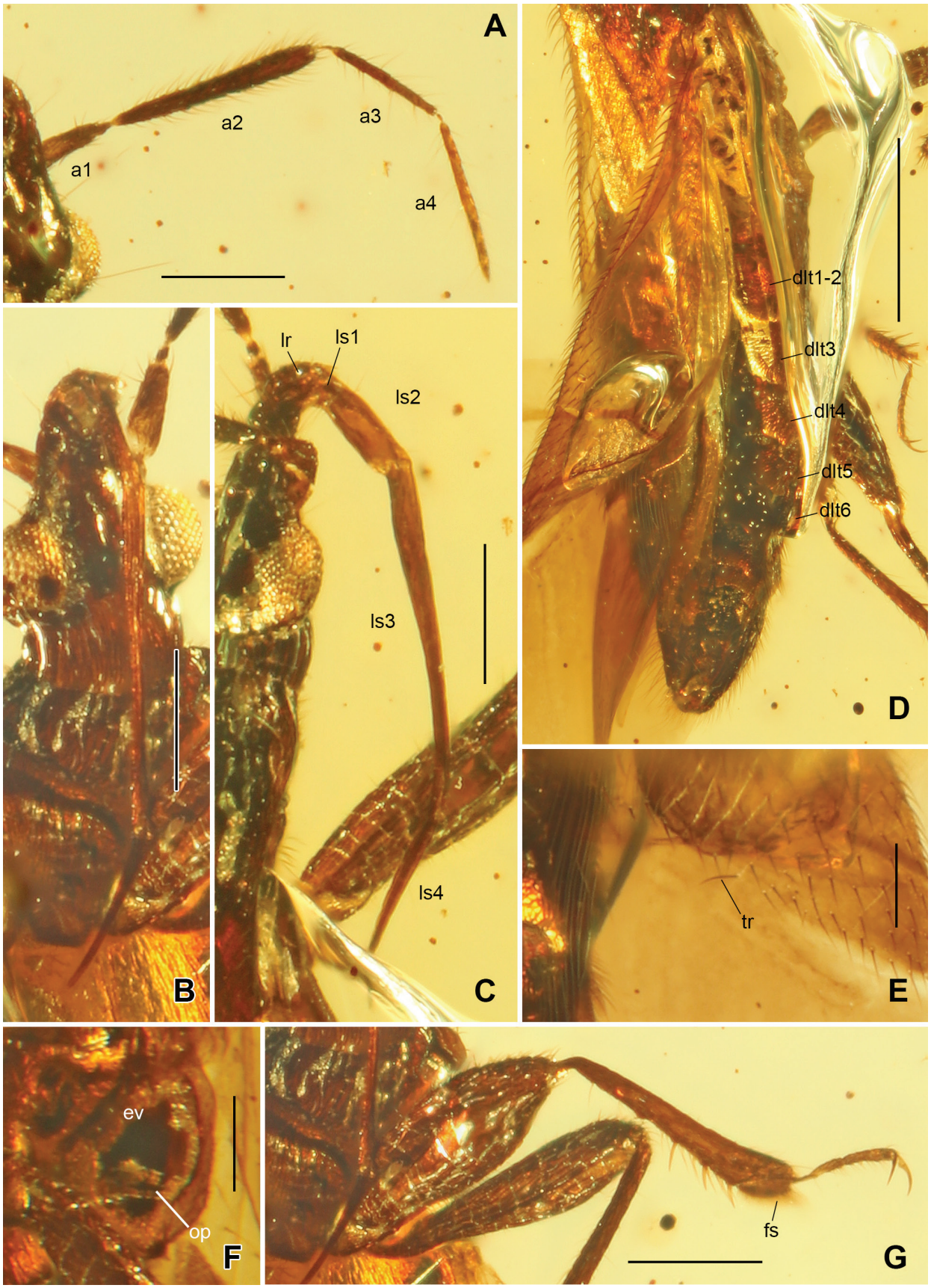

Figure 2. *Ecpaglocoris ditomeus* gen. et sp. nov., male, holotype (AMNH Bu-SY33). **A.** Right antenna, laterodorsal view; **B, C.** Labium, ventral (**B**) and right lateral (**C**) views; **D.** Thorax and abdomen, right laterodorsal view; **E.** Trichobothrium on corium-membrane boundary of right hemelytron; **F.** Ostiolar peritreme and evaporatorium, left lateroventral view; **G.** Right fore-leg, outer view. Abbreviations: a1–4, antennal segment 1–4; dlt1–6, dorsal laterotergite 1–6; ev, evaporatorium; fs, fossula spongiosa; lr, Labrum; ls1–4. labial segment 1–4; op, ostiolar peritreme; tr, trichobothrium. Scale bars: 0.5 mm (**D**); 0.2 mm (**A–C, E–G**).

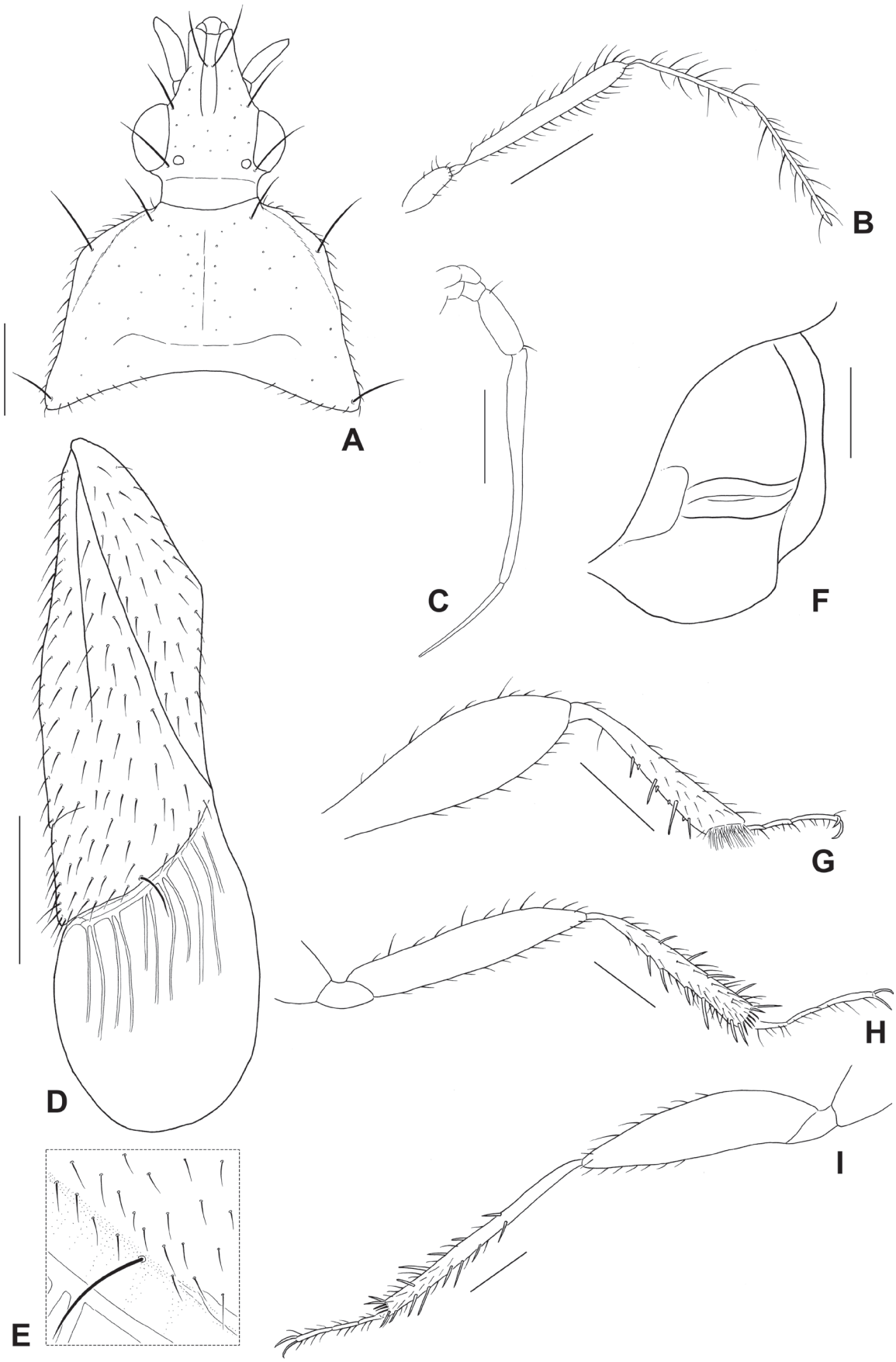

Figure 3. *Ecpaglocoris ditomeus* gen. et sp. nov., male, holotype (AMNH Bu-SY33). **A.** Head and pronotum, dorsal view; **B.** Right antenna, laterodorsal view; **C.** Labium, lateral view; **D.** Left hemelytron, as seen in situ, not flattened; **E.** Trichobothrium on corium-membrane boundary of right hemelytron; **F.** Ostiolar peritreme and evaporatorium, left lateroventral view; **G.** Right fore-leg, outer view; **H.** Right middle leg, outer view; **I.** Right hind leg, inner view. Scale bars: 0.5 mm (**D**); 0.2 mm (**A–C, F–I**).

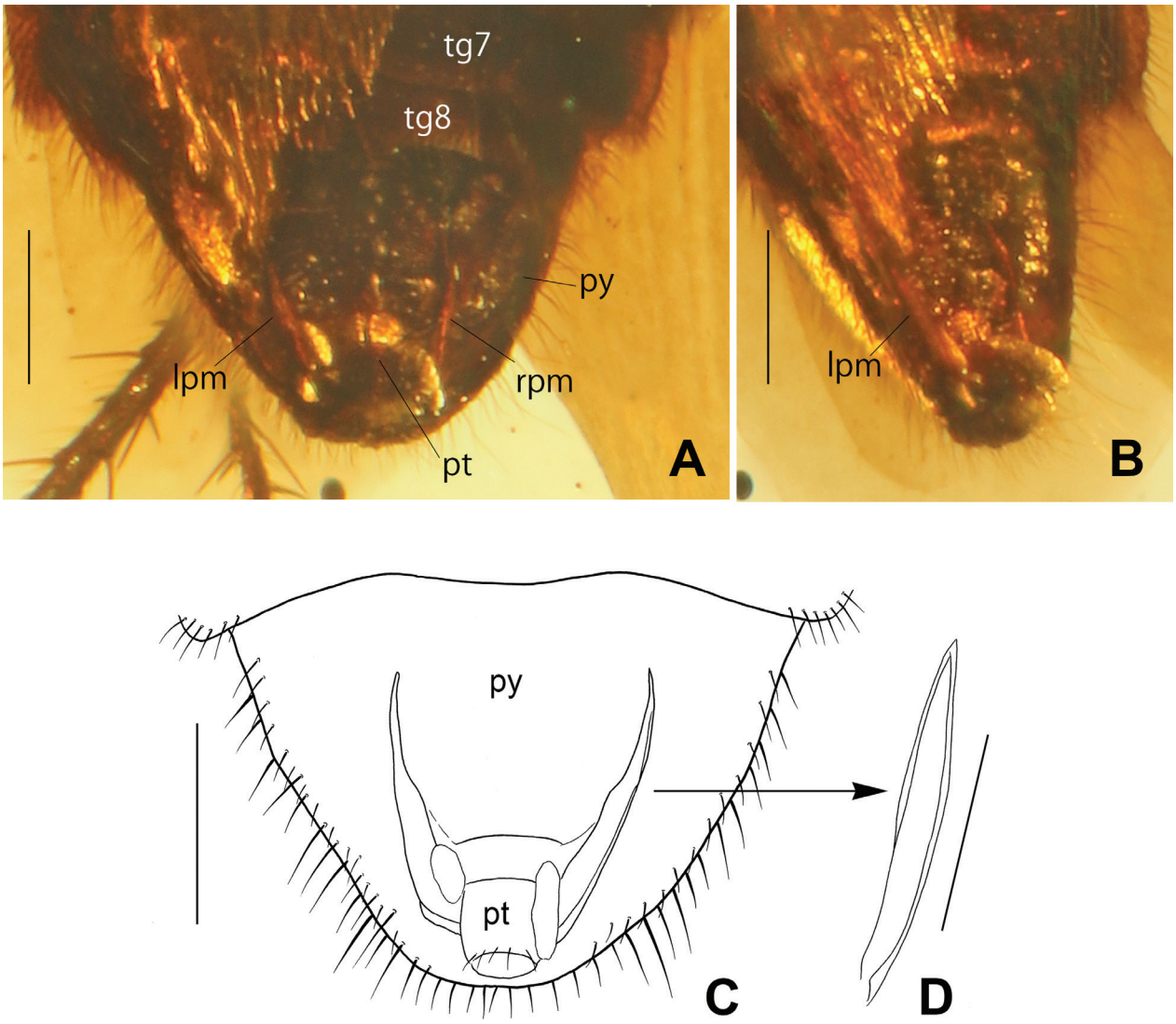

Figure 4. *Ecpaglocoris ditomeus* gen. et sp. nov., male, holotype (AMNH Bu-SY33). **A, B.** Apex of abdomen, dorsal (**A**) and left laterodorsal (**B**) views; **C.** Pygophore with parameres, dorsal view; **D.** Right paramere, right lateral view. Abbreviations: lpm, left paramere; pt, proctiger; py, pygophore; rpm, right paramere; tg7–8, tergite 7–8. Scale bars: 0.1 mm.

opening(s) of uradenia (paired abdominal glands) on either abdominal sternum 4 or 5, which is also an autapomorphy of Scolopini (e.g. Carayon (1972); Schuh and Slater (1995)). *Ecpaglocoris* gen. nov. lacks femoral teeth and an opening of uradenia on the abdominal sternum and it has an ostiolar peritreme continuing to a fine carina (Figs 2F, 3F). *Ecpaglocoris* gen. nov. has leg characteristics similar to those of *Xylocoris* and *Blaptostethus* as follows: each tibiae bearing several long, stout spines that are as long as or longer than the width of the tibia (Figs 1B–D, 2G, 3G–I); fore tibia expanded towards the apex, with developed fossula spongiosa at the apex (Figs 1B–D, 2G, 3G). However, the fossula spongiosa is also present on the middle and hind tibiae in *Xylocoris* and *Blaptostethus*, but it is absent in *Ecpaglocoris* gen. nov. (e.g. Carayon (1972); Schuh and Slater (1995)). This new genus is characterised by a combination of morphological features found in some anthocorid taxa of different tribes, but lacks synapomorphies in each genus (tribe) in Anthocoridae. Considerable differences in male genitalia are recognised between the new genus and anthocorid groups. The superficial morphological similarities between these taxa may represent the convergence of habits and habitats.

Although symmetrical male genitalia in *Ecpaglocoris* gen. nov. are also found in Microphysoidea (Joppeicidae and Microphysidae) and Naboidea (Medocostidae, Nabidae and Velocipedidae), which are closely related to Cimicoidea, all these groups possess a conspicuous paramere insertion on the left side of the pygophore and the various-shaped paramere, which is never sickle-like in shape (Schuh and Štys 1991; Schuh et al. 2009; Schuh and Weirauch 2020). These features clearly distinguish *Ecpaglocoris* gen. nov. from both the superfamilies. In addition, Microphysoidea has reduced or no evaporatorium in the metapleuron and two-segmented tarsi and Naboidea has a membrane with 2–3 short or elongate cells usually with numerous emanating veins. The new genus may belong to neither Microphysoidea nor Naboidea.

Of the above-mentioned unusual features in *Ecpaglocoris* gen. nov., membrane venation and dorsal laterotergites on the abdomen are also recognised in the extinct family Vetanthocoridae. Tang et al. (2016) re-evaluated Vetanthocoridae as a member of Cimicoidea and suggested two synapomorphies to support the monophyly of the family, based on their phylogenetic analysis: antennal segments III and IV smooth without setae and 10 or more simple longitudinal veins on the hemelytral membrane. However, the former was not considered a synapomorphic character for the family by Tang et al. (2022), because *Pubivetanthocoris carinalis* Tang, Wang & Yao, 2022, described as the first record of the Vetanthocoridae from Kachin amber, has antennal segments III and IV with discrete setae. However, the membrane venation and dorsal laterotergites on the abdomen found in Vetanthocoridae and *Ecpaglocoris* gen. nov. clearly distinguish both taxa from Recent cimicoids and can be regarded as important diagnostic features for Vetanthocoridae. Thus, we should place *Ecpaglocoris* gen. nov. in the family Vetanthocoridae.

Relationships within Vetanthocoridae

Although *Ecpaglocoris* gen. nov. is best placed in Vetanthocoridae, the genus has several remarkable characteristics amongst the vetanthocorid genera: body very small (Fig. 1) (in Vetanthocoridae, 4.3–13.7 mm vs. 3.1 mm); hemelytra parallel-sided (Fig. 1A) (in Vetanthocoridae, generally curved-sided); embolar fracture on hemelytra absent (Figs 1A, B, 3D) (in Vetanthocoridae, present); a very long trichobothrium present on the middle of the corium-membrane boundary (Figs 2E, 3D, E) (in Vetanthocoridae, absent; at least not confirmed in the descriptions of all members); and fore tibia strongly expanded towards apex (Figs 2G, 3G) (in Vetanthocoridae, generally straight) (Yao et al. 2006; Tang et al. 2016, 2022). Based only on the condition of antennal segments III and IV (both distinctly narrower than segment II) (Yao et al. 2006; Tang et al. 2022), *Ecpaglocoris* gen. nov. can be assigned to the tribe Vetanthocorini; however, the above-mentioned distinctive characters are all exceptional in Vetanthocoridae. Therefore, the tribal placement of this new genus cannot be determined yet.

Limited information is available regarding the male genital features of Vetanthocoridae. Based on the figures by Yao et al. (2006: pp. 10, 17), *Vetanthocoris decorus* Yao, Cai & Ren, 2006 and *Collivetanthocoris rapax* Yao, Cai & Ren, 2006 may have symmetrical and well-developed pygophores. Shcherbakov (2007) also indicated that the family Vetanthocoridae has symmetrical male genitalia; however, no detailed discussion was provided. The general appearance of pygophore from the ventral aspect in *E. ditomeus* gen. et sp. nov. is relatively similar to those of *V. decorus* and *C. rapax*; however, it is not possible to determine whether they have the same characteristics owing to limited morphological information available from their fossils.

Male genitalic morphology

Male genitalia and insemination mechanisms are the most important characteristics for determining the family level systematic position within Cimicoidea. Asymmetrical male genitalia are one of the peculiarities of all extant Cimicoidea, except for Plokiophilidae. Sinistral asymmetry affects the pygophore and parameres, indicating that the right paramere is usually completely lost. Asymmetry, as seen in parameres, occurs in many groups that appear to be distantly related, judging by other characters, including Nepomorpha, Dipsocoridae, Schizopteridae and Miroidea (Ford 1979; Weirauch et al. 2019). Male genital asymmetry has arisen independently of several evolutionary lineages. Symmetrical male genitalia in *Ecpaglocoris* gen. nov. and Plokiophilidae are clearly plesiomorphic within the Cimicoidea.

Traumatic (haemocoelic) insemination is the most prevalent mating strategy in the true bug infraorder Cimicomorpha, where it occurs in at least seven families (Carayon 1966, 1972, 1977; Ford 1979; Tatarnic et al. 2014). With some exceptions, the members of Cimicoidea practise traumatic insemination. Male genitalic characteristics associated with these insemination mechanisms include: 1) aedeagus (endosoma) with sclerotised organ (needle-like acus) and 2) copulatory left paramere. The former is found in Lyctocoridae and Plokiophilidae, as well as in several other non-cimicoid heteropterans (Nabidae: Prostemmatinae). Their paramere has no grooves because the aedeagus itself serves as an intromittent organ. The latter is found in Anthocoridae, Cimicidae and Polyctenidae. Their paramere itself functions as an intromittent organ and has a distinct groove with an acute apex, which serves as a guide for the membranous aedeagus. The paramere of some Lasiochilidae species has a similar condition with those of three families, but its function is unknown (Carpintero 2014). Although the grooved paramere is also seen in *Coridromius* (Miridae), suggesting an independent derivation for traumatic insemination, it can be regarded as a unique condition within the Cimicoidea. The parameres of *Ecpaglocoris* gen. nov. are sickle-shaped and possess a groove throughout the paramere (Fig. 4). Due to the male genitalic structure of this new fossil genus, they have very significant differences from the extant species which have traumatic insemination and no direct behavioural evidence showed in the amber specimen. Although the possibility of this new fossil species mating by traumatic insemination is existing, based on their male genitalic characteristics, our insight is completely speculative.

The mating posture of *E. ditomeus* gen. et sp. nov. might be quite different from that of other cimicoid groups. Available evidence suggests that its posture is presumably almost the same as that of other heteropterans with symmetrical male genitalia, showing that the male takes its place under the female (Ceratocombidae, Melber and Köhler 1992; Aradidae, Schuh and Weirauch 2020) or that the male places the dorsal side of the tip of the abdomen

under the tip of the female abdomen (Nepidae, Larsén 1938; Joppeicidae, Davis and Usinger 1970). Whereas, another hypothesis can predict that *E. ditomeus* gen. et sp. nov. also practised the most common "male-above" position for genital coupling in cimicoid members with grooved parameres. In this case, the male bends his abdomen from the female's right (or left) side and inserts his paramere into a certain part of the ventral side of the abdomen (e.g. Péricart (1972); Huber et al. (2007); Tatarnic et al. (2014)). In the case of *E. ditomeus* gen. et sp. nov., the mating posture may be an alternating two-sided position because it has double parameres as an intromittent organ.

Male genital asymmetry in Recent Cimicoidea is overwhelmingly directional (sinistrally curved) (Huber et al. 2007; Schuh and Weirauch 2020). Directional asymmetry is also seen in females of Cimicoidea, because traumatic insemination often occurs via a specific copulatory site (Carayon 1977). Their morphological modifications are thought to have evolved through a mating strategy in association with sexually antagonistic types of behaviour (e.g. Parker (1979); Arnqvist and Rowe (2005)); however, no hypothesis explains why sinistral male genitalia are dominant over symmetry in Cimicoidea.

According to Schuh et al. (2009), Jung et al. (2010), Jung and Lee (2012) and Weirauch et al. (2019), cimicoid groups with grooved paramere (Anthocoridae, Cimicidae, Polyctenidae and some Lasiochilidae) do not form a monophyletic group, placing Lasiochilidae as a base for the remaining Cimicoidea. Thus, the grooved paramere occurs separately in the superfamily and that their possession has no strong systematic significance, at least within Cimicoidea. *Ecpaglocoris* gen. nov. also has grooved parameres; however, owing to the combination of the unique characters mentioned above, it is unlikely that this genus would be closely related to these taxa with grooved parameres. Within Heteroptera, *Ecpaglocoris* gen. nov. is characterised by plesiomorphic symmetrical pygophore and parameres and a unique grooved paramere. This peculiar combination of male genital characteristics prevents their placement in any of the extant cimicoid families. If this characteristic is recognised in members of the Vetanthocoridae, it could undoubtedly be a synapomorphy in this extinct family.

Conclusions

Although our investigation of these *Ecpaglocoris* gen. nov. characteristics produced unexpected results and produced doubt that this taxon belongs to Cimicoidea, we are reasonably certain that it should be placed in this superfamily, based on salient characteristics. Consequently, *Ecpaglocoris* gen. nov. can be assigned to the extinct family Vetanthocoridae because of the presence of venation of the hemelytral membrane and dorsal laterotergites on abdominal segments I to VIII, which are unique amongst the extant cimicoid taxa. In extant Heteroptera, the parameres of the species that are used as the intromittent organ are all strongly asymmetrical, never symmetrical. However, the male genitalia of *Ecpaglocoris ditomeus* gen. et sp. nov. is characterised by a combination of plesiomorphic (symmetrical pygophore and paramere) and unique (a groove that runs throughout the paramere) characteristics within Heteroptera. The characteristics of the parameres indicate that traumatic insemination was practised in this genus. If this characteristic in the male genitalia is recognised in the members of Vetanthocoridae, it could undoubtedly be a synapomorphy in the extinct family. Since relationships amongst the family level taxa within Cimicoidea remain controversial, assessment of the phylogenetic position of *Ecpaglocoris* gen. nov. or Vetanthocoridae requires detailed phylogenetic studies to rigorously evaluate the monophyly of the currently-recognised family level groups in extant Cimicoidea.

Data availability

The single material (holotype) is deposited in the American Museum of Natural History, New York, USA (AMNH). All data and results are presented in the main text and figures. Higher-resolution images are also available through the Zenodo repository (https://doi.org/10.5281/zenodo.7472713).

Author contributions

KY, SY and YT conceived the study. YT and SY prepared for cutting, grinding and polishing an amber piece containing an inclusion. KY identified and described the specimen. SY produced the photos. KY edited and assembled the figures. KY, SY and YT prepared the paper and contributed to the editing.

Competing interests

The authors declare that they have no conflict of interest.

Financial support

This study was partly supported by Grant-in-Aid for Scientific Research (B) from the Japan Society for the Promotion of Science (JSPS) to KY (No. JP16K07502; head: Kazunori Yoshizawa) and Grant-in-Aid for JSPS Fellows given to SY (No. 20J00159).

Acknowledgements

We express our appreciation to Carolin Haug (editor), Jacek Szwedo, Jun Chen and an anonymous reviewer for their careful review and constructive comments and suggestions. KY thanks Michael S. Engel (University of

Kansas, Kansas, USA) and Yunzhi Yao (Capital Normal University, Beijing, China) for providing literature and information of several essential publications. We would like to thank Editage (www.editage.jp) for English language editing.

References

Arnqvist G, Rowe L (2005) Sexual Conflict. Princeton University Press, Princeton, NJ, 328 pp. https://doi.org/10.1515/9781400850600

Balashov I (2021) The first records of mollusks from mid-Cretaceous Hkamti amber (Myanmar), with the description of a land snail, *Euthema myanmarica* n. sp. (Caenogastropoda, Cyclophoroidea, Diplommatinidae). Journal of Paleontology 95(5): 994–1003. https://doi.org/10.1017/jpa.2021.26

Carayon J (1966) Traumatic insemination and the paragenital system. In: Usinger RL (Ed.) Monograph of Cimicidae. The Thomas Say Foundation, volume VII. Entomological Society of America, Lanham, MD, 81–166.

Carayon J (1972) Caractères systématiques et classification des Anthocoridae. Annales de la Société Entomologique de France 8: 309–349. [Hemipt.] [Nouvelle Série]

Carayon J (1977) Insémination extra-génitale traumatique In: Grassé PP (Ed.) Traité de Zoologie. Anatomie, Syste'matique, Biologie. Tome VIII: Insectes. Gamétogenè ses, Fécondation, Métamorphoses. Masson, Paris, 351–390.

Carpintero DL (2014) Western Hemisphere Lasiochilinae (Hemiptera: Heteroptera: Anthocoridae) with comments on some extralimital species and some considerations on suprageneric relationships. Zootaxa 3871(1): 1–87. https://doi.org/10.11646/zootaxa.3871.1.1

Chhibber HL (1934) The Mineral Resources of Burma. MacMillan, London, [i–xv +] 320 pp.

Cruickshank RD, Ko K (2003) Geology of an amber locality in the Hukawng Valley, northern Myanmar. Journal of Asian Earth Sciences 21(5): 441–455. https://doi.org/10.1016/S1367-9120(02)00044-5

Davis NT, Usinger RL (1970) The biology and relationships of the Joppeicidae (Heteroptera). Annals of the Entomological Society of America 63(2): 577–586. https://doi.org/10.1093/aesa/63.2.577

Engel MS (2008) A stem-group cimicid in mid-Cretaceous amber from Myanmar (Hemiptera: Cimicoidea). Alavesia 2: 233–237.

Ford LJ (1979) The Phylogeny and Biogeography of the Cimicoidea (Insecta: Hemiptera). MSc. Thesis. University of Connecticut, Storrs, 308 pp.

Haug JT, Azar D, Ross A, Szwedo J, Wang B, Arillo A, Baranov V, Bechteler J, Beutel R, Blagoderov V, Delclòs X, Dunlop J, Feldberg K, Feldmann R, Foth C, Fraaije RHB, Gehler A, Harms D, Hedenäs L, Hyžný M, Jagt JWM, Jagt-Yazykova EA, Jarzembowski E, Kerp H, Khine PK, Kirejtshuk AG, Klug C, Kopylov DS, Kotthoff U, Kriwet J, McKellar RC, Nel A, Neumann C, Nützel A, Peñalver E, Perrichot V, Pint A, Ragazzi E, Regalado L, Reich M, Rikkinen J, Sadowski E-M, Schmidt AR, Schneider H, Schram FR, Schweigert G, Selden P, Seyfullah LJ, Solórzano-Kraemer MM, Stilwell JD, van Bakel BWM, Vega FJ, Wang Y, Xing L, Haug C (2020) Comment on the letter of the Society of Vertebrate Paleontology (SVP) dated April 21, 2020 regarding "Fossils from conflict zones and reproducibility of fossil-based scientific data": Myanmar amber. PalZ 94(3): 431–437. https://doi.org/10.1007/s12542-020-00524-9

Huber BA, Sinclair BJ, Schmitt M (2007) The evolution of asymmetric genitalia in spiders and insects. Biological Reviews of the Cambridge Philosophical Society 82(4): 647–698. https://doi.org/10.1111/j.1469-185X.2007.00029.x

Jung S, Lee S (2012) Correlated evolution and Bayesian divergence time estimates of the Cimicoidea (Heteroptera: Cimicomorpha) reveal the evolutionary history. Systematic Entomology 37(1): 22–31. https://doi.org/10.1111/j.1365-3113.2011.00596.x

Jung S, Kim H, Yamada K, Lee S (2010) Molecular phylogeny and evolutionary habitat transition of the flower bugs (Heteroptera: Anthocoridae). Molecular Phylogenetics and Evolution 57(3): 1173–1183. https://doi.org/10.1016/j.ympev.2010.09.013

Larsén O (1938) Untersuchungen über den Geschlechtsapparat der aquatilen Wanzen. Opuscula Entomologica (Supplement 1): 1–388.

Latreille PA (1802) Histoire naturelle, générale et particulière des crustacés et des insectes 3. F. Dufart, Paris, [i–xii +] 467 pp. https://doi.org/10.5962/bhl.title.15764

Latreille PA (1810) Considerations generales sur l'ordre naturel des animaux composant Ies classes des crustaces, des arachnides, et des insectcs; avec tableau methodique de leurs genres, disposes en families. Schnell, Paris, 444 pp. https://doi.org/10.5962/bhl.title.34917

Linnaeus C (1758) Systema naturae per regna tria naturae, secundum classes, ordines, genera, species, cum characteribus, differentiis, synonymis, locis. Editio decima, reformata. Salvii, Holmiae, [i–v +] 824 pp. https://doi.org/10.5962/bhl.title.542

Melber A, Köhler R (1992) Die Gattung *Ceratocombus* Signoret, 1852 in Nordwestdeutschland (Heteroptera, Ceratocombidae). Bonner Zoologische Beitrage 43: 229–246.

Parker GA (1979) Sexual selection and sexual conflict. In: Blum MS, Blum NA (Eds) Sexual Selection and Reproductive Competition in Insects. Academic, London, 123–166. https://doi.org/10.1016/B978-0-12-108750-0.50010-0

Peretti A (2021) An alternative perspective for acquisitions of amber from Myanmar including recommendations of the United Nations Human Rights Council. Journal of International Humanitarian Action 6(1): 12. https://doi.org/10.1186/s41018-021-00101-y

Péricart J (1972) Hémiptères Anthocoridae, Cimicidae, Microphysidae de l'Ouest-Paléarctique. Faune de l'Europe et du bassin Méditerranéen. Vol. 7. Masson et Cie Éditeurs, Paris, 402 pp.

Poinar G, Ellenberger S (2020) Burmese amber fossils, mining, sales and profits. Geoconservation Research 3: 12–16. https://doi.org/10.30486/gcr.2020.1900981.1018

Popov YA (2003) New flower bugs from Baltic and Ukrainian amber (Heteroptera: Anthocoridae, Lyctocorinae). Mitteilungen aus dem Geologisch-Paläontologischen Institut der Universität Hamburg 87: 183–202.

Popov YA (2016) A new family of anthocoroid hemipterans (Hemiptera: Heteroptera, Cimicomorpha) from Cretaceous Taimyr amber. Paleontological Journal 50(4): 406–411. https://doi.org/10.1134/S0031030116040109

Popov YA, Herczek A, Brozek J (2011a) The first fossil Dufouriellini (Hemiptera: Heteroptera: Anthocoridae: Lyctocorinae) from the Eocene Baltic amber. Zootaxa 2760(1): 53–60. https://doi.org/10.11646/zootaxa.2760.1.5

Popov YA, Herczek A, Brozek J (2011b) *Brachypicritus ribesi* n. gen., n. sp., a new fossil Cardiastethini (Hemiptera: Heteroptera: Anthocoridae) from the Eocene Baltic amber. Heteropterus Review of Entomology 11: 323–327. https://heteropterus.org/images/HRE/articulos/Heteropterus_Rev_Entomol_11(2)_323-327.pdf

Schuh RT, Slater JA (1995) True Bugs of the World (Hemiptera: Heteroptera): Classification and Natural History. Cornell University Press, Ithaca, NY, 336 pp.

Schuh RT, Štys P (1991) Phylogenetic analysis of cimicomorphan family relationships (Heteroptera). Journal of the New York Entomological Society 99: 298–350.

Schuh RT, Weirauch C (2020) True bugs of the world (Hemiptera: Heteroptera). Classification and Natural history. 2nd edn. Monograph Series. Vol. 8. Siri Scientific Press, Manchester, 800 pp.

Schuh RT, Weirauch C, Wheeler WC (2009) Phylogenetic relationships within the Cimicomorpha (Hemiptera: Heteroptera): a total-evidence analysis. Systematic Entomology 34(1): 15–48. https://doi.org/10.1111/j.1365-3113.2008.00436.x

Shcherbakov DE (2007) Mesozoic Velocipedinae (Nabidae s. l.) and Ceresopseidae (Reduvioidea), with notes on the phylogeny of Cimicomorpha (Heteroptera). Russian Entomological Journal 16: 401–414.

Shi G, Grimaldi DA, Harlow GE, Wang J, Wang J, Yang M, Lei W, Li Q, Li X (2012) Age constraint on Burmese amber based on U-Pb dating of zircons. Cretaceous Research 37: 155–163. https://doi.org/10.1016/j.cretres.2012.03.014

Sokol J (2019) Troubled treasure. Science 364(6442): 722–729. https://doi.org/10.1126/science.364.6442.722

Statz G, Wagner E (1950) Geocorisae (Landwanzen) aus den Oberoligocner Ablagerungen von Rott. Palaeontographica. Abteilung A, Paläozoologie, Stratigraphie 98: 97–136.

Tang D, Yao YZ, Ren D (2016) Phylogenetic position of the extinct insect family Vetanthocoridae (Heteroptera) in Cimiciformes. Journal of Systematic Palaeontology 15(9): 697–708. https://doi.org/10.1080/14772019.2016.1219779

Tang HY, Wang Y, Ren D, Yao YZ (2022) The first record of vetanthocorids (Hemiptera: Heteroptera: Vetanthocoridae) from mid-Cretaceous amber of northern Myanmar. Cretaceous Research 131: 105090. https://doi.org/10.1016/j.cretres.2021.105090

Tatarnic NJ, Cassis G, Siva-Jothy MT (2014) Traumatic insemination in terrestrial arthropods. Annual Review of Entomology 59(1): 245–261. https://doi.org/10.1146/annurev-ento-011613-162111

Weirauch C, Schuh RT, Cassis G, Wheeler WC (2019) Revisiting habitat and lifestyle transitions in Heteroptera (Insecta: Hemiptera): insights from a combined morphological and molecular phylogeny. Cladistics 35(1): 67–105. https://doi.org/10.1111/cla.12233

Yao YZ, Cai WZ, Ren D (2006) Fossil flower bugs (Heteroptera: Cimicomorpha: Cimicoidea) from the Late Jurassic of Northeast China, including a new family, Vetanthocoridae. Zootaxa 1360(1): 1–40. https://doi.org/10.11646/zootaxa.1360.1.1

Fossil Record 26 (1) 2023, 39–50 | DOI 10.3897/fr.26.99995

New species of Tanaidacea from Cretaceous Kachin amber, with a brief review of the fossil record of tanaidacean crustaceans

Paula G. Pazinato[1], Patrick Müller[2], Joachim T. Haug[1,3]

1 *Biocenter, Ludwig-Maximilians-Universität München (LMU Munich), Großhaderner Str. 2, 82152 Planegg-Martinsried, Germany*
2 *Kreuzbergstr. 90, 66482 Zweibrücken, Germany*
3 *GeoBio-Center at LMU, Richard-Wagner-Str. 10, 80333 München, Germany*

https://zoobank.org/DD3534AA-4A28-4992-B364-C094D541D995

Corresponding author: Paula G. Pazinato (paula.pazinato@palaeo-evo-devo.info)

Academic editor: Alexander Schmidt ♦ **Received** 6 January 2023 ♦ **Accepted** 30 January 2023 ♦ **Published** 31 January 2023

Abstract

Tanaidaceans are benthic, mostly marine, crustaceans that live burrowed in the substrate or in self-built tubes. The fossil record of Tanaidacea reaches back to the Carboniferous, 350 million years ago, but it is especially species-rich in Cretaceous amber sites from Spain and France. We report and formally describe a new species of Tanaidacea from 100-million-year-old Kachin amber, from the Hukawng Valley, Northern Myanmar, the first record of Cretaceous tanaidaceans outside Europe. The combination of character states of *Tanaidaurum kachinensis* **gen. nov. et sp. nov.** suggests that the new species is a representative of the early diversification of an unnamed group (Paratanaoidea+Tanaidoidea), an ingroup of the monophyletic group Tanaidomorpha. We briefly review the biased fossil record of Tanaidacea and present its abundance in European amber sites.

Key Words

Cretaceous, Myanmar amber, Peracarida, Tanaidacea, Tanaidomorpha

Introduction

Tanaidacea, an ingroup of Peracarida, is a group of crustaceans with currently about 1,200 formally described extant species and 26 fossil species. As for all representatives of Peracarida, such as woodlice, females carry their offspring in a ventral brood pouch. Tanaidaceans distantly resemble representatives of Isopoda (woodlice, slaters etc.), but can easily be differentiated from the latter by the presence of a pair of prominent chelae.

Most tanaidaceans are marine and are found at all depths; four species live in freshwater; all species live borrowed in the substrate, some in self-built tubes (Hassack and Holdich 1987; Kakui and Hiruta 2017; Kakui 2021). The body size ranges from one up to seven millimeters. The body is organised of 20 segments (one ocular and 19 post-ocular segments), as is ancestrally for Eumalacostraca. The anterior eight segments form the functional head ("cephalothorax"), followed by six segments of the anterior trunk (free thorax segments; "pereon") and six segments of the posterior trunk (pleon). The prominent chelae are formed by the appendages of the last segment of the functional head. The fossil record of Tanaidacea reaches back into the Carboniferous, but is especially species-rich in Cretaceous amber from France and Spain, together with 13 of the 26 formally described species, with some amber formations, such as the Spanish Álava amber alone recording six species.

In the last decades, amber deposits from the Cretaceous have provided expressively high numbers of different lineages of Euarthropoda, especially Insecta, giving a window of the past diversity and abundance of some ingroups of Insecta (e.g. Badano et al. 2018; Ross 2018, 2019; Haug et al. 2021). Eumalacostracans are quite rare in such ambers in comparison to beetles, bees and their kin; so far there are records in Cretaceous amber of Decapoda (shrimps, lobsters and crabs) and of three ingroups of Peracarida: Amphipoda, Isopoda

Copyright *Paula G. Pazinato et al.* This is an open access article distributed under the terms of the Creative Commons Attribution License (CC BY 4.0), which permits unrestricted use, distribution, and reproduction in any medium, provided the original author and source are credited.

and Tanaidacea (Ross 2018, 2019). Kachin amber (also known as Burmese amber or Burmite), from the Hukawng Valley, Northern Myanmar, is one example of Cretaceous amber sites that have expressively high numbers of fossils (Ross 2018, 2019) and, so far, a remarkably low number of eumalacostracans, represented by four formally described species of Isopoda (Broly et al. 2015; Poinar 2020; Schädel et al. 2021a, b).

Here we report a new species of Tanaidacea, the first record in Kachin amber, expanding the knowledge of the Cretaceous diversity of Tanaidacea. We briefly review the overall fossil record of Tanaidacea and compare some abundance aspects.

Materials and methods

Materials

Two pieces of Burmese (Myanmar) amber containing three specimens are in the center of this study. Sample SNHMB.G 8008 contains one specimen accessible in dorso-ventral view. Sample BUB 4227 has two specimens preserved, one accessible in lateral view (BUB 4227-1), the other in ventral view (BUB 4227-2). The latter is poorly accessible due to impurities of the amber. Sample SNHMB.G 8008 is deposited in the collections of the Staatliches Naturhistorisches Museum Braunschweig, Germany. Sample BUB 4227 is from the collection of one of the authors (collection Müller) and is available for further study on request. All specimens were legally purchased. The amber pieces present small fragments of plants as syninclusions.

Methods

The amber pieces were documented using a Keyence VHX-6000 digital microscope. The amber pieces were placed in a petri dish, we added one drop of distilled water and a cover glass on top of the specimens of interest for documentation. Different light settings, cross-polarized light (Haug et al. 2013a) and ring light (Haug et al. 2019), were used against a white and a black background to enhance visibility of the details of the specimen. Fully focused images were obtained by recording stacks and fusing these with the built-in software. Larger images were created by recording several adjacent image details (each with a stack) and merging these to a larger panorama image. All images were recorded as HDR (High Dynamic Range; cf. Haug et al. 2013b). Measurements of the specimens were made on the images using the open-source software ImageJ. The histograms of the images were optimized and some structures were artificially color-marked using Photoshop CS2. Figure plates were arranged using the open-source vector-graphics editor Inkscape.

Note on terminology: To provide a wider comparative frame we apply general terminology for Euarthropoda and Eucrustacea. This is necessary as many specialist terms are used very differently in different ingroups of Eucrustacea with very different criteria behind each version of the same term (e.g. ‘carapace’ which is therefore substituted by shield). Specialist terms (following Larsen 2003) were added in single quotation marks.

Results

The three specimens are interpreted here as representatives of a single species of Tanaidacea due to their great similarity and lack of distinctive characters. The species is treated as new to science since it presents a unique combination of characters so far unknown from the fossil and extant record of Tanaidacea.

Taxonomic treatment

Euarthropoda sensu Walossek, 1999
Eucrustacea sensu Walossek, 1999
Peracarida Calman, 1904
Tanaidacea Dana, 1849
Tanaidomorpha Sieg, 1980

***Tanaidaurum* gen. nov.**
https://zoobank.org/EC1E9DC2-E223-494E-9379-FE20F10700D2

Type species. *Tanaidaurum kachinensis* sp. nov.

***Tanaidaurum kachinensis* sp. nov.**
https://zoobank.org/E14D2DF3-4675-4421-98F2-A2E32E11ADC1

Type material. ***Holotype*** SNHMB.G 8008.

Etymology. “Tanaid” in reference to Tanaidacea + “*aurum*” (“gold” in Latin) in reference to the golden appearance of the preservation. The specific epithet “kachinensis” refers to the Kachin State in Myanmar, where the specimens come from.

Diagnosis. Body cylindrical, surface smooth. Shield with set off triangular sclerite postero-laterally on each side. Antennula with four elements. Antenna uniramous, four elements. Appendages of post-ocular segment 7 (‘cheliped’) with ischium not separated from basipod. Appendages of post-ocular segments 8–10 (trunk appendages 1–3; ‘pereopods’ 1–3) slender, ischium separated from basipod; distal part of dactylus (‘unguis’) distinctly sclerotized, elongated, separated from proximal part of dactylus. Appendages of post-ocular segments 11–13 (trunk appendages 4–6; ‘pereopods’ 4–6) stouter, ischium separated from basipod; one pair of distal spines on merus, carpus and propodus; dactylus curved, specialized as a claw, no distinct separate part (‘unguis’’) apparent. Group of short setae in the lateral margin of pleon segments. Uropods with endopod and exopod differing slightly in length, two elements in both rami with terminal long setae.

Description. ***Overall morphology.*** Body longer than wide, differentiated into functional head and trunk, the

latter further subdivided into an anterior part and posterior part. Functional head ('cephalothorax') composed of eight segments: six segments of the ancestral eucrustacean head (ocular segment + post-ocular segments 1–5: segments of antennula and antenna accessible, mandible, maxillula and maxilla not accessible) + two anterior trunk segments (post-ocular segments 6–7: segments of maxilliped and 'cheliped' accessible). Segments of functional head dorsally conjoined forming a distinct shield ('carapace'). Anterior part of the trunk ('pereon') composed of six segments (post-ocular segments 8–13, 'pereon' segments 1–6). Posterior part of the trunk (pleon) composed of five free segments (post-ocular segments 14–19, pleon segments 1–5) and a pleotelson (post-ocular segment 14, pleon segment 6 conjoined to the telson) (Figs 1–3).

Functional head (cephalothorax). Dorsally accessible, one-fourth of the length of the entire body (body length measured from anterior edge of shield to tip of telson (Table 1); surface of shield smooth, postero-lateral edges with set off triangular sclerites. Compound eyes, protruding antero-laterally (Figs 2B, 4). Appendages of functional head. Antennula and antenna (appendages of post-ocular segments 1, 2) arising anterior-medially. Most mouthparts not accessible (appendages of post-ocular segments 3–5). Two distal elements of maxilliped (appendage of post-ocular segment 6) and cheliped (appendage of post-ocular segment 7).

Antennula longer, broader and dorsally displaced in relation to antenna; four elements, proximal-most element longest and broadest, subsequent elements progressively shorter than proximal one, at least one long seta arising in the connective joint between elements 1 and 2, as well as 3 and 4, at least five shorter setae in the anterior part of distal-most element.

Antenna shorter and slenderer than antennula, four elements, proximal-most elements 1 (coxa?) and 2 (basipod?) shorter and broader than subsequent elements

Table 1. Measurements of Tanaidacea specimens preserved in amber. All measurements in millimetres, except ratios.

Measurements	Specimens	
	SNHMB.G 8008	BUB 4227-1
Body (B)	1.77	1.84
'Cephalothorax' (Ct)	0.30	0.39
Anterior trunk (T)	1.08	0.97
Pleon (Pl)	0.40	0.48
Anterior trunk segment 3 (Ts3)	0.12	0. 12
Anterior trunk segment 4 (Ts4)	0.14	0. 12
Anterior trunk segment 5 (Ts5)	0.16	0. 13
Anterior trunk segment 6 (Ts6)	0.25	0.20
Anterior trunk segment 7 (Ts7)	0.24	0.21
Anterior trunk segment 8 (Ts8)	0.18	0. 18
Pleon segment 1 (Pl 1)	0.06	0.06
Pleon segment 2 (Pl2)	0.07	0.06
Pleon segment 3 (Pl3)	0.06	0.07
Pleon segment 4 (Pl4)	0.05	0.06
Pleon segment 5 (Pl5)	0.05	0.07
Pleotelson (Plt)	0.11	0.16

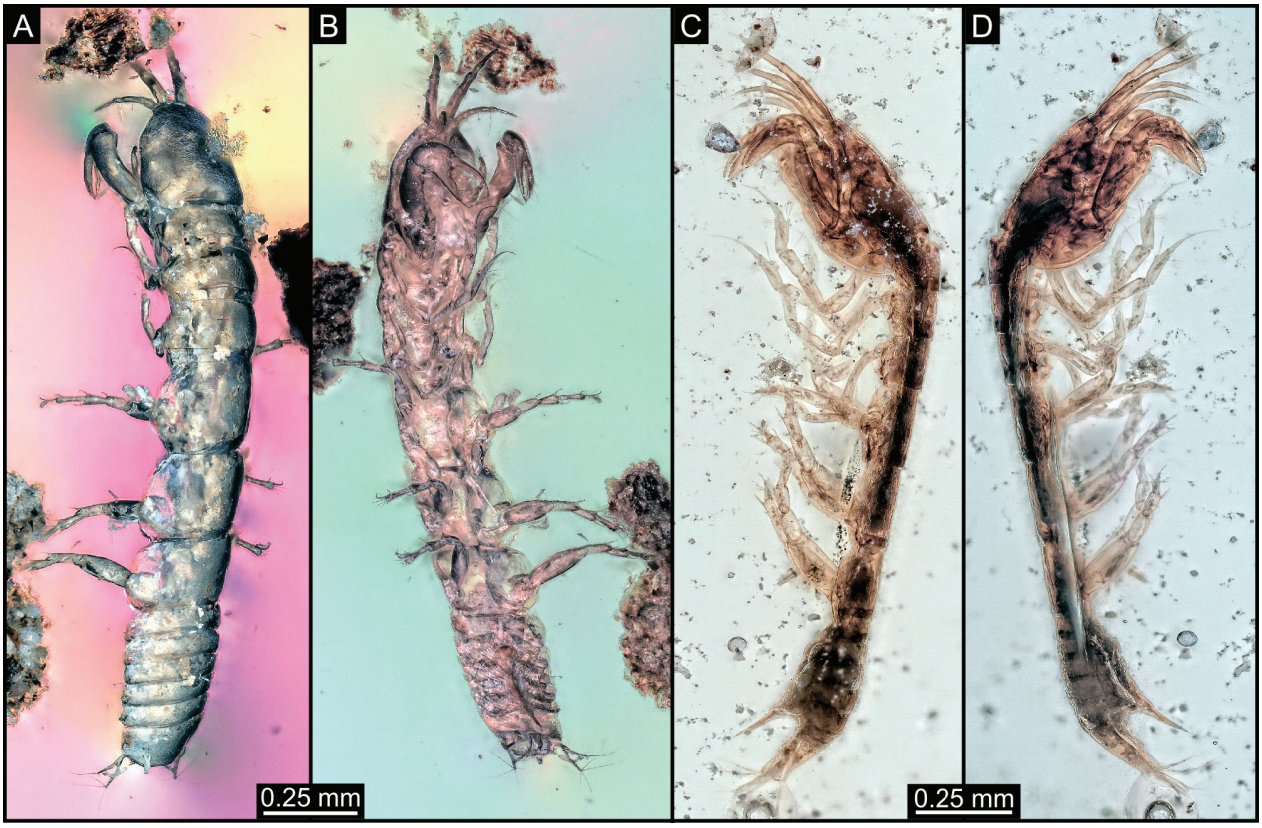

Figure 1. Digital microscopy images of *Tanaidaurum kachinensis* gen. et sp. nov.. Specimen SNHMB.G 8008 in dorsal (**A**) and ventral (**B**) views. Specimen BUB 4227-1 in lateral view, left (**C**) and right (**D**) sides. Co-axial polarized light with black (**A, D**) and white (**B, C**) backgrounds.

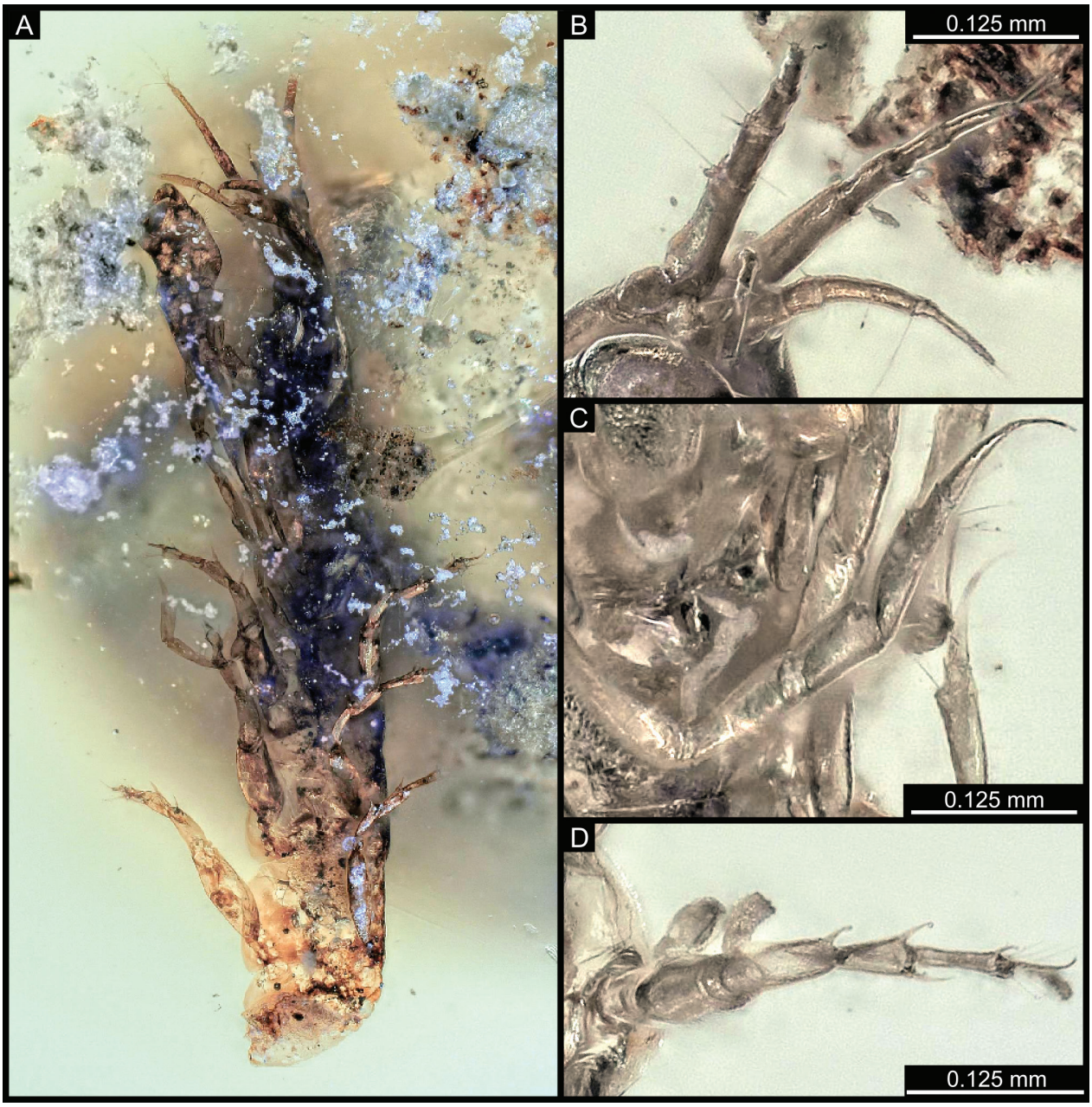

Figure 2. Digital microscopy images of *Tanaidaurum kachinensis* gen. et sp. nov. Specimen BUB 4227-2 in ventral view (**A**), ring light with white background. Detail of anterior part of functional head, showing compound eye, antennula and antenna (**B**). Detail of trunk appendage 1 (**C**), detail of trunk appendage 4 (**D**) of the holotype.

(endopod?), element 3 longest, at least one long seta arising in the connective joint between elements 3 and 4, at least two shorter setae in the anterior part of distal-most element.

Maxilliped with two distal elements accessible, anterior margin of distal-most element convex with at least five setae. 'Cheliped' with five elements accessible most likely representing basipod, merus, carpus, propodus and dactylus; basipod wider than long (2×), merus sub-triangular in ventral view, carpus longer than wide (2×), propodus with cone-like projection (fixed-finger) longer than wide (2×), fixed finger with five setae on inner surface, dactylus as long and wide as fixed finger, tapering distally (Figs 1, 4).

Anterior trunk (free thorax, 'pereon'). Six free segments, dorsally each with a tergite; tergites sub-equal in shape, anterior and posterior margins straight, lateral margins semi-circular; tergite of trunk segments 3–5 (post-ocular segments 8–13) gradually increasing in length, tergites of trunk segments 6 and 7 (post-ocular segments 11 and 12) longest, tergite of trunk segment 8 (post-ocular segment 13) slightly shorter than previous segment; width not accessible. Surface of tergites smooth, except for transversal rim near the posterior margin; sclerites of ventral surface (sclerites) smooth.

Anterior trunk appendages ('pereopods'). Appendages of trunk segments 3–5 sub-equal in shape, each with seven elements: coxa, basipod, ischium, merus, carpus,

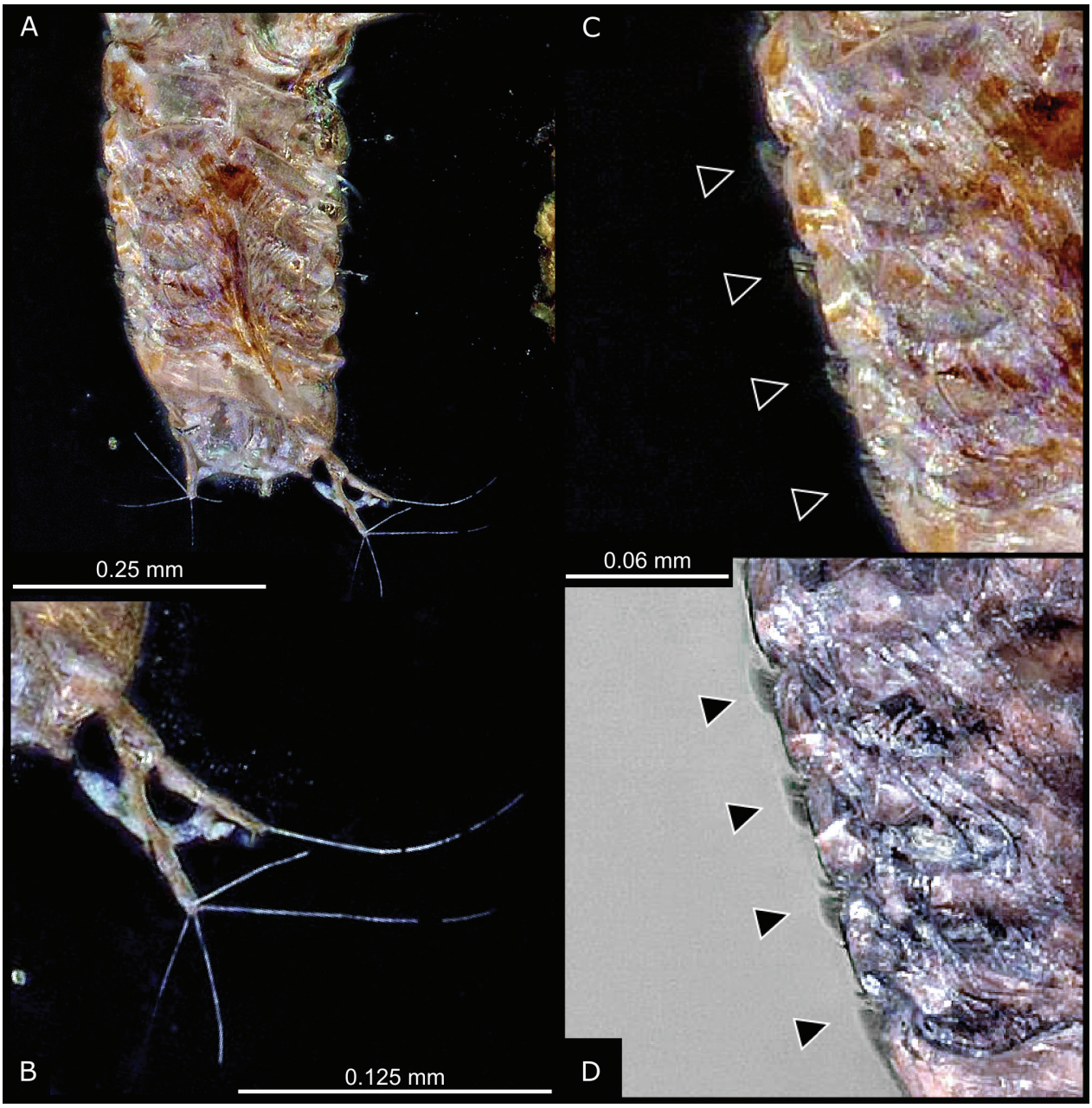

Figure 3. Digital microscopy images of *Tanaidaurum kachinensis* gen. et sp. nov. Holotype, ventral view of the pleon (**A**). Detail of uropod (**B**). Detail of pleon segments (**C, D**), arrow heads point to bundles of setae in the lateral margin of the pleon segments.

propodus and dactylus; coxa wider than long (1.8×), basipod longest element, longer than wide (3.5×), ischium wider than long (1.5×), carpus, merus and propodus subequal, longer than wide (1.5×), dactylus almost as long as basipod, proximal part of dactylus short, as long as wide, distal part of dactylus ('unguis') slender and elongated, tapering distally, at least one seta in carpus/propodus and one in propodus/dactylus connective joints; trunk appendages 6–8 sub-equal in shape, stouter than trunk appendages 3–5, six elements, from proximal to distal: possibly basipod, ischium, merus, carpus, propodus and dactylus; basipod longest and widest element, longer than wide (2×), ischium ring-like, merus, carpus and propodus sub-equal in length and shape, longer than wide (2.5×) with two spines latero-distally positioned, dactylus without distinct differentiation (no 'unguis' apparent), dactylus sickled-shaped (specialized as claw), at least four setae in propodus/dactylus connective joint (Figs 2C, D, 4).

Posterior trunk (pleon). Five free segments, dorsally with tergites; tergites sub-equal in shape, each half of the length of the tergites of the first free thorax segment and same width of these anterior and posterior margins straight, lateral margins semi-circular with group of short setae (Fig. 3), surface smooth; sclerites in ventral surface (sternites) with mid furrow in antero-posterior direction; pleotelson about twice the length of last free pleon segment, semi-circular posterior margin, dorsal and ventral surfaces smooth.

Pleon appendages (pleopods). Each free pleon segment bears one pair of appendages (pleopods), only distal por-

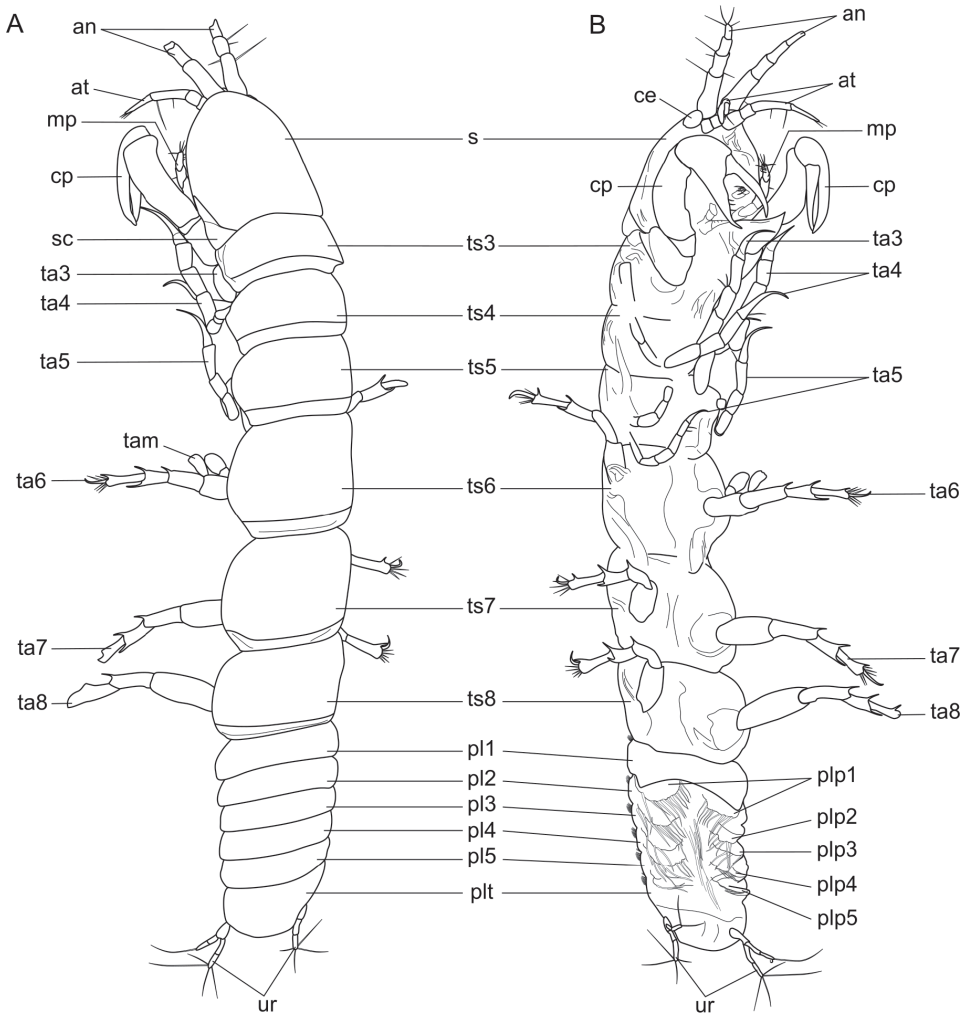

Figure 4. Digital drawing of *Tanaidaurum kachinensis* gen. et sp. nov. Holotype in dorsal (**A**) and ventral (**B**) views. Abbreviations: at: antenna, an: antennula, ce: compound eyes, cp: 'cheliped', mp: maxilliped, pl1–5: pleon segment 1–5, plp1–5: pleopod 1–5, plt: pleotelson, s: shield ('carapace'), sc: sclerite, ta3–8: trunk appendage 3–8, tam: trunk appendage muscle tissue, ts3–8: trunk segment 3–8, ur: uropod.

tion of pleopods accessible, distal margin semi-circular bearing many setae. Unclear if uniramous or biramous; pleotelson bearing one pair of uropods (appendage of pleon segment 6) latero-posteriorly arising from pleotelson; uropods with basipod bearing two rami – endopod and exopod; basipod shorter and wider than rami; endopod longer than exopod (1.18×), two elements: proximal element longer than wide (5×), distal element longer than wide (2.5×), at least four long setae distally; exopod with two elements: proximal element longer than wide (3×), distal element longer than wide (5×), at least two long setae distally (Fig. 3B).

Discussion

Systematics and fossil record of Tanaidacea

Generally three morphotypes are recognized within Tanaidacea: anthracocaridomorphan-type tanaidaceans, apseudomorphan-type tanaidaceans and tanaidomorphan-type tanaidaceans. Only the third appears to correspond to a distinct monophyletic group Tanaidomorpha, the other two groups seem to be characterised by plesiomorphies only and do not seem to represent natural groups. All three morphotypes are known from fossils.

Anthracocaridomorphan-type tanaidaceans (often erroneously recognised as a monophyletic group "Anthracocaridomorpha") are only known from fossils. The morphotype is recognized by the plesiomorphic condition of a pleon having six free segments and telson. All of the five anthracocaridomorphan-type species are based on rock fossils. Their records range from the early Carboniferous (Mississippian, circa of 358 million years ago) with *Anthracocaris scotica* (Peach, 1882), which provided the name for the morphotype, to the Middle Jurassic (between approximately 170 to 166 million years ago) with *Niveotanais brunnensis* Polz, 2005 (Fig. 5).

The ingroup of Tanaidacea including the apseudomorphan-type representatives and Tanaidomorpha has mostly extant representatives, but has a quite intriguing fossil record. The novelty characterizing this group is the presence of a pleotelson (sixth pleon segment conjoined to the telson). The oldest fossil of the apseudomorphan-type

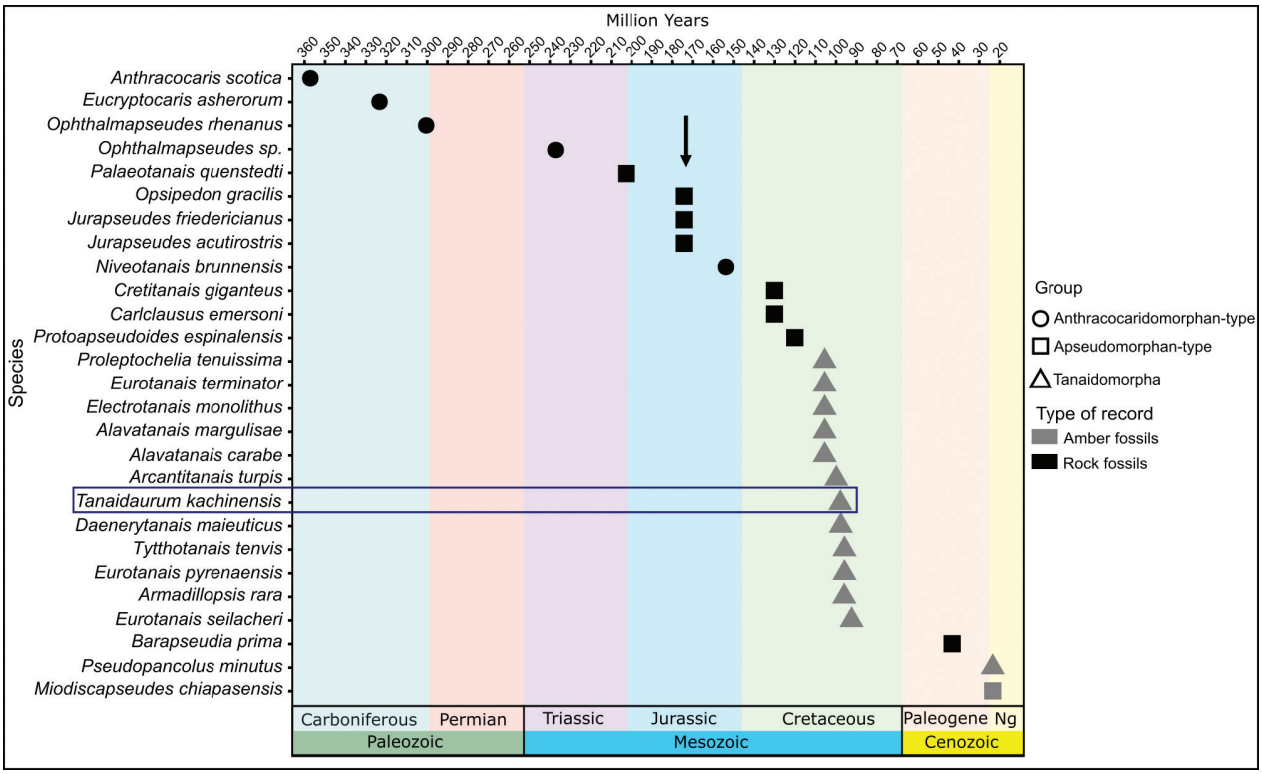

Figure 5. Temporal distribution of the fossil record of Tanaidacea. The black arrow indicates the first record of a tanaidacean with a pleotelson preserved, and the new species is highlighted by a blue rectangle.

(the supposed group "Apseudomorpha" was shown to be not a natural group repetitively; Siewing 1953; Drumm 2010; Kakui et al. 2011) is *Palaeotanais quenstedti* Reiff, 1936 from the Early Jurassic of Germany (Rhaetian to Toarcian, circa of 200 to 180 million years ago). The fragmentary condition of the trunk does not provide information whether the species indeed had a pleotelson or not. Still, it was interpreted as an apseudomorphan-type tanaidacean due to the combination of: 1) presence of antero-lateral processes in the anterior trunk segments, and 2) presence of lateral protrusions in the pleon segments (tergopleura). These two characters in combination are found only in extant apseudomorphan-type tanaidaceans (Schädel et al. 2019). Unfortunately, there is no preservation of the appendages of *Palaeotanais quenstedti*.

The oldest fossil record of a tanaidacean with a pleotelson preserved is *Opsipedon gracilis* (Heer, 1865) from the Middle Jurassic (lower Aalenian, circa of 174 to 172 million years ago). Currently, there are nine formally described species of apseudomorphan-type fossils; most are rock fossils, the only exception so far is *Miodiscapseudes chiapensis* Heard, 2018, from the Early Miocene (Aquitanian, circa of 23 million years ago) Mexican Amber of the Chiapas region (also known as "Chiapas amber") (Heard et al. 2018).

The group Tanaidomorpha, and the corresponding morphotype, is characterised by several apomorphic characters: 1) antennula uni-flagellate, 2) antenna uniramous, 3) cheliped and trunk appendage 1 without exopod. The monophyly of Tanaidomorpha is further supported by molecular phylogenetic analyses (Drumm 2010; Kakui et al. 2011). The fossil record of Tanaidomorpha is restricted to fossils preserved in amber (Fig. 5). Most of the species are from the Cretaceous, with the exception of *Pseudopancolus minutus* from early Miocene Mexican Chiapas Amber (Aquitanian, circa of 23 million years old; Heard et al. 2018). The fossils described here possess apomorphies that characterize Tanaidomorpha and are therefore an addition to the Cretaceous record of tanaidomorphans.

Relationships and fossil record of Tanaidomorpha

When dealing with fossils, there is a limited number of characters available to differentiate species. Mouthparts that are usually used for differentiating among extant species are rarely visible in fossils. Here we will focus in discussing characters that are available in most of the fossils of Tanaidomorpha.

Tanaidomorpha is generally differentiated into three morphotypes, tanaidoidean-type, paratanaoidean-type and neotanaoidean-type (Kakui et al. 2011, 2012). The first two seem to correspond to monophyletic groups, Tanaidoidea and Paratanaoidea. Neotanaoidean-type tanaidaceans are only characterised by plesiomorphies (cheliped and anterior trunk appendages with ischium separated from basipod, five pairs of pleopods, uropods biramous). A possible apomorphic character uniting them is the number of elements of the uniramous antenna: neotanaoidean-type tanaidaceans have nine elements in the antenna, while tanaidoideans and paratanaoideans usual-

ly have less than that. Yet, this number is highly variable within Tanaidacea.

Neotanaoidean-type tanaidaceans are restricted to deep-sea environments and have no fossil record so far. Regarding relationship of neotanaoidean-type tanaidaceans within Tanaidomorpha, there are two competing hypotheses: ((Neotanaoidea + Tanaidoidea) + Paratanaoidea) which is supported by molecular data (Kakui et al. 2011), while (Neotanaoidea+(Paratanaoidea+Tanaidoidea)) is supported by morphological data (Lang 1956). Given the fact that even the monophyly of a supposed group "Neotanaoidea" is not well established, we follow here the scheme of (neotanaoidean-type tanaidaceans + (Paratanaoidea+Tanaidoidea)).

The group Tanaidoidea is characterised by three apomorphic characters: 1) pleon segments 4 and 5 narrower than pleon segments 1–3, 2) only three pairs of pleopods, and 3) uropods uniramous. Additionally, tanaidoideans have antennae with 6–8 elements. The only fossil record of the ingroup Tanaidoidea is *Pseudopancolus minutus* (Heard et al. 2018) from early Miocene Chiapas, Mexico.

All other fossils from Cretaceous ambers have been considered to be representatives of Paratanaoidea. However, the relationships of the fossils to extant ingroups of Paratanaoidea are not clearly resolved. Chelipeds with the ischium not separated from the basipod (also referred as "absence of ischium" in the literature) can be considered as a synapomorphy of the unnamed group Paratanaoidea + Tanaidoidea. There seem to be chelipeds with an ischium separated from the basipod that occur in the tanaidoidean species-group *Tanais*, but this would then represent an evolutionary reversal. Anterior trunk appendages with the ischium not separated from the basipod was considered an apomorphic character of Tanaidoidea (Sieg 1980). Yet, also here one ingroup represents an exception: representatives of the species-group *Arctotanais* have anterior trunk appendages with the ischium separated from the basipod (Kakui et al. 2012). Also here this character state needs to be understood as a reversal.

The fossils described here, like most tanaidaceans from Cretaceous ambers, have the following characters states: 1) chelipeds without a separated ischium (apomorphy of Paratanaoidea+Tanaidoidea), 2) anterior trunk appendages with a separated ischium (plesiomorphy of Tanaidacea), 3) biramous appendages (plesiomorphy of Tanaidacea), and 4) the last two free pleon segments are never reduced in width (plesiomorphy of Tanaidacea). This combination of characters suggests the Cretaceous fossils are representatives of the group Paratanaoidea+Tanaidoidea. Furthermore, they lack the apomorphic character for Tanaidoidea. Therefore, they basically resemble modern paratanaoideans. Yet, with this character combination the fossils could indeed be branching off the lineage towards modern paratanaoideans, but also off the early lineage towards modern tanaidoideans (before their apomorphy has evolved), but also in the direct (stem-)lineage towards Paratanaoidea+Tanaidoidea.

Species delimitation: comparison to other Cretaceous fossils

The body ratios are quite stable among Cretaceous tanaidaceans (Fig. 6), also seen in extant tanaidaceans

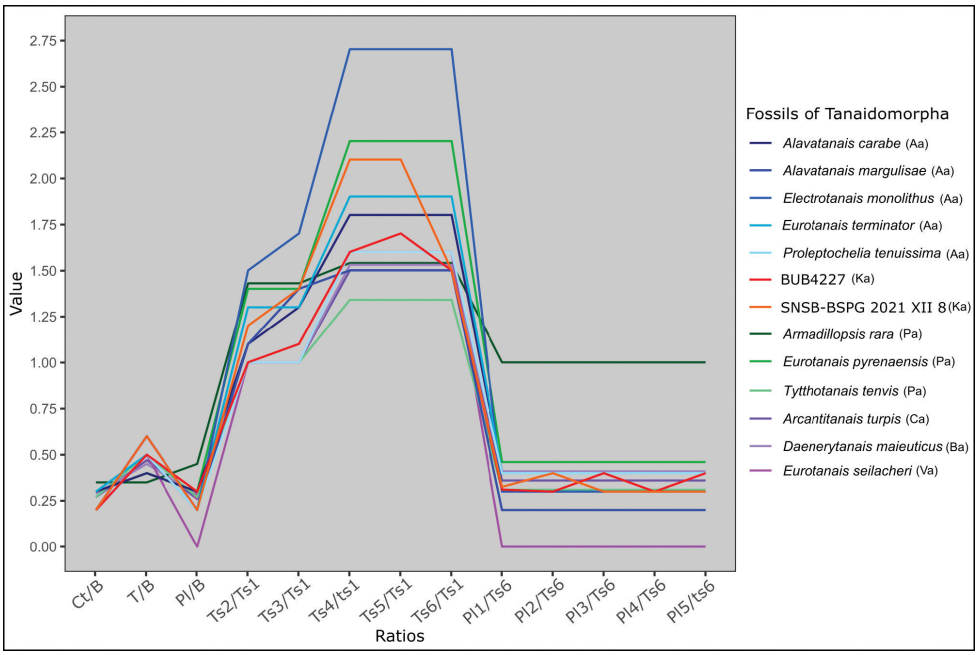

Figure 6. Parallel coordinates chart of the body ratios of Cretaceous tanaidomorphan crustaceans. The ratios were obtained dividing the lengths of different body parts. Abbreviations: Aa: Álava amber, B: body (except of appendages), Ba: La Buzinie amber, Ca: Charentese Amber, Ct: functional head ("cephalothorax"), Ka: Kachin amber, Pa: Pyrenean amber, Pl: pleon, Pl1–5: pleon segments 1–5, T: anterior trunk (free thorax), Ts: anterior trunk segments, Ts3–8: trunk segments 3–8, Va: Vendean amber.

(Schädel et al. 2019). Still, there are some variances, like *Armadillopsis rara* from Pyrenean Amber of France, which has a shorter anterior trunk in relation to the pleon, and the new Kachin fossils described here in which the last trunk segment is shorter than the previous ones. In the remaining Cretaceous tanaidaceans, the last three anterior trunk segments have the same length (Fig. 6).

From the species preserved in Cretaceous amber, *Tanaidaurum kachinensis* gen. et sp. nov. has most morphological similarities to *Proleptochelia tenuissima* Vonk & Schram, 2007 from the Álava Amber, Upper Cretaceous (Albian, circa of 110–105 million years old), the oldest representative of Paratanaoidea+Tanaidoidea, especially in the shape of the chelipeds, anterior trunk appendages and the uropods. The biramous uropods of Cretaceous tanaidomorphans have either symmetric or asymmetric rami, i.e., endopod and exopod with a small (< 2) or large (≥ 4) difference in length, respectively (Fig. 7). In the Kachin species both rami have a small difference in length, are more symmetric, and have two elements with terminal long setae, as *Proleptochelia tenuissima*.

The number of elements in the antennula and antenna of tanaidomorphans varies greatly, and although it is useful to differentiate among species, its phylogenetic value remains to be investigated. Different from all other fossil or extant tanaidaceans, *Tanaidaurum kachinensis* gen. et sp. nov. has four elements in both antennula and antenna. The shape of the anterior trunk appendages is conspicuously similar among Cretaceous tanaidaceans, including the species here described. Trunk appendages 4–6 have a hook-shaped dactylus. Today, this character is present in different ingroups of Paratanaoidea, almost exclusively in shallow-water forms (Larsen and Wilson 2002). This is compatible with a fossil preserved in amber. Likewise, it is safe to assume that *Tanaidaurum kachinensis* gen. et sp. nov. lived in shallow water specimen; however, it is unclear from its morphology if it represents a freshwater or marine organism. Kachin amber is formed by resin from trees possibly in a proximity to the sea, in an area with occasional flooding (Schädel et al. 2021a, b).

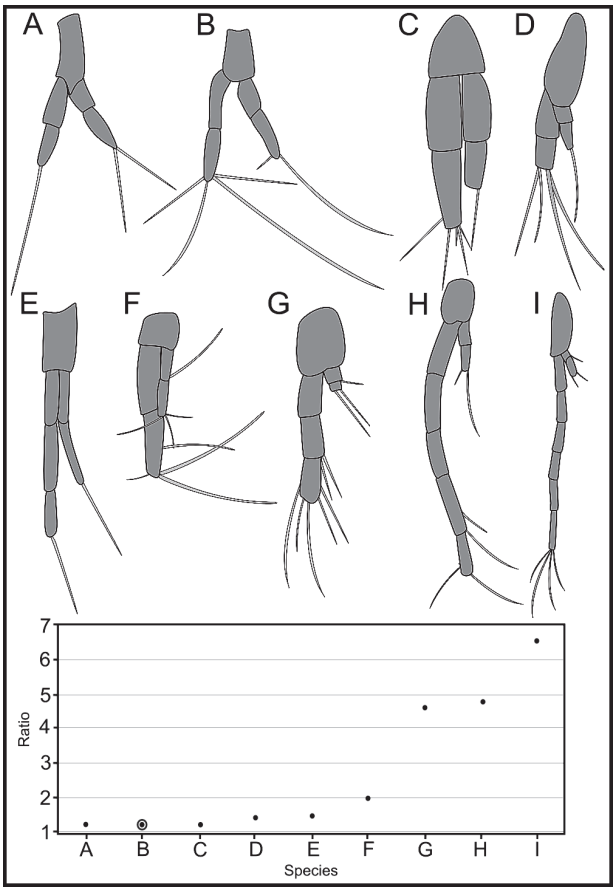

Figure 7. Restoration of the preserved uropods of Cretaceous tanaidomorphan crustaceans. **A.** *Proleptochelia tenuissima* (after Vonk and Schram 2007, fig. 3–5); **B.** *Tanaidaurum kachinensis* gen. et sp. nov.; **C.** *Armadillopsis rara* (after Sánchez-García et al. 2016, fig. 6C); **D.** *Tytthotanais tenvis* (after Sánchez-García et al. 2016, fig. 7A); **E.** *Alavatanais margulisae* (after Sánchez-García et al. 2017, fig. 6F); **F.** *Arcantitanais turpis* (after Sánchez-García et al. 2016, fig. 10C); **G.** *Alavatanais carabe* (after Sánchez-García et al. 2015, fig. 1E); **H.** *Electrotanais monolithus* (after Sánchez-García et al. 2015, fig. 9H); **I.** *Eurotanais pyrenaensis* (after Sánchez-García et al. 2016, fig. 3F), and plot of the uropods ratio (length of the endopod / length of the exopod). The uropod of the new species (**B**) is highlighted by a grey circle.

The biased fossil record of Tanaidacea

It is important to note that the fossil record of Tanaidacea is largely biased and, therefore, we need to make some remarks before continuing. So far, all records come from the northern hemisphere. This point is very likely to be of historical aspect than representing true palaeogeographic distribution, since most of palaeontological research has been developed in the northern hemisphere in the last centuries. About half of the fossil species described are based on specimens preserved as rock fossils and about the other half are specimens preserved in amber (Fig. 4). This situation possibly leads to an underestimating of the number of species in some ingroups. Specimens preserved as rock fossils preserve less details, specimens preserved in amber are usually preserved in greater detail.

This fact appears especially problematic, because the rock fossils interpreted as representatives of Tanaidacea are very fragmentary and some species, such as *Carlclausus emersoni* Schram et al., 1986, have been described from isolated pieces of the anterior trunk and pleon. Also, isolated pieces such as chelae, rather common in some fossil sites, have been attributed to species described from other body parts. This "fossil-Frankenstein" approach is quite common and to a certain degree useful in palaeontology because it avoids description of new species to every isolated remain found. Yet, it is not ideal, because most fossil groups have a rather complicated fossil record. The strategy is likely driven as many researchers believe that to attribute a name to a specimen facilitates communication. In an attempt to cope with the

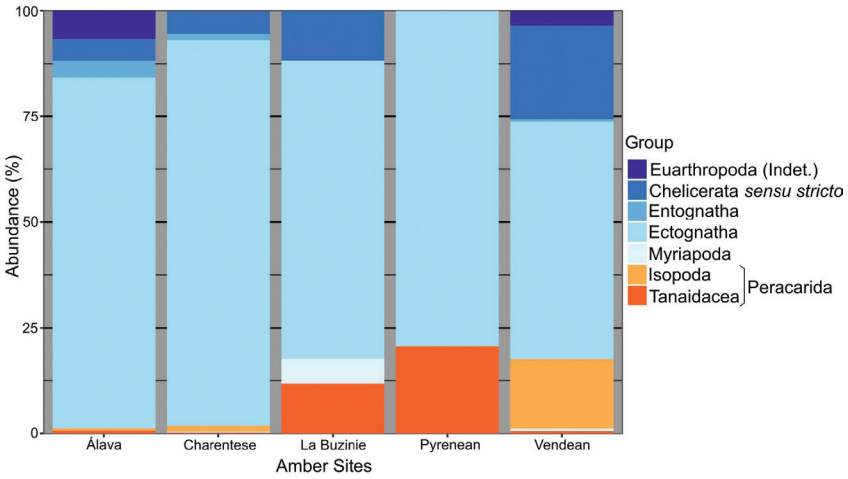

Figure 8. Relative abundances of different ingroups of Euarthropoda in different amber deposits from the Cretaceous.

fragmentary record of Tanaidacea, Schädel et al. (2019) employed a morphometric approach to interpret an isolated fragment of anterior trunk and pleon to Tanaidacea, which proved to be useful. Their analysis showed the ratios of anterior trunk and pleon segments are very stable in different ingroups of Eumalacostraca (except for Isopoda), especially in Tanaidacea. Yet, it is not clear if this relationship has phylogenetic value among different ingroups of Tanaidacea.

Amber inclusions: relative abundance of tanaidaceans

Cretaceous ambers are a great window for past diversity, especially morphological diversity, in many lineages of Euarthropoda. So far, tanaidaceans have been reported from Cretaceous amber sites in Spain and France. The fossils reported here represent the first record of Cretaceous tanaidaceans outside Europe. Aquatic organisms are not likely to be preserved in tree resins when compared to mainly terrestrial animals, such as beetles and alike, but it is taphonomically possible as shown, for example, by Schmidt and Dilcher (2007), Schmidt et al. (2018), or Schädel et al. (2021a, b). The abundance (i.e., number of specimens) of eumalacostracan records in Cretaceous amber sites is usually very low when compared to other lineages of Euarthropoda. Still there are some amber deposits, such as the French La Buzinie and Pyrenean, where tanaidaceans account for a great percentage of the discoveries (Fig. 8). According to Perrichot et al. (2007), La Buzinie yields seventeen specimens of Euarthropoda preserved in amber, two specimens are tanaidaceans comprising circa 11% of the records. From the 29 specimens of Euarthropoda found in the Pyrenean amber, six specimens are tanaidaceans, circa 20% (Perrichot et al. 2007). In the Vendean amber, from 171 fossil of Euarthropoda, 29 are representatives of Isopoda, accounting for remarkably circa 16% of the assemblage (Perrichot and Néraudeau 2014).

These numbers of crustaceans are extremely high when compared to the French Charentese amber, where from the 760 fossils of Euarthropoda, circa 2.58% are peracaridans, namely one specimen of Tanaidacea and eleven of Isopoda. Also, in the Spanish Álava amber, where from more than 2,300 fossils of Euarthropoda have been found, peracaridan crustaceans (Isopoda and Tanaidacea) represent circa of 1.22% of the total assemblage (Delclòs et al. 2007; Peñalver and Delclòs 2010).

Future studies increasing the overall number of specimens will likely approximate the relative abundance of different euarthropodan groups of the French La Buzinie, Pyrenean and Vendean amber deposits to Charentese and the Spanish Álava. Until this date there is no information on how many specimens of Euarthropoda Kachin amber has provided, but we can possibly expect similar numbers of abundance as Charentese and Álava.

Regarding diversity, from the 49 specimens of Tanaidacea found in Cretaceous amber deposits, there are 14 different formally described species. All of them are representatives of the group Paratanaoidea+Tanaidoidea, suggesting the Cretaceous was a period of diversification of Tanaidomorpha. Still, the gross morphology of the Cretaceous species is very similar to modern day paratanaoideans, and the only record of a fossil tanaidacean presenting the apomorphies of modern tanaoideans, *Pseudopancolus minutus* Heard, 2018, is from the Miocene (circa of 20 million years ago) Mexican Chiapas amber. This suggests that the diversification of Tanaidoidea happened after the Cretaceous-Paleogene extinction.

Conclusions

We describe a new species of Tanaidacea, *Tanaidaurum kachinensis* gen. et sp. nov., from Kachin amber (100 million years old). The new species is a representative of the group Tanaidomorpha, part of the Cretaceous diversification of the unnamed ingroup Paratanaoidea+Tanaidoidea. It has most morphological similarities to *Proleptochelia tenuissima*

Vonk & Schram, 2007 from the Álava Amber, Upper Cretaceous (Albian, ca. 110–105 million years old) of Spain. This is the first record of a Cretaceous tanaidacean outside Europe. So far, all Cretaceous tanaidaceans are representatives of Paratanaoidea+Tanaidoidea. Modern tanaidoideans only appear in the Miocene, suggesting the diversification of Tanaidoidea happened after the Cretaceous-Paleogene extinction.

Acknowledgements

We sincerely thank the editor Alexander Schmidt, Ronald Vonk and an anonymous reviewer for their comments and contribution to this paper. We are grateful to the Museum für Naturkunde, Berlin, for support with the coverage of the Article Processing Charges. PGP was supported by Capes/Doctoral Program (CAPES/DAAD/CNPQ, Notice n°. 15–2017/ Process n° 88887.161379/2017–00). JTH is supported by the Volkswagen Foundation with a Lichtenberg Professorship.

References

Badano D, Engel MS, Basso A, Wang B, Cerretti P (2018) Diverse Cretaceous larvae reveal the evolutionary and behavioural history of antlions and lacewings. Nature Communications 9: 3257. https://doi.org/10.1038/s41467-018-05484-y

Broly P, Maillet S, Ross AJ (2015) The first terrestrial isopod (Crustacea: Isopoda: Oniscidea) from Cretaceous Burmese amber of Myanmar. Cretaceous Research 55: 220–228. https://doi.org/10.1016/j.cretres.2015.02.012

Calman WT (1904) On the classification of the Crustacea Malacostraca. Annals & Magazine of Natural History 13(74): 144–158. https://doi.org/10.1080/00222930408562451

Dana JD (1849) Conspectus Crustaceorum quae in Orbis Terrarum Circumnavigatione, Carolo Wilkes e Classe Reipublicae Foederatae Duce, lexit et descripsit. The American Journal of Science and Arts, Series 2 8: 424–428. https://doi.org/10.2307/20021076

Delclòs X, Arillo A, Peñalver E, Barrón E, Soriano C, Valle RLD, Bernárdez E, Corral C, Ortuño VM (2007) Fossiliferous amber deposits from the Cretaceous (Albian) of Spain. Comptes Rendus. Palévol 6(1–2): 135–149. https://doi.org/10.1016/j.crpv.2006.09.003

Drumm DT (2010) Phylogenetic relationships of Tanaidacea (Eumalacostraca: Peracarida) inferred from three molecular loci. Journal of Crustacean Biology 30(4): 692–698. https://doi.org/10.1651/10-3299.1

Hassack E, Holdich DM (1987) The tubicolous habit amongst the Tanaidacea (Crustacea, Peracarida) with particular reference to deep-sea species. Zoologica Scripta 16(3): 223–233. https://doi.org/10.1111/j.1463-6409.1987.tb00069.x

Haug C, Shannon KR, Nyborg T, Vega FJ (2013a) Isolated mantis shrimp dactyli from the Pliocene of North Carolina and their bearing on the history of Stomatopoda. Boletín de la Sociedad Geológica Mexicana 65(2): 273–284. https://doi.org/10.18268/BSGM2013v65n2a9

Haug JT, Müller CHG, Sombke A (2013b) A centipede nymph in Baltic amber and a new approach to document amber fossils. Organisms, Diversity & Evolution 13(3): 425–432. https://doi.org/10.1007/s13127-013-0129-3

Haug JT, Müller P, Haug C (2019) A 100-million-year-old predator: A fossil neuropteran larva with unusually elongated mouthparts. Zoological Letters 5(1): 29. https://doi.org/10.1186/s40851-019-0144-0

Haug JT, Haug GT, Zippel A, van der Wal S, Müller P, Gröhn C, Wunderlich J, Hoffeins C, Hoffeins H-W, Haug C (2021) Changes in the morphological diversity of larvae of lance lacewings, mantis lacewings and their closer relatives over 100 million years. Insects 12(10): 860. https://doi.org/10.3390/insects12100860

Heard RW, Serrano-Sánchez ML, Vega FJ (2018) Early Miocene Tanaidacea (Crustacea: Malacostraca) preserved in amber from Chiapas, Mexico, with the preliminary descriptions of new taxa. Neues Jahrbuch für Geologie und Paläontologie. Abhandlungen 288(1): 107–120. https://doi.org/10.1127/njgpa/2018/0726

Heer O (1865) Die Urwelt der Schweiz. Schulthess, Zürich (Switzerland), 700 pp.

Kakui K (2021) Tube-constructing paratanaoidean tanaidaceans (Crustacea: Peracarida): a brief review. Aquatic Animals AA2021: 1–5. https://doi.org/10.34394/aquaticanimals.AA2021.0_AA2021-4_4

Kakui K, Hiruta C (2017) Tube construction by a tanaidacean crustacean using a novel mucus secretion system involving the anal opening. Zoological Letters 3(1): 20. https://doi.org/10.1186/s40851-017-0082-7

Kakui K, Katoh T, Hiruta SF, Kobayashi N, Kajihara H (2011) Molecular systematics of Tanaidacea (Crustacea: Peracarida) based on 18S sequence data, with an amendment of suborder/superfamily-level classification. Zoological Science 28(10): 749–757. https://doi.org/10.2108/zsj.28.749

Kakui K, Kobayashi N, Kajihara H (2012) Phylogenetic position of *Arctotanais* in the suborder Tanaidomorpha (Peracarida: Tanaidacea). Journal of Crustacean Biology 32(1): 127–139. https://doi.org/10.1163/193724011X615406

Lang K (1956) Neotanaidae nov. fam., with some remarks on the phylogeny of the Tanaidacea. Arkiv för Zoologi 9: 469–475.

Larsen K (2003) Proposed new standardized anatomical terminology for the Tanaidacea (Peracarida). Journal of Crustacean Biology 23(3): 644–661. https://doi.org/10.1651/C-2363

Larsen K, Wilson GDF (2002) Tanaidacean phylogeny, the first step: The superfamily Paratanaidoidea. Journal of Zoological Systematics and Evolutionary Research 40(4): 205–222. https://doi.org/10.1046/j.1439-0469.2002.00193.x

Peach BN (1882) On some new Crustacea from the lower Carboniferous rocks of Eskdale and Liddesdale. Proceedings of the Royal Society of Edinburgh 30(1): 73–91. https://doi.org/10.1017/S0080456800028982

Peñalver E, Delclòs X (2010) Spanish amber. In: Penney D (Ed.) Biodiversity of Fossils in Amber from the Major World Deposits. Siri Scientific Press, Manchester (UK), 236–269.

Perrichot V, Neraudeau D, Nel A, De Ploeg G (2007) A reassessment of the Cretaceous amber deposits from France and their palaeontological significance. African Invertebrates 48(1) 213–227.

Perrichot V, Néraudeau D (2014) Introduction to thematic volume – Fossil arthropods in Late Cretaceous Vendean amber (northwestern France). Paleontological Contributions 2014(10A): 1–4.

Poinar Jr G (2020) A new genus of terrestrial isopods (Crustacea: Oniscidea: Armadillidae) in Myanmar amber. Historical Biology 32(5): 583–588. https://doi.org/10.1080/08912963.2018.1509964

Polz H (2005) *Niveotanais brunnensis* g. nov. sp. nov. (Crustacea: Tanaidacea: Anthracocaridomorpha) eine fossile Scherenassel aus den Plattenkalken von Brunn. Archaeopteryx 23: 57–66.

Reiff E (1936) Isopoden aus dem Lias Delta (Amaltheenschichten) Schwabens. Palaontologische Zeitschrift 18(1–2): 49–90. https://doi.org/10.1007/BF03041710

Ross AJ (2018) Burmese (Myanmar) amber taxa, on-line checklist v.2018.2, 105, n.d. https://doi.org/10.11646/palaeoentomology.2.1.5

Ross AJ (2019) Burmese (Myanmar) amber taxa, on-line supplement v.2019.2, 34, n.d. https://doi.org/10.11646/palaeoentomology.2.1.5

Sánchez-García A, Peñalver E, Pérez-de la Fuente R, Delclòs X (2015) A rich and diverse tanaidomorphan (Crustacea: Tanaidacea) assemblage associated with Early Cretaceous resin-producing forests in North Iberia: palaeobiological implications. Journal of Systematic Palaeontology 13(8): 645–676. https://doi.org/10.1080/14772019.2014.944946

Sánchez-García A, Peñalver E, Bird GJ, Perrichot V, Delclòs X (2016) Palaeobiology of tanaidaceans (Crustacea: Peracarida) from Cretaceous ambers: extending the scarce fossil record of a diverse peracarid group. Zoological Journal of the Linnean Society 178(3): 492–522. https://doi.org/10.1111/zoj.12427

Sánchez-García A, Delclòs X, Engel MS, Bird GJ, Perrichot V, Peñalver E (2017) Marsupial brood care in Cretaceous tanaidaceans. Scientific Reports 7(1): 4390. https://doi.org/10.1038/s41598-017-04050-8

Schädel M, Pazinato PG, van der Wal S, Haug JT (2019) A fossil tanaidacean crustacean from the Middle Jurassic of southern Germany. Palaeodiversity 12(1): 13–30. https://doi.org/10.18476/pale.v12.a2

Schädel M, Hyžný M, Haug JT (2021a) Ontogenetic development captured in amber – the first record of aquatic representatives of Isopoda in Cretaceous amber from Myanmar. Nauplius 29: e2021003. https://doi.org/10.1590/2358-2936e2021003

Schädel M, Hörnig MK, Hyžný M, Haug JT (2021b) Mass occurrence of small isopodan crustaceans in 100-million-year-old amber: An extraordinary view on behaviour of extinct organisms. PalZ 95(3): 429–445. https://doi.org/10.1007/s12542-021-00564-9

Schmidt AR, Dilcher DL (2007) Aquatic organisms as amber inclusions and examples from a modern swamp forest. Proceedings of the National Academy of Sciences of the United States of America 104(42): 16581–16585. https://doi.org/10.1073/pnas.0707949104

Schmidt AR, Grabow D, Beimforde C, Perrichot V, Rikkinen J, Saint Martin S, Thiel V, Seyfullah LJ (2018) Marine microorganisms as amber inclusions: Insights from coastal forests of New Caledonia. Fossil Record [Weinheim] 21(2): 213–221. https://doi.org/10.5194/fr-21-213-2018

Schram FR, Sieg J, Malzahn E (1986) Fossil Tanaidacea. Transactions of the San Diego Society of Natural History 21: 127–144. https://doi.org/10.5962/bhl.part.24579

Sieg J (1980) Sind die Dikonophora eine polyphyletische Gruppe? Zoologischer Anzeiger 205: 401–416.

Siewing R (1953) Morphologische Untersuchungen an Tanaidaceen und Lophogastriden. Zeitschrift für Wissenschaftliche Zoologie 157: 333–426.

Vonk R, Schram FR (2007) Three new tanaid species (Crustacea, Peracarida, Tanaidacea) from the Lower Cretaceous Álava amber in northern Spain. Journal of Paleontology 81(6): 1502–1509. https://doi.org/10.1666/05-020.1

Fossil Record 26 (1) 2023, 51–84 | DOI 10.3897/fr.26.100059

The easternmost record of the largest anguine lizard that has ever lived – *Pseudopus pannonicus* (Squamata, Anguidae): new fossils from the late Neogene of Eastern Europe

Erwan Loréal[1], Elena V. Syromyatnikova[2,3], Igor G. Danilov[3], Andrej Čerňanský[1]

1 *Department of Ecology, Laboratory of Evolutionary Biology, Faculty of Natural Sciences, Comenius University in Bratislava, Mlynská dolina, 84215 Bratislava, Slovakia*

2 *Borissiak Paleontological Institute, Russian Academy of Sciences, Profsoyuznaya 123, 117997, Moscow, Russia*

3 *Zoological Institute, Russian Academy of Sciences, Universitetskaya Emb. 1, 199034 St. Petersburg, Russia*

https://zoobank.org/EB01E77B-10FD-4D7F-82C3-6A241635F0FD

Corresponding author: Andrej Čerňanský (cernansky.paleontology@gmail.com)

Academic editor: Florian Witzmann ♦ **Received** 8 January 2023 ♦ **Accepted** 16 February 2023 ♦ **Published** 1 March 2023

Abstract

We here report on new material of *Pseudopus pannonicus*, the iconic and largest-known representative of the lizard clade Anguinae, from several late Neogene localities across Moldova, Ukraine, and regions of the North Caucasus – the last representing the easternmost known occurrence of this extinct species. Today, *Pseudopus apodus*, the last extant *Pseudopus* representative, is found in a variety of habitats ranging from South-East Europe to Central Asia. In the late Cenozoic of Europe, however, several extinct species of *Pseudopus* existed. Among them, interestingly, *P. pannonicus* displayed the largest spatiotemporal range of the genus, occurring from Spain to the North Caucasus and known from the Late Miocene to the Early Pleistocene. Although it has been reported in a plethora of European localities, *P. pannonicus* is a taxon "with several questionings related to its few diagnostic features vs. numerous features shared with *P. apodus*". The elements described here exhibit some variability, but their overall morphology undoubtedly resembles that of previously described material of *P. pannonicus*. The lacrimal from Tatareshty, moreover, represents the first fossil lacrimal reported for *P. pannonicus*. Besides, the fairly complete maxilla with a length of almost 3.7 cm is the largest maxilla ever reported for this taxon, expanding our knowledge of its gigantism. In addition, several features are described and discussed regarding their diagnostic relevance for *P. pannonicus*. The relationship between body size and some of these features was tested statistically. Consequently, two cranial characters and one vertebral feature peculiar to *P. pannonicus* were retained in the diagnosis of the species.

Key Words

Anguimorpha, Miocene, Moldova, North Caucasus, Pliocene, Ukraine

Introduction

This study is part of a larger project aimed at the taxonomical revision of *Pseudopus pannonicus* (Kormos, 1911). Among squamates, Anguidae represent a diversified and widely distributed group of reptiles from which Anguinae is the most derived clade (Augé 2005). Although there have been recent alterations to phylogenetical conceptions that have been stable for decades (e.g., Pyron et al. 2013; Burbrink et al. 2020) and the position of Diploglossidae is still debated (as a subclade of Anguidae, e.g., see Conrad 2008; Gauthier et al. 2012; Pyron et al. 2013; as a distinct clade outside of Anguidae, e.g., see Zheng and Wiens 2016; Burbrink et al. 2020), besides Anguinae three other extant clades are traditionally included in Anguidae. These are Gerrhonotinae, Anniellinae, and the extinct Glyptosaurinae (Sullivan 1979, 2019; Gauthier et

Copyright *Erwan Loréal et al.* This is an open access article distributed under the terms of the Creative Commons Attribution License (CC BY 4.0), which permits unrestricted use, distribution, and reproduction in any medium, provided the original author and source are credited.

al. 2012; Georgalis et al. 2021). Nowadays, anguines are represented solely by legless forms (note, however, that some fossil taxa were not legless, see Sullivan et al. 1999; Čerňanský and Klembara 2017) included in three genera: the glass lizard *Ophisaurus* Daudin, 1803 from Northern America, Southeast Asia [=*Dopasia* Gray, 1853], and Northern Africa [=*Hyalosaurus* Günther, 1873]; the slow worm *Anguis* Linnaeus, 1758 from Europe and Western Asia; and the Sheltopusik *Pseudopus* Merrem, 1820, from southeastern Europe, the Middle East and Central Asia (Estes 1983; Sindaco and Jeremčenko 2008; Jablonski et al. 2021). All three taxa are also present in the Neogene of Europe. A fourth anguine taxon, *Ragesaurus* Bailon & Augé, 2012, is also known from the Quaternary of Spain. This taxon is known by only a subcomplete dentary and is restricted to one locality on Islas Medas (Catalonia, Spain) (Bailon and Augé 2012). Recently, a fifth taxon - *Smithosaurus* Vasilyan, Čerňanský, Szyndlar & Mörs, 2022 was described from the Early and Middle Miocene of Germany and Austria (Vasilyan et al. 2022). Today, *Pseudopus* is represented only by a single extant species *Pseudopus apodus*. Populations of this species are considered to pertain to three sub-species: *Pseudopus apodus thracius* Obst, 1978 from the western-most part of the geographic range of the species (i.e., coastal Croatia, Greece, Northwestern Anatolia), *Pseudopus apodus apodus* Pallas, 1775 from Asia Minor and Central Asia, and *Pseudopus apodus levantinus* Jablonski, Ribeiro-Junior, Meiri, Maza, Mikulíček & Jandzik, 2021 from the Levant (Jandzik et al. 2018; Glavaš et al. 2020; Jablonski et al. 2021). The genus *Pseudopus* is also known in the fossil record by a plethora of upper Cenozoic remains from localities all across Europe (Klembara 1981; Klembara and Rummel 2018). There are currently four fossil species described: *Pseudopus ahnikoviensis* Klembara, 2012, *Pseudopus confertus* Klembara & Rummel, 2018, *Pseudopus laurillardi* (Lartet, 1851), and *P. pannonicus* (Kormos, 1911) (see Klembara and Rummel 2018). The latter is the largest anguine known with a skull length estimated around 90–100 mm (Estes 1983; Roček 2019). The temporal range of *P. pannonicus* spans the Upper Miocene (MN9) to the Lower Pleistocene (e.g., Čerňanský et al. 2017). As great as the temporal range of this species is its geographic range. Indeed, although most common in Central Europe, the presence of this species has been reported from fossil localities in Spain (Bailon 1991; Blain et al. 2016) to Ukraine (Alexejew 1912; Zerova 1993; Roček 2019) since its original description by Kormos (1911). On the other hand, apart from some notable contributions (Fejérváry-Lángh 1923; Roček 2019), few works tackled the diagnosis of *P. pannonicus* or examined intraspecific variation. In addition, few recent works described various fossil remains that were only identified as indeterminate anguines (Georgalis et al. 2018) or *Pseudopus* sp. (Georgalis et al. 2019a; Georgalis and Delfino 2022) because of preservation issues or restricted material for instance but for which suspicions of affinities towards *P. pannonicus* were hinted at. These reports are from the Balkans area, namely from Late Miocene Greek localities of Ravin de la Pluie and of Maramena, in which is recorded the Miocene-Pliocene transition (Georgalis et al. 2018, 2019a). If the *P. pannonicus* affinities, especially strong from Maramena, suggested by these authors were to be confirmed (see comments later in Results), these reports would thus document the most southward occurrences currently known for that species. The material described by Kormos (1911) originated from the type locality of Polgárdi 2 (Upper Miocene, Hungary) and consisted only of isolated remains, i.e., one premaxilla, one pterygoid and three dentaries of which none was formally established as either the holotype or as lectotypes for this newly described species. Therefore, in accordance with the ICZN (1999), these original specimens are, by definition, automatically and equally designated as the syntypes of this taxon. Several decades later, Estes (1983) referred to one of the most informative dentary from the original material figured by Kormos (1911), i.e., actually a syntype of *P. pannonicus* as emphasized hereabove, as the neotype of *P. pannonicus*:

"Neotype: HGI, dentary (KORMOS 1911, fig. 19); Pliocene, Polgardi, Hungary." (Estes 1983, 141).

More recently, Klembara and Rummel (2018) and Roček (2019) followed that statement from Estes (1983) and referred to that specimen from Polgárdi as a neotype as well, the former authors stating that no collection number was assigned to that particular specimen. However, by the ICZN definition, this specimen cannot be considered as a neotype. It is still unclear why this syntype specimen was referred to as a neotype rather than a lectotype or even an inferred holotype in the first place. It is especially puzzling when the apparent intent behind the words of this author is closest to that of a lectotype usage, and where, in the same publication, multiple uses of lectotypes can be recorded. Prior to the study of Estes, Młynarski (1956) does use the term "holotype" while mentioning the work of Kormos (1911). However, the former author did not specify any specimen in particular: "good photograph of his holotype (fragment of skull)" (Młynarski 1956, 142). Nonetheless, following the ICZN, as neither the exact term of "lectotype" was explicitly used, nor a holotype has been inferred from the original syntypes, the actions of Estes (1983) do not constitute a lectotype designation ([Art. 74], [ICZN] 1999). Thus, no lectotype is currently fixed for *Pseudopus pannonicus*. To alleviate this issue, we here formerly designate a lectotype for the anguine *Pseudopus pannonicus*. The lectotype specimen we select here is the left dentary MÁFI V 2023.1.14.1., the same specimen that was figured in the original description of this taxon (Kormos 1911, 63, Fig. 19 [i.e., the leftmost specimen]) and that was later referred to as a "neotype" by Estes (1983) and Roček (2019). Several features of that dentary are undoubtedly allowing us to identify it as the specimen figure by Kormos, but it should be noted that it has been

slightly damaged since its discovery. Indeed, a few anterior teeth are now broken off and the posterior end of the dentary is lightly damaged as well. In the prior literature, this specimen can be found under the former collection number Ob. 5058, following an older number formatting used previously by the Hungarian Geological Institute in Budapest, Hungary. With the designation of the lectotype here, all other remaining specimens figured by Kormos (1911) therefore lose the status of syntypes and are given the paralectotype status. These include two right dentaries, one premaxilla (currently missing) and a pterygoid (currently missing as well).

In any case, as of today, very few clearly defined apomorphic features are known for *Pseudopus pannonicus*. Yet, many works, including recent ones, have attributed numerous specimens to this taxon with limited argumentation or use of clear apomorphic criteria, sometimes even pointing at the lack of differences with *P. apodus* except for the large size of the bones described (e.g., Młynarski 1956, 1962; Bachmayer and Młynarski 1977; Młynarski et al. 1984; Kotsakis 1989; Tempfer 2009; see Blain et al. 2016 for summarizing comments about the *Pseudopus* material from the Iberian peninsula). Some of these identifications are not necessarily erroneous and are nothing more than the product of their time when differences between both taxa were not yet clearly established. Nonetheless, revisions of these copious amounts of fossils are much desired to update and complete these taxonomic statements with either restricted or no supporting evidence.

Moreover, due to the establishment of other binomina from nearby areas as well as several synonymization actions, the early taxonomic history of this taxon has been subjected to some confusion. Indeed, Bolkay (1913), following the work of Kormos (1911), described the new species *Ophisaurus intermedius*, *Anguis polgardiensis*, and *Varanus deserticolus*. The former two taxa, *O. intermedius* and *A. polgardiensis*, were subsequently treated as junior synonyms of *P. pannonicus* by Fejérváry-Lángh (1923). The third species, *V. deserticolus* is a chimaera taxon, with its syntypes of both a varanid and an anguine (see Georgalis et al. 2017b). At the same time, Alexejew (1912) described *Ophisaurus novorossicus* from the Upper Miocene of Ukraine. According to him, this new species could be distinguished from other *Ophisaurus* (=*Pseudopus*) species based on its tooth count and its stratigraphic position. Similar to the specimens described by Bolkay (1913), the work of Fejérváry-Lángh (1923) led to the synonymization of *O. novorossicus* with *P. pannonicus*. To add to the taxonomical confusion surrounding *P. pannonicus*, because few differences were identified between *P. pannonicus* and *P. apodus* in the past, a rather popular idea started to spread among the palaeoherpetological community. It was suggested that this taxon was in reality a very large morphotype of *P. apodus* (Młynarski 1964; Estes 1983). However, Klembara (1986) stated that he was able to recognize both species in the Early Pliocene (MN 15) locality of Ivanovce, Slovakia. To that can be added the minute report of *Ophisaurus apodus dzhafarovi* (Alekperov, 1978) from the Pleistocene locality of Fatmai village, Azerbaijan, in which incomplete and disarticulated elements from the skull (upper and lower jaws, and frontals), the vertebral column (a mention of over 30 vertebrae, from which 20 are decently preserved), as well as ribs and numerous osteoderms are briefly mentioned. In this publication, it is stated that these fossils were closest to the modern form of *Ophisaurus* (=*Pseudopus*) *apodus*, but that some peculiarities allowed to distinguish this fossil form from the modern one. Following this, a subspecific status was given to that material from Azerbaijan, under the name of *Ophisaurus apodus dzhafarovi*. These peculiarities are given as follows: wider and thicker frontal bones than *P. apodus*, marked ornamentation of osteoderms displaying a network of irregular ridges and grooves, palatine teeth closely packed together. Following the works of Klembara (1979, 1981) in which the validity of the genus *Pseudopus* was reaffirmed, the taxon *O. apodus dzhafarovi* should probably be attributed to the genus *Pseudopus* as well. Very limited information about *O. apodus dzhafarovi* is available in the literature but the brief descriptions provided here (Alekperov 1978) are reminiscent of the tendency toward larger and more robust morphology of *P. pannonicus*. The latter taxon has been reported up until the Early Pleistocene of central and eastern Europe (e.g., Klembara et al. 2010; Čerňanský et al. 2017), but also in Italian (Delfino 2002) and Iberian (Blain and Bailon 2006) localities. The temporal distribution of *P. apodus* overlaps the tail-end of the temporal distribution of *P. pannonicus*, henceforth and without more osteological information and a more detailed stratigraphic position for the material from Azerbaijan, it is a delicate matter to exclude an attribution of the *O. apodus dzhafarovi* material to *P. pannonicus* or to confirm its current attribution. Access to and revision of this material would be much desirable to clarify the status of this taxon. More recently, material from the Upper Miocene of Gritsev (Ukraine) allowed for the study of intraspecific variation and the amendment of the diagnosis of *P. pannonicus*. To conclude, there are currently seven features that are considered to be useful to discriminate *P. pannonicus* from the other species of the genus *Pseudopus*. These features mostly encompass characters from the skull and a single vertebral character (Roček 2019; for mandibular feature, see Čerňanský et al. 2017).

We here describe new material of *P. pannonicus* from nine localities from the Miocene and Pliocene of Ukraine, Moldova, and the North Caucasus where it was previously not documented (or reported but not formerly described), thus broadening the already impressive geographic range of this species to the east. Indeed, some elements from Gaverdovsky and Volchaya Balka herein studied were briefly mentioned by Tesakov et al. (2017). These authors reported the presence of anguines, including *P. pannonicus*, from these Late Miocene localities, namely by the posterior portion of a large braincase, some vertebrae, and osteoderms. These reports were, however, restricted to a short mention of "abundant" material

of *P. pannonicus*. No detailed descriptions or collection numbers were provided. Only a single osteoderm from this material was figured (Tesakov et al. 2017: pl. 7, fig. 15). Pending the clarification of the status of *O. apodus dzhafarovi* (Alekperov 1978) mentioned earlier, in the outcome in which that material from Azerbaijan was to be confidently identified as *P. pannonicus*, hence also becoming the most oriental report of *P. pannonicus*, our occurrences from Volchaya Balka and Gaverdovsky are considered to be the most oriental reports of *P. pannonicus* currently known.

The aims of this paper are as follows: 1) to describe the materials in detail and compare them with previously described material of *Pseudopus pannonicus* including newly rediscovered type material of this taxon from Polgárdi as well as its newly designated lectotype; 2) to compare the material with the other known species of *Pseudopus* with a special emphasis on *P. apodus*; and 3) to discuss the taxonomic implications of our findings.

Institutional abbreviations

DE, Department of Ecology, Comenius University in Bratislava, Slovakia; **GIN**, Geological Institute of the Russian Academy of Sciences, Moscow, Russia; **ISEZ**, Institute of Systematics and Evolution of Animals, Polish Academy of Sciences, Krakow, Poland; **MÁFI**, Hungarian Geological Institute (Magyar Állami Földtani Intézet) in Budapest, Hungary; **ZIN PH**, Zoological Institute, Russian Academy of Sciences, St. Petersburg, Russia.

Geological settings

The following study is reporting on material from several localities scattered across Ukraine, the Republic of Moldova, and the North Caucasus.

Ukraine

A single Ukrainian locality, the Petroverovka village from the Odesa Oblast, is discussed in the present work. It can be found in the literature under the former name of Zhovten (alternatively romanized as Zhoften). It is close to the northern coast of the Black Sea (Fig. 1A). The *Pseudopus* material herein presented originates from deposits of the Lower Maeotian, a regional stage also referred to as Meotian (see Palcu et al. 2019, 36), which correlates to the early-middle Turolian (MN 11–MN 12) of the European continental biochronologic scheme (Fig. 1C). Petroverovka, located near the Novoelizavetovka village, is known for the presence of fossil anguids and snakes (Alexejew 1912; Zerova et al. 1987; Zerova 1993), mammals (e.g., Petronio et al. 2007; Krakhmalnaya 2008; Rosina and Sinitsa 2014), and fishes (Kovalchuk and Ferraris 2016).

Moldova

From the Republic of Moldova, the following localities are studied (Fig. 1B): Kalfa (alternatively Calfa) from the Anenii Noi District, Tatareshty (alternatively Tătărești) from the Cahul District, Lucheshty (alternatively Lucești), Etulia (alternatively Etuliya) from the Vulkanesthy Region, and Khadzhi-Abdul from the Cahul District. From Etulia, it should be acknowledged that herpetological material was retrieved from three local points, respectively Ovrag Nadezhda, Tretiy Ovrag, and Strausovyj Ovrag. The locality of Kalfa is known for the presence of vipers (Zerova et al. 1987; Zerova 1993) and several mammalian taxa (e.g., Delinschi 2014; Čermák 2016; Sinitsa and Delinschi 2016). This locality has yielded the oldest specimens of our material. Indeed, although the exact levels of excavation were not stated, these samples were reported from the Sarmatian regional stage. According to Zerova (1993), Kalfa is more precisely of the middle Sarmatian age (=Vallesian) and correlated to the MN 9b zone. This is the consensus view based on mammalian assemblage compositions (e.g., Koretsky 2001; Krakhmalnaya 2008; Delinschi 2014). However, the exact age of Kalfa has been questioned, as only very few mammal fossils found at Kalfa hold strong biochronological signals (Sinitsa and Delinschi 2016). Moreover, recent studies based on magnetostratigraphic analyses have tentatively suggested a slightly younger age (early MN 10) for Kalfa. As pointed out by some authors (Čermák 2016; Sinitsa and Delinschi 2016; and references therein), the magnetostratigraphic data are more congruent with the overall biochronological markers. Here, we are following the more recent and revised age estimations. Henceforth, the deposits from Kalfa are here treated as from the early MN 10 (Fig. 1C).

The locality of Tatareshty is known to have hosted a faunistic assemblage that is part of the Moldavian Faunal Complex (Redkozubov 2003; Nadachowski et al. 2006). Therefore, the estimated age of the Tatareshty deposits is the late Ruscinian (MN 15) of the European continental scale (Fig. 1C).

The locality of Lucheshty is about 4 km southwest of Tatareshty and of a similar age to Tatareshty. Indeed, the fossiliferous levels examined in Lucheshty have yielded an assemblage of mammals that is also indicative of the Moldavian Faunal Complex. The presence of some taxa, however, has highlighted the possibility of a record of the early MN 16a in Lucheshty. Moreover, remains of fishes, amphibians, turtles, and snakes have also been reported from Lucheshty (Redkozubov 2005; Nadachowski et al. 2006).

The fossiliferous deposits of the Etulia area have been associated with the Moldavian Mammal Complex, i.e., MN 15 (Nadachowski et al. 2006; Baryshnikov and Zakharov 2013). Apart from mammalian remains, fossils of mollusks (Nadachowski et al. 2006 and references therein), amphibians, and reptiles (Szyndlar 1991a, 1991b; Redkozubov 2003, 2008; Syromyatnikova 2017a; Syromyatnikova et al. 2022) have been reported from deposits around Etulia.

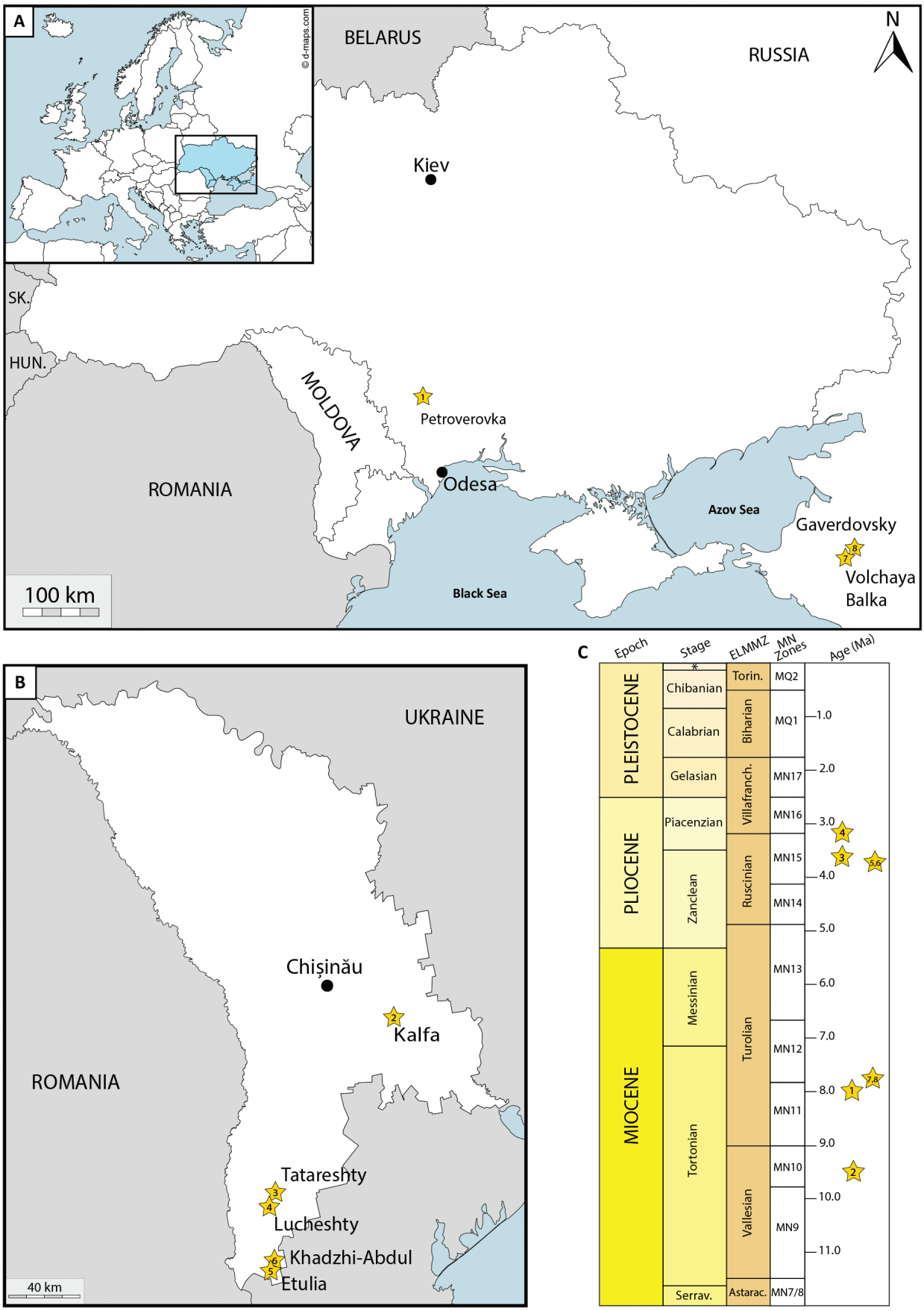

Figure 1. A. Location map of the studied localities. **B.** Close-up on the localities of Moldova. **C.** Stratigraphic position of each locality. Abbreviations: Astarac.: Astaracian; ELMMZ: European Land Mammal Mega Zone; Torin.: Toringian; Serrav.: Serravallian; Villafranch.: Villafranchian; *: Late Pleistocene.

The locality of Khadzhi-Abdul is located near Etulia (Fig. 1B). It was mentioned in the work of Godina and David (1973) under the name of Suvorovo-1, near the Suvorovo village (today named Alexandru Ioan Cuza) from the Cahul district of Moldova. The deposits of Khadzhi-Abdul are from the late Ruscinian, being stratigraphically similar to Etulia.

The North Caucasus

Two localities from the North Caucasus (Russia) are herein presented, viz., Gaverdovsky and Volchaya Balka (Fig. 1A). These localities have yielded palaeobatrachid remains as well as a diverse fauna comprising other amphibians (both caudates and anurans), mollusks, fishes, and reptiles, as well as both micromammal and large-sized mammal taxa (Tesakov et al. 2017; Syromyatnikova 2017b, 2018; Syromyatnikova and Roček 2019). The correlation of several proxies (stratigraphy, ostracod assemblage composition, palynology, mammalian assemblage composition) estimated an age range of 8.1–7.6 Ma (Tesakov et al. 2017) (Fig. 1C), which translates to the early Turolian (MN 11). Although geographically close to one another, Gaverdovsky and Volchaya Balka are associated respectively with a densely forested shore under strong marine water influence and a fresh-water basin with more open vegetation (Tesakov et al. 2017).

Material and methods

The specimens described here were collected on several expeditions in Eastern Europe during the beginning of the second half of the twentieth century. To our knowledge, these campaigns are from the years 1957 (Kalfa), 1959 (Kalfa, Lucheshty), 1961 (Kalfa, Tatareshty, Etulia), 1964 (Etulia), 1965 (Lucheshty), and 1965 (Etulia). One campaign was conducted in Petroverovka with no precise temporal indication, but most likely during the year 1961. More recent campaigns have been conducted in the North Caucasus. Indeed, the material from both Gaverdovsky and Volchaya Balka were collected in 2012.

Specimens examined and terminology

All materials are represented by disarticulated specimens in which the preservation is quite variable, ranging from very poor to fairly complete in some cases. Our samples consist of eight dentaries, five maxillae, four frontals, 11 parietals, one lacrimal, and two fragmentary braincases (for the cranial remains) and 133 osteoderms, 18 vertebrae, and one rib (for the postcranial remains).

The fossil material from Moldova and Ukraine is deposited in the collections of the Zoological Institute of the Russian Academy of Sciences, Saint Petersburg, Russia (collection numbers prefixed by "ZIN PH"), whereas the fossil material from Gaverdovsky and Volchaya Balka is deposited in the collection of the Geological Institute of the Russian Academy of Sciences, Moscow, Russia (collection numbers prefixed by "GIN").

Standard anatomical orientation is used. The anatomical terminology of the individual structures follows, with few exceptions, Meszoely (1970) and Klembara et al. (2014, 2017) for the cranial elements and Čerňanský et al. (2019) for the vertebral elements.

Photography, X-ray microtomography, three-dimensional visualization, and statistical analysis

Specimens were photographed under a Leica M125 binocular microscope with an axially mounted DFC500 camera [LAS software (Leica Application Suite) v.4.1.0 (build 1264)] at the Department of Ecology, Comenius University in Bratislava. Several fossil specimens were scanned using the micro-computed tomography (CT) facility at the Slovak Academy of Sciences in Banská Bystrica, using a phoenix v|tome|x L 240 micro-CT. The CT data sets were analyzed using Avizo v.8.1. and VG Studio Max 3. The type material from Polgárdi was photographed under a scanning electron microscope Thermo Scientific Prisma E SEM housed at the GEOCORE Core Sample, Collection and Laboratory Knowledge Center of the Supervisory Authority for Regulatory Affairs in Rákóczibánya, Hungary. The specimens were left uncoated and photographed under Low Vacuum Mode. The LVD detector was set at various different accelerating voltages, respecting the individual preservation state of the specimens and minimizing unnecessary charging.

Measurements of centrum length (CL) and neural arch width (NAW) follow Szyndlar (1984). The image processing program ImageJ (Schneider et al. 2012) was used for measurements. Statistical analyses were performed with the PAST software (v4.09; Hammer et al. 2001).

Published descriptions and figures of *Pseudopus pannonicus* and *Pseudopus apodus* specimens were used for comparative purposes. Such data were employed as long as there were no ambiguities or doubts associated with these specimens (e.g., descriptions without figures, figures of poor quality, and/or specimens poorly preserved and inappropriate for comparisons). When suited, some of these data from the literature were also included in some of the statistical analyses presented in this work. The analyses made here encompass correlation matrices to understand the various relationships between size measurements, and Student's *t*-tests to compare populations means. Due to the nature of the tests used for the creation of correlation matrices, issues related to multiple comparisons may arise. Thus, to circumvent these issues, a Bonferroni correction is applied when needed and the proper thresholds of significance (i.e., traditionally p-value < 0.05) are adjusted to new corrected values. These values are provided in the section dedicated to the statistical analyses of this manuscript as well as in the

Suppl. materials 1–3. A detailed list of the specimens of *P. pannonicus* and *P. apodus* that were included in the statistical analyses herein presented is provided in the Suppl. materials 1–3 (i.e., Suppl. material 1: *P. pannonicus* specimens, Suppl. material 2: *P. apodus* specimens, and Suppl. material 3: detailed measurements and statistical data for each studied elements).

Data resources

All specimens are catalogued and accessible in the fossil collection of the Russian Academy of Sciences. Digital surface models of the figured fossil specimens are available on Morphosource and Virtual Collections: https://www.morphosource.org/projects/000497477?locale=en.

Results

Systematic palaeontology

Squamata Oppel, 1811
Anguimorpha Fürbringer, 1900
Anguidae Gray, 1825 sensu Gauthier et al. 2012
Anguinae Gray, 1825
***Pseudopus* Merrem, 1820**

***Pseudopus pannonicus* (Kormos, 1911)**
Figs 2–15

Locality, horizon and material. 1. Petroverovka, early-middle Turolian (MN 11 – MN 12): one trunk vertebra (ZIN PH 7/281); four caudal vertebrae (ZIN PH 8/281, 9/281, 10/281, 11/281); and 49 osteoderms (ZIN PH 1-6/281; 12-54/281).

2. Kalfa, Middle Sarmatian age (=Vallesian; MN 10a): five dentaries (ZIN PH 1/277; 2/277; 3/277; 4/277; 5/277); three maxillae (ZIN PH 6/277; 7/277; 8/277); two parietals (ZIN PH 17/277, 18/277); and 57 osteoderms (ZIN PH 9-15/277; 19-68/277).

3. Lucheshty, late Ruscinian (MN 15): one frontal (ZIN PH 2/278); one parietal (ZIN PH 6/278); one fragment of the braincase (ZIN PH 1/278); one presacral vertebra (ZIN PH 7/278); and four osteoderms (ZIN PH 3-5/278; 8/278).

4. Etulia (Ovrag Nadezhda, Tretiy Ovrag, Strausovyj Ovrag local points), late Ruscinian (MN 15): five parietals (ZIN PH 2/279, 3/279, 4/279, 5/279, 6/279), one dentary (ZIN PH 1/279), one presacral vertebra (ZIN PH 7/279), and 11 osteoderms (ZIN PH 8-18/279).

5. Khadzhi-Abdul, late Ruscinian (MN 15): one maxilla (ZIN PH 1/282), two frontals (ZIN PH 2/282, 3/282), two parietals (ZIN PH 4/282, 5/282).

6. Tatareshty, late Ruscinian (MN 15, ?MN 16a): one dentary (ZIN PH 1/280); and one lacrimal (ZIN PH 2/280).

7. Gaverdovsky, Turolian (MN 11): one dentary (GIN 1144/230); one maxilla (GIN 1144/231); one parietal (GIN 1144/232); three trunk vertebrae (GIN 1144/233; 1144/234; 1144/235).

8. Volchaya Balka, Turolian (MN 11): one frontal (GIN 1143/600); one portion of a braincase (GIN 1143/605); five trunk vertebrae (GIN 1143/602; 1143/603; 1143/606; 1143/607; 1143/608); three caudal vertebrae (GIN 1143/601; 1143/604; 1143/609); and 12 osteoderms (GIN 1143/610-621).

Description. Maxilla. Most maxillae available in the material are incomplete except for the right maxilla ZIN PH 1/282 (Figs 2–3). This specimen is fairly complete and very large with a length of 36.93 mm and a height of 11.05 mm, thus making it the largest *Pseudopus*, or anguine even, maxilla ever found. To our knowledge, this is the largest maxilla found among anguids as a whole; see Fig. 2). In any case, all maxillae are robust and relatively large. The exception is GIN 1144/231 which is small and fragile.

The maxilla is anteroposteriorly long and relatively robust with a slight medial curvature at its anterior end. It consists of two major portions: the dental portion bearing the marginal dentition and the dorsally extending nasal process. The nasal process is roughly trapezoidal in shape. It is tall, forming an almost perpendicular wall, although it curves slightly medially at its dorsal extremity. The anterolateral wall of the lacrimal bone was abutting the nasal process of the maxilla where it begins to rise dorsally (i.e., at the level of the lacrimal recess). The anterodorsal margin of this process joins the nasal, whereas its posterodorsal portion broadly overlaps the prefrontal; the latter facet is clearly visible. The dental portion is almost complete, bearing teeth, although a few are missing anteriorly. The tooth row possesses 19 tooth positions (16 teeth are still attached). A short area posterior to the last tooth lacks dentition. In the anterior portion, the maxilla is forked, being divided into two rami. The septomaxillary ramus is thinner and taller than the external ramus. It is also anteromedially flexed and bordered by a small shallow fossa. In medial view, a prominent, concave, and relatively thick, horizontal supradental shelf is present. In the anterior region, a well-developed lip of bone is located on the dorsal surface of the dental shelf. This lamina can be referred to as the septomaxillary lamina (sensu Klembara et al. 2017). The superior alveolar foramen is deep and wide, located at the level of the posterior margin of the nasal process – at the level between the 9th and 10th tooth positions (counted from posterior, see Fig. 2C, D). The adjacent supradental shelf is expanded medially in this area, forming a prominent palatine articulation. The jugal articulation is located in the posterodorsal portion of the posteroventral process, it is wide and deep. The ectopterygoid articulation is present on the posterior end of the maxilla, reaching the level of the 4th tooth position (counted from posterior). In lateral view, the otherwise more-or-less smooth dental portion is pierced by labial foramina in the area ventral to the nasal process. In ZIN PH 1/282, eight foramina are present, being located in a row. However, fewer are present in other maxillae, possibly related to differing preservation states (Fig. 3B, E).

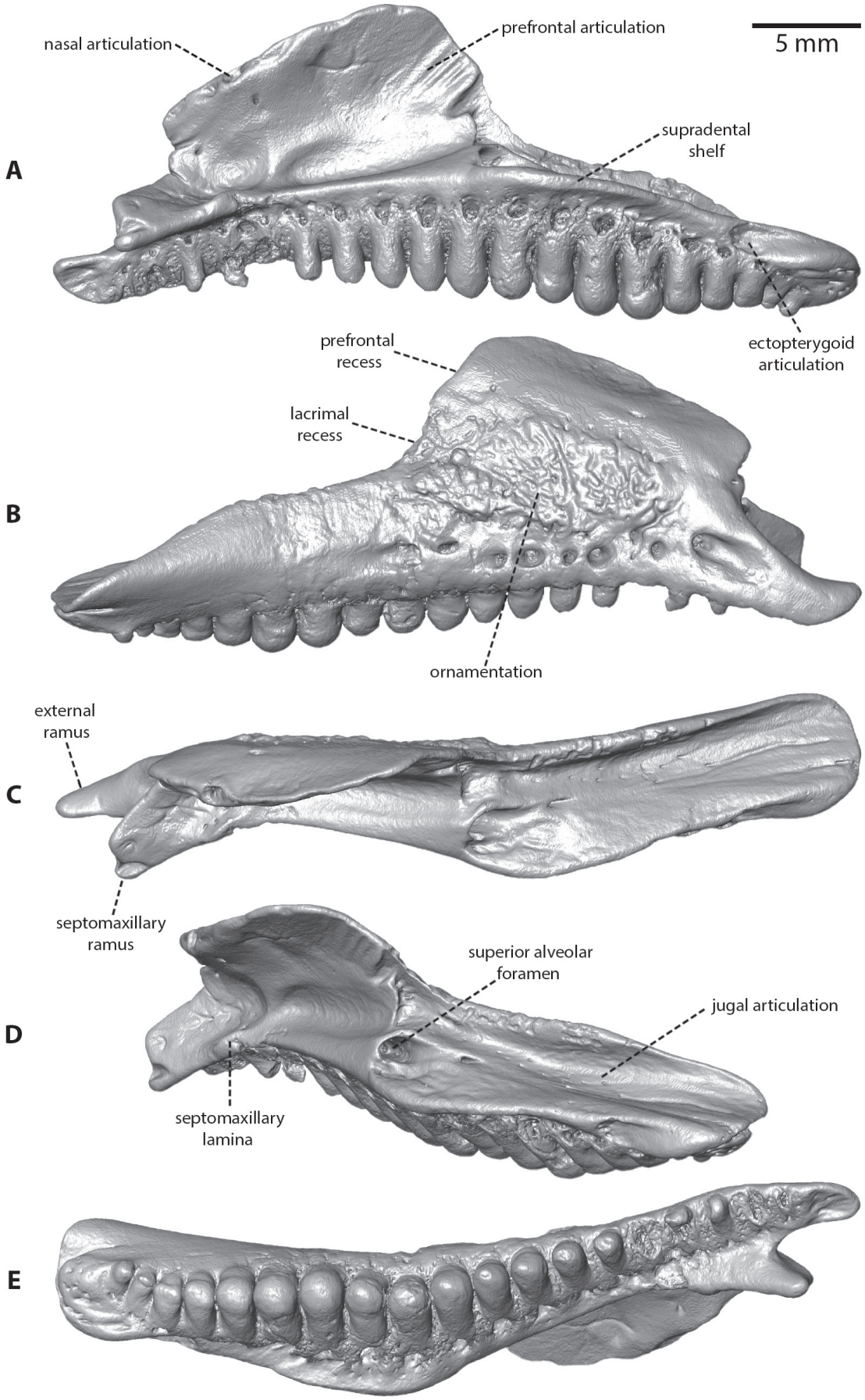

Figure 2. *Pseudopus pannonicus*: virtually segmented model of a right maxilla (ZIN PH 1/282) in medial (**A**), lateral (**B**), dorsal (**C**), posterodorsomedial (**D**), and ventral (**E**) views.

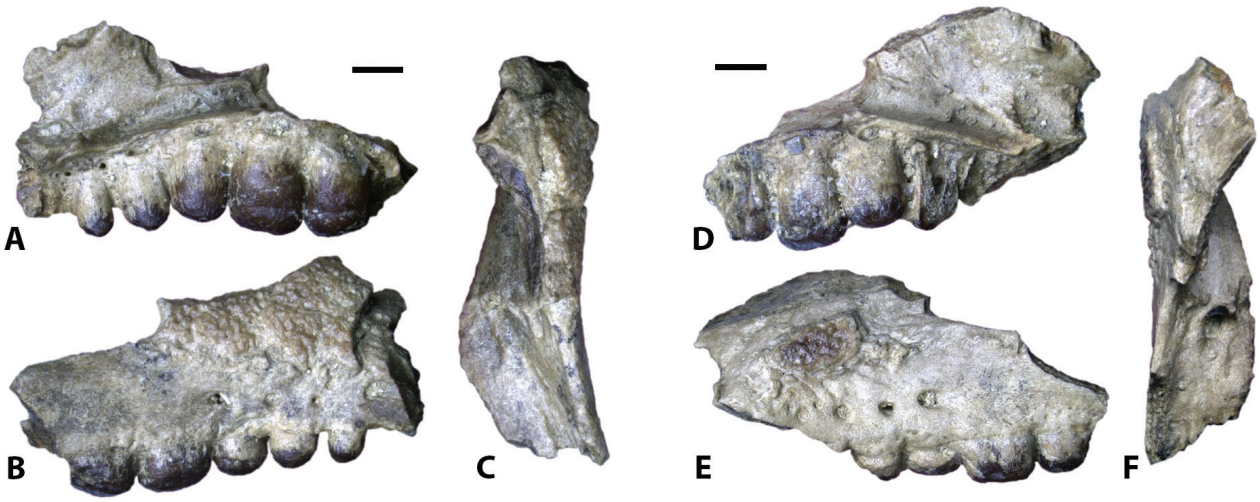

Figure 3. *Pseudopus pannonicus*: right maxilla (ZIN PH 8/277) in medial (**A**), lateral (**B**), and dorsal (**C**) views; left maxilla (ZIN PH 6/277) in medial (**D**), lateral (**E**), and dorsal (**F**) views. Scale bars: 2 mm.

The area above the foramina, which also reaches the ventral region of the nasal process, is covered with several fused, ornamented osteoderms. This ornamentation consists of several irregular ridges and grooves (Figs 2B, 3B, E). The dorsal portion of the nasal process is smooth.

Remarks. The rather small size of maxilla GIN 1144/231, very light lateral dermal ornamentation, and its overall fragility are indications of an early ontogenetic stage, likely of a juvenile and not fully developed individual. In ZIN PH 1/282 with its length of 36.93 mm, the ectopterygoid articulation reaches the level of the 4th tooth position (counted from posterior). This seems to be different from *Pseudopus apodus*, where it reaches the penultimate tooth position (Klembara et al. 2017: fig. 14B). However, this may be subject not only to individual variation but especially to ontogenetic variation, because the ectopterygoid articulation reaches the level of the last tooth in the specimen of *P. pannonicus* from Hambach (see Čerňanský et al. 2017: fig. 7C; its length is 17 mm) and the level of the third position (counted from posterior) in the specimen from Gritsev (Roček 2019: 15C; its length is 24 mm).

Lacrimal. This is a paired bone. The specimen ZIN PH 2/280 is the only lacrimal available in the material (Fig. 4). It is a left element. In lateral view, two distinguishable portions can be recognized. The first, dorsal portion of the lacrimal is roughly rectangular. It is slightly ornamented by a few ridges and grooves. The anterior margin of the lacrimal forms the maxilla articulation. The second, ventral portion of the lacrimal is elongated, extending posteroventrally (Fig. 4A). In medial view, the posteroventrally extending ventral portion of the lacrimal bears a prefrontal articulation.

Remarks. The lacrimal from Tatareshty is the only lacrimal bone reported for *P. pannonicus* (in the fossil members of the genus *Pseudopus*, the partly preserved remains of this element were reported only in *P. laurillardi*, see Klembara et al. 2010). As emphasized by Villa and Delfino (2019a), lacrimal bones are generally quite rare in the fossil record of European lizards, thus making our find noteworthy. However, because of the scarcity of this element in fossil representation and the lack of knowledge about morphological variation, lacrimal bones are of rather marginal interest for fossil identification purposes. This lacrimal generally matches the morphology of the lacrimal known for *P. apodus* (Klembara et al. 2017). The lacrimal from Tatareshty is ornamented, which is a feature that is known in *P. apodus*. However, in the latter species, it is linked to

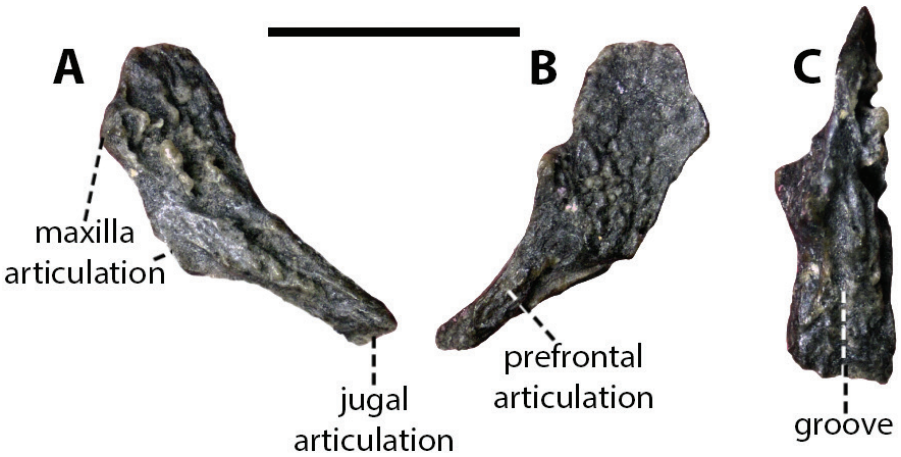

Figure 4. *Pseudopus pannonicus*: lacrimal (ZIN PH 2/280) in lateral (**A**), medial (**B**), and ventral (**C**) views. Scale bar: 2 mm.

size parameters as this condition is known only for large specimens (Klembara et al. 2017). Yet, and interestingly, this lacrimal is relatively small in comparison to that of *P. apodus*. If dermal ornamentation of the lacrimal in *P. pannonicus* is related to size as in *P. apodus*, then the lacrimal of *P. pannonicus* would be among the rare bones to be smaller in *P. pannonicus* than in *P. apodus*. Nevertheless, this lacrimal is the first and only known for *P. pannonicus*.

Frontal. When complete, frontals are large, anteroposteriorly long bones (Fig. 5). In our available material, these paired-bones are all disarticulated and none are found coalesced. The anteriormost portion of the frontal is markedly narrow, extending into a pointed nasal (=anteromedial) process. The anterolateral portion of the process bears the narrow facet for the nasal bone. The facet is sculptured by longitudinal grooves and ridges, indicating strong contact between the frontal and the nasal. The posterior portion of the frontal is the widest. Here, the posterolateral corner of the frontal is distinct and extends into the posterolateral process. In dorsal view, almost the whole dorsal surface is covered by ornamented osteodermal crust, which is fused to the bone. The ornamented surface is even extending far onto the nasal process of the frontal (Fig. 5A, C). The only exception is present in the nasal facet and posteroventral process bearing postfrontal articulation. The ornamentation consists of short grooves, ridges and pits in the central portion of the ornamented surface. The bottoms of some pits are pierced by small foramina. The grooves and ridges diverge from the center to the periphery of the bone, becoming longer (note that this is especially prominent, in the anterior portion of the ornamented surface). The sulci, which separate epidermal osteoscutes (i.e., "shield(s)" of other authors, e.g., Klembara et al. 2010, 2017; Klembara 2012; Čerňanský et al. 2020; Georgalis and Scheyer 2021; Vasilyan et al. 2022, or "ossicula dermalia", e.g., Fejérváry-Lángh 1923; Roček 2019), are less well defined, almost difficult to recognize in some specimens. The incomparably largest osteoscute is the frontal one. It is separated from the frontoparietal and small, posteromedially located interparietal osteoscute (its triangular anterior region overlaps the posterior region of the frontal on the midline; note, however, that it is not preserved in some specimens) by the lateral frontal sulcus and the medial frontal sulcus. The first one is slightly longer than the latter. The lateral frontal sulcus runs in the anterolateral-posteromedial direction, whereas the medial, shorter one has a mediolateral course. The postfrontal articulation extends more posteriorly than laterally.

In ventral view, a large and robust frontal cranial crest can be observed. In its anterior portion, it extends into a rather well-defined and rounded prefrontal (=subolfactory) process. The anteromedial margin of this crest is thin and lightly convex. Posteriorly, it widens and gradually diminishes. It fades out at the posterolateral process of the frontal. Medially, the triangular wedge-shaped parietal tab is indicated by a facet. The anterior portion of the frontal crest is less deep, forming a sharp, medially directed ridge. In the anterior region, lateral to the frontal crest (including its lateral surface), a facet for the prefrontal is located. Its surface is rough and striated. The striation is relatively light on ZIN PH 2/282 in comparison with other specimens. The prefrontal facet is large and occupies anterior two-thirds of the frontal length, and reaches about mid-orbit level. The prefrontal and postfrontal facets are, however, not in contact, so a small lateral portion of the frontal is exposed on the orbital margin.

Parietal. Parietals (Figs 6–7) are medium-sized to large. The parietal is a large azygous element consisting of the parietal table with an ornamented surface and two posterolaterally diverging supratemporal processes. The parietal tab, when preserved, is small. The anterolateral processes are well developed, and their margins are rounded. The lateral margins of the parietal table are more-or-less straight. In dorsal view, the surface of the parietal table can be divided into two areas – a typical

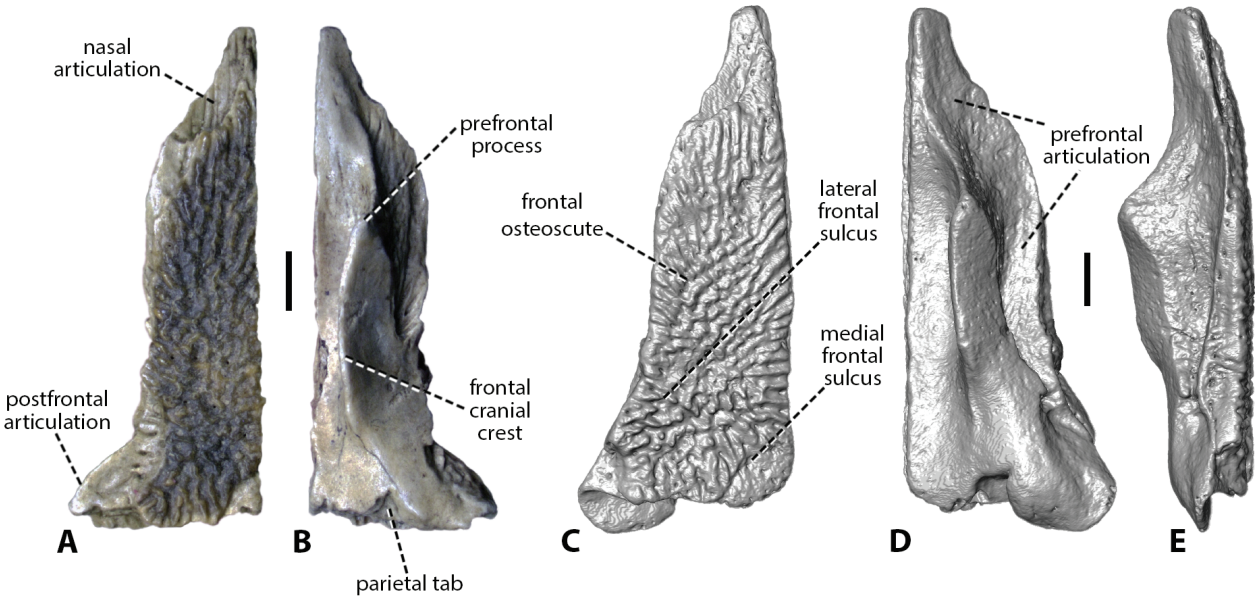

Figure 5. *Pseudopus pannonicus*: photographs of a left frontal (ZIN PH 2/278) in dorsal (**A**) and ventral (**B**) views; virtually segmented model of a left frontal (ZIN PH 2/282) in dorsal (**C**), ventral (**D**), and lateral (**E**) views. Scale bars: 2 mm.

ornamented surface made of osteodermal crusts occupying most of the dorsal surface and a smooth area located posteriorly. The ornamented surface is large and roughly rectangular, being slightly wider than long in large specimens. The interparietal, lateral, and occipital osteoscutes are more or less well-delimited by the interparietal and occipital sulci (Fig. 6G). In the large individual ZIN PH 6/278, however, the sulci are not recognized (see Fig. 7C).

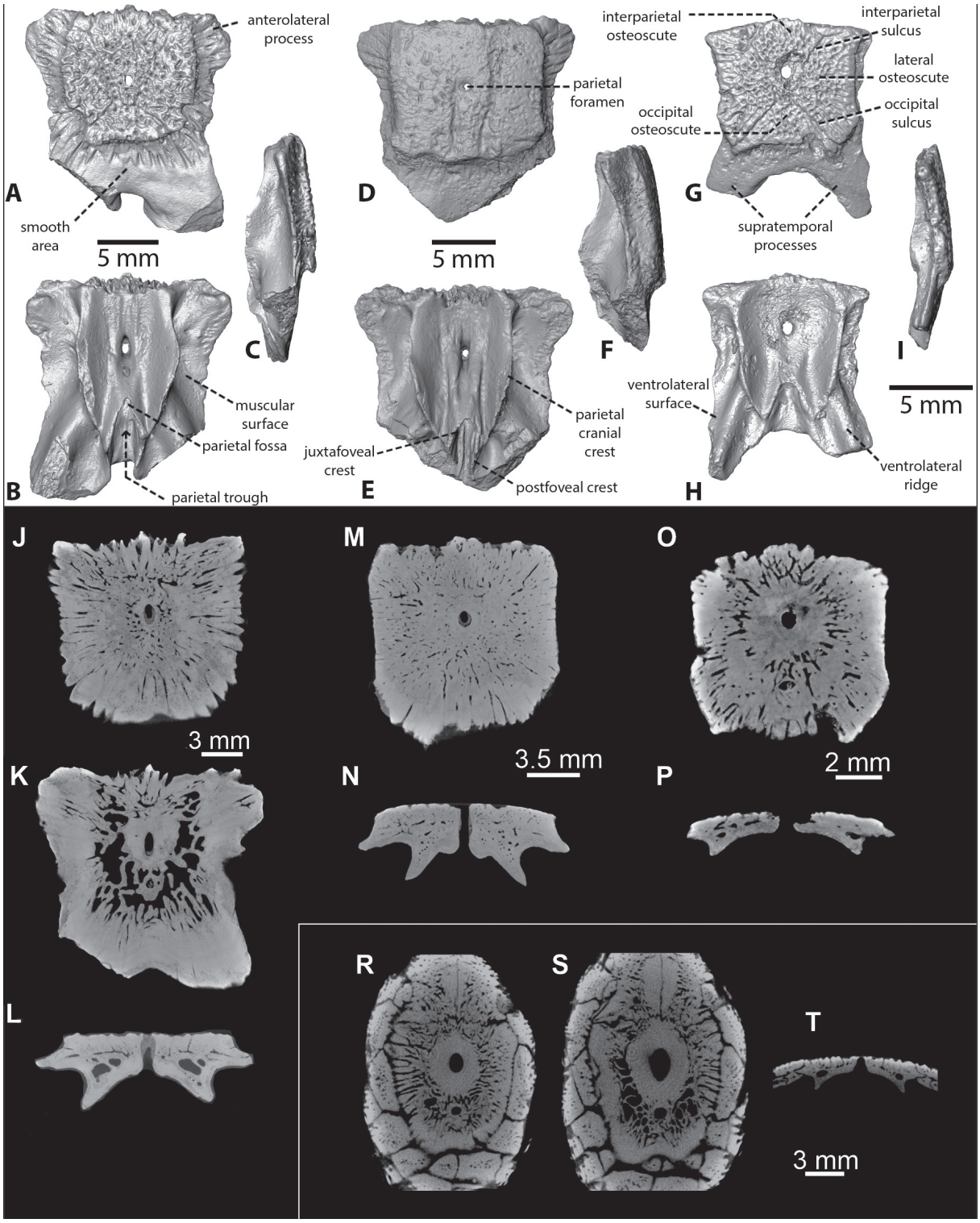

Figure 6. *Pseudopus pannonicus*: virtually segmented models of the parietal ZIN PH 17/277 in dorsal (**A**), ventral (**B**), and lateral left (**C**) views; parietal ZIN PH 18/277 in dorsal (**D**), ventral, and lateral left (**F**) views; parietal ZIN PH 6/279 in dorsal (**G**), ventral (**H**), and lateral left (**I**) views. Virtual slices of the parietal ZIN PH 17/277: axial section at the mid-level of the dorsoventral thickness of the parietal table (**J**), at the ventral level inside of the parietal table (**K**) and coronal section at the level of the parietal foramen (**L**); ZIN PH 18/277: axial section at the mid-level of the parietal table (**M**) and coronal section (**N**); ZIN PH 6/279: axial section at the mid-level of the parietal table (**O**) and coronal section (**P**). Extant *Pseudopus apodus* DE 52, part of the dorsal skull roof: axial section at the mid-level of the dorsoventral thickness of the parietal table (**R**), at the ventral level inside of the parietal table (**S**) and coronal section (**T**).

The dermal sculpture is made of an irregular network of grooves, ridges, and tubercles, being densely distributed. The interparietal osteoscute, when recognized, is pierced by the rounded parietal foramen. The foramen varies in size, being small in some specimens (Fig. 6A), but larger in others (Figs 6G, 7E). The preserved portions of the parietal osteoscutes are the largest relative to others in regard to their size. They are butterfly-wing shaped. As well as the interparietal osteoscute, their anterior portions overlap the frontal. The occipital osteoscute is large. Although its shape slightly varies in the specimens, its posterior margin is usually more-or-less straight. Posteriorly located smooth area of the parietal table is large but shorter than the ornamented surface. The supratemporal processes are not well preserved, being either damaged or broken off in most specimens. In some specimens (e.g., ZIN PH 17/277; ZIN PH 3/279; ZIN PH 6/279; and to a lesser extent ZIN PH 4/282), parts of the supratemporal processes are still preserved. They gradually taper posterolaterally.

by the parietal trough. The anterior margin of the fossa is slightly elevated, so this region has a slightly bulged (or swollen) appearance. The fossa is laterally bordered by a sharp juxtafoveal crest. The postfoveal crest is strong and well defined. It is present as a massive ridge continuing from the junction of the end of the juxtafoveal crest and the parietal cranial crest. The supratemporal processes bear the ventrolateral ridges. These ridges are medially bordered by the parietal arch and laterally bordered by the ventrolateral surface. The base of these ridges abuts the lateral wall of the posterior portion of the parietal cranial crest. In lateral view, parietals are slightly externally convex, and the supratemporal processes are flexed posteroventrally.

Virtual microanatomy and histology. The three micro-CT scans of the parietals revealed a robust bone structure with a very similar internal microanatomy in terms of a vascular network (Fig. 6J, M, O). It revealed relatively large, but not complex meshwork of channels and small cavities. The larger interconnecting vascular cavities of irregular shape are located only in the ventral

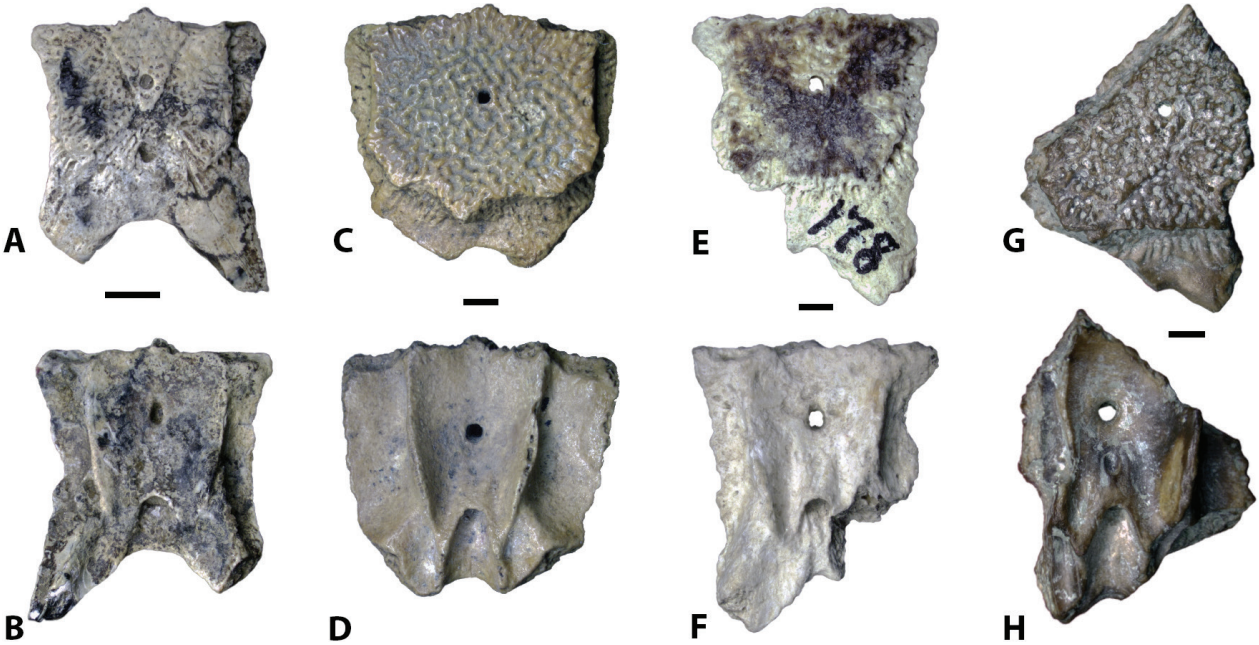

Figure 7. *Pseudopus pannonicus*: photographs of the parietal ZIN PH 3/279 in dorsal (**A**) and ventral (**B**) views; parietal ZIN PH 6/278 in dorsal (**C**) and ventral (**D**) views; parietal ZIN PH 4/282 in dorsal (**E**) and ventral (**F**) views; parietal GIN 1144/232 in dorsal (**G**) and ventral (**H**) views. Scale bars: 2 mm.

In ventral view, the most conspicuous structure is the parietal cranial crest. These crests form sharp walls on each side, so marking the cranial vault. They run generally anteroposteriorly but are slightly convex at mid-length. Lateral to the crest, a distinct muscular attachment surface is present. Its width varies among individuals. In large specimens, its width is equal to the distance between the parietal foramen and parietal cranial crest, whereas in smaller individuals, this distance can be smaller (in some specimens, almost about one-third of the distance between the foramen and the crest). On GIN 1144/232, a small pit is opened posteriorly to the parietal foramen (Fig. 7B, H). The parietal fossa is large and deep, followed posteriorly

section of the parietal table of ZIN PH 17/277 (Fig. 6K, L). At this level, they are arranged around the central region, laterally and posteriorly from the parietal foramen (the bony area surrounding the foramen itself is, however, without cavities or channels). From here, a network of thinner interconnected channels extends anterolaterally and mainly posterolaterally (beneath the smooth area). The ZIN PH 18/277 and smaller specimen ZIN PH 6/279 are slightly different - large cavities are absent (Fig. 6M, N, O, P). Here, the extensive, but very fine interconnecting vascular spaces form a dense network. Overall, the condition in *Pseudopus pannonicus* resembles the one in the extant *Pseudopus apodus* (Fig. 6R–T). However,

parietals ZIN PH 17/277 and ZIN PH 18/277 of *P. pannonicus* are distinctly thicker than the one in the latter taxon (see Fig. 6L, N vs. T).

In *P. apodus* - and to a certain degree in the parietals of *P. pannonicus* here - the dorsal portion of the parietal shows numerous foramina which lie inside of pits (for *P. apodus*, see Klembara et al. 2017: fig. 12A). CT coronal section (Fig. 6L, N, P, T) revealed that the foramina represent openings of canals which continue inside to the bone and are connected to meshwork. Note that the finer histological details such as growth marks and cell lacunae of the bone are not visible.

Remarks. Although the dorsal opening of the parietal foramen is varying in diameter in our specimens, when closely observed in ventral view, it seems that the foramina piercing the parietals are of similar size across specimens. Thus, it is possible that this apparent variability in the size of the parietal foramen mentioned here above may likely be explained by differing degrees of osteodermal crust development rather than representing an actual range of individual variation. To support this idea, when observing specimen ZIN PH 6/279 (Fig. 6G, H) in which the osteodermal crust surrounding the parietal foramen is damaged, one can see that both the internal and external openings of the parietal foramen are of the same size. When observing specimen ZIN PH 17/277 in ventral view, a part of the osteodermal crust overlapping the dorsal opening of the parietal foramen can be seen through its ventral opening (Fig. 6B). The small secondary pit described on the parietal GIN 1144/232 (Fig. 7H) is related to individual variation. A similar condition has also been described and discussed for *Pseudopus pannonicus* specimens from Gritsev (Ukraine) by Roček (2019). This can be seen in other taxa such as *Ophisaurus* as well (see Čerňanský and Klembara 2017). As pointed out in more detail by Smith et al. (2018), the apparition of this secondary pit is caused by the "pineal-related cartilage" immediately underlying the bone.

Braincase. The following description is mostly based on specimen GIN 1143/605 as the other specimen from Lucheshty is rather poorly preserved, displaying few features. The specimen from Volchaya Balka is large (Fig. 8). The sphenoid, otic and occipital bones are completely fused in this specimen, and the sutures between the individual bones are hardly distinguishable. Despite its rather damaged right paroccipital process and both alar processes, it is in an overall good shape. In dorsal view, the unpaired supraoccipital lies at the midline and forms the dorsal portion of the posterior braincase, the dorsal part of the inner ear capsule, and the dorsal margin of the foramen magnum. It has a high ascending process with which the ventral crest of the parietal articulates. In lateral view, the process gradually rises dorsally. In dorsal view, the posterior margin of the supraoccipital possesses a wide, V-shaped notch located over the foramen magnum.

In posterior view, the foramen magnum is large, roughly hexagonal. The occipital condyle, which is formed by otooccipital and basioccipital, is heavily damaged. Only its base is present. The latter is flat and trapezoidal (Fig. 8D). Its dorsal margin is much longer than its ventral one. Its lateral margins are rather straight and diverging dorsally. Dorsolaterally from the base of the condyle, there is set of foramina (preserved on the left side): two foramina for hypoglossal nerve (XII) – one is located closer to the occipital condyle, whereas the second more anterolaterally – both located in the depression; here, dorsal to the second one, a foramen for vagus nerve (X) is present and dorsal to it, there is a fourth foramen - potentially for accessory nerve (XI). The otooccipitals are strongly posterolaterally expanded to form the paroccipital processes - only the left one is preserved. It is well-developed, being robust and laterally expanded. A well-developed dorsal ridge runs posterolaterally along the entire dorsal surface of the paroccipital process. This dorsal ridge is slightly curved, mildly convex. The dorsal margin of the spheno-occipital tubercle is well-developed. The spheno-occipital tubercles are rectangular and slightly depressed between their dorsal and ventral margins. These tubercles are expanded ventrolaterally, well below the level of the ventral margin of the occipital condyle. There is a small and medially-pointed extension on the ventral margin of the spheno-occipital tubercles (Fig. 8D). A swelling of the internal surface of the braincase ("bulla tympani" sensu Klembara et al. 2010) is present, well visible inside through the foramen magnum (Fig. 8C, D).

In ventral view, there is a saddle between the basal (spheno-occipital) tubercles, immediately anterior to the area of the occipital condyle. Anterior to the saddle, there is a longitudinal depression running far on the sphenoid. The depression diminishes anteriorly and disappears at the level of the 1/3 of the anterior length of the braincase. The ventrolateral margins of the basal tubercles are prominent, stout.

In lateral view, beginning on the anterior margin of the paroccipital process and continuing strongly onto the prootic is a groove for the vena capitis lateralis (sensu Klembara et al. 2010), which is dorsally bounded by the prootic crest. The prootic crest is well-developed, being sharp. The area ventral to the prootic crest is quite significantly depressed. It is pierced by the fenestra ovalis: the oval window of the braincase in which the footplate of the stapes fits. Ventral to the fenestra is the large occipital recess. These two are separated by a fine, sharp interfenestral crest (Fig. 8H). Anteriorly, immediately below the prootic crest, there is a small foramen for the facial nerve (V). It lies inside the groove for the vena capitis lateralis and is covered by the crest in lateral view. Slightly dorsal to the prootic crest and below the alar process, an additional crest is found. It is running on both sides of the braincase, its course being parallel to the prootic crest. It is not as sharp as the prootic crest but it is sufficiently well defined to be easily observed. More anteriorly, more- or less at the level of the ventral portion of the occipital recess, the bone is pierced by the large posterior opening of the Vidian canal (Fig. 8G, H).

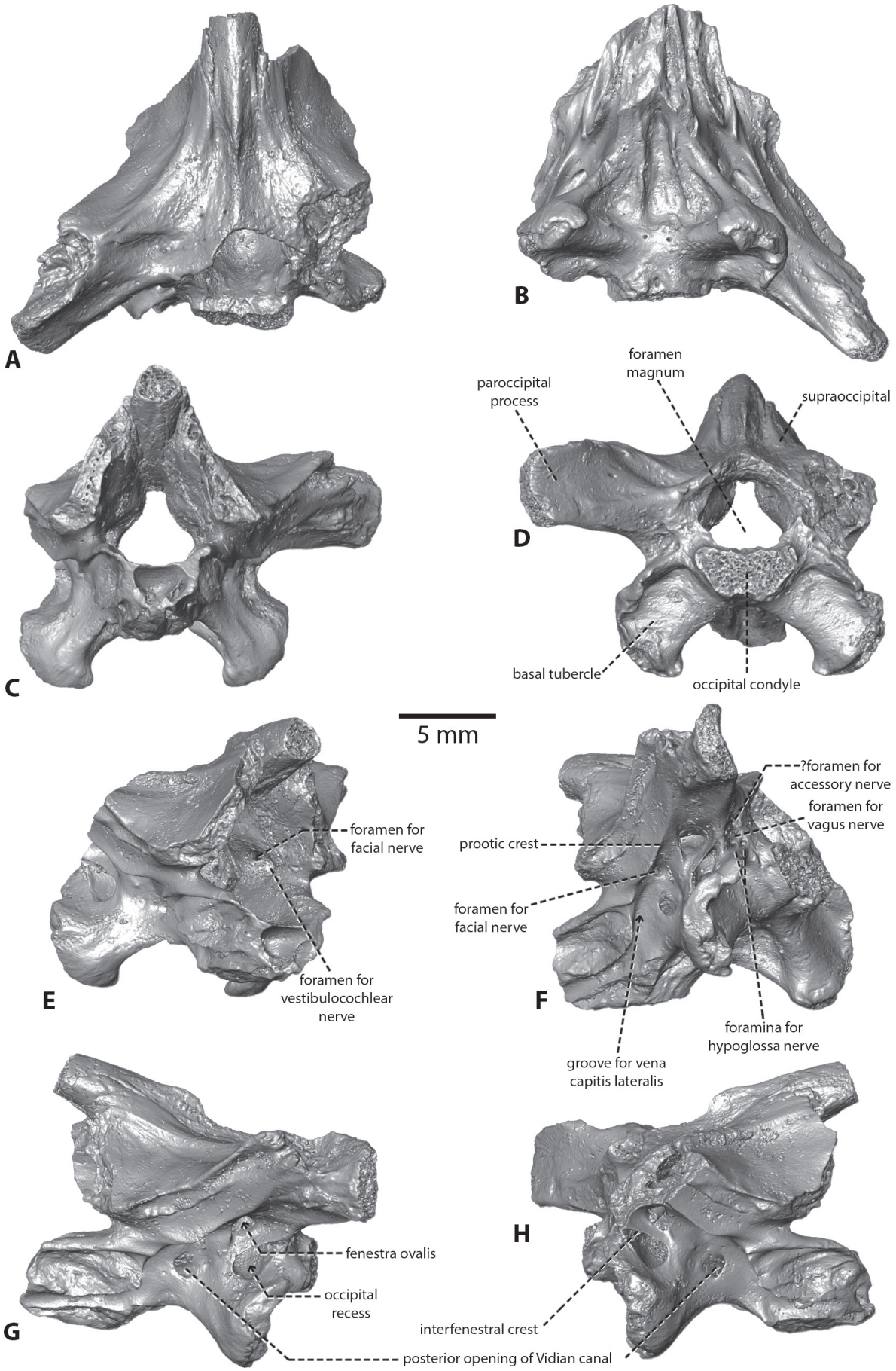

Figure 8. *Pseudopus pannonicus*: virtually segmented model of the posterior portion of a braincase GIN 1143/605 in dorsal (**A**), ventral (**B**), anterior (**C**), posterior (**D**), anterolateral (**E**), posteroventrolateral (**F**), lateral left (**G**), and lateral right (**H**) views.

Anteriorly, the Vidian canal opens lateral to the base of the parasphenoid process (Fig. 8C). The anterior foramen for the abducens nerve (VI) is located directly above the anterior opening of the Vidian canal. A pair of the internal carotid foramina are located centrally, dorsal to the base of parasphenoid process. A sharp crista sellaris is found dorsal to these foramina and runs between the well-developed alar processes. A foramen for a facial nerve opens ventromedially (inside of the braincase) from the prootic crest, inside of the oval depression. In the internal side of this depression, a foramen for the vestibulocochlear nerve (VIII) is also present. The posterior internal area of the braincase is pierced by the perilymphatic foramen. Further posteriorly, the foramen for the vagus nerve and for the hypoglossal nerve are located, piercing the internal posterior area.

Dentary. Several dentaries are available in the material. Because the preservation quality varies among these specimens (Figs 9–11), the following description is mainly based on the best-preserved mature individuals, i.e., specimens ZIN PH 1/277 (Fig. 11A, B), ZIN PH 3/277 (Fig. 9), and to an extent ZIN PH 1/280 (Fig. 10; this specimen represents, however, an immature individual). Tooth rows are mostly incomplete in all specimens, except for ZIN PH 1/280; thus, the total number of tooth positions is difficult to observe.

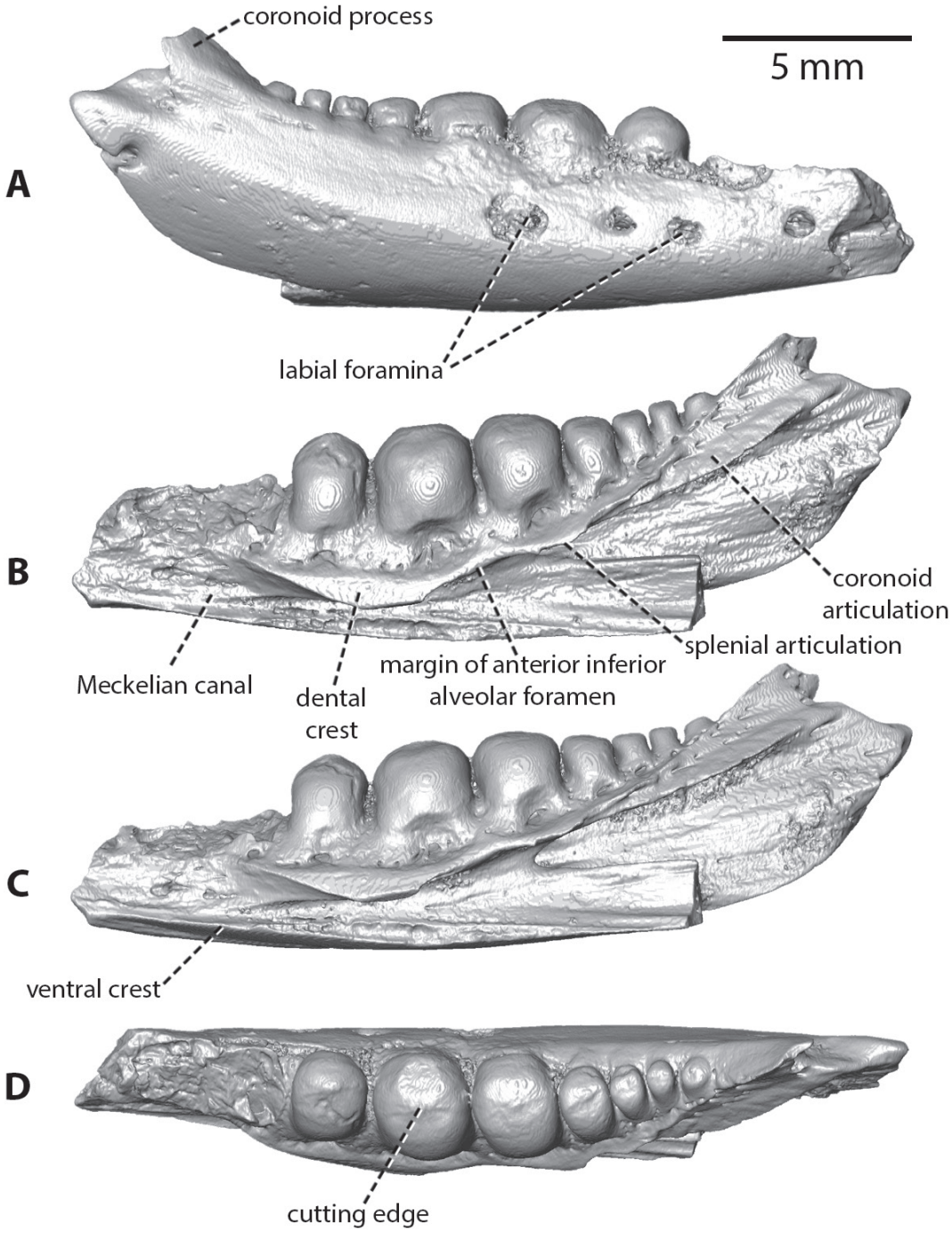

Figure 9. *Pseudopus pannonicus*: virtually segmented model of the right dentary ZIN PH 3/277 in lateral (**A**), medial (**B**), ventromedial (**C**), and dorsal (**D**) views.

Among the best-preserved specimens, ZIN PH 1/280 displays 16 tooth positions (all teeth are still attached except for the small last one; Fig. 10B). The other preserved specimens are large-sized. In medial view, both ZIN PH 1/277 and ZIN PH 1/280 possess their symphyseal region being preserved at the anterior end of the bone (Figs 10B–D, 11A). The symphysis is provided with a kidney-shaped symphyseal facet. The Meckelian canal is fully opened. Anteriorly, it reaches the symphysis in these two above-mentioned specimens, notching it ventrally. Further, the canal continues as a narrow groove, but it widens in the posterior portion of the bone due to the rising of the dental crest in this section. The Meckelian canal is dorsomedially roofed by an almost concave dental crest, whereas it is ventrally bordered by the ventral crest. The ventral crest is more-or-less straight. The ventral and dental crests bear facets for the splenial articulation. In the complete, but immature specimen ZIN PH 1/280, the facets reach anteriorly the level of the 7th tooth position (counted from anterior).

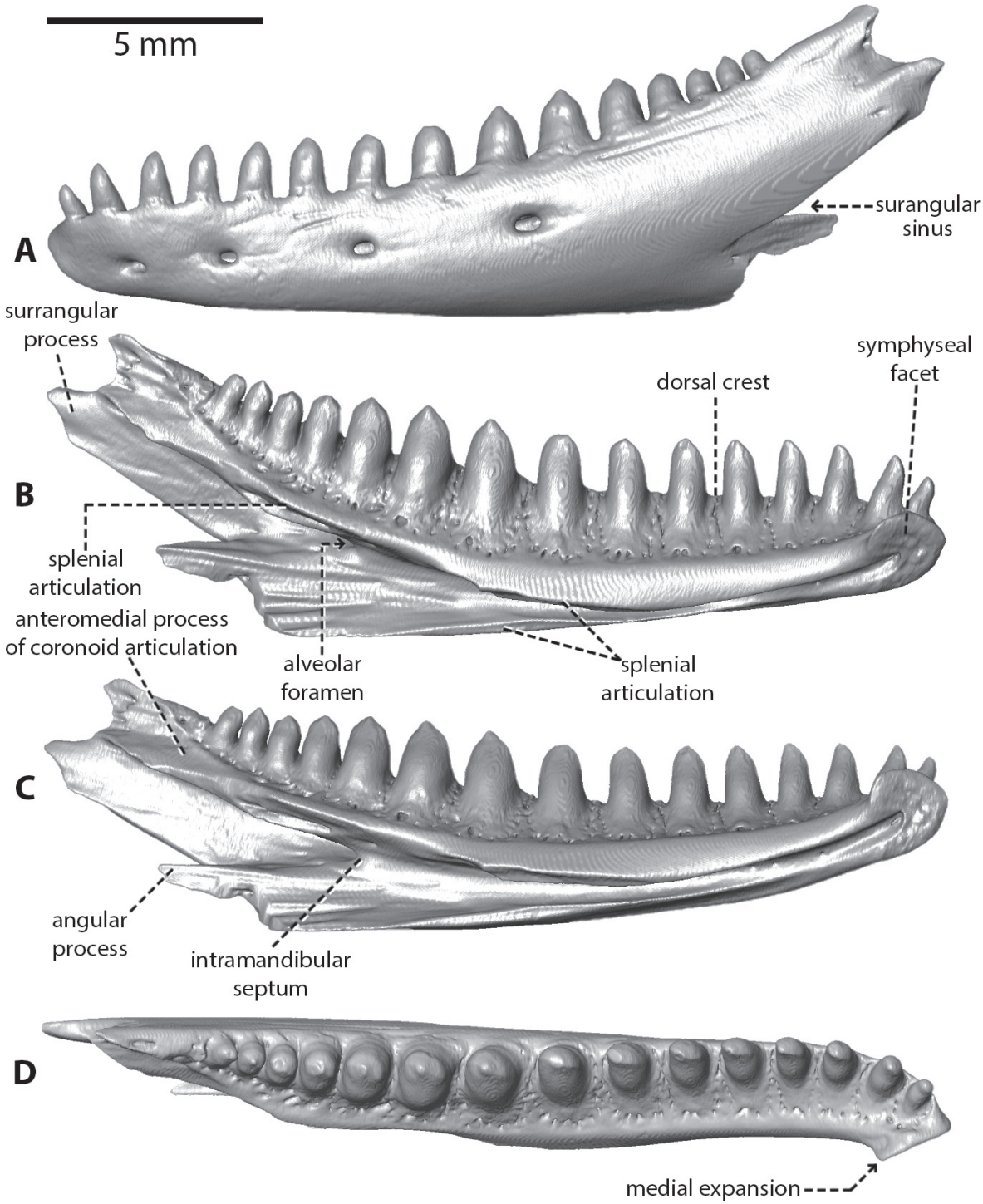

Figure 10. *Pseudopus pannonicus*: virtually segmented model of the left dentary ZIN PH 1/280 (juvenile individual) in lateral (**A**), medial (**B**), ventromedial (**C**), and dorsal (**D**) views.

The anterodorsal margin of the anterior inferior alveolar foramen forms a shallow, elongate notch (the splenial spine is not preserved) at the dental crest, being located at the level of the 5th tooth position in ZIN PH 5/277, at the level between 5th–6th tooth position in ZIN PH 3/277 and at the level of the 6th tooth position in ZIN PH 1/280. The opening of the alveolar canal, the alveolar foramen, is located at the level of the posterior portion of the anterior inferior alveolar foramen (Fig. 11C). The intramandibular septum, which separates the alveolar canal from the Meckelian canal, is almost horizontal. In the posterior portion, the dental crest bears a large facet for an anteromedial process of the coronoid bone. This facet has a rough surface and extends anteriorly to the level of the 4th tooth position (counted from posterior) in the larger individuals and to the level of the 3rd tooth position in ZIN PH 1/280. However, there is a small area that separates the anterior end of the facet from the anterior inferior alveolar foramen, thus the coronoid facet does not reach the foramen. This separating area is difficult to interpret in larger individuals - most likely represents a facet for the splenial (see Discussion). In any case, there is a clear dorsal facet for the splenial posterior to the anterior inferior alveolar foramen in ZIN PH 1/280 – the foramen only interrupts the facet here. This posterior portion of the dorsal facet for the splenial reaches the level of the 3rd tooth position (counted from posterior). The angular process is well-preserved only on ZIN PH 1/280 whereas it is damaged – only the root portion is preserved in other specimens. In ZIN PH 1/280, the posterior tip of this process does not surpass the coronoid process but terminates just anterior to the latter process. The coronoid process is posterodorsally oriented and slightly pointed on several specimens. The surangular process is preserved in some specimens (e.g., ZIN PH 2/277, ZIN PH 1/280). It is large and surpasses both angular and coronoid processes posteriorly (Fig. 11D). The ventral edge of the surangular process bears a distinct notch forming the anterior margin of the anterior surangular foramen. In ZIN PH 2/277 (Fig. 11C, D), the foramen is located completely in the slit in the posteriormost portion of the surangular process, and the slit is posteriorly not completely closed. The foramen seems to be absent in ZIN PH 1/280. The ventral edge of the surangular process of this specimen is rather straight (Fig. 10B). On this particular specimen, the surangular sinus (sensu Klembara et al. 2014; i.e., sinus supraangularis in Roček 1984, 2019), located between the surangular and angular processes, is wedge-shaped.

In lateral view, the otherwise more-or-less smooth surface of the bone is pierced by labial foramina. These form a series located in the mid-line of the bone, and they number four in the best-preserved specimens.

Remarks. The specimen ZIN PH 1/280 is very well preserved and displays a different tooth morphology in comparison to any of the other larger specimens presented here. This specimen displays typical features of *Pseudopus* (Klembara et al. 2014) such as the teeth being rather conical and slenderer with tips slightly curved posteriorly in the anterior half of the dentary, and becoming gradually stouter and more robust in the posterior half. Moreover, the tooth morphology (i.e., thick and conical teeth with pointed apices and posterior teeth being larger and stouter) displayed here is reminiscent of that of juvenile *Pseudopus apodus* (see Klembara e al. 2014). As pointed out in *P. apodus*, the spacing of teeth varies during the ontogeny and as the individuals mature, the teeth of the dentary become more densely spaced (Klembara et al. 2014). Although for a different clade, tooth spacing was also hinted at as a possible juvenile feature by Smith (2011). Henceforth, the general morphology and spacing of teeth is suggesting that ZIN PH 1/280 pertained to a juvenile individual of *Pseudopus*. Klembara (2012) stated that teeth from dentaries of *Pseudopus ahnikoviensis* from the type locality were all devoid of striations. However, as emphasized by Čerňanský et al. (2015, 2017a), this could be linked to intraspecific variability or taphonomy as the latter authors reported for *Pseudopus* cf. *ahnikoviensis* material from the Early Miocene and Middle Miocene of the German localities of Amöneburg (Čerňanský et al. 2015) and Hambach (Čerňanský et al. 2017a) respectively. Similar variability has been shown for *P. apodus* (Klembara et al. 2014). All currently known *P. ahnikoviensis* are confined to the Early and Middle Miocene (MN 3–MN5; Klembara 2012; Čerňanský et al. 2015, 2017; Klembara and Rummel 2018) of Central Europe whereas ZIN PH 1/280 originates from the much younger deposits of Tatareshty

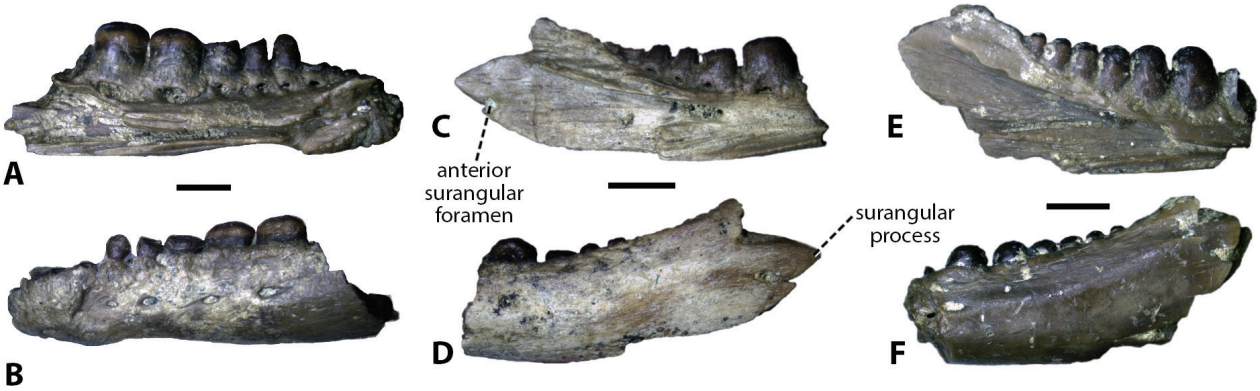

Figure 11. *Pseudopus pannonicus*: left dentary (ZIN PH 1/277) in medial (**A**) and lateral (**B**) views; left dentary (ZIN PH 2/277) in medial (**C**) and lateral (**D**) views; left dentary (ZIN PH 5/277) in medial (**E**) and lateral (**F**) views. Scale bars: 2 mm.

(MN 15). This juvenile specimen is relatively similar in size (20.73 mm in length) to the range known among the adults of *P. ahnikoviensis*. On the other hand, *P. ahnikoviensis* is distinguished from all other *Pseudopus* species by the autapomorphic feature of the dentary in the presence of a surangular spine. Here, ZIN PH 1/280 does not bear a surangular spine but rather a damaged angular process on closer examination. The morphology of the dentary of *Pseudopus confertus* is not currently known. Moreover, this species is solely restricted to a single locality from the Early Miocene (MN3) of the Czech Republic. The dentary of *Pseudopus laurillardi* is known in much more detail than the aforementioned *Pseudopus* species. This species is slightly younger. It is known from Miocene localities ranging from MN4 to MN7/8 (Rage and Bailon 2005; Klembara et al. 2010; Ivanov et al. 2020). One of the most conspicuous and autapomorphic features of the dentary in *P. laurillardi* is the distinct and medially-extending subdental shelf, thus forming a markedly deep sulcus as well as a large medial ridge (Klembara et al. 2010). The latter authors also state that the development of the subdental shelf is affected by ontogenetic processes, being rather narrow in smaller specimens and growing throughout development. Our specimen does not show signs of any subdental shelf, alike *P. ahnikoviensis*, *P. pannonicus*, or *P. apodus*. The posteriormost portion of the dentary of *P. laurillardi* is described as being very short, reaching a length equating to roughly the length occupied by the two posteriormost teeth (Klembara et al. 2010). Here, the posterior portion of ZIN PH 1/280 is notably longer, reaching almost twice that length. It is possible, however, that the immature state of this individual affects the expression of that character. In addition to the various differences with several *Pseudopus* species exposed here, the stratigraphical position of the deposits of Tatareshty is also more congruent with the temporal range of either *P. pannonicus* or *P. apodus*. Finally, ZIN PH 1/280 exhibits an interesting feature in its facet for the splenial. It is most similar to that described for other dentaries of *P. pannonicus* presented here, which appear to have much taxonomical interest (see Discussion), thus comforting the attribution of this juvenile dentary to *P. pannonicus*.

Dentition. Maxillary teeth are small, cylindrical, and slender anteriorly (Fig. 2). These gradually increase in size posteriorly, becoming more bulbous up to the fifth-to-last teeth. Teeth are closely packed. Apices of teeth are lightly striated, both lingually and labially, and pointed. On some teeth, a more-or-less faint anteroposterior cutting edge can be observed. In the dentary, teeth are rather closely packed as well. The most complete specimens show a variation in teeth size along the tooth row. In the anterior portion of the tooth row, teeth are generally more cylindrical and slender, gradually increasing in size and robustness. The largest tooth is located slightly posterior to the mid-length of the dentary. The last four to five teeth are smaller, gradually decreasing in size. In ZIN PH 1/280, the apices of teeth are pointed and slightly striated. A cutting edge is distinct (Fig. 10D).

Trunk vertebra. These presacral vertebrae are relatively well preserved. They are medium-sized to large. These vertebrae are overall rather robust, more compressed rather than elongated (Fig. 12).

They are procelous with the centrum in the shape of a conical frustum. In dorsal view, the vertebrae are constricted at mid-length. Prezygapophyses and postzygapophyses are laterally expanded. The articular facets of the prezygapophyses are oval, slightly elongated in the anterolateral-posteromedial direction, and dorsomedially inclined. The prezygapophyses slightly surpass the level of the anterior margin of the cotyle (e.g., GIN 1143/602), whereas the postzygapophyses do not reach the level of the posterior end of the condyle. The articulation facets of the postzygapophyses are oval, laterally expanded, and ventrolaterally inclined. In lateral view, the prezygapophyses and postzygapophyses are connected by the well-developed interzygapophyseal ridge. The neural arch is lightly depressed medial to the prezygapophyses. The dorsal region of the neural arch slightly rises in height posteriorly. The posteriorly developed neural spine starts to rise at about vertebral mid-length. Unfortunately, it is not complete in any of these specimens, the tip of the neural spine being broken in most specimens (Fig. 12C, H, M, R, W). It thickens posteriorly, thus displaying a hatchet-like morphology in a cross-section. The neural canal is sub-circular, tunnel-like. Its dorsal height is smaller than the dorsal height of the cotyle (for this character, see Čerňanský et al. 2019). In lateral view, the synapophyses are broad, more or less kidney-shaped, and laterally directed. Some specimens display small tubercles located medial to each synapophysis. In ventral view, the centrum is wide but gradually narrows posteriorly - the subcentral ridges are straight and gradually converge posteriorly. The ventral surface is flat. A faint ridge runs anteromedially in some specimens (e.g., GIN 1144/234). Both condyle and cotyle are markedly depressed. The condyle is separated from the body of the centrum by a distinct narrowing, although note that a distinct precondylar constriction (as seen in varanids; e.g., Čerňanský et al. 2022: fig. 5) is absent (Fig. 12B).

Remarks. The two features indubitably allow the allocation of these vertebrae to *Pseudopus* (see Čerňanský et al. 2019): (1) the straight course of the lateral margins of the centrum convergent posteriorly; and (2) the dorsoventral height of the cotyle is higher than the height of the neural canal.

These dorsal vertebrae are robust and large, having short and compressed appearance in comparison to the more elongated vertebrae of *P. apodus*.

Caudal vertebra. The caudal vertebrae are rather poorly preserved. These are medium-sized and rather narrow and anteroposteriorly elongated (Fig. 13).

They are procelous. In dorsal view, the vertebrae are constricted at mid-length. Prezygapophyses slightly surpass the anterior margin of the cotyle. The articular facets of the prezygapophyses are oval, laterally expanded, and dorsomedially inclined. There is a faint ridge

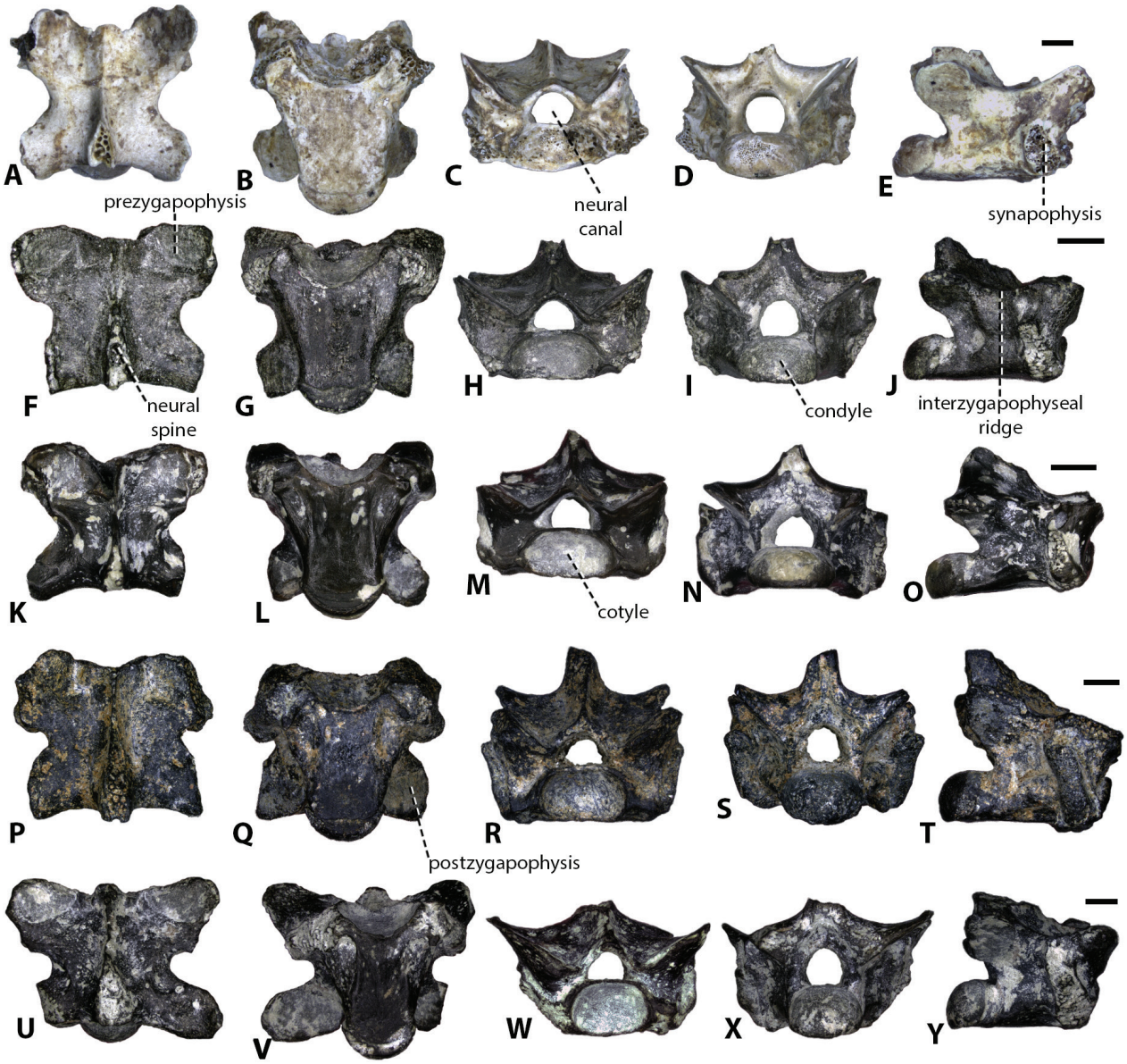

Figure 12. *Pseudopus pannonicus*: trunk vertebra (ZIN PH 7/281) in dorsal (**A**), ventral (**B**), anterior (**C**), posterior (**D**), and right lateral (**E**) views; trunk vertebra (GIN 1143/602) in dorsal (**F**), ventral (**G**), anterior (**H**), posterior (**I**), and right lateral (**J**) views; trunk vertebra (GIN 1144/234) in dorsal (**K**), ventral (**L**), anterior (**M**), posterior (**N**), and right lateral (**O**) views; trunk vertebra (GIN 1143/606) in dorsal (**P**), ventral (**Q**), anterior (**R**), posterior (**S**), and right lateral (**T**) views; trunk vertebra (GIN 1143/607) in dorsal (**U**), ventral (**V**), anterior (**W**), posterior (**X**), and right lateral (**Y**) views. Scale bars: 2 mm.

deriving from the posterolateral corner of the prezygapophyseal facet. These ridges meet medially. In some specimens from Volchaya Balka (e.g., GIN 1143/601; GIN 1143/604; GIN 1143/609), a small apophysis (i.e., the dorsal paraseptal apophysis; Hoffstetter and Gasc 1969, 271) sits atop the level where these ridges meet (Fig. 13P). The articular facets of the postzygapophyses are oval, laterally expanded, and ventrolaterally inclined. The neural spine on these vertebrae is only ever partly preserved. It is slender and pointed. The cross-section of the neural spine is sub-circular. The neural canal is oval, clearly smaller than the cotyle. The subcentral ridges are more-or-less straight. The centrum possesses pleurapophyses. However, only their bases are preserved. These are broad and laterally directed, and gradually narrow distally. The prezygapophyses and pleurapophyses are connected by a vertical wall. The posteromedial margins of the pleurapophyses do not overlap the anterior margins of the postzygapophyses. Some vertebrae (e.g., GIN 1143/604) possess an autotomy foramen at the base of each pleurapophysis, but no transverse autotomic split is present in any of these caudal vertebrae. The centrum is also pierced by several foramina. Only the bases of the haemapophyses are partly preserved on some vertebrae (Fig. 13B, G, L, Q). These bases are posteroventrally oriented. The cotyle and condyle are both depressed. The condyle is slightly smaller than the cotyle.

Remarks. Caudal vertebrae are usually difficult to confidently identify between anguine lizards and are commonly only attributed to indeterminate anguines (e.g., Čerňanský

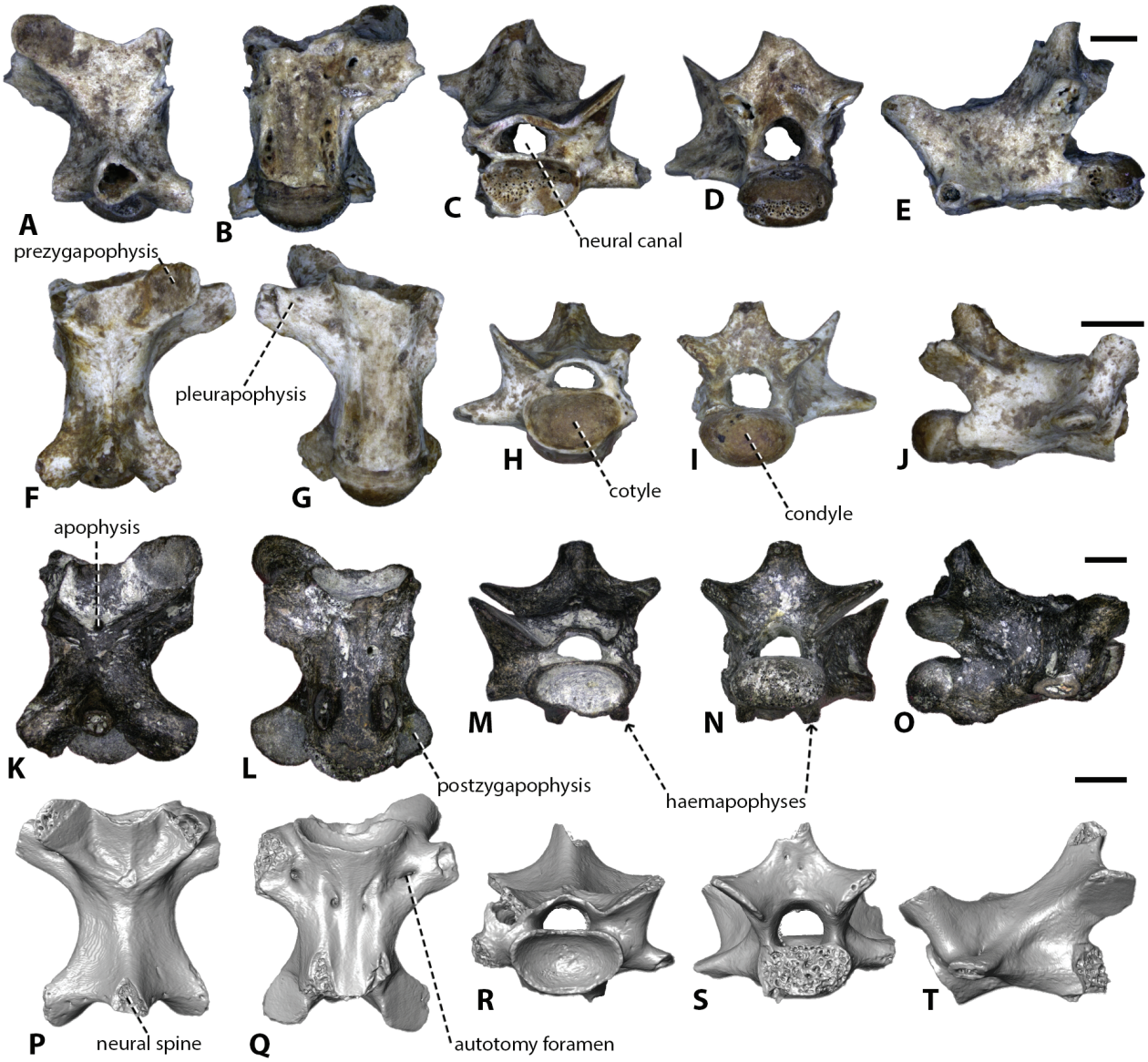

Figure 13. *Pseudopus pannonicus*: photographs of caudal vertebra (ZIN PH 10/281) in dorsal (**A**), ventral (**B**), anterior (**C**), posterior (**D**), and right lateral (**E**) views; caudal vertebra (ZIN PH 11/281) in dorsal (**F**), ventral (**G**), anterior (**H**), posterior (**I**), and right lateral (**J**) views; caudal vertebra (GIN 1143/609) in dorsal (**K**), ventral (**L**), anterior (**M**), posterior (**N**), and right lateral (**O**) views; virtually segmented model of the caudal vertebra GIN 1143/604 in dorsal (**P**), ventral (**Q**), anterior (**R**), posterior (**S**), and right lateral (**T**) views. Scale bars: 2 mm.

et al. 2017; Georgalis et al. 2017, 2018), even though more precise affinities can sometimes be supposed (e.g., Georgalis et al. 2018, 2019a). This becomes even more difficult in the case of large anguid caudal vertebrae as these are strongly similar to those of varanids (Estes 1983; Georgalis et al. 2018). As summarized by Georgalis et al. (2018), some features can nonetheless be used to distinguish caudal vertebrae between large anguids and varanids. Essentially, haemapophyses in the former clade are directly fused to the centrum whereas these are sitting on articulation facets in the latter clade (i.e., pedicles in Georgalis et al. 2018). Additionally, as pointed out by these authors as well, the neural spine also proves useful in distinguishing between anguid and varanid caudal vertebrae, although the distinction is a more delicate matter for the anteriormost caudal vertebrae of anguids which are closer to the morphology exhibited in varanids than the more posterior vertebrae (Georgalis et al. 2018). Among anguids, the neural spine is tube-like and posteriorly inclined whereas, among varanids, the neural spine is rather laterally-compressed and sub-vertical to wholly vertical (Georgalis et al. 2018). In the case of the material presented here, the structures present ventrally in the posterior portion of the centrum are unlikely to be facets for articulation and are, on the contrary, fused directly to the centrum. Moreover, although incomplete in most specimens, the neural spine of the vertebrae of our material are tube-like and rather posteriorly inclined. Therefore, potential varanid affinities among our material can be discarded. Then, as stated previously, identifications of caudal vertebrae among anguines are

difficult and tend to be only referred to as indeterminate anguines, thus rendering our attribution less conservative than usual in comparison. A similar suggestion, although more conservative, was offered by Georgalis et al. (2018) for a limited amount of material (i.e., specimen RP1 299: a single caudal vertebra, likely among the most anterior caudals based on the morphology of its neural spine) from the Late Miocene (MN10) of Greece. These authors referred this specimen to an indeterminate anguine, discarding (although not completely) its possible varanid affinities following a reasoning similar to ours. These authors stated that this specimen could tentatively be attributed to *Pseudopus pannonicus* due to its large size and geographic and stratigraphic positions. Acknowledging that this matter is more sensitive in the case of such limited material, the argumentations of these authors as well as the replacing of that specimen inside a spatiotemporal rationale appear rather sensible. Thus this specimen could warrant a more precise attribution to *P. pannonicus*, hence documenting additional occurrences of that species in the European Neogene. Here, we attribute the caudal vertebrae from our material to the genus *Pseudopus* because none are showing an autotomic split, a feature that is present and well-visible in either *Anguis* or *Ophisaurus* (Hoffstetter and Gasc 1969; Čerňanský et al. 2019). This condition is, however, currently unknown in either *Ragesaurus* and *Smithosaurus* based on the material available (Bailon and Augé 2012; Vasilyan et al. 2022). We refer the vertebrae described here to the species *P. pannonicus* due to the fact that this species is the sole (with the exception of the recently described and rare occurrences of *Ophisaurus* from Lucheshty and Etulia; Syromyatnikova et al. 2022) and most abundant representant of anguines in the localities studied here as evidenced by the additional cranial material described here.

Interestingly and as mentioned in the description above, although some vertebrae are bearing autotomy foramina, none are displaying an autotomic split. To add to these observations, it can be noted that neither "half-vertebra" that could be attributed to autotomized *Pseudopus* elements, nor halves separated post-mortem were found in our material.

Rib. In the available material, a single rib is present (Fig. 14A–C). It is medium-sized. It is lightly bent ventrally as well as lightly compressed anteroposteriorly. The head of the rib is only partly preserved. It displays a more-or-less kidney-shaped articular facet. The anterior process of the proximal end of the rib is preserved whereas its posterior process is not. The distal end of the rib is also lightly damaged. Dorsally, the rib bears a distinct ridge.

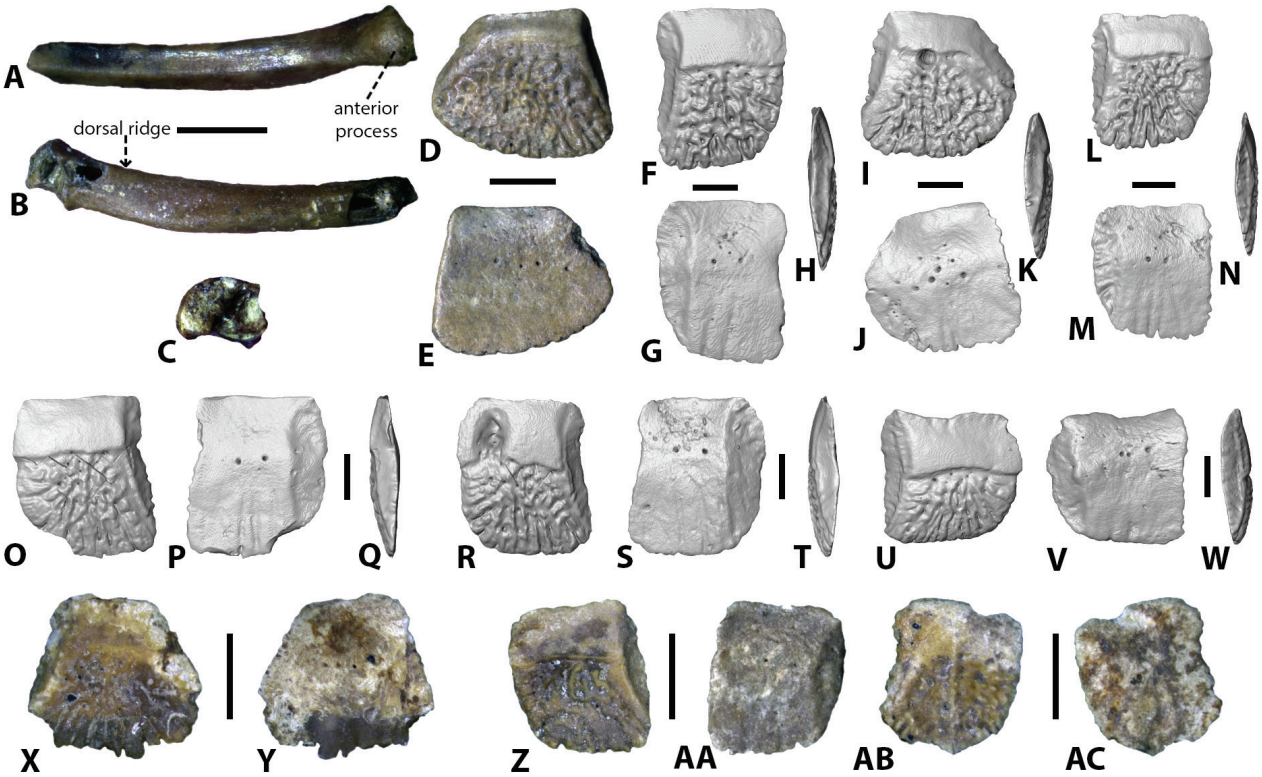

Figure 14. *Pseudopus pannonicus*: rib (ZIN PH 16/277) in anterior (**A**), posterior (**B**), and proximal (**C**) views; photographs of osteoderm from Lucheshty (ZIN PH 3/278) in external (**D**) and internal (**E**) views; virtually segmented model of osteoderms from Kalfa, specimen ZIN PH 9/277 in external (**F**), internal (**G**), and lateral (**H**) views, specimen ZIN PH 10/277 in external (**I**), internal (**J**), and lateral (**K**) views; specimen ZIN PH 11/277 in external (**L**), internal (**M**), and lateral (**N**) views; specimen ZIN PH 19/277 in external (**O**), internal (**P**), and lateral (**Q**) views; specimen ZIN PH 20/277 in external (**R**), internal (**S**), and lateral (**T**) views; specimen ZIN PH 21/277 in external (**U**), internal (**V**), and lateral (**W**) views; photographs of osteoderms from Petroverovka, specimen ZIN PH 1/281 in external (**X**) and internal (**Y**) views; specimen ZIN PH 2/281 in external (**Z**) and internal (**AA**) views; specimen ZIN PH 3/281 in external (**AB**) and internal (**AC**) views. Scale bars: 2 mm.

Osteoderms. Among the herein studied material, osteoderms represent the most common element. Indeed, a total of 133 single osteoderms are recorded. These elements are most abundant in the Kalfa locality and rarest from Lucheshty. In general, some osteoderms are more rectangular and slightly more elongated (e.g., Fig. 14F, R) whereas other osteoderms are more trapezoidal, shorter, and stouter (e.g., Fig. 14D, I). However, all these elements share the following features: rather large, flat, thick, and rather robust. The external surface of the osteoderms can be divided into two distinct areas: a short and smooth gliding surface in the anterior portion and a large, ornamented posterior portion. This ornamentation consists of tubercles mainly in the central part of the ornamented surface and a network of grooves and ridges around the periphery (Fig. 14). Occasionally, pits are found inside these grooves. Some osteoderms have a low, elongate ridge running almost along their middle (e.g., Fig. 14P). In addition, some specimens possess a lateral narrow bevel (i.e., longitudinal crest in Vasile et al. 2021). This feature is, however, certainly most variable as this bevel can be seen on either side of the osteoderms, sometimes both, or rarely on neither side. These different beveling conditions are likely to reflect different placements on the body and can be indicative of left-sided or right-sided osteoderms (e.g., Gauthier 1982; Vasile et al. 2021). In ventral view, osteoderms are rather smooth. Some specimens show light grooves and/or are pierced by foramina (e.g., Fig. 14G, J). In lateral view, these osteoderms are to be rather thick (e.g., Fig. 14H, K).

Remarks. Osteoderms are generally difficult to identify precisely and rarely useful for alpha-taxonomic determinations. Although the morphology of anguid osteoderms tends to be rather generic (i.e., vermicular ornamentation of the external surface; Gauthier 1982; Georgalis et al. 2019b), some possibilities of differentiation between the various anguine genera exist and have been heavily used for fossil osteoderms. For instance, it has been very common to distinguish between osteoderms of *Anguis*, *Pseudopus* and *Ophisaurus*. Indeed, osteoderms of the former are rather small and thin, not rectangular, and devoid of a longitudinal keel (Tesakov et al. 2017; Syromyatnikova et al. 2019; Loréal et al. 2020), whereas osteoderms of the latter two genera are rectangular, larger and both keeled (Čerňanský and Klembara 2017). However, even the keeled feature is not entirely reliable for isolated osteoderms because it is known that some osteoderms of *Pseudopus* can be devoid of this keel, as shown by several authors (Schmidt 1914; Spinner et al. 2015; Vasile et al. 2021). Initially described by Schmidt (1914), the presence of a longitudinal keel in specimens of *Pseudopus apodus* is indeed variable at the individual scale, following a gradient of expression both anteroposteriorly and dorsoventrally across the body. In addition, as pointed out more recently by Vasile et al. (2021), in *Pseudopus*, osteoderms of the dorsomedial region display a medial ridge whereas those of the laterodorsal and lateroventral regions do not. Such results were reaffirmed recently by Spinner et al. (2015). Therefore, the variability described on the presence or absence of a medial ridge is likely reflecting different body topology rather than reflecting actual taxonomical differences. As for the range of variability in the bearing of a lateral bevel, as mentioned above, it can be explained by the positions on the body on which each osteoderm was originally located rather than by taxonomical differences.

Discussion

The allocation of the material to *Pseudopus* is beyond doubt. However, some doubts concerning the distinguishing of *Pseudopus pannonicus* and recent *P. apodus* still exist. In phylogenetic analyses, the two were recovered as sister-taxa and, together with *P. laurillardi* and *P. ahnikoviensis*, formed the clade *Pseudopus* (see Klembara et al. 2019; Vasilyan et al. 2022). The taxonomic allocation of the various elements studied here from different localities to *P. pannonicus* is based not only on the generally large size that characterized this taxon, but also on the presence of several diagnostic features. However, because of the current knowledge of the osteology of *P. pannonicus* and/or the degree of preservation, there are some specimens in this material for which identification to the species level could be questioned (i.e., the lacrimal as it is the first one known in the fossil record for the taxon, vertebrae, especially some that are poorly preserved and osteoderms as these are usually difficult to identify to species-level).

Indeed, several traits are not peculiar to *P. pannonicus* and are shared with other *Pseudopus* taxa, especially *Pseudopus apodus*. The affinities of some of these unremarkable elements with *P. pannonicus* are here justified because of their general morphology, overall large size (similar to, or slightly larger than in *P. apodus*), stratigraphic, and geographic positions. The simultaneous occurrences with other elements more confidently allocated to *P. pannonicus*, in localities where no other anguine reptiles are currently known, are also taken into account. It appears that in the localities herein studied *P. pannonicus* is the most common, sometimes the only, representative of anguine reptiles, thus somewhat strengthening the attribution to *P. pannonicus* of these more generic and non-diagnostic elements. However, it should be noted that some rare occurrences of *Ophisaurus* specimens are known in the Early Pliocene of Moldova. Indeed, two parietals confidently attributed to two distinct *Ophisaurus* species, *Ophisaurus spinari* Klembara, 1979 and *Ophisaurus fejfari* Klembara, 1979, were recently described from Etulia and Lucheshty by Syromyatnikova et al. (2022): the first record of the genus from the Pliocene of Eastern Europe. These findings are quite interesting given how this anguine genus was widely distributed in the Miocene of Eastern Europe and was previously thought to be absent from the Pliocene of this area. Besides, despite these recent rare findings that should not be discarded in any case, very little or no material of anguine reptiles except *Pseudopus*, is known from

Upper Cenozoic fossil sites of Moldova, whereas other squamates such as cf. *Lacerta* sp. or various snake representatives (e.g., Erycidae, Viperidae, or Colubridae) comprise the fossil squamate fauna of the area (Nadachowski et al. 2006). Although it is admitted that there has been a general tendency in the past for lesser attention given to reptile and amphibian fossil assemblages in comparison to other groups such as mammals in Europe (Villa and Delfino 2019b, and references therein), the relatively diverse palaeoherpetofaunas known for these localities would attest that such sampling biases are not the primary explanation for the absence of an otherwise quite common member of vertebrate fossil faunas. The material we document here is interesting as it is supplementing other reports of *P. pannonicus* from that area (Alexejew 1912; Roček 2019) and thus also adds to the range of variation known for this species. Most relevant are both materials from Gritsev (Roček 2019) and especially Novoelizavetovka (Alexejew 1912) as these are well preserved and numerous. Material from the latter locality, originally described as *Ophisaurus novorossicus* and then synonymized with *P. pannonicus* by Fejérváry-Lángh (1923) presents also a notable interest. Indeed, the specimens that have been described and figured from this locality are documenting some of the most common fossil elements in the fossil record of *P. pannonicus* (e.g., maxillae, frontals, parietal, dentaries, vertebrae, osteoderms) in an exceptional state of preservation (i.e., one of the largest specimens from this locality and partially articulated; Alexejew 1912, 30, pl. II., figs 1, 2) but also more scarce elements such as pterygoids, palatines, jugals, quadrates and braincases. Based on the descriptions and figures available, it is difficult to state confidently if the specimens from this locality display some of the characters we present here (e.g., exclusion of the coronoid from the anterior inferior alveolar foramen by the splenial articulation facet of the dentary). The maxillae presented by Alexejew (1912) are bearing rather apparent and well-developed ornamentation, similar to the condition typically observed in *P. pannonicus* that is supplemented by our data and studied further later in this work. The large parietals from that material are displaying wide muscular surface ventrally, almost as wide as the width between the parietal cranial crest and the parietal foramen, a character that is focused on in the present work. The braincase from the Miocene of Novoelisavetovka is exceptionally well-preserved, possibly the best preserved currently known. Unfortunately, its description is most succinct, and the figures provided are limited as well. It would be interesting to see if that specimen also bears, in lateral view, the supplementary longitudinal crest that is located between the alar process and the prootic crest on the specimen from our material and also seemingly on the specimen from Gritsev (specimen NMNHU-P 3390; Roček 2019, 832). Henceforth, as suggested here, this ancient material would benefit most to be revisited, following the many advancements made in regard of the taxonomy of *Pseudopus*, and be revised accordingly to more modern practices and scientific standards.

Intrageneric comparisons with a special emphasis on *Pseudopus apodus*

Currently, *Pseudopus pannonicus* is distinguished from other *Pseudopus* taxa by a limited number of features – some of the previous ones are summarized in the recently amended diagnosis of the taxon (Roček 2019). For a long time, however, *P. pannonicus* has proven to be a rather problematic taxon because of the close osteological similarities to the extant *Pseudopus apodus*. This striking resemblance between the two taxa is something that has long been known and frequently pointed out (Fejérváry-Lángh 1923; Młynarski 1964; Estes 1983; Holman 1998; Roček 2019). It has been the source of several questions about the relationships of *P. pannonicus* to *P. apodus* (e.g., Młynarski 1964), and the true nature of this fossil taxon as a whole (e.g., a fully distinct taxonomic entity, a larger phenotype of *P. apodus*, etc.; see Introduction). On the other hand, Klembara (1986) stated that he was able to recognize both species in the Early Pliocene (MN 15) Ivanovce locality (Slovakia) based on several features, not only their different sizes. Although the material described here as *P. pannonicus* exhibits many similarities with *P. apodus*, there are also several diagnostic features that appear to distinguish it not only from the other fossil members of the genus *Pseudopus*, but especially from *P. apodus*. These features (treated in detail below) are as follows: (1) a more strongly developed ornamentation of the nasal process of the maxilla in comparison to *P. apodus*; (2) well-developed and wider muscular surfaces of the ventral surface of the parietal; (3) splenial facet reaches posterior to the anterior inferior alveolar foramen, thus excluding the coronoid from this foramen; and (4) short and compressed presacral vertebrae in comparison to the more elongated vertebrae of *P. apodus*.

It should be noted, however, that some of these features discussed here or some diagnostic features of *P. pannonicus* are notorious among other groups of squamates for being rather variable in their respective expressions. The variability of some of these features can be explained by the influence of ontogeny and body size (e.g., increasingly marked dermal ornamentation of the prefrontal and frontal among lacertids; degree of concavity of the compound bone among scincids; size-related individual variation of the compound bone in *Lacerta viridis*; Villa and Delfino 2019b). This is mainly the case for character states such as the development of dermal ornamentations, – which in the case of the present study could affect the first character and, e.g., the number of teeth. Although the character states suggested here were either never observed in *P. apodus*, or are somewhat different in *P. apodus*, a correlation to body-size parameters for some of the traits herein discussed cannot be fully discarded. As such, statistical analyses of these features are presented in a dedicated part later in this work.

Maxilla. *Pseudopus pannonicus* is differentiated from other members of the genus, especially *Pseudopus apodus*, by its higher number of labial foramina piercing the

lateral surface of the maxilla as well as by its different number of teeth (Roček 2019). In *P. apodus*, the maxilla is pierced by a maximum of five labial foramina (Klembara et al. 2017). The tooth account of this extant species is up to 14 teeth (Klembara et al. 2014). However, the tooth account of *P. pannonicus* is stated to have a maximum of 12 tooth positions (Bachmayer and Młynarski 1977; Klembara 1986). For example, eleven tooth positions are present in the largest specimen (24 mm) from Gritsev (Roček 2019), and 12 in the smaller specimen (17 mm) from Hambach. The particularly large ZIN PH 1/282 (its length is 36.93 mm, being relatively much larger than the previously described maxillae) described here possesses eight labial foramina (the same as the smaller maxilla from Hambach, see Čerňanský et al. 2017) and displays typical traits of *P. pannonicus* (see Description above for more detail). It has, however, 19 tooth positions, thus markedly surpassing the previously expected maximum of 12 teeth. This is a good example that tooth number in anguines, as in virtually all lizards, is quite variable and also likely to be size related, so these numbers should not be interpreted as absolutes. Therefore, as such a range of variability exists, a restricted amount of teeth might not prove to be the most pertinent of characters to help differentiate taxa (not only to the very least). Drastic variations in the number of teeth should not be overlooked, of course, but in the case of less clearcut differences, a degree of variability should most likely be accounted for.

Laterally, the osteoderms fused to the nasal processes of the maxillae in our material possess a well-developed ornamented surface, better developed than in *P. apodus*.

Frontal. The frontals in our material show clear differences from both *Pseudopus ahnikoviensis* and *Pseudopus laurillardi* while sharing similar characters with *Pseudopus apodus*. The lateral margins of the frontals are straight and gradually converging anteriorly. Additionally, unlike in *P. ahnikoviensis* and *P. laurillardi*, the orbital margins of the frontal are not smooth, but are covered by the ornamented surface. The latter condition is shared with adult individuals of *P. apodus* (Klembara et al. 2017).

Parietal. The parietal shows a combination of characters that are shared across species of the genus. In our *Pseudopus pannonicus* material, the anterolateral processes are rather well-developed, more than in *Pseudopus apodus*, but slightly less than in *Pseudopus laurillardi*. In ventral view, the muscular surfaces of the medium and large-sized specimens are well-developed and large - their width (abbreviated MSw hereafter) approaches, and sometimes equals, the distance between the parietal foramen and parietal cranial crest (abbreviated PCC-MedP hereafter) (e.g., ZIN PH 17/277 and ZIN PH 6/278). In *P. laurillardi* and *P. apodus*, the width of the muscular surfaces is smaller, and narrower (Klembara et al. 2010). In *P. apodus*, the muscular surface is generally half as wide as the distance between the parietal cranial crest and the median plane of the parietal. Comparatively, the observations of our material tend to highlight a width of the muscular surface closer to the PCC-MedP distance. As mentioned previously, this particularity of the parietals of *P. pannonicus* from our material might prove to be diagnostic and will be studied more in-depth later in this work.

Virtual microanatomy. The internal microanatomy in terms of a vascular network is similar in all studied specimens. Small differences might represent individual and/or ontogenetic variations. Interestingly, the meshwork of *Pseudopus pannonicus* with its large interconnected cavities and channels in ventral section of the parietal table (in regard to ZIN PH 17/277) slightly resembles the type present in *Pseudopus apodus* (Fig. 6K vs. S). It should be noted, however, that the parietal ZIN PH 17/277 is clearly thicker and the cavities are much larger and also more variable, irregular in shape. In *P. apodus*, the meshwork in the mid-level is formed by radially diverging channels running to the periphery of the bone. Here, the channels appear to be slightly larger relative to the overall size of the parietal bone than in ZIN PH 17/277. In *P. apodus*, few cavities are present only at the ventral level inside of the parietal table. They are rather small, oval (or box-shaped) and regularly arranged. On the other hand, above mentioned distinct cavities are absent in the large specimen ZIN PH 18/277 and comparative physiological studies of extant anguines are needed to resolve the exact function of the strong parietal vascularization in these lizards. It should be noted that the general type of meshwork in *Pseudopus* slightly differs from the heavily vascularized type present in *Ophisaurus* (the parietal bone appears to be less compact in both axial and coronal sections; see Georgalis and Scheyer 2021: fig. 7). Such small differences in vascular arrangements could indicate some differences in the thermoregulatory function – this might reflect the large body size of *Pseudopus*.

Braincase. The occipital segment of the braincase, although the quantity of our material is strongly limited, shows some interesting features. Braincase elements are not currently known for *Pseudopus ahnikoviensis* and *Pseudopus confertus*, thus hindering any valuable comparisons. Different from *Pseudopus laurillardi* but somewhat similar to *Pseudopus apodus*, the dorsal ridges [i.e., ala otosphenoidea sensu Roček (2019)] are slightly curved. These dorsal ridges are somewhat more prominent than in *P. apodus*. The high ascending process of the supraoccipital crest seems more prominent and more strongly defined than in *P. laurillardi* (although it is partly broken in the only known specimen; Klembara et al. 2010) and in *P. apodus* (Villa and Delfino 2019a). The basal tubercles of our *Pseudopus pannonicus* braincase appear to be somewhat wider than what is known in *P. apodus* (e.g., Villa and Delfino 2019a; CT scans from the Digimorph CT-repository at the University of Texas at Austin, Maisano 2003). The distal ends of the basal tubercles seem also to be somewhat more rounded in appearance than in *P. apodus* (although the difference is admittedly low). This roundness is reminiscent of the condition displayed by *P. laurillardi* (Klembara et al. 2010). In lateral view, there is a mild crest running dorsal to the prootic crest, its course being parallel to that of the prootic crest.

According to our observations, such a crest is not present in *P. apodus*. It is still unclear if this additional crest holds much, if any, taxonomical value but its presence is noteworthy, nonetheless. The Gritsev *P. pannonicus* specimen drawn and figured by Roček (2019) seems to display a similar (although slightly less well defined?) structure but no particular attention has been drawn to it. It is unclear if such a crest is present in *P. laurillardi*¸ although it does seem to be absent. In *P. apodus* and among extant anguids more generally, the ventral surface of the sphenoid is mostly flattened, showing a mild depression in its middle area (Villa and Delfino 2019a). Here, the ventral surface of our specimen is distinctly sunken in its middle area, showing an anteroposteriorly elongated depression. However, braincases of *P. pannonicus* are particularly scarce in the fossil record, and only a handful have been reported, including ours. In the case of the specimen reported from Gritsev (Roček 2019), the ventral surface of the sphenoid is depressed in its middle, but not the extent shown here. With such limited material overall, it is delicate to weigh on the interest of the feature displayed by our specimen. Taphonomic processes could have been at play here and damaged our specimen, for instance. In *P. laurillardi*, such marked depression is not reported (Klembara et al. 2010).

Dentary. The dentary of anguines usually possesses many clear diagnostic features, and this is especially true for *Pseudopus*, which shows the highest number of apomorphies of all anguine genera (Klembara et al. 2014). In contrast to *Pseudopus laurillardi*, the dentaries described here are neither ventrally arched, and nor is the dental crest medially expanded. The surangular spine, a structure present only in *P. ahnikoviensis* within the genus *Pseudopus* (Klembara 2012; Čerňanský et al. 2015), is absent in our specimens. Aside from their overall large size, the dentaries in our material show several similarities with *P. apodus*. The positions of surangular foramen and surangular sinus are similar to that of *P. apodus* contra both *P. laurillardi* and *P. ahnikoviensis*. The angular process of our dentaries does not surpass the coronoid process, a feature characteristic of the genus as a whole (Klembara et al. 2014). The surangular process of our dentaries is similar to that in *P. apodus*. The coronoid processes of our dentaries express some degree of variability in their morphology, which is a tendency also known among *P. apodus* specimens (Klembara et al. 2014). The dentition of our dentaries is also similar to that of *P. apodus*. The number of tooth positions herein observed is well within the ontogenically related range of 11 to 18 teeth known for *P. apodus* (Klembara et al. 2014). Roček (1980, 2019) reported that among ontogenically advanced individuals of *P. apodus*, there were tendencies for the posterior teeth of the dentary to stop being replaced, thus displaying a fused aspect at their bases. This feature should probably be treated carefully when dealing with limited fossil material because of its relationships with ontogenetic series. Nonetheless, the specimens described here tend to be on the lower end of the size spectrum of dentaries known for *P. pannonicus* – namely when compared with specimens from Gritsev (Roček 2019) – and there are no signs of such fusing of teeth in our material. In addition, such fusion has never been described in the literature for specimens attributed to *P. pannonicus*.

There is one dentary character state which might distinguish *Pseudopus pannonicus* from *P. apodus*. In *P. apodus*, the posterior margin of the anterior inferior alveolar foramen is formed by the anteromedial process of the coronoid, a condition not present in the extinct *Pseudopus* species. However, as was previously suggested by Čerňanský et al. (2017a) on the material of *P. pannonicus* from Hambach, a facet for the splenial in this taxon appears to be present posterior to the anterior inferior alveolar foramen – thus, the coronoid is excluded from this foramen. The same condition is present in *P. laurillardi* (see Klembara et al. 2010) and in *P. ahnikoviensis*. In our dentary material, the facet for the anteromedial process of the coronoid clearly does not reach the foramen but is separated from it by an area. This area could be interpreted as a splenial facet (if the splenial attached this area when the mandible was complete). The same condition is present in the lectotype MÁFI V 2023.1.14.1 specimen from Hungary (see Fig. 15) as well as the material from Gritsev (see Roček 2019: "Only the dorsal facet is interrupted by a rounded section that in complete mandible takes part in the formation of a foramen called by Meszoely [1970, figure 4] the anterior inferior alveolar foramen."). In any case, there is a clear facet for the splenial posterior to the anterior inferior alveolar foramen in ZIN PH 1/280.

In summary, we can consider the character state in *P. pannonicus* as different from that of *P. apodus* and support the suggestion of Čerňanský et al. (2017). Note, however, that in juvenile medium-sized individuals of *P. apodus*, the anteromedial process of the coronoid is shorter and pointed, and does not reach the posterior margin of the anterior inferior alveolar foramen. But this points to the fact that the condition in *P. apodus* is peramorphic (see Klembara et al. 2014). In the largest specimen DE 13 of *P. apodus* in Klembara et al. (2014; the length of the mandible of this specimen is 56.8 mm), the condition is slightly different as above mentioned – although the termination of the anteromedial process of the coronoid is rounded and participates in the anterior inferior alveolar foramen, so that the splenial is also not excluded here (see Klembara et al. 2014: fig. 2C).

Trunk vertebra. In our material, the height of the neural canal is lower than the height of the cotyle. This is a character state shared typically with *Pseudopus apodus* as opposed to *Ophisaurus*, one exception being *Ophisaurus harti* as highlighted by Čerňanský et al. (2019). In addition, the trunk vertebrae described here appear to be wider, being markedly less elongated, than the trunk vertebrae of *P. apodus*. Trunk vertebrae of the latter taxon are somewhat elongated, as highlighted by their centrum length and neural arch width ratio of 62% (Čerňanský et al. 2019). Here, our material is associated with a CL/NAW ratio closer to 90%. This characteristic will be developed more thoroughly later in this work.

Figure 15. The lectotype, MÁFI V 2023.1.14.1. (former Ob. 5058) of *Pseudopus pannonicus*: left dentary from the Late Miocene of Polgárdi 2, Hungary, in medial (**A**) and lateral (**B**) views.

Caudal vertebra. Caudal vertebrae are unknown for *Pseudopus ahnikoviensis* and *Pseudopus confertus* (Klembara 2012, 2015; Klembara and Rummel 2018), whereas a few, albeit not particularly informative, are known for *Pseudopus laurillardi* (Klembara et al. 2010) and a handful are known for *Pseudopus pannonicus* (including the ones presented here; e.g., Alexejew 1912; Klembara 1986; Roček 2019). Noteworthy is the fact that several caudal vertebrae have been reported as either indeterminate anguines or *Pseudopus* sp. but with hints of potential affinities towards *P. pannonicus* (e.g., Georgalis et al. 2017a, 2018). As mentioned briefly earlier in this work, some specimens with such suspected affinities could potentially be reassigned to *P. pannonicus*. As it has been also emphasized previously, the distinction of anguine taxa based solely on osteological features of caudal vertebrae is difficult and a traditionally more conservative approach is preferred by only referring such specimens to indeterminate anguines (Čerňanský et al. 2017a, 2017b; Georgalis et al. 2018). Unfortunately, few to no features (supposing there are any) allowing for the confident distinction between *Pseudopus* species, especially *P. pannonicus* and *P. apodus* are currently known. Thus, additional insights from other rationales (e.g., stratigraphy, geography, compositions of fossil assemblages, etc.) need to be considered to argue for any particular specific identification. Here, our material is most similar to the morphology of caudal vertebrae known in *Pseudopus*, namely *P. apodus*. Indeed, these are generally narrower than the presacral vertebrae observed here. No autotomic split is apparent despite the presence of autotomy foramen in some specimens. This material is also rather similar to better preserved caudal vertebrae from Gritsev (Roček 2019) or other similarly preserved specimens (e.g., Alexejew 1912; Bachmayer and Młynarski 1977; Klembara 1986; Venczel 2006).

Osteoderms. The osteoderms allocated to this form are large and thick. As mentioned earlier, due to the difficulties of alpha taxonomic determinations linked to osteoderms, an identification as an indeterminate anguine would be totally admissible because of the vermicular ornamented surface. Here, in the case of our material, we argue that the features displayed by these osteoderms exclude an *Anguis* identification, thus leaving *Ophisaurus*, *Pseudopus*, *Ragesaurus*, and *Smithosaurus* as the remaining anguine taxa that these osteoderms could be attributed to. The osteoderms of either *Ragesaurus* or *Smithosaurus* are still unknown as these taxa are known only by limited

material respectively from the Quaternary of Spain (Bailon and Augé 2012), and from the Early and Middle Miocene of Germany and Austria (Vasilyan et al. 2022). The larger size and robustness of these elements seems to be more congruent with *Pseudopus*. An identification of some of our osteoderms to *Ophisaurus* is not necessarily excluded as two different members of this genus have been reported recently by Syromyatnikova et al. (2022) in both Lucheshty and Etulia, coexisting with *Pseudopus* representatives (this study). However, because of the age of these specimens, their size, as well as the relative scarcity of *Ophisaurus* material from the Pliocene of Eastern Europe (i.e., two damaged parietals) in comparison to the amount of material confidently attributed to *Pseudopus* here, we tentatively identify our osteoderms from Lucheshty and Etulia, and the remaining specimens from Kalfa, Petroverovka, and Volchaya Balka, as belonging to *Pseudopus* and more particularly *Pseudopus pannonicus*, due to their robustness and thickness. Although the morphology of these osteoderms is roughly similar to those known in *P. apodus*, the osteoderms of our material are generally markedly thicker.

Statistical analyses

Dermal ornamentation of the maxilla. The preservation of three of the five maxillae available in the material allows observation of the size of the ornamentation of the nasal process. Besides these three specimens, data from nine maxillae of *Pseudopus pannonicus* described and figured in the literature were added. Specimens, either from our samples or the literature, with heavily damaged or missing nasal process, have been excluded from the samples tested, leaving thus only specimens suited for the analyses conducted here. The height and width of the ornamented surface and the total height and width of each maxilla are measured (Fig. 16) and a correlation matrix was established.

This matrix (Fig. 17) shows with statistical significance (i.e., p-values less than the Bonferroni correction) on one hand that both the width and height of the dermal ornamentation are positively correlated to each other, and that the overall width and length of the maxillae are positively correlated to each other as well. On the other hand, the dimensions of the ornamentation are also positively correlated to the size of the maxilla, although slightly less to its height than its length. However, there is only statistical significance for the relationship between the ornamentation dimensions and the total height of the maxillae. Our sample size is admittedly rather small and more well-preserved specimens would be most welcomed but our results are nonetheless interesting regarding intraspecific variability. Although there is a seemingly positive correlation between the development of the ornamentation of the nasal process of the maxilla and the body size, our data only really support a correlation with the height of the maxilla (i.e., stronger ornamentation on more developed nasal process and vice versa). This suggests that the ornamentation of the nasal process is a character that is subject to changes throughout the ontogeny of *P. pannonicus* and that older individuals would tend to display larger and more developed dermal ornamentation than younger, less mature, individuals. The smaller individuals of our material as well as the ones from the literature used here for comparisons tend to display a degree of ornamentation at least similar to that of adults of *Pseudopus apodus*, if not more strongly developed, whereas larger individuals tend to bear more developed ornamentation. Studies focusing on this feature of the maxilla of *P. apodus* throughout different ontogenetic series would be most interesting to compare the intraspecific variation among these two taxa. Based on the pattern that our results are suggesting, it could be assumed that the ornamentation of the nasal process of the maxilla is also subject to ontogenetic changes in *P. apodus*.

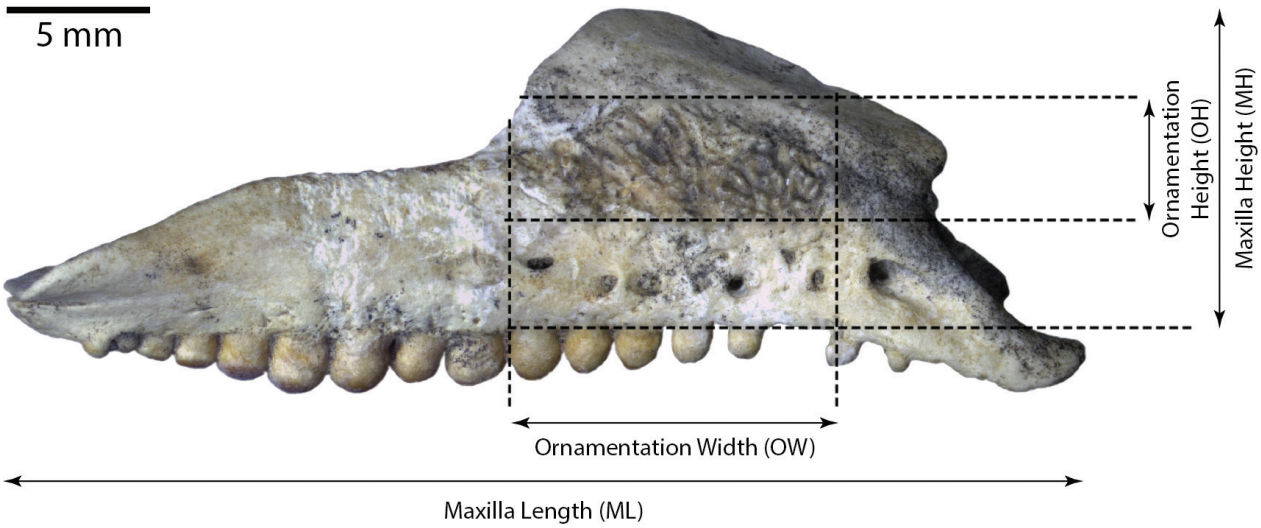

Figure 16. Measurements of the maxilla of *Pseudopus pannonicus* used in statistical analyses in the present work (here, ZIN PH 1/282 in lateral view).

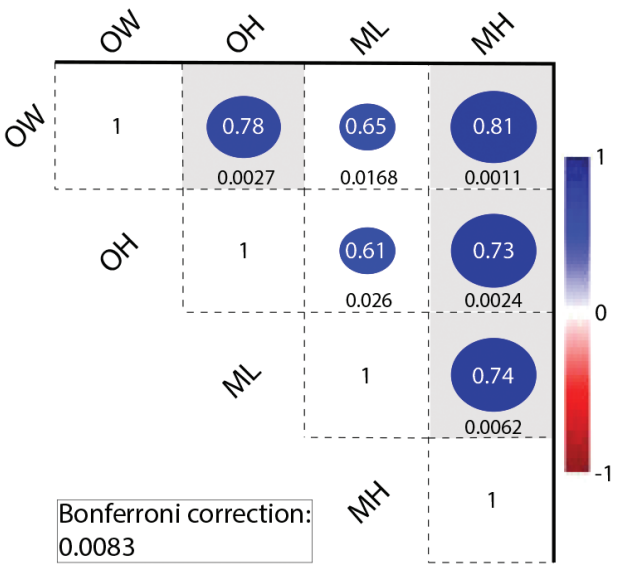

Figure 17. Correlation matrix of the studied parameters of the maxillae of *Pseudopus pannonicus*. Diagonal terms of this matrix (e.g., "OW – OW" correlation index = 1) are ignored. Terms of this matrix that are in a greyed box are statistically significant ($p < P_{Bonferroni}$). Individual p-values for each combination are shown below the corresponding correlation indexes. Abbreviations: MH: maxilla height; ML: maxilla length; OH: ornamentation height; OW: ornamentation width.

Currently, osteological studies on *P. apodus* have highlighted that the lateral surface of the maxillae of this taxon bears only light ornamentation (Klembara 1981; Klembara et al. 2017; Villa and Delfino 2019a) that is supposedly thinner and located slightly higher up on the nasal process than in *P. pannonicus*. Maxillae of *Pseudopus laurillardi* are known to exhibit various types of ornamentation, somewhat similar to the condition known in *P. pannonicus*, and more pronounced in the larger specimens (Klembara et al. 2010). This condition of the maxilla is not known for *Pseudopus ahnikoviensis* and *Pseudopus confertus*. As emphasized by Roček (2019), this character state might be of interest in distinguishing between *P. pannonicus* and *P. apodus*. If the trend observed in our material and suggested by our statistical analyses were to be confirmed by the input of new material, then hypotheses on the cause(s) of the differences in character expression between *P. pannonicus* and *P. apodus* could be made. For instance, heterochronic processes may likely be at play here. Indeed, the evolution of several features of the lower jaw, skull, and vertebral column of *P. apodus* have already been shown to be influenced by heterochronic processes (Klembara et al. 2014, 2017; Čerňanský et al. 2019).

Muscular surface of the parietal. The feature of the parietal discussed here is the relative width of the muscular surface observed in *Pseudopus pannonicus* in comparison to the overall size of the parietal. Following observations and as mentioned earlier, among *P. pannonicus* the muscular surfaces appear to be rather wide, approximately equal to the PCC-MedP distance. In comparison, among *Pseudopus apodus* the MSw is approximately equal to half the PCC-MedP distance. To summarize, the conditions observed are an MSw/PCC-MedP ratio ≈ 1.0 and an MSw/PCC-MedP ratio ≈ 0.5 for *P. pannonicus* and *P. apodus* respectively. Of the 11 parietals from our material, these data could be measured on 10 of them. To the data of these 10 specimens, the data from 16 additional parietals attributed to *P. pannonicus* were added. These data were then compared with the material of *P. apodus*.

The MSw and the PCC-MedP distances were measured (Fig. 18) and an MSw/PCC-MedP ratio was attributed to each specimen.

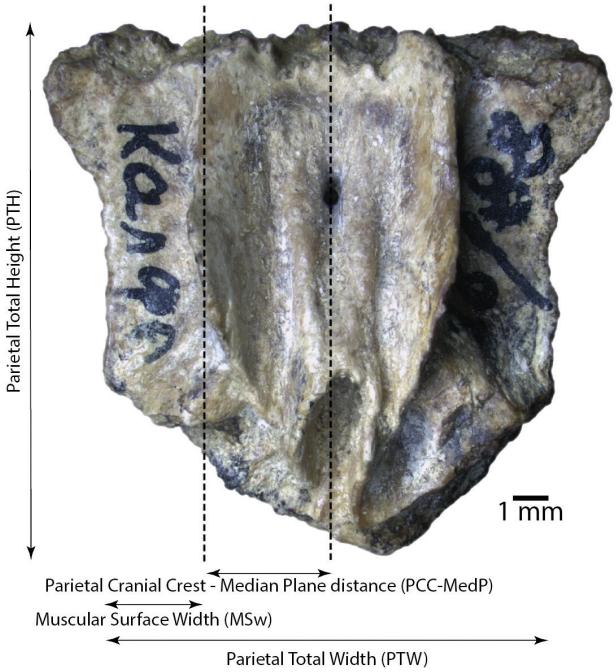

Figure 18. Measurements of the parietal of *Pseudopus pannonicus* used in statistical analyses in the present work (here, ZIN PH 18/277 in ventral view).

Following these measurements, the average ratio in *P. pannonicus* is of 0.885 (min: 0.406; max: 1.734; σ: 0.262) and the average ratio in *P. apodus* is of 0.534 (min: 0.177; max: 0.872; σ: 0.233). To determine if these ratios are significantly different from one another, a Student's *t*-test was done. The null hypothesis H_0 of this test is: "the samples are taken from a population with the given mean". The result of this test shows that the mean values of the elements sampled as *P. pannonicus* and the one of *P. apodus* are significantly different from each other (Table 1). Indeed, the sample mean (i.e., the mean ratio among *P. pannonicus*; $\bar{x} = 0.885$, N = 26) is significantly different from the given mean of 0.534 (Student's $t = 6.833$; $p_{(same\text{-}mean)} = 3.67 \times 10^{-7}$). Therefore, the null hypothesis is rejected, and it can be established that the populations (taxa) represented by the specimens are clearly distinct from one another.

Consequently, a test of correlation between these various parameters was done to evaluate the influence of body size on the relative width of the muscular surface. The correlation matrix shows, with statistical significance, that these parameters are quite strongly influenced by body size (Fig. 19). Thus, this character state presum-

Table 1. Summary of the Student *t*-test parameters regarding the parietal of *Pseudopus pannonicus* and *Pseudopus apodus*.

Samples data				
	N	**Mean**	**Std. Dev**	**Std. Error Mean**
P. apodus	6	0.534	0.233	0.095
P. pannonicus	26	0.885	0.262	0.051

t-Test results				
Mean difference	**Lower bound of the 95% confidence interval of the difference**	**Upper bound of the 95% confidence interval of the difference**	***t***	$p_{(same\ mean)}$
0.351	0.113	0.589	6.833	3.67 × 10^–7

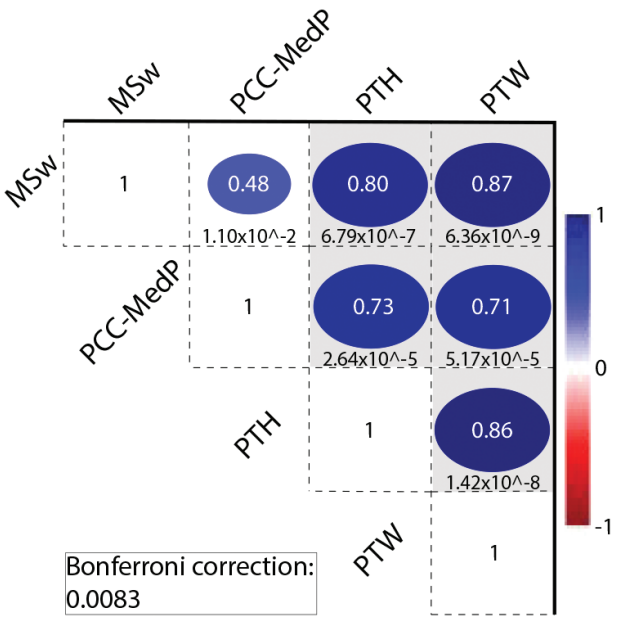

Figure 19. Correlation matrix of the studied parameters of the ventral surface of the parietal bones of *Pseudopus pannonicus*. Diagonal terms of this matrix are ignored. Terms of this matrix that are in a greyed box are statistically significant ($p < 0.05$). Abbreviations: MSw: muscular surface width; PCC-MedP: distance between the parietal cranial crest and the median plane of the parietal; PTH: parietal table height; PTW: parietal table width.

ably peculiar to *P. pannonicus* is not reliable enough to distinguish this taxon from *P. apodus*.

Vertebral elongation. As mentioned previously, the trunk vertebrae of our *P. pannonicus* material, as well as the ones described in the literature, are rather stout and compressed. These are thus quite distinct from the comparatively notably elongated trunk vertebrae of *Pseudopus apodus* (Čerňanský et al. 2019). Here, the relevance of the degree of vertebral elongation for identification purposes is examined.

The eleven presacral vertebrae from our material are here considered. To these elements, literature data from 16 additional presacral vertebrae identified as *P. pannonicus* are included. These data are then compared to the presacral vertebrae of *P. apodus*, such as the ones studied in details by Čerňanský et al. (2019). The degree of elongation of a vertebra is determined by the ratio between the centrum length and the neural arch width (i.e., CL/NAW ratio hereafter). A ratio closer to 1, or greater than 1, is equivalent to a stouter and more compressed vertebra, whereas a more elongated vertebra is associated with a ratio lesser than 1. Another assumption resides in the fact in both *P. pannonicus* and *P. apodus*, although the absolute values of both NAW and CL might very well vary throughout the relative position of a given vertebra in the column, the respective proportions of the vertebrae (i.e., the CL/NAW ratios) remain similar. It has been highlighted that the presacral vertebrae posterior to the atlas and axis of *P. apodus* display very uniform morphology despite increasing steadily in relative sizes anteroposteriorly (Hoffstetter and Gasc 1969; Čerňanský et al. 2019). Only the very first few anterior trunk vertebrae appear to diverge from this general tendency. Moreover, this tendency is seemingly not limited to *Pseudopus* or anguines as a whole. Indeed, as Hoffstetter and Gasc (1969) also pointed out, vertebrae from the presacral region of the column tend to show relative morphological uniformity among snake-like, limbless and elongated organisms. In addition, because *P. pannonicus* and *P. apodus* are admittedly similar in many regards (Fejérváry-Lángh 1923; Klembara et al. 2010, 2014, 2017; Čerňanský et al. 2019), it is not too far-fetched to expect a similar condition for such a general tendency in *P. pannonicus*.

Presacral vertebrae of *P. apodus* are quite elongated. Their ratio of elongation has been previously estimated to be about 0.62 (Čerňanský et al. 2019). The average NAW/CL ratio of the herein described presacral vertebrae is closer to 1 ($\bar{x} = 0.96$). However, there is some variability among these ratios (min = 0.79; max = 1.37; $\sigma = 0.156$). To determine whether the values of the ratios obtained for *P. pannonicus* are different from the average elongation ratio of *P. apodus*, a Student's *t*-test was conducted. The null hypothesis H_0 of this test is: "The samples are taken from a population with the given mean". The results of this test show that the elongation ratios differ significantly between these taxa (Table 2). Indeed, the sample mean ($\bar{x} = 0.96$, N = 27) is significantly different from 0.62 (Student's $t = 11.132$; $p_{(same\text{-}mean)} = 1.4768 \times 10^{-11}$). Therefore, the null hypothesis is here rejected.

Table 2. Summary of the Student *t*-test parameters of trunk vertebrae of *Pseudopus pannonicus* and *Pseudopus apodus*.

Samples data				
	N	**Mean**	**Std. Dev**	**Std. Error Mean**
P. apodus	N/A	(*)0.620	N/A	N/A
P. pannonicus	27	0.96	0.156	0.03

t-Test results				
Mean difference	**Lower bound of the 95% confidence interval of the difference**	**Upper bound of the 95% confidence interval of the difference**	***t***	$p_{(same\ mean)}$
0.34	0.278	0.402	11.132	1.4768 × 10^–11

(*): Average ratio data for *P. apodus* from Čerňanský et al. (2019). N/A: Not Available.

Following this result, the character state of "stout presacral vertebrae with reduced elongation" appears to be important for comparisons between *P. pannonicus* and *P. apodus*.

Conclusions

Here were studied and described various cranial and vertebral elements attributed to the fossil anguine *Pseudopus pannonicus*. This material originates from several localities spread across Eastern Europe and the North Caucasus. The fossiliferous deposits are spanning the Upper Cenozoic (MN 10 to MN 15 / early MN 16). This material extends our knowledge of *P. pannonicus* in several aspects. Besides taxonomical discussion, the report of the elements from the localities from the Northern Caucasus represents some of the most, if not the most, easternmost occurrences currently documented for *P. pannonicus*, pending the revision and clarification of *Ophisaurus apodus dzhafarovi* from the Pleistocene of Azerbaijan. Although with limited taxonomic implications because of the high scarcity of this particular element, we report on the first lacrimal bone known in the fossil record of this species. Several osteological features and their validity in regard to comparisons between the fossil *P. pannonicus* and the very similar extant *Pseudopus apodus* were described and discussed. This new material included a handful of caudal vertebrae that unfortunately did not provide any new meaningful insight toward potentially distinctive features among *Pseudopus* species (supposing there is any in the first place). When data were suitable, statistical analyses were performed to study the influence of body-size parameters on the expression of a set of cranial and vertebral traits. It was shown that several of these traits were rather strongly linked to body size, thus rendering them unreliable for diagnostical purposes between *P. pannonicus* and *P. apodus*. Two newly recognized traits in *P. pannonicus* in comparison to *P. apodus* are respectively related to the development of the osteodermal crust of the maxilla and the degree of elongation of the trunk vertebrae. Finally, the following three features are suggested as being diagnostic of *P. pannonicus*: (1) more strongly developed ornamentation of the nasal process of the maxilla in comparison to *P. apodus*; (2) splenial facet reaches posterior to the anterior inferior alveolar foramen – thus excluding the coronoid from this foramen; and (3) short and compressed presacral vertebrae in comparison to the more elongated vertebrae of *P. apodus*.

Acknowledgments

We thank Andrea Villa for his comments and insights regarding the influence of body-size parameters that inspired the statistical analysis section presented here. Our gratitude is also addressed towards Georgios Georgalis and Zbigniew Szyndlar of the Institute of Systematics and Evolution of Animals of the Polish Academy of Sciences for allowing loans and access to some of the comparative material of *Pseudopus pannonicus* from Poland included in Suppl. material 1 to E. L. and A. Č. We are deeply indebted to László Makádi and the Department of Collections of the Supervisory Authority for Regulatory Affairs in Budapest, Hungary, for providing E. L. access to their collections, hosting the original material in addition to comparative specimens of *Pseudopus pannonicus*, and for their precious help in the acquisition of SEM pictures of this valuable material figured in the present work. We are indebted to Jozef Klembara (Comenius University in Bratislava) for the access to CT scans of the extant *Pseudopus apodus* (DE 52). We thank Krister T. Smith (Senckenberg Research Institute, Germany) and Georgios Georgalis (Polish Academy of Sciences, Poland) for their comments and revisions on the manuscript. This work was supported by the Scientific Grant Agency of the Ministry of Education of Slovak Republic and Slovak Academy of Sciences, Grant Nr. 1/0191/21 (to A. Č), and Grant Nr. UK/49/2022 (to E. L.) and by the Zoological Institute, Russian Academy of Sciences (project 122031100282-2. The Scanning Electron Microscope used in this study, and the pictures subsequently acquired, was established thanks to the GINOP-2.3.3-15-2017-00043 grant.

References

Alekperov AM (1978) Zemnovodnye i presmykayushchiesya Azerbaydzhana [Amphibians and reptiles in Azerbaijan].

Alexejew A (1912) Description de la faune méotique des vertébrés des environs du Village Petroviérovak (District Tiraspol). I. Anguidae. Zapiski matematicheskogo otdeleniya Novorossiiskogo obshchestva. estestvoispytatelei 39: 13–40.

Augé M (2005) Évolution des lézards du Paléogène en Europe. Mémoires du Muséum national d'Histoire naturelle 192: 1–369.

Bachmayer F, Młynarski M (1977) Bemerkungen über die fossilen *Ophisaurus*-Reste von Österreich und Polen. Akademie der Wissenschaften 186: 285–299.

Bailon S (1991) Amphibiens et reptiles du Pliocène et du Quaternaire de France et d'Espagne: mise en place et évolution des faunes. Paris-Diderot.

Bailon S, Augé M (2012) Un nouveau genre, *Ragesaurus* (Squamata, Anguidae, Anguinae), du Pléistocène inférieur des îles Medas (Catalogne, Espagne). Bulletin de la Société géologique de France 183: 683–688. https://doi.org/10.2113/gssgfbull.183.6.683

Baryshnikov GF, Zakharov DS (2013) Early Pliocene bear *Ursus thibetanus* (Mammalia, Carnivora) from Priozernoe locality in the Dniester Basin (Moldova Republic). Proceedings of the Zoological Institute RAS 317: 3–10. https://doi.org/10.31610/trudyzin/2013.317.1.3

Blain H-A, Bailon S (2006) Catalogue of Spanish Plio-Pleistocene amphibians and squamate reptiles from the Museu de Geologia de Barcelona. Treballs del Museu de Geologia de Barcelona 14: 61–80.

Blain H-A, Bailon S, Agustí J (2016) The geographical and chronological pattern of herpetofaunal Pleistocene extinctions on the Iberian Peninsula. Comptes Rendus Palevol 15: 731–744. https://doi.org/10.1016/j.crpv.2015.05.008

Bolkay SJ (1913) Additions to the fossil herpetology of Hungary from the Pannonian and Praeglacial periods. Mitteilungen aus dem Jahrbuche der königlich ungarischen Geologischen Reichsanstalt 21: 217–230.

Burbrink FT, Grazziotin FG, Pyron RA, Cundall D, Donnellan S, Irish F, Keogh JS, Kraus F, Murphy RW, Noonan B (2020) Interrogating genomic-scale data for Squamata (lizards, snakes, and amphisbaenians) shows no support for key traditional morphological relationships. Systematic biology 69: 502–520. https://doi.org/10.1093/sysbio/syz062

Čermák S (2016) The Late Miocene species *Ochotona kalfense* (Mammalia, Lagomorpha) of Moldova: The oldest European record of the genus in the context of the earliest Ochotoninae. Comptes Rendus Palevol 15: 927–940. https://doi.org/10.1016/j.crpv.2016.04.010

Čerňanský A, Klembara J (2017) A skeleton of *Ophisaurus* (Squamata: Anguidae) from the middle Miocene of Germany, with a revision of the partly articulated postcranial material from Slovakia using micro-computed tomography. Journal of Vertebrate Paleontology 37: e1333515. https://doi.org/10.1080/02724634.2017.1333515

Čerňanský A, Rage J-C, Klembara J (2015) The Early Miocene squamates of Amöneburg (Germany): the first stages of modern squamates in Europe. Journal of Systematic Palaeontology 13: 97–128. https://doi.org/10.1080/14772019.2014.897266

Čerňanský A, Szyndlar Z, Mörs T (2017a) Fossil squamate faunas from the Neogene of Hambach (northwestern Germany). Palaeobiodiversity and Palaeoenvironments 97: 329–354. https://doi.org/10.1007/s12549-016-0252-1

Čerňanský A, Vasilyan D, Georgalis GL, Joniak P, Mayda S, Klembara J (2017b) First record of fossil anguines (Squamata; Anguidae) from the Oligocene and Miocene of Turkey. Swiss Journal of Geosciences 110: 741–751. https://doi.org/10.1007/s00015-017-0272-5

Čerňanský A, Yaryhin O, Ciceková J, Werneburg I, Hain M, Klembara J (2019) Vertebral Comparative Anatomy and Morphological Differences in Anguine Lizards with a Special Reference to *Pseudopus apodus*. The Anatomical Record 302: 232–257. https://doi.org/10.1002/ar.23944

Čerňanský A, Singh NP, Patnaik R, Sharma KM, Tiwari RP, Sehgal RK, Singh NA, Choudhary D (2022) The Miocene fossil lizards from Kutch (Gujarat), India: a rare window to the past diversity of this subcontinent. Journal of Paleontology 96: 213–223. https://doi.org/10.1017/jpa.2021.85

Conrad JL (2008) Phylogeny and systematics of Squamata (Reptilia) based on morphology. Bulletin of the American Museum of Natural History 2008: 1–182. https://doi.org/10.1206/310.1

Daudin FM (1803) Histoire naturelle, générale et particulière des reptiles: ouvrage faisant suite à l'histoire naturelle générale et particulière, composée par Leclerc de Buffon, et rédigée par C.S. Sonnini. Tome septième. F. Dufart. Paris, 436 pp. https://doi.org/10.5962/bhl.title.60678

Delfino M (2002) Erpetofaune italiane del Neogene e del Quaternario. Università degli Studi di Modena e Reggio Emilia.

Delinschi A (2014) Late Miocene lagomorphs from the Republic of Moldova. Annales de Paléontologie 100: 157–163. https://doi.org/10.1016/j.annpal.2013.10.004

Estes R (1983) Sauria terrestria, Amphisbaenia, Handbuch Der Paläoherpetologie, Part 10A. Gustav Fischer Verlag, Stuttgart, Germany, 249 pp.

Fejérváry-Lángh A (1923) Beiträge zu einer Monographie der fossilen Ophisaurier. Palaeontologia Hungarica 1: 123–220.

Fürbringer M (1900) Zur vergleichenden anatomie des Brustschulterapparates und der Schultermuskeln. Jenaische Zeitschrift für Naturwissenschaft 34: 215–718. https://doi.org/10.5962/bhl.title.52377

Gauthier JA (1982) Fossil xenosaurid and anguid lizards from the early Eocene Wasatch Formation, southeast Wyoming, and a revision of the Anguioidea. Rocky Mountain Geology 21: 7–54.

Gauthier JA, Kearney M, Maisano JA, Rieppel O, Behlke ADB (2012) Assembling the Squamate Tree of Life: Perspectives from the Phenotype and the Fossil Record. Bulletin of the Peabody Museum of Natural History 53: 3–308. https://doi.org/10.3374/014.053.0101

Georgalis G, Villa A, Ivanov M, Vasilyan D, Delfino M (2019a) Fossil amphibians and reptiles from the Neogene locality of Maramena (Greece), the most diverse European herpetofauna at the Miocene/Pliocene transition boundary. Palaeontologia Electronica 22.3.: 1–99. https://doi.org/10.26879/908

Georgalis GL, Scheyer TM (2021) Lizards and snakes from the earliest Miocene of Saint-Gérand-le-Puy, France: an anatomical and histological approach of some of the oldest Neogene squamates from Europe. BMC Ecology and Evolution 21: 1–22. https://doi.org/10.1186/s12862-021-01874-x

Georgalis GL, Delfino M (2022) The fossil record of lizards and snakes (Reptilia: Squamata) in Greece. In: Fossil Vertebrates of Greece Vol. 1. Springer, 205–235. https://doi.org/10.1007/978-3-030-68398-6_7

Georgalis GL, Villa A, Delfino M (2017a) Fossil lizards and snakes from Ano Metochi–a diverse squamate fauna from the latest Miocene of northern Greece. Historical Biology 29: 730–742. https://doi.org/10.1080/08912963.2016.1234619

Georgalis GL, Villa A, Delfino M (2017b) The last European varanid: demise and extinction of monitor lizards (Squamata, Varanidae) from Europe. Journal of Vertebrate Paleontology 37: e1301946. https://doi.org/10.1080/02724634.2017.1301946

Georgalis GL, Čerňanský A, Klembara J (2021) Osteological atlas of new lizards from the Phosphorites du Quercy (France), based on historical, forgotten, fossil material. Geodiversitas 43: 219–293. https://doi.org/10.5252/geodiversitas2021v43a9

Georgalis GL, Rage J-C, de Bonis L, Koufos GD (2018) Lizards and snakes from the late Miocene hominoid locality of Ravin de la Pluie (Axios Valley, Greece). Swiss Journal of Geosciences 111: 169–181. https://doi.org/10.1007/s00015-017-0291-2

Georgalis GL, Villa A, Ivanov M, Roussiakis S, Skandalos P, Delfino M (2019b) Early Miocene herpetofaunas from the Greek localities of Aliveri and Karydia – bridging a gap in the knowledge of amphibians and reptiles from the early Neogene of southeastern Europe. Historical Biology 31: 1045–1064. https://doi.org/10.1080/08912963.2017.1417404

Glavaš OJ, Počanić P, Lovrić V, Derežanin L, Tadić Z, Lisičić D (2020) Morphological and ecological divergence in two populations of European glass lizard, *Pseudopus apodus* (Squamata: Anguidae). Zoological Research 41: 172–181. https://doi.org/10.24272/j.issn.2095-8137.2020.025

Godina AY, David AI (1973) Neogenoviye mestonahozhdeniya pozvonochnyh na territorii Moldavskoy SSR [Neogene localities of vertebrates on the territory of the USSR]. Chisinau: Shtiintsa.

Gray JE (1825) A synopsis of the genera of reptiles and Amphibia, with a description of some new species. Annals of Philosophy Series 2: 193–217.

Gray JE (1853) Descriptions of some undescribed species of reptiles collected by Dr. Joseph Hooker in the Khassia mountains, East Bengal, and Sikkim Himalaya. Annals and Magazine of Natural History 12: 386–392. https://doi.org/10.1080/03745485709495063

Günther A (1873) Description of a new saurian (*Hyalosaurus*) allied to *Pseudopus*. Annals and Magazine of Natural History 11: 351–351. https://doi.org/10.1080/00222937308696828

Hammer Ø, Harper DA, Ryan PD (2001) PAST: Paleontological statistics software package for education and data analysis. Palaeontologia Electronica 4: 9.

Hoffstetter R, Gasc J-P (1969) Vertebrae and ribs of modern reptiles. Biology of the Reptilia 1: 201–310.

Holman JA (1998) Pleistocene amphibians and reptiles in Britain and Europe. Oxford University Press, New York. https://doi.org/10.1093/oso/9780195112320.001.0001

[ICZN] IC on ZN (1999) International Commission on Zoological Nomenclature. 4th ed. International Trust for Zoological Nomenclature, London, 306 pp.

Ivanov M, Čerňanský A, Bonilla-Salomón I, Luján ÀH (2020) Early Miocene squamate assemblage from the Mokrá-Western Quarry (Czech Republic) and its palaeobiogeographical and palaeoenvironmental implications. Geodiversitas 42: 343–376. https://doi.org/10.5252/geodiversitas2020v42a20

Jablonski D, Ribeiro-Júnior MA, Meiri S, Maza E, Kukushkin OV, Chirikova M, Pirosová A, Jelić D, Mikulíček P, Jandzik D (2021) Morphological and genetic differentiation in the anguid lizard *Pseudopus apodus* supports the existence of an endemic subspecies in the Levant. Vertebrate Zoology 71: 175–200. https://doi.org/10.3897/vz.71.e60800

Jandzik D, Jablonski D, Zinenko O, Kukushkin OV, Moravec J, Gvoždík V (2018) Pleistocene extinctions and recent expansions in an anguid lizard of the genus *Pseudopus*. Zoologica Scripta 47: 21–32. https://doi.org/10.1111/zsc.12256

Klembara J (1979) Neue Funde der Gattungen *Ophisaurus* und *Anguis* (Squamata, Reptilia) aus dem Untermiozän Westböhmens (CSSR). Věstník Ústředního ústavu geologického 54: 163–169.

Klembara J (1981) Beitrag zur Kenntnis der Subfamilie Anguinae (Reptilia, Anguidae). Acta Universitatis Carolinae, Geologica 2: 121–168.

Klembara J (1986) Neue Funde der Gattungen *Pseudopus* und *Anguis* (Reptilia, Anguinae) aus drei Pliopleistozänen Mitteleuropätischen Lokalitäten. Geologický zborník 37: 91–106.

Klembara J (2012) A new species of *Pseudopus* (Squamata, Anguidae) from the early Miocene of Northwest Bohemia (Czech Republic). Journal of Vertebrate Paleontology 32: 854–866. https://doi.org/10.1080/02724634.2012.670177

Klembara J (2015) New finds of anguines (Squamata, Anguidae) from the Early Miocene of Northwest Bohemia (Czech Republic). Paläontologische Zeitschrift 89: 171–195. https://doi.org/10.1007/s12542-014-0226-4

Klembara J, Rummel M (2018) New material of *Ophisaurus*, *Anguis* and *Pseudopus* (Squamata, Anguidae, Anguinae) from the Miocene of the Czech Republic and Germany and systematic revision and palaeobiogeography of the Cenozoic Anguinae. Geological Magazine 155: 20–44. https://doi.org/10.1017/S0016756816000753

Klembara J, Böhme M, Rummel M (2010) Revision of the anguine lizard *Pseudopus laurillardi* (Squamata, Anguidae) from the Miocene of Europe, with comments on paleoecology. Journal of Paleontology 84: 159–196. https://doi.org/10.1666/09-033R1.1

Klembara J, Hain M, Dobiašová K (2014) Comparative anatomy of the lower jaw and dentition of *Pseudopus apodus* and the interrelationships of species of subfamily Anguinae (Anguimorpha, Anguidae): Anatomy of lower jaw and teeth of Anguinae. The Anatomical Record 297: 516–544. https://doi.org/10.1002/ar.22854

Klembara J, Hain M, Čerňanský A (2019) The first record of anguine lizards (Anguimorpha, Anguidae) from the early Miocene locality Ulm – Westtangente in Germany. Historical Biology 31: 1016–1027. https://doi.org/10.1080/08912963.2017.1416469

Klembara J, Dobiašová K, Hain M, Yaryhin O (2017) Skull anatomy and ontogeny of legless lizard *Pseudopus apodus* (Pallas, 1775): Heterochronic influences on form. The Anatomical Record 300: 460–502. https://doi.org/10.1002/ar.23532

Koretsky IA (2001) Morphology and systematics of Miocene Phocinae (Mammalia: Carnivora) from Paratethys and the north Atlantic region. Geologica Hungarica, Series Palaeontologica 54: 1–109.

Kormos T (1911) Der Pliozäne Knochenfund bei Polgárdi. Földtani Közlöni 41: 1–19.

Kotsakis T (1989) Late Turolian amphibians and reptiles from Brisighella (northern Italy): preliminary report. Bollettino della Società paleontologica italiana 28: 277–280.

Kovalchuk O, Ferraris C (2016) Late Cenozoic catfishes of Southeastern Europe with inference to their taxonomy and palaeogeography. Palaeontologia Electronica: 1–17. https://doi.org/10.26879/616

Krakhmalnaya T (2008) Proboscideans and ungulates of Late Miocene fauna of Ukraine. In: 6th Meething of The European Association of Vertebrate Palaeontologists, 51.

Lartet E (1851) Notice sur la colline de Sansan, suivie d'une récapitulation des diverses espèces d'animaux vertébrés fossiles, trouvés soit à Sansan, soit dans d'autres gisements du terrain tertiaire du miocène dans le bassin sous-pyrénéen. J.A. Portes, Auch.

Linnaeus C (1758) Tomus 1 Systema naturæ per regna tria naturae, secundum classes, ordines, genera, species cum characteribus, differentiis, synonymis, locis. Decima. Laurentii Salvius, Stockholm, 824 pp. https://doi.org/10.5962/bhl.title.542

Loréal E, Villa A, Georgalis G, Delfino M (2020) Amphibians and reptiles from the late Miocene and early Pliocene of the Ptolemais area (Western Macedonia, Greece). Annales de Paléontologie 106: 102407. https://doi.org/10.1016/j.annpal.2020.102407

Maisano J (2003) The Deep Scaly Project, "*Ophisaurus apodus*" (Online). Digital Morphology. [Available from:] http://digimorph.org/specimens/Ophisaurus_apodus/ [December 15, 2022]

Merrem B (1820) Versuch eines systems der Amphibien. Krieger. https://doi.org/10.5962/bhl.title.5037

Meszoely CA (1970) North American fossil anguid lizards. Bulletin of the Museum of Comparative Zoology 139: 87–149.

Młynarski M (1956) Lizards from the Pliocene of Poland. Acta Palaeontologica Polonica 1: 135–152.

Młynarski M (1962) Notes on the amphibian and reptilian fauna of the Polish Pliocene and early Pleistocene. Państwowe Wydawnictwo Naukowe-Oddział Kraków.

Młynarski M (1964) Die jungpliozäne Reptilienfauna von Rebielice Królewskie, Polen. Senckenbergiana biologica 45: 325–347.

Młynarski M, Szyndlar Z, Estes R, Sanchiz B (1984) Amphibians and reptiles from the Pliocene locality of Weže II near Dzialoszyn (Polen). Acta Palaeontologica Polonica 29: 209–226.

Nadachowski A, Mirosław-Grabowska J, David A, Tomek T, Garapich A, Pascaru V, Obadă T, Szyndlar Z (2006) Faunal assemblages and biostratigraphy of several Pliocene sites from Moldova. Cour. Forsch.-Inst. Senckenberg 256: 249–259.

Obst F (1978) Zur geographischen Variabilitat des Scheltopusik, *Ophisaurus apodus* (Pallas) (Reptilia, Squamata, Anguidae). Zoologische

Abhandlungen Staatliches Museum für Tierkunde in Dresden 35: 129–140. https://doi.org/10.1515/9783112598764-002

Oppel M (1811) Die ordnungen, familien und gattungen der reptilien als prodrom einer naturgeschichte derselben. Comm. Lindauer, München, 87 pp. https://doi.org/10.5962/bhl.title.4911

Palcu DV, Vasiliev I, Stoica M, Krijgsman W (2019) The end of the Great Khersonian Drying of Eurasia: Magnetostratigraphic dating of the Maeotian transgression in the Eastern Paratethys. Basin Research 31: 33–58. https://doi.org/10.1111/bre.12307

Pallas PS (1775) *Lacerta apoda* descripta. Novi Commentarii Academiae Scientiarum Imperialis Petropolitanae 19: 435–454.

Petronio C, Krakhmalnaya T, Bellucci L, Di Stefano G (2007) Remarks on some Eurasian pliocervines: Characteristics, evolution, and relationships with the tribe Cervini. Geobios 40: 113–130. https://doi.org/10.1016/j.geobios.2006.01.002

Pyron R, Burbrink FT, Wiens JJ (2013) A phylogeny and revised classification of Squamata, including 4161 species of lizards and snakes. BMC Evolutionary Biology 13: 93. https://doi.org/10.1186/1471-2148-13-93

Rage J-C, Bailon S (2005) Amphibians and squamate reptiles from the late early Miocene (MN 4) of Béon 1 (Montréal-du-Gers, southwestern France). Geodiversitas 27: 413–441.

Redkozubov OI (2003) Pliocene and Lower Pleistocene fauna reptiles of Republic Moldova. In: 12th Ordinary General Meeting, Societas Europaea Herpetologica (SEH). Zoological Institute of the Russian Academy of Sciences, Saint-Petersburg, Russia, 138–139.

Redkozubov OI (2005) Herpetofauna of the middle-Pliocene reference location Lucheshty (Republic of Moldova). In: Problems of paleontology and archeology of the south of Russia and neighbouring territories. Materials of international conference. Rostov-on-Don: Ltd. "CVVR," 138.

Redkozubov OI (2008) Pliocene snakes of R. Moldova (Viperinae). In: Structura şi funcţionarea ecosistemelor în zona de interferenţă biogeografică. Simpozion internaţiona, 219–221.

Roček Z (1980) The dentition of the European glass lizard *Ophisaurus apodus* (Pallas, 1775) (Reptilia, Sauria: Anguidae), with notes on the pattern of tooth replacement. Amphibia-Reptilia 1: 19–27. https://doi.org/10.1163/156853880X00033

Roček Z (1984) Lizards (Reptilia: Sauria) from the Lower Miocene locality Dolnice (Bohemia, Czechoslovakia). Rozpravy Československé Akademie věd. Řada matematických a přírodních věd 93.

Roček Z (2019) A contribution to the herpetofauna from the late Miocene of Gritsev (Ukraine). Comptes Rendus Palevol 18: 817–847. https://doi.org/10.1016/j.crpv.2019.07.003

Rosina VV, Sinitsa MV (2014) Bats (Chiroptera, Mammalia) from the Turolian of the Ukraine: phylogenetic and biostratigraphic considerations. Neues Jahrbuch für Geologie und Paläontologie - Abhandlungen 272: 147–166. https://doi.org/10.1127/0077-7749/2014/0403

Schmidt WJ (1914) Studium am Integument der Reptilien. V. Anguiden. Zoologische Jahrbücher 38: 1–102.

Schneider CA, Rasband WS, Eliceiri KW (2012) NIH Image to ImageJ: 25 years of image analysis. Nature Methods 9: 671–675. https://doi.org/10.1038/nmeth.2089

Sindaco R, Jeremčenko VK (2008) 1 The Reptiles of the Western Palearctic: Annotated checklist and distributional atlas of the turtles, crocodiles, amphisbaenians and lizards of Europe, North Africa, Middle East and Central Asia. Edizioni Belvedere Latina.

Sinitsa MV, Delinschi A (2016) The earliest member of *Neocricetodon* (Rodentia: Cricetidae): a redescription of *N. moldavicus* from Eastern Europe, and its bearing on the evolution of the genus. Journal of Paleontology 90: 771–784. https://doi.org/10.1017/jpa.2016.72

Smith KT (2011) The evolution of mid-latitude faunas during the Eocene: late Eocene lizards of the Medicine Pole Hills reconsidered. Bulletin of the Peabody Museum of Natural History 52: 3–105. https://doi.org/10.3374/014.052.0101

Smith KT, Bhullar B-AS, Köhler G, Habersetzer J (2018) The Only Known Jawed Vertebrate with Four Eyes and the Bauplan of the Pineal Complex. Current Biology 28: 1101–1107.e2. https://doi.org/10.1016/j.cub.2018.02.021

Spinner M, Bleckmann H, Westhoff G (2015) Morphology and frictional properties of scales of *Pseudopus apodus* (Anguidae, Reptilia). Zoology 118: 171–175. https://doi.org/10.1016/j.zool.2014.11.002

Sullivan RM (1979) Revision of the Paleogene genus *Glyptosaurus* (Reptilia, Anguidae). Bulletin of the American Museum of Natural History 163: 1–72.

Sullivan RM (2019) The taxonomy, chronostratigraphy and paleobiogeography of glyptosaurine lizards (Glyptosaurinae, Anguidae). Comptes Rendus Palevol 18: 747–763. https://doi.org/10.1016/j.crpv.2019.05.006

Syromyatnikova E (2018) Palaeobatrachid frog from the late Miocene of Northern Caucasus, Russia. Palaeontologia Electronica: 1–16. https://doi.org/10.26879/861

Syromyatnikova E, Roček Z (2019) New *Latonia* (Amphibia: Alytidae) from the late Miocene of northern Caucasus (Russia). Palaeobiodiversity and Palaeoenvironments 99: 495–509. https://doi.org/10.1007/s12549-018-0350-3

Syromyatnikova E, Klembara J, Redkozubov O (2022) The Pliocene *Ophisaurus* (Anguidae) from Eastern Europe: new records and additions to the history of the genus and its palaeoenvironment. Palaeobiodiversity and Palaeoenvironments: 1–10. https://doi.org/10.1007/s12549-022-00556-w

Syromyatnikova E, Georgalis GL, Mayda S, Kaya T, Saraç G (2019) A new early Miocene herpetofauna from Kilçak, Turkey. Russian Journal of Herpetology 26: 205. https://doi.org/10.30906/1026-2296-2019-26-4-205-224

Syromyatnikova EV (2017a) Redescription of *Pelobates praefuscus* Khosatzky, 1985 and new records of *Pelobates* from the late Miocene–Pleistocene of Eastern Europe. Historical Biology 31: 888–897. https://doi.org/10.1080/08912963.2017.1402015

Syromyatnikova EV (2017b) Two pelobatid frogs from the Late Miocene of Caucasus (Russia). Palaeontologia Electronica 20: 1–12. https://doi.org/10.26879/772

Szyndlar Z (1984) Fossil snakes from Poland. Acta Zoologica Cracoviensia 28: 1–156.

Szyndlar Z (1991a) A review of Neogene and Quaternary snakes of Central and Eastern Europe. Part I: Scolecophidia, Boidae, Colubrinae. Estudios Geológicos 47: 103–126. https://doi.org/10.3989/egeol.91471-2412

Szyndlar Z (1991b) A review of Neogene and Quaternary snakes of Central and Eastern Europe. Part II: Natricinae, Elapidae, Viperidae. Estudios Geológicos 47: 237–266. https://doi.org/10.3989/egeol.91471-2412

Tempfer PM (2009) The early Vallesian vertebrates of Atzelsdorf (Late Miocene, Austria). 3. Squamata, Scleroglossa. Annalen des Naturhistorischen Museums in Wien 111: 489–498.

Tesakov AS, Titov VV, Simakova AN, Frolov PD, Syromyatnikova EV, Kurshakov SV, Volkova NV, Trikhunkov YI, Sotnikova MV, Kruskop SV, Zelenkov NV, Tesakova EM, Palatov DM (2017) Late Miocene (Early Turolian) vertebrate faunas and associated biotic record of the Northern Caucasus: Geology, palaeoenvironment, biochronology. Fossil Imprint 73: 383–444. https://doi.org/10.2478/if-2017-0021

Vasile Ștefan, Venczel M, Petculescu A (2021) Early Pleistocene amphibians and squamates from Copăceni (Dacian Basin, southern Romania). Palaeobiodiversity and Palaeoenvironments 101: 967–983. https://doi.org/10.1007/s12549-020-00465-w

Vasilyan D, Čerňanský A, Szyndlar Z, Mörs T (2022) Amphibian and reptilian fauna from the early Miocene of Echzell, Germany. Fossil Record 25: 99–145. https://doi.org/10.3897/fr.25.83781

Venczel M (2006) Lizards from the late Miocene of Polgárdi (W-Hungary). Nymphaea 33: 25–38.

Villa A, Delfino M (2019a) A comparative atlas of the skull osteology of European lizards (Reptilia: Squamata). Zoological Journal of the Linnean Society 187: 829–928. https://doi.org/10.1093/zoolinnean/zlz035

Villa A, Delfino M (2019b) Fossil lizards and worm lizards (Reptilia, Squamata) from the Neogene and Quaternary of Europe: an overview. Swiss Journal of Palaeontology 138: 177–211. https://doi.org/10.1007/s13358-018-0172-y

Zerova GA (1993) Late Cainozoic localities of snakes and lizards of Ukraine. Revue de Paléobiologie 7: 273–280.

Zerova GA, Lungu AN, Chkhikvadze VM (1987) Large fossil vipers from northern Black Seaside and Transcaucasus. Trudy Zoologicheskogo Instituta 158: 89–99.

Zheng Y, Wiens JJ (2016) Combining phylogenomic and supermatrix approaches, and a time-calibrated phylogeny for squamate reptiles (lizards and snakes) based on 52 genes and 4162 species. Molecular Phylogenetics and Evolution 94: 537–547. https://doi.org/10.1016/j.ympev.2015.10.009

Supplementary material 1

List of the *Pseudopus pannonicus* fossil specimens used for comparative purposes

Authors: Erwan Loréal, Elena V. Syromyatnikova, Igor G. Danilov, Andrej Čerňanský

Data type: table (Excel file)

Copyright notice: This dataset is made available under the Open Database License (http://opendatacommons.org/licenses/odbl/1.0). The Open Database License (ODbL) is a license agreement intended to allow users to freely share, modify, and use this Dataset while maintaining this same freedom for others, provided that the original source and author(s) are credited.

Link: https://doi.org/10.3897/fr.26.100059.suppl1

Supplementary material 2

List of the *Pseudopus apodus* specimens used for comparative purposes

Authors: Erwan Loréal, Elena V. Syromyatnikova, Igor G. Danilov, Andrej Čerňanský

Data type: table (Excel file)

Copyright notice: This dataset is made available under the Open Database License (http://opendatacommons.org/licenses/odbl/1.0). The Open Database License (ODbL) is a license agreement intended to allow users to freely share, modify, and use this Dataset while maintaining this same freedom for others, provided that the original source and author(s) are credited.

Link: https://doi.org/10.3897/fr.26.100059.suppl2

Supplementary material 3

Detailed measurements and statistical data for each studied elements

Authors: Erwan Loréal, Elena V. Syromyatnikova, Igor G. Danilov, Andrej Čerňanský

Data type: tables (Excel file)

Copyright notice: This dataset is made available under the Open Database License (http://opendatacommons.org/licenses/odbl/1.0). The Open Database License (ODbL) is a license agreement intended to allow users to freely share, modify, and use this Dataset while maintaining this same freedom for others, provided that the original source and author(s) are credited.

Link: https://doi.org/10.3897/fr.26.100059.suppl3

Fossil Record 26 (1) 2023, 85–101 | DOI 10.3897/fr.26.97686

Recognising and quantifying the evolution of skeletal paedomorphosis in Plesiosauria

Ricardo Araújo[1], Adam S. Smith[2]

1 *Instituto de Plasmas e Fusão Nuclear, Instituto Superior Técnico, Lisbon, Portugal*
2 *Nottingham Natural History Museum, Wollaton Hall, Nottingham, UK*

https://zoobank.org/1128975D-7A2B-4624-870E-926469C943C1

Corresponding author: Ricardo Araújo (ricardo.araujo@tecnico.ulisboa.pt)

Academic editor: Johannes Müller ♦ **Received** 21 November 2022 ♦ **Accepted** 3 April 2023 ♦ **Published** 20 April 2023

Abstract

Plesiosaurs are one of the longest-ranging tetrapod groups in the Mesozoic and underwent a major adaptive radiation in the Late Triassic/Early Jurassic, so they are an ideal clade to study the long-term implications and deep-time evolution of specific developmental patterns. We compiled a database of all published plesiosaur specimens and recorded their skeletal maturity status. We use statistical modelling to demonstrate that the abundance of allegedly 'juvenile' specimens increases through time, which contradicts the null hypothesis that the relative proportion of juvenile to adult specimens should remain constant throughout evolution. These results indicate that many 'juvenile' specimens are really adults exhibiting heterochronic traits, particularly paedomorphism. Heterochrony is a developmental pattern particularly widespread in secondarily adapted organisms such as plesiosaurs. However, heterochronic patterns are typically only studied in individual genera/species or restricted clades. We demonstrate that the pervasiveness of paedomorphism in plesiosaurs increased gradually throughout the evolution of the clade, rather than being a specialization of specific clades.

Key Words

heterochrony, histology, osteological maturity, sexual maturity

Introduction

Plesiosaurs (=Plesiosauria) are a globally distributed group of extinct predatory aquatic reptiles that formed an important component of Jurassic and Cretaceous marine ecosystems. All plesiosaurs have a short torso, a short tail, and four large flippers, but their skull and neck proportions vary greatly. Plesiosaur morphotypes range between two extremes: plesiosauromorphs with a long neck and small head, and pliosauromorphs with a short neck and large head (O'Keefe 2002). The first studies of plesiosaur ontogeny were conducted by Andrews (1895, 1910) on *Cryptoclidus* from the Middle Jurassic (Callovian) Oxford Clay Formation of the UK. Brown (1981) followed up on this work and set the modern standard for determining ontogenetic growth stages within Plesiosauria, herein referred to as the 'Brown model'. Brown (1981) analysed ontogenetic sequences of two cryptoclidids, *Cryptoclidus* and *Muraenosaurus*, both from the Oxford Clay Formation of the UK. This foundational work established intraspecific ontogenetic variability patterns among plesiosaurs. *Cryptoclidus* provides an especially good case study because it is known from abundant and substantially complete material representing different growth stages. The Brown model *sensu stricto* uses osteological maturity, specifically the degree of fusion between the vertebral centra and neural arch, as a proxy for sexual maturity. Under this model there are three categories: in 'juveniles' the neural arches and centra are unfused, in 'adults' the neural arches and centra are fused but a neurocentral suture is still visible, and in 'old adults' the neural arches and centra are fused and the neurocentral suture is obliterated (Brown 1981). Caldwell (1997a) expanded on this work by investigating ossification patterns in the limbs of *Cryptoclidus*. The Brown model has been adopted by all subsequent

Copyright *Ricardo Araújo & Adam S. Smith*. This is an open access article distributed under the terms of the Creative Commons Attribution License (CC BY 4.0), which permits unrestricted use, distribution, and reproduction in any medium, provided the original author and source are credited.

workers and the patterns observed for *Cryptoclidus* have been generalized to all other plesiosaurs, including pliosauroids and elasmosaurids, to determine their sexual maturity. The problems with applying the Brown model in this way are three-fold: (1) sexual maturity does not necessitate osteological maturity, so assuming the two correlate omits the possible ontogenetic effects of paedomorphism; (2) different parts of the skeleton may ossify at different stages of maturity; (3) ontogenetic patterns observed in *Cryptoclidus* and *Muraenosaurus* may not be applicable to all plesiosaurs. In summary, the Brown model conflates osteological maturity with ontogenetic or sexual maturity.

The possible importance of paedomorphism within plesiosaurs and the potential implications of paedomorphic characters for plesiosaur paleobiology, paleoecology, evolution, and systematics, has received little research attention to date (Buchy et al. 2005; Araújo et al. 2015; Wintrich et al. 2017). Paedomorphic traits have been identified in various secondarily-adapted tetrapods (Delfino and Sánchez-Villagra 2010). However, the long-term evolution of paedomorphism has not been investigated in plesiosaurs, or any other clade. The Plesiosauria is a long-lived clade that survived for 135 Ma, witnessing the breakup of Pangea, various major oceanic anoxic events (AOEs), dramatic changes in thermohaline oceanic circulation, and the rise and fall of various other Mesozoic marine reptiles such as thalattosuchians, ichthyosaurs and mosasaurs (Polcyn et al. 2014; Ősi et al. 2018; Moon 2019). This unique clade is therefore an ideal candidate to study the long-term, large-scale evolutionary persistence of heterochronic mechanisms affecting skeletal morphology.

Heterochrony is the dissociation of the relative timing of developmental events during the ontogeny of ancestral and descendant organisms (Raff 1996). Gould (1977) partitions heterochrony into two fundamental divisions: paedomorphism denotes an underdevelopment in descendants relative to the ancestor, while peramorphosis denotes an overdevelopment of ontogenetic traits. These concepts can be further subdivided into distinct processes. There are three types of paedomorphism: progenesis (early finishing/offset), neoteny (slower growth rate), and postdisplacement (delayed starting/onset). But to extricate which of these processes affects a given ontogenetic trait requires underlying knowledge of the rates of development. Smith (2001) proposed an alternative, sequence heterochrony, to avoid the need to calculate these rates and to make it feasible to apply a conceptual framework of heterochrony to museum or paleontological specimens. Sequence heterochrony simply denotes changes in the offset or onset of a given phenotypic trait. So, even without accurate information on the developmental rates it is possible to recognise and understand underdeveloped or overdeveloped morphological traits relative to the ancestor condition in fossils.

Speciation events may undergo a mosaic of heterochronic processes, with different traits being affected by peramorphosis and paedomorphosis concomitantly. For example, peramorphic processes result in convergent evolution of polydactyly and hyperphalangy in multiple Mesozoic marine reptile lineages (Caldwell 1997b). However, paedomorphism is observed more often in secondarily-adapted amniotes, probably due to the staggering degree of convergence between distantly related clades, ranging from porpoises to thalattosuchians. Inspired by the work of Piveteau and Dechaseaux (1955) and Lehman (1955), de Ricqlès (1975) coined the term "aquatic neoteny" referring to the juvenilized morphology of tetrapods as an adaptation to the aquatic environment. However, neoteny refers to a specific paedomorphic process referring to slower growth rate (Gould 1977; Raff 1996; McNamara 1997), and other paedomorphic processes, such as progenesis, can be related to adaptations to the aquatic environment (Galatius 2010). The term 'skeletal paedomorphosis' (Rieppel 1989a) is more appropriate because it refers to the heterochronic process more generally but can be applied to the specific anatomical loci affected by it.

Miniaturized taxa are often, but not always, paedomorphic. Some authors have proposed that some aristonectines may be miniaturized paedomorphic plesiosaurs (Araújo et al. 2015; Otero et al. 2015). Clades with dramatic minimum size limits also tend to be more diverse (Angielczyk and Feldman 2013) and, coincidently, the Aristonectinae is the most diverse plesiosaur clade by the Campanian-Maastrichtian. Miniaturization is a pathway for evolutionary novelty and diversification because dwarfed forms can partition resources and occupy ecological niches that are otherwise inaccessible to larger forms (Miller 1996; Angielczyk and Feldman 2013). However, most paedomorphic traits in Mesozoic marine reptiles do not seem to be related to body size, as they are mostly reflected in the axial and appendicular skeleton (Rieppel 1989a). Paedomorphism produces sexually mature organisms that otherwise retain a juvenile morphology by promoting the developmental truncation, deceleration or deletion of some traits (Britz et al. 2009; Angielczyk and Feldman 2013). The meristic deletion of mesopodial elements in sauropterygians (Rieppel 1989b) is a typical example of aquatic skeletal paedomorphism. Although several paedomorphic traits were attained in the early radiation of Sauropterygia, it is unclear how these traits evolved in plesiosaurs. Brown (1981) standardized the way to assess plesiosaur ontogeny but did not take into account the confounding effects of heterochrony.

A clear extrication of juvenile and paedomorphic characters in relation to the ancestral state, as well as complementary evidence from histology, is crucial for understanding plesiosaur evolution. This paper presents the results of an analysis of osteological maturity in hundreds of plesiosaur specimens across all clades, spanning the entire stratigraphic history of the group, to help elucidate the presence of juvenile vs. paedomorphic characters, to test the Brown model, and to avoid a biased view of plesiosaur ontogeny.

Methods

Data collection

We compiled an extensive database of hundreds of published records of plesiosaur specimens to assess their osteological maturity. The database contains 712 plesiosaur specimens representing different individuals. The database contains all plesiosaur publications known to us up until December 2022, excluding descriptions of isolated teeth or other material for which the osteological maturity could not be determined. The number of specimens that have been published since then are negligible and should not change the results significantly. Each entry corresponds to one specimen, to which we provide the most recent consensus concerning its systematic classification, following (in most cases) the higher-ranking taxonomy of Benson and Druckenmiller (2014). We have classified each specimen based on a bipartite scheme of classification (Plesiosauroidea and Pliosauroidea). Plesiosauroidea comprises Microcleididae, Polycotylidae, Leptocleididae, Cryptoclididae and Elasmosauridae. Pliosauroidea comprises Rhomaleosauridae and Pliosauridae. 34 specimens were taxonomically ascribed to Plesiosauria indet. and those without a firm systematic placement (13) were excluded from the clade-by-clade analysis. These are '*Plesiosaurus*' *cliduchus*, *Eoplesiosaurus antiquior*, *Sthenarosaurus dawkinsi*, *Bobosaurus forojuliensis*, *Raptocleidus blakei*, *Raptocleidus bondi*, *Macroplata tenuiceps*, *Plesiopterys wildii*, '*Plesiosaurus*' *macrocephalus*, '*Plesiosaurus*' *costatus*, '*Plesiosaurus*' *rugosus* (BRSMG Cb2458), '*Thaumatosaurus*' *indicus* and '*Plesiosaurus hesternus*'.

For each specimen we recorded the following information: specimen number; its Superfamily (Plesiosauroidea or Pliosauroidea); its Family; the operational taxonomic unit (i.e. lowest possible taxonomy, genus and species when possible); its ontogenetic stage under the Brown model in a binary system ('mature' or 'partially mature or immature)', its ontogenetic stage under the Brown model in a tripartite system ('mature', 'partially mature', or 'immature'); its ontogenetic traits; its geological range in Stages; its average age in Ma; and references.

The specimens' ontogenetic maturity was classified based upon anatomical descriptions and figures found in the literature and/or personal observations. Table 1 lists the criteria we used to determine the osteological maturity of each specimen. We used a bipartite scheme (mature vs. immature), which is a modification of the tripartite scheme (mature vs. partially mature vs. immature), by including mature and *partially mature* specimens under the term 'mature'. The tripartite classification scheme is inspired by Brown (1981), where: a mature specimen has the neural arch and vertebral centrum completely fused leaving no neurocentral suture visible, a partially mature specimen has the neural arch and the vertebral centrum partly co-ossified but has the neurocentral suture visible, and an immature specimen has separate neural arch and vertebral centra. Based on the geological and stratigraphic data provided in the literature for each specimen we convert it into an approximate absolute age of occurrence based on Ogg et al. (2016).

Table 1. Criteria used to determine the osteological maturity of each specimen.

Osteological maturity	Vertebrae	Limbs	Girdles
Immature	Neural arch unfused to centrum	Rounded edges, no trochanter or tuberosity	Rounded edges, girdle elements unfused
Partially mature	Neural arch fused to centrum but neuro-central suture visible	Angular edges, Trochanter or tuberosity partially separated from propodial head	Angular edges, Girdle elements partially fused
Mature	Neural arch completely fused to centrum, no neuro-central suture visible	Angular edges, trochanter or tuberosity completely separated from propodial head	Angular edges, girdle elements completely fused

Terminology

It is important to clarify terminology, especially because the meaning of 'maturity' can be applied in several ways. Specifically, we must consider the differences and areas of overlap between 'osteological maturity', 'sexual maturity', and 'ontogenetic maturity'. The term 'sexual maturity' as a proxy for maturity in a given specimen is unsatisfactory in practice because it cannot be assessed in the fossil record and does not untangle heterochronic issues. Therefore, an alternative terminology for assessing maturity is required.

Osteological maturity: immature, partially mature, and mature

The abundant Callovian plesiosaur record amassed from the Oxford Clay Formation of the UK consists mainly of different cryptoclidid and pliosaurid taxa. In addition to the Brown (1981) criterium *sensu stricto*, Brown identified other characters that change through ontogeny that should therefore be excluded from taxonomic purposes (Brown 1981). Among these, two characters have been widely cited for all major plesiosaur clades as representing a juvenile state (Table 1): (1) a humeral tuberosity or femoral trochanter unseparated by a condylar isthmus from the capitulum; and (2) an unfaceted distal propodial epiphysis. However, there are few records of pliosaurs (except for *P. funkei*, see Knutsen et al. 2012, *P. irgisensis*, see Storrs 2000 and some specimens of *Peloneustes*, Tarlo 1960) and few rhomaleosaurids (with the exception of *R. zetlandicus* and *R. thorntoni*) with faceted distal epiphyses (e.g., Sollas 1881; Tarlo 1959; Hampe 2005; Smith 2007; Vincent 2010; Ketchum and Benson 2011a, 2011b; Benson et al. 2013). Also, to date no rhomaleosaurids

have been found possessing an isthmus separating the humeral or femoral head (Smith 2007). Moreover, in several plesiosaur clades all individuals have visible neurocentral sutures or separated neural arches and centra (Rhomaleosauridae, Pliosauridae, Leptocleididae, except *Gronausaurus wegneri* see Hampe 2013; fig. 12). This apparent contradiction can be explained by the retention of the plesiomorphic condition of Pistosauria, which themselves exhibit paedomorphism (Rieppel 2000). So, in *Cryptoclidus* and *Muraenosaurus*, faceted propodials and separated humeral and femoral tubercles/trochanters are apomorphic traits (Druckenmiller and Russell 2008).

Sexual maturity: juveniles, adults, and old adults

This issue requires a careful definition of different sexual stages, namely the contrast between 'juveniles' and 'adults'. The 'adult' condition usually refers to an individual that has reached sexual maturity. This definition of adulthood is exclusively biological (e.g., legal adulthood in humans is a different issue). However, sexual maturity can rarely be confidently determined in the paleontological record, with one exception in the plesiosaur fossil record represented by a pregnant individual (O'Keefe and Chiappe 2011). By looking at the degree of fusion between the centra and neural arches, Brown (1981) refers instead to the degree of osteological maturity. For example, an osteologically immature specimen has unfused neural arches. A modern analogue exemplifying sexual maturity before osteological maturity as a result of paedomorphism is the harbour porpoise, *Phocoena phocoena* (fig. 10; Galatius and Kinze 2003; Galatius et al. 2006, 2011; Galatius 2010). Hereinafter we use the terms 'juvenile', 'adult', and 'old adult' (in inverted commas) according to Brown 1981; so when single quotes are not used we refer to true juveniles, excluding paedomorphism.

Ontogenetic maturity

This term simply refers to the actual age (i.e., time since birth) of the animal. This concept differs from sexual maturity as it does not make any suppositions about reproducibility of the organism.

Rationale and caveats

To assess the evolution of paedomorphism in plesiosaurs we used a ratio of the frequency of osteologically immature specimens (I) to the frequency of the sum between partially osteologically mature specimens (P) and fully osteologically mature specimens (M), the I/(P+M) ratio, through time bins representing the evolutionary history of plesiosaurs. The null hypothesis is that this ratio should remain constant through time. There is no reason to think that fertility ratios should vary through time given the available evidence that plesiosaurs are K-selectors (O'Keefe and Chiappe 2011), nor should there be any variation or taphonomic biases towards osteologically immature (or osteologically mature) specimens through time (Benson et al. 2010). There are some intrinsic collection, temporal and geographical biases in the fossil record, but correction protocols are always dependent on the existing face-value paleontological record (Benson et al. 2021). In other words, it may be spurious to 'correct' the record if the attempted correction is not known to be true itself.

The alternative hypothesis we propose is that variations of I/(P+M) ratio through geological time reflect variations of heterochronic processes, namely paedomorphism, through the evolutionary history of plesiosaurs. It is important to note that our results could be overly conservative because we lump partially mature specimens together with fully mature specimens in the denominator. However, this is intentional. If we can observe a pattern of variation of the I/(P+M) ratio through time then, it would only be more conspicuous if partially mature specimens were lumped with immature specimens.

Statistical modelling of plesiosaur paedomorphism evolution

We divided geologic time from 234.55 Ma (Early Carnian) up to 66 Ma (Late Maastrichtian) into equally sized time-bins of 4.5 Ma each. 4.5 Ma was the minimum age range, required to provide a meaningful assessment of our hypothesis given the abundance of plesiosaurs in the fossil record. In other words, 4.5 Ma is the minimum spread of time required to avoid having various time periods without any plesiosaur specimens, which would give the impression of an interrupted record. Figure 1 shows the specimen frequency based on tripartite division of osteological maturity into different time bins of 2, 4.5, 6 and 10 Ma. The time bins, therefore, do not correspond directly to stratigraphic stages.

We calculated the ratio of the frequency of osteologically immature versus osteologically mature specimens (and osteologically immature versus osteologically mature + partially osteologically mature specimens) in each time bin. The time bin refers to the average between the maximum and minimum age.

We optimised the dataset according to different types of equations to model the evolution of paedomorphism, using the ratio of immature versus mature + partially mature specimens per time bin as a proxy, hereinafter I/(P+M) ratio. The I/(P+M) ratio may be over-conservative towards reducing the real effects of paedomorphism because it lumps partially osteologically mature specimens together with osteologically mature specimens. Partially osteologically mature specimens may also be affected by paedomorphism. On the other hand, osteologically immature specimens through time should be retrieved in fossil collections at a constant rate.

Each equation was limited to a maximum of four estimated parameters to ensure optimization using the

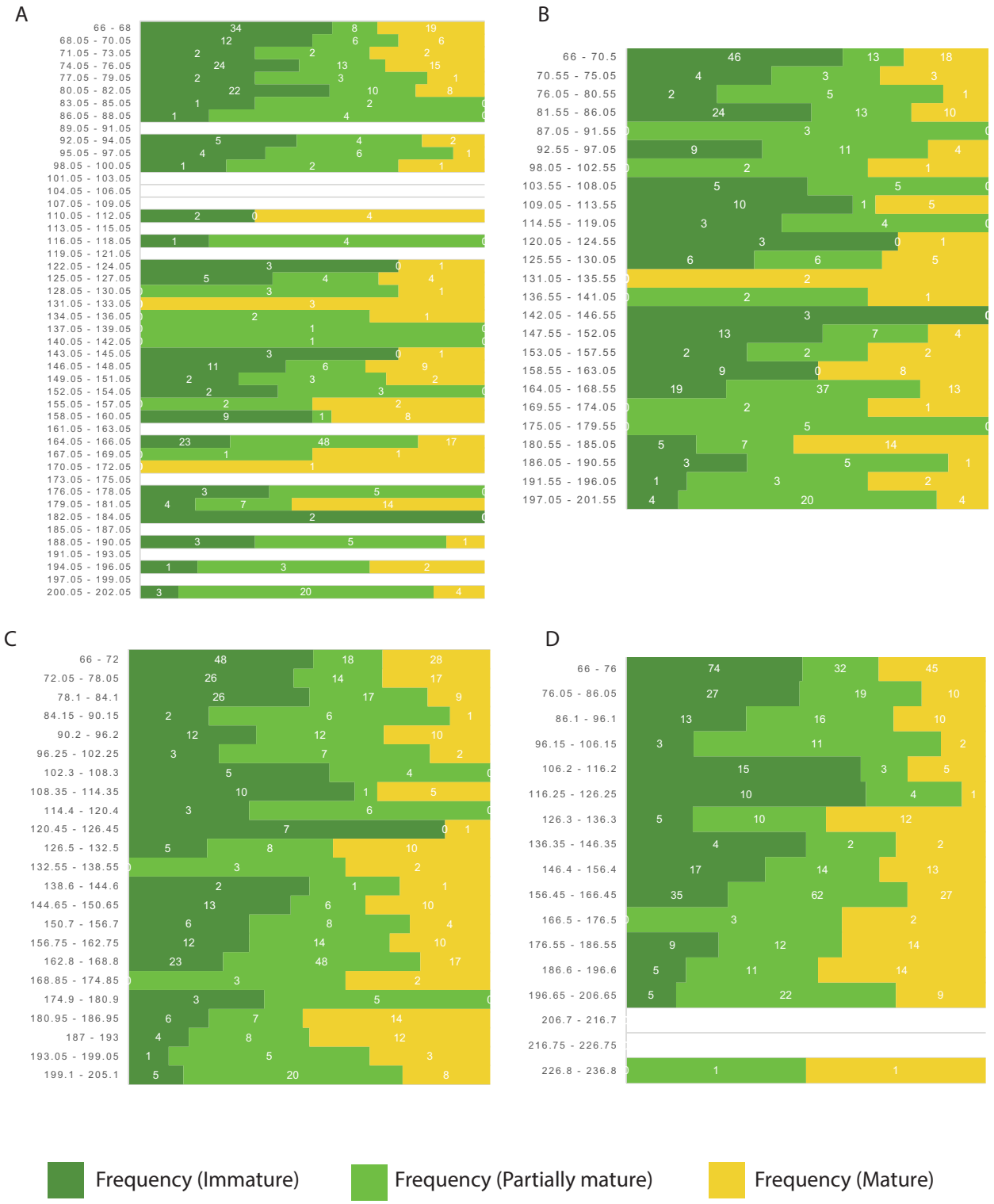

Figure 1. Frequencies of immature (dark green), partially mature (light green) and mature (yellow) specimens through time. **A.** 2 Ma time bin. **B.** 4.5 Ma bin. **C.** 6 Ma bin. **D.** 10 Ma bin. Note that the frequency of immature specimens increases through time independent to the time bin scheme used.

simplest, thus more parsimonious, models possible. The parametric models include linear, exponential, and other equations types (see Tables 2, 3). To ensure that the models were not being affected by outliers we ran a Grubbs tests and calculated Z scores. Statistical outliers are here identified when there is an anomalously high I/(P+M) ratio. The ratio is null or incalculable when there are simply no plesiosaur records for a given time bin. We optimized a linear model, without the outlier, for which we calculated the confidence intervals based on a significance level of 5%, the Cook's distances, the mean of the squares of the errors (MSE) and the square root mean square of the

Table 2. Statistical assumption tests for each time bin for linear models. Marginally non-significant regressions are in bold.

		2 Ma	4.5 Ma	6 Ma	10 Ma
Correlation coefficient	Spearman	-0.537	-0.415	-0.613	-0.637
Analysis of variance model	p-value	0.010	**0.095**	0.015	**0.065**
Statistical tests for linear regression assumptions					
Outliers	Grubbs	Yes	Yes	Yes	Yes
Removed outliers	Z-score	Berriasian + Aptian	Aptian	Aptian	Aptian/ Albian
Multicolinearity	VIF (<5)	1.339	1.184	1.400	1.383
Homoscedasticity	White test p-value (>0.05)	0.274	0.115	0.175	0.279
Autocorrelation	Durbin-Watson p-value (>0.05)	0.929	0.656	0.393	0.157

errors (RMSE), and various other statistics (Suppl. material 1). Optimal models have lower MSE, AIC and AICc values because these statistics essentially account for the amount of deviation from the linear or nonlinear model. All models were calculated using XLSTAT2014.3.

Non-parametric regression

We performed a non-parametric regression that relaxes the assumptions made by the linear regression model (Fig. 2C, Table 4). We performed a LOWESS regression and a robust LOWESS regression (Cleveland 1979) for all time bin partitions, which are locally weighted scatterplot smoothing techniques performed in XLSTAT2014.3.

Clade-by-clade analyses

We partitioned and analysed the plesiosaur dataset into various clades to assess the weight of phylogeny on the global evolution of paedomorphism in Plesiosauria, and to understand if there was any particular trend through time in individual plesiosaur clades (Figs 3, 4). We reproduced the same methodology as outlined above, but with subsets of the database and we only plotted the I/(P+M) ratio through time. We drew simple frequency graphs in instances where very few entries exist for each clade per time bin (Microcleididae,

Table 3. The type of function, the general tendency demonstrated by the function fitted to the data, relative likelihood and the mean square errors (MSE), for each model and time bin. Green model, relative likelihood RL > 0.05 for all time bins Green, RL > 0.05. Red, model with RL < 0.05 for every time bin. BM, best model.

Model	2 Ma time bin			4.5 Ma time bin			6 Ma time bin			10 Ma time bin			Tendency through time
	MSE	RL AIC	RL AICc	MSE	RL AIC	RL AICc	MSE	RL AIC	RL AICc	MSE	RL AIC	RL AICc	
Linear	0.077	BM	-	0.237	BM	-	0.127	BM	-	0.205	BM	-	Increase
Beta Growth	0.080	0.135	0.064	0.252	0.135	0.186	0.127	0.236	0.594	0.219	0.164	0.132	Increase
Exponential Growth	0.076	0.402	0.315	0.237	0.367	0.832	0.133	0.241	BM	0.214	0.277	BM	Increase
Boltzman Sigmoidal	0.075	0.215	0.062	0.256	0.079	0.040	0.174	0.007	0.007	0.228	0.092	0.016	Uniform, burst increase
One phase decay	0.071	0.587	0.278	0.252	0.136	0.186	0.135	0.135	0.339	0.226	0.135	0.109	Increase
Two phases decay	0.071	0.248	0.043	0.258	0.052	0.006	0.153	0.018	0.006	0.283	0.018	0.000	Increase, step increase
One phase association	0.103	0.010	0.007	0.280	0.074	0.168	0.178	0.013	0.053	0.284	0.045	0.161	Uniform
Two phases association	0.084	0.050	0.014	0.268	0.050	0.025	0.136	0.085	0.079	0.243	0.061	0.011	Increase
Second order polynomial	0.080	0.140	0.066	0.252	0.135	0.186	0.127	0.242	0.608	0.219	0.163	0.131	Increase
Third order polynomial	0.064	1.366	0.393	0.258	0.073	0.037	0.134	0.096	0.089	0.242	0.063	0.011	Increase, plateau, increase
Fourth order polynomial	0.064	0.943	0.165	0.272	0.031	0.003	0.137	0.056	0.019	0.255	0.035	0.000	Increase, plateau, increase
Quadratic one variable	0.282	0.000	0.000	0.432	0.002	0.007	0.381	0.000	0.000	0.466	0.003	0.016	Decrease
One parameter exponential	0.289	0.000	0.000	0.469	0.001	0.003	0.325	0.000	0.000	0.457	0.003	0.018	Uniform
Asymptotic regression	0.071	0.587	0.278	0.252	0.136	0.186	0.135	0.135	0.339	0.226	0.135	0.109	Increase
Michaelis-Menten	0.069	1.279	BM	0.232	0.441	BM	0.146	0.094	0.388	0.237	0.145	0.523	Increase then burst increase
Gompertz	0.164	0.000	0.000	0.598	0.000	0.000	0.633	0.000	0.000	0.740	0.000	0.000	Decrease
Substrate inhibition	0.072	0.470	0.223	0.247	0.162	0.223	0.144	0.068	0.171	0.244	0.081	0.065	Increase, burst increase
One site competition	0.093	0.020	0.009	0.240	0.214	0.294	0.173	0.011	0.027	0.279	0.034	0.027	Increase, step increase
Two site competition	0.180	0.000	0.000	0.271	0.032	0.004	0.153	0.018	0.006	0.314	0.009	0.000	Double step increase
Gaussian	0.080	0.146	0.069	0.252	0.135	0.185	0.129	0.202	0.507	0.216	0.179	0.144	Increase
Lerentzian	0.079	0.163	0.077	0.251	0.136	0.187	0.133	0.152	0.382	0.221	0.157	0.126	Increase
Allometric 2	0.087	0.051	0.024	0.272	0.064	0.087	0.161	0.023	0.058	0.280	0.033	0.027	Increase
Power	0.289	0.000	0.000	0.469	0.001	0.003	0.325	0.000	0.000	0.457	0.003	0.018	Uniform

Table 4. The mean square errors for non-parametric regressions, for each time bin. The best model is in bold.

Type of regression	2 Ma MSE	4.5 Ma MSE	6 Ma MSE	10 Ma MSE
LOWESS	**0.075**	0.354	0.172	0.446
Robust LOWESS	0.078	0.339	0.149	0.285

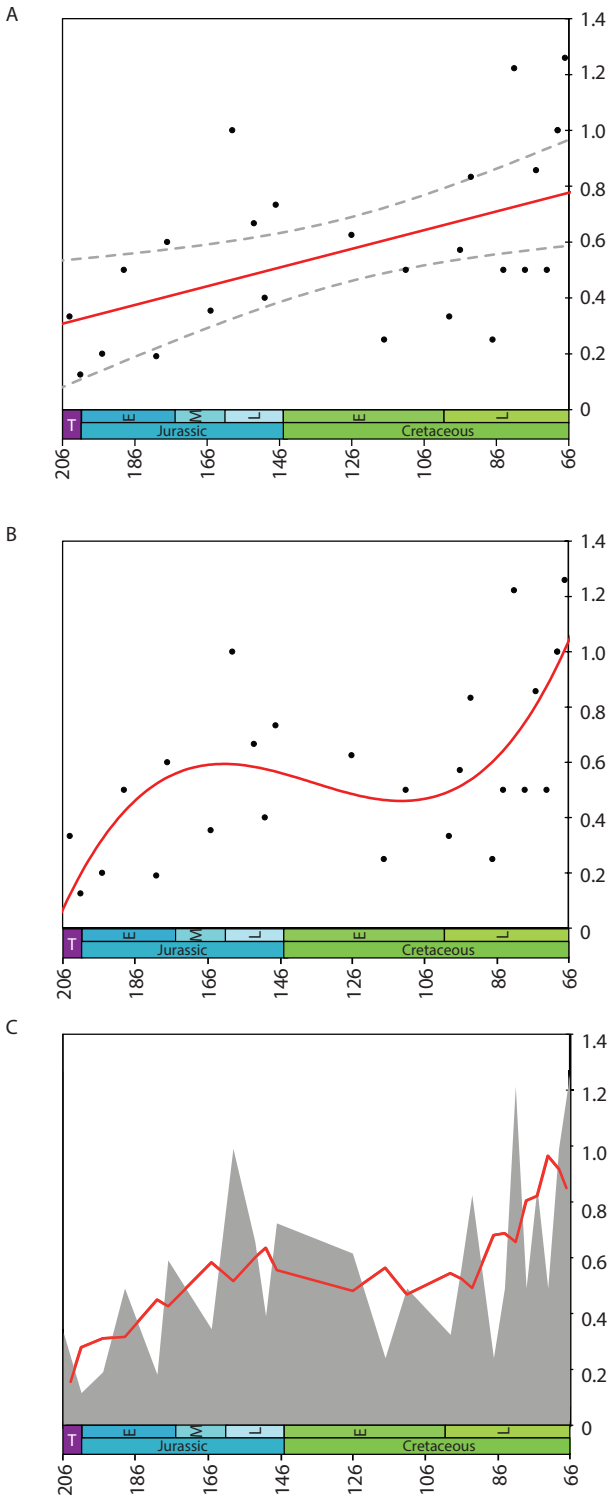

Figure 2. Evolution of paedomorphism through geological time in Plesiosauria, as expressed by the I/(M+P) ratio. Geological time in Ma is represented in the abscissa and I/(M+P) in the ordinate. **A.** Best linear model. **B.** Best nonlinear model. **C.** Best nonparametric model.

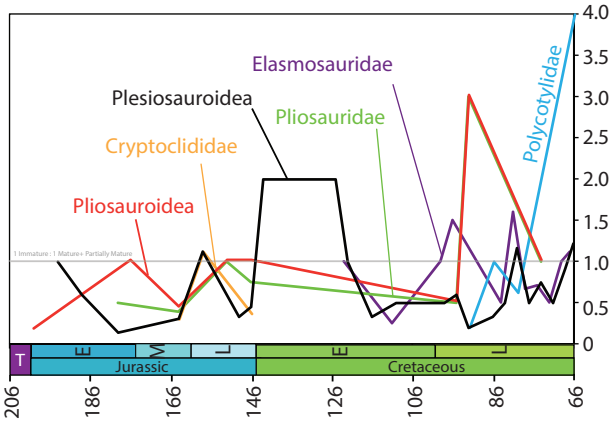

Figure 3. Evolution of paedomorphism through time in selected plesiosaurian clades for 2 Ma time bins. Geological time in Ma is represented in the x-axis and I/(M+P) in the y-axis. Higher I/(M+P) values indicate higher proportion of osteological immature specimens.

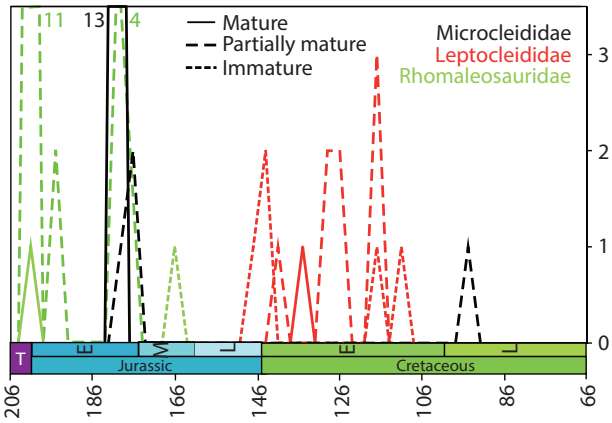

Figure 4. Evolution of paedomorphism as expressed by the I/(M+P) in families with few specimens. Frequencies of osteologically immature, partially mature, and mature specimens of leptocleidids, microcleidids and rhomaleosaurids through time. Geological time in Ma is represented in the abscissa and frequency (number) of specimens in the ordinate for each of the categories (mature, partially mature and immature).

Leptocleididae and Rhomaleosauridae) (Fig. 4). Data was partitioned into high level clades Plesiosauroidea and Pliosauroidea, and then into various subsets equivalent to the families Microcleididae, Polycotylidae, Leptocleididae, Cryptoclididae, Elasmosauridae, Pliosauridae and Rhomaleosauridae. Two time bins were used with durations of 2 and 4.5 Ma respectively, to evaluate if the patterns are affected by different time bin partitions.

Results

We found a statistically significant increase in the relative abundance of osteologically immature specimens through time. This finding is at odds with what should be expected from a taphonomic standpoint: the ratio of juvenile to adult specimens should have remained uniform through geological time. Figure 2 shows an average 50% of 'immature' specimens (i.e., specimens previously reported

as 'juveniles' or 'subadults') during the latest Cretaceous (82–66 Ma). This average might be an overestimation because several specimens considered as 'immature' may, in fact, be adult species of taxa displaying paedomorphosis. Steadily increasing rates of paedomorphism would explain this trend, and this data suggests that paedomorphism was widespread throughout plesiosaur clades, notably present in Rhomaleosauridae, Elasmosauridae, Pliosauridae, and Polycotylidae (Figs 3, 4).

Outliers. We found that the time bin for (approximately) the Early Aptian (120.05–124.55 Ma) was an outlier (Suppl. material 1). There is an evident peak of the ratio I/(P+M) at the Early Aptian that contrasts with the general gradual increase tendency through plesiosaur history. Before the Early Aptian the average I/(P+M) ratio is 0.40, and after it is 0.83, for the 4.5 Ma time bin partition. At the Early Aptian the I/(P+M) ratio is 3.0. For understanding this issue, please refer to the discussion.

Parametric regressions assumption tests

All of the linear regression tests that we conducted verify the assumptions to draw the parametric regression models. The Grubbs test and Z-scores find the Aptian time bin as an outlier independent of the time bin partition used, except for the Grubbs test for the 4.5 and 10 Ma partition (Table 2). There is no evidence for autocorrelation; the Durbin-Watson p-value is at least 0.157 for any time bin partition. The residuals are homoscedastic because the White's test p-value is at least 0.115, and we found no evidence for multicollinearity as the variance inflation factor is smaller than 5 for all time bin partitions. It is important to note that we only aim to find a tendency through time with these models, not necessarily to use the model parameters for estimation of I/(P+M) ratios.

Linear regression statistical modelling

The linear models are statistically significant ($p < 0.02$), except for the 4.5 and 10 Ma time bin partition ($p = 0.095$ and $p = 0.065$, see Discussion). The most significant time bin partition is for 2 Ma ($p = 0.001$), followed by the 6 Ma time bin partition ($p = 0.015$), Fig. 2A. The 10 Ma time bin partition shows the highest Spearman's correlation coefficient of -0.637, with the 4.5 Ma time bin partition showing the lowest (-0.415).

Nonlinear regression statistical modelling

The best fitting parametric models to the dataset show an increase of the I/(P+M) ratio – increased osteological immaturity – through time independent of the time bin partition used (Table 2, Fig. 2B). Overall, there is an increase of the MSE values with larger time bin partitions (see Table 2). The third order polynomial model performs best (i.e., lowest mean squares of errors, here abbreviated as MSE). However, Exponential Growth and Michaelis-Menten models could be selected irrespective of the time bin partition scheme used (relative likelihood > 0.05). Overall, the lowest MSE values are for the Exponential Growth for 10 Ma time bin partition, Beta Growth and second order polynomial for 6 Ma partition, and Michaelis-Menten for the 4.5 Ma time bin partition. Notably, all these models show a marked increase of the I/(P+M) ratio through time. Linear regressions are also among the best performing models in our analysis. Also importantly, the worst performing models show a decreasing or uniform tendency through time (e.g., Power function, Gompertz function, One Parameter exponential).

The best parametric model, the third order polynomial, shows a sharp increase of the I/(P+M) ratio until the end of the Jurassic, stabilizing during the Early Cretaceous, and subsequently increasing markedly up to ~1.0 (Fig. 2B).

Non-parametric LOWESS regression statistical modelling

The non-parametric regression models showed a consistent increase of the I/(P+M) ratio through time (Fig. 2C). There are no significant differences between the LOWESS and the robust LOWESS plots. However, the MSE scores are lower for the robust LOWESS model than for the LOWESS model, except for the 2 Ma time bin partition. The LOWESS model for the 2 Ma time bin partition draws a curve similar to the third order polynomial (see Fig. 2C and Discussion). All other models simply show a gradual increase of the I/(P+M) ratio through time.

Results by clade

Plesiosauroidea

In this superfamily as a whole there is only a sharp increase in the I/(M+P) ratio in the Early Cretaceous (Fig. 3). Otherwise, the ratio is relatively constant, but high, through time. It peaks at 2 in the Early Cretaceous, and dips to 0.2 in the Early Jurassic.

Pliosauroidea

There is a slight increase in I/(M+P) ratio through time, independent of the time bin partition used. In the Early Jurassic the I/(M+P) ratio is around 0.2 but by the Middle Jurassic and Early Cretaceous it is about 1 (Fig. 3).

Polycotylidae

The temporal range of polycotylids spans from the Aptian (Kear 2005) to the Maastrichtian (Welles and Gregg 1971; Fig. 3). Osteologically immature (~38%) and partially osteologically mature specimens account for 75% of the

specimens. The I/(M+P) ratio increases through time independently from the time bin partition used. By the end of the Cretaceous there are four more osteologically immature specimens than partially osteologically mature and osteologically mature polycotylid specimens combined, and the I/(M+P) ratio is ~4, whereas by the beginning of the Late Cretaceous the I/(M+P) ratio is ~0.2.

Various specimens of indeterminate polycotylids create an outlier in the latest Aptian (Vavrek et al. 2014), which was removed from the final results for this clade because of their uncertain taxonomic position (they could be leptocleidids). In fact, there are no published records of polycotylids by this time (109–113 Ma), and those reported by Vavrek et al. (2014) are all osteologically immature, except NUFV 1996 which is partially osteologically mature.

Elasmosauridae

Among elasmosaurids there is typically a ratio of one osteologically immature specimen per partially osteologically mature and osteologically mature specimen throughout the clade's longevity (Fig. 3). There is no statistically significant trend towards increasing or decreasing the I/(P+M) ratio through time.

Pliosauridae

Pliosauridae is a clade with a long temporal range, with records from the Early Jurassic (Hettangian) with taxa such as *Thalassiodracon*, to the Late Cretaceous (Late Campanian), such as indeterminate pliosaurid specimens recovered from New Zealand (Wiffen and Moisley 1986). Our database accounts for 72 specimens, of which ~34% are osteologically immature and only ~14% are fully osteologically mature (Fig. 3). There is a trend for increased I/(P+M) ratio through time, but this tendency seems to be affected by the patchy record of pliosaurids through time. Several osteologically immature specimens of *Kronosaurus queenslandicus* have been reported from the Aptian-Albian of Australia (McHenry 2009), thus creating a sudden increase around this time.

Cryptoclididae

Cryptoclidids are a clade with a temporal range from the Callovian to the Tithonian and are represented by 88 specimens in our database. There is a trend for increased I/(P+M) ratio through time; by the Callovian the ratio is ~0.4 and by the Tithonian it is 3 for the 6 Ma partition and 0.75 for the 4.5 Ma-partition (Fig. 3). Only ~27% of the specimens are fully osteologically mature and 25% of the specimens are osteologically immature.

Rhomaleosauridae

The rhomaleosaurid fossil record consists of very few published specimens (n = 22) and it is a clade with a short temporal range (Early to Middle Jurassic). Therefore, it is hard to obtain broad patterns on the evolution of paedomorphism in this clade (Fig. 4). However, most of the specimens are osteologically immature or partially osteologically mature (95.2%), suggesting paedomorphism in this clade.

Microcleididae

Microcleidids are a clade of plesiosauroids with a short temporal range at the end of the Early Jurassic and records of this group amount to only 17 published specimens (Fig. 4). The vast majority of the specimens are osteologically mature (76%), and the remaining (n = 4) are partially osteologically mature.

Leptocleididae

Leptocleidids have a temporal range within the Cretaceous from the Berriasian to the Albian and are represented in our database by 18 published specimens (Fig. 4). Only two specimens are osteologically mature: *Leptocleidus capensis* (SAM-K5822) and *Gronausaurus wegneri* (GMM-A3B.2). These represent only ~11% of the dataset. The counts of osteologically immature specimens (n = 8) equal those of partially osteologically mature specimens (n = 8).

Discussion

Several authors have considered ontogeny in plesiosaurs. For example, Andrews (1895) investigated ontogeny of the shoulder girdle of *Cryptoclidus*, Carpenter (1999) discussed the ontogenetic series for *Styxosaurus snowii* (p. 162), Carpenter (1996, p. 266) discussed the ontogenetic series for *Dolichorhynchops*, Caldwell (1997a) discussed ossification patterns in *Cryptoclidus*, Cruickshank and Long (1997) discussed sexual maturity in specimens of *Leptocleidus* (p. 273), Hiller et al. (2005, p. 269) discussed ontogeny in *Mauisaurus*, Wiffen and Moisley (1986) illustrated a growth series of elasmosaurid girdles, Wiffen et al. (1995) investigated ontogeny of bone structure in plesiosaurs, Talevi and Fernandez (2015) investigated microstructure of plesiosaur bone as an ontogenetic indicator, O'Keefe et al. (2019) studied polycotylid long bone ontogeny, Miller et al. (2020) considered ontogenetic variability in the plesiosaur pelvis, and Otero et al. (2014, 2018) and O'Gorman et al. 2014, O'Gorman and Coria 2017) discussed ontogeny in elasmosaurids. However, paedomorphism in plesiosaurs has not been considered as much.

Paedomorphism in Plesiosauria

Paedomorphism is a common trait among secondarily aquatically-adapted organisms (Fordyce and Barnes 1994; Galatius 2010). It has also been reported in stem-group sauropterygians (Carroll and Gaskill 1985;

Rieppel 1989a, 1989b; Klein 2010), and is suspected to occur also in Plesiosauria (Caldwell 1997a; Wintrich et al. 2017). The incongruent external morphology versus the histology of the propodials of Angolan specimens (Araújo et al. 2015) and *Abyssosaurus* (Berezin 2019) supports the idea of paedomorphism in Plesiosauria. Furthermore, as Galatius (2010) noted for some cetaceans, in the Angolan specimens the juvenile morphology and the smaller absolute size of the adults (as compared to other limb elements, for example) agrees with the idea of paedomorphism. However, this statement should be considered with caution because it is anchored on the small sample of data derived from Wiffen et al. (1995). Araújo et al. (2015) and Liebe and Hurum (2012) underscore that the histology of plesiosaurs is poorly known and needs to be systematically surveyed across both taxa and ontogeny. For example, the presence of pachyosteoslerotic and osteoporotic histology in sections that are a few centimeters apart in the same bone complicates the interpretation and indicates the need for more comprehensive histological analyses. Paedomorphism in whale lineages seems to only arise in derived forms (Fordyce and Barnes 1994). Analogous evidence for this heterochronic condition is most obvious in Late Cretaceous taxa (this paper). Thus, ontogenetic assessments should be a critical basis for taxonomic ascriptions in derived plesiosaur lineages. Pending histological analysis, plesiosaur specimens previously considered to be juveniles may simply be paedomorphic adults, unless osteologically mature specimens of the same species also exist to show this is not the case (e.g., Andrews 1910; Brown 1981; Bardet et al. 2008). External morphology is not always sufficient to determine the ontogenetic status of the specimens.

Implications for plesiosaur systematics

Following Brown (1981), many plesiosaur species were considered *nomina dubia* due to their 'juvenile' condition (e.g., *Tuarangisaurus? cabazai*, Gasparini et al. 2007; *Leurospondylus ultimus*, Sato and Wu 2006). However, paedomorphism is an equally parsimonious hypothesis to explain the osteologically immature external morphology seen in many plesiosaur specimens. Brown (1981) did not critically assess the confounding heterochronic effects and their potential taxonomic implications because he was working on a clade with a typical ontogenetic pattern with (comparatively) reduced heterochrony and complete fossilized ontogenetic sequences. An analysis of external morphological characters is necessary, but not sufficient, to assess a specimen's ontogenetic stage, particularly in plesiosaurs and other secondarily aquatically-adapted organisms. In order to avoid a circular argument, additional lines of evidence are ultimately required to test paedomorphism as an alternative hypothesis.

Our data suggests that not all plesiosaur clades co-ossify neural arches and centra at the same rate and extent. Thus, in certain clades these differences will bear a phylogenetic signal. In other words, the apomorphic condition is a paedomorphic trait. For example, neural arches remain separated throughout ontogeny in every taxon of the rhomaleosaurid clade.

Implications for plesiosaur paleoecology - Paedomorphism or nurseries?

The presumption that osteologically immature external morphological traits imply a 'juvenile' condition led several authors to propose breeding ground and nursery hypotheses for certain plesiosaur assemblages (Wiffen et al. 1995; Kear 2006). For example, Kear (2006) suggested that the relatively high number of 'juvenile' elasmosaurids (and other marine amniotes) in the Bulldog Shale, Australia, was a result of favorable ecological conditions for 'safe calving grounds' and refuges for young animals prior to their entering the open sea as adults. Welles and Gregg (1971, p. 171) suggested that "infant mortality must have been high among the plesiosaurs" when looking at the late Campanian-early Maastrichtian elasmosaurid fauna of New Zealand. Conversely, other marine reptiles from the same assemblage (mosasaurs and turtles) do not exhibit the same pattern.

The perception of relative 'juvenile' abundance is dependent upon the assemblages and taxa under study (e.g., "juvenile plesiosaurs are relatively rare in the fossil record", Storrs 1995, p. 75; "complete juvenile plesiosaurs are indeed relatively rare in the fossil record …", Vincent 2010, p. 45).

The interpretation of these assemblages as plesiosaur nurseries rests on the assumption that the osteological immature specimens represent sexually immature and ontogenetically immature individuals. The hypothesis that coastal environments served as nurseries for plesiosaurs remains speculative pending histological studies except for one outlier: the Aptian-Albian. Kear (2006) proposed that an explanation for the high proportion of immature specimens in the Bulldog Shale (Early Aptian-Early Albian) could be explained by nutrient-rich cold-water coastal habitats serving as both 'safe calving grounds' and refuges for young animals prior to their entering the open sea as adults. This hypothesis was first proposed by Wiffen et al. (1995) when analysing the unique pattern of the osteohistology of Late Cretaceous elasmosaurids from New Zealand. Similarly, Sachs (2004) reports various specimens with "[neural arches] not fused with the centra" from the Late Aptian. In fact, in all our analyses, the Aptian time bin was found to be a statistically significant outlier. A close look at the dataset reveals that the vast majority of specimens are ascribed to the elasmosaurid taxon *Woolungasaurus glendowerensis* which is mostly composed of immature specimens (Sachs 2004). However, the use of the I/(P+M) ratio is insensitive to the sampling quality. Specimen sampling for the Aptian-Albian is poor, and although the nursery hypothesis cannot be rejected based upon presented evidence, we acknowledge that

more findings from this time bin might either eliminate this outlier or emphasize and verify the nursery hypothesis. At this point, the Aptian-Albian outlier represents a major decrease of fossil record quality. Converse to the Aptian-Albian pattern, other better sampled time bins show a gradual increase of paedomorphism through time.

The contribution of paleohistology to understanding paedomorphism

Paleohistology provides an alternative line of evidence for determining paedomorphism in plesiosaurs (Houssaye 2009). The available literature on plesiosaur histology is scarce (see Liebe and Hurum 2012 for a review), although there has been some expansion of knowledge on non-plesiosaurian sauropterygians (e.g., Klein 2010; Hugi et al. 2011). Wiffen et al. (1995) presented a thorough analysis of plesiosaur histology by analyzing several bones of different ontogenetic stages from Late Cretaceous specimens from New Zealand. The histology of isolated elasmosaurid propodials allowed the contrasting of two different ontogenetic stages: the 'juvenile' humerus is pachyostotic; i.e., has a thick layer of cortical bone and the medullary zone is pierced by some erosional lacunae; whereas the 'adult' specimen is cancellous and has intense Haversian remodeling, although it bears a relatively compact cortex locally. The 'Wiffen et al. (1995) juvenile' histological traits correlate with the 'Brown juvenile' (Brown 1981) external morphological traits; i.e., unfaceted propodials, relatively small dimensions, undeveloped tuberosity/trochanter, and overall propodial proportions. Nevertheless, new evidence seems to question the view that this material represents different ontogenetic stages and it may represent different taxa instead (Talevi and Fernández 2015), but data from more specimens needs to be gathered. For example, Fostowicz-Frelik and Gaździcki (2001) also compared the histology and external morphology of an elasmosaurid (cf. *Mauisaurus*) from the Campanian-Maastrichtian of Antarctica. They concluded that the Antarctic specimen was a sub-adult based on the presence of the humeral trochanter and bone dimensions, which were in accordance with the presence of bone remodeling, the proportion of cortical versus medullar bone in the humerus, and the concentration of secondary osteons.

In Angolan aristonectine specimens the humeri have an osteosclerotic histology, there are secondary osteons nearly all the way to the outermost regions of the sectioned bones, and there is a presence of three lines of arrested growth (Araújo et al. 2015). This set of traits points to a 'Wiffen et al. (1995) adult' condition. In addition, the muscle scars are formed by deeply grooved and reworked periosteum which is indicative of late ontogenetic stages as observed in other vertebrates (e.g., Tumarkin-Deratzian et al. 2006). In contrast, the external morphology, in particular the small size, the unfaceted distal propodials, the flat articular facets of the vertebrae, the non-fusion of the neural arches with the centra, the near absence of the posterior cornua of the coracoids, and the absence of the pectoral bar, implies a 'Brown juvenile' condition. The combination of these ontogenetically incongruent characters indicates: (1) paedomorphism; or (2) that Wiffen et al.'s (1995) ontogenetic classes are not fully and appropriately defined. On the other hand, Liebe and Hurum (2012) described the internal structure and microstructure of various cryptoclidids at different ontogenetic states. This is significant for the present study as a null hypothesis based on a phylogenetically significant outgroup. Liebe and Hurum (2012) detected the presence of secondary osteons in 'adult' specimens and an absence in 'juvenile' specimens. Also, the external morphology exhibits typically 'juvenile' traits, such as unfaceted propodials, which contrasts with the condition in the Angolan specimens. Synchrotron tomography techniques offer a modern, non-destructive, and scalable approach to assess the histologically maturity of specimens. This could be adopted to test the observed patterns of the plesiosaur fossil record as has been done for other taxa (e.g., Sanchez et al. 2012).

Early Cretaceous: changing seas, acquisition of new life history strategies, or poor specimen sampling?

The Early Cretaceous is characterized by elevated climatic volatility and major tectonic changes due to the accelerated breakup of Pangea (Fischer et al 2016; Föllmi 2012). The pre-Aptian Early Cretaceous witnessed a cold greenhouse climate with ephemeral ice sheets (Hay and Floegel 2012; Hu et al. 2012; Föllmi 2012), followed by one of the hottest period of the Mesozoic starting from the Aptian (Kidder and Worsley 2010). There were also major reversals of thermohaline ocean circulation and a major Oceanic Anoxic Event had occurred by the Early Aptian (Kidder and Worsley 2010; Sames et al. 2016). These major global oceanic transformations oceans could have led plesiosaurs to important radiation events and/or the acquisition of new life history strategies. During this time some of the most important and diverse plesiosaur clades originated: Polycotylidae and Elasmosauridae. Indeed, residual diversity for plesiosaurs, alongside chelonioids and derived ichthyosaurs, was high yet unaffected by Lagerstätten effects (Benson and Butler 2011). Elasmosaurids are already a paedomorphic clade when they originate in the Early Cretaceous. The origin of these important Late Cretaceous plesiosaur clades coincides with a common pattern detected from our models where there were significant changes in the I/(P+M) ratio during the Early Cretaceous (see nonlinear regression results). However, the Early Cretaceous is also the poorest sampled epoch of plesiosaur existence. The Early Cretaceous represents ~33% of plesiosaur longevity, but only ~11% of the specimens in this analysis are from this interval. Conversely, the Late Cretaceous contains ~37% of the published specimens for ~25% of plesiosaur longevity, and the Middle Jurassic specimens are also

overrepresented (11% of the published specimens for 8% of plesiosaur longevity). The Early Cretaceous seems to be inadequately sampled for various Mesozoic marine reptiles (Benson et al. 2010, 2013; Fischer et al. 2016). Likewise, the "fish" fossil record, which is less prone to sampling effort/success biases, shows elevated percentage of ghost lineages by the pre-Aptian Early Cretaceous, which is a proxy for sampling quality (Guinot and Cavin 2015, 2016). Therefore, the sudden increase of the I/(P+M) ratio during the Early Cretaceous found by our best models, may be an artefact of poor sampling during this period.

The rate of paedomorphic evolution in Plesiosauria

By using alternative methods to linear regression modelling, the nonparametric LOWESS regression of the I/(P+M) ratio through time indicates a linear tendency. Furthermore, the linear model was retrieved consistently among the best statistical modelling techniques. This linear tendency implies a steady increase of I/(P+M) through geological time, allowing us to speculate about a possible rate of paedomorphism. The rate of paedomorphic evolution in Plesiosauria as whole is 0.6%/Ma with 95% confidence bounds oscillating between 0.3 to 0.9%/Ma. Whereas plesiosaurs seem to have a slow rate and gradual evolution of paedomorphic traits, a contrasting pattern is present in the odontocete phocoenids. Widespread paedomorphism seems to have been attained at a relatively accelerated rate in phocoenids, whose entire body plan has become paedomorphic in less than ~11 Ma (Barnes 1985) with heterochronic modifications on the brain (Racicot and Colbert 2013), postcranial skeleton (Galatius 2010) and skull (Barnes 1985). However, the plesiomorphic condition in non-plesiosaurian sauropterygians already shows a significant degree of aquatic skeletal paedomorphism (Rieppel 2000). The absence of a calcified sternum, the reduced number of carpal and tarsal elements, or the absence of the neurocentral fusion are some of the external morphological traits indicative of paedomorphism (Rieppel 2000). Paedomorphism in plesiosaurs is an aggregation of the basal sauropterygian condition.

However, some aristonectines represent extreme examples of paedomorphism by the Campanian-Maastrichtian (Araújo et al. 2015; Otero et al. 2015). The extremely 'juvenilized' external morphology of the skeleton, contrasts with the histologically maturity of the long bones (Araújo et al. 2015). The typical plesiosaur pattern is not as extreme, affecting only skeleton morphology to a lesser degree or in a combination of traits. Nevertheless, there are some consistent pleiotropic effects of paedomorphosis among Mesozoic marine reptiles. In plesiosaurs (see dataset), and also in other Mesozoic marine reptiles, paedomorphism not only affects vertebral closure, but also rib co-ossification, epicondyle morphology, and meristic reduction of mesopodial ossification concomitantly (Seeley 1908; Carroll 1997; Caldwell 2002; Herrera et al. 2013). Further study and refinement of the data collected here may shed light on the evolutionary patterns of pleiotropic effects resulting from heterochronic modifications.

Paedomorphism and secondarily-adapted tetrapods

Paedomorphic traits are widespread among tetrapods, with salamanders and newts being a quintessential example where paedomorphic traits are viewed as adaptations to their complex life cycle (e.g., Oromi et al. 2016). However, paedomorphic characters have been linked to various major adaptive events such as flight in avian dinosaurs (Bhullar et al. 2012), adaptations to insularity in elephants (Larramendi and Palombo 2015), or even the human condition (Godfrey and Sutherland 1996; Mitteroecker et al. 2004).

While gravity is a primary constraint for tetrapod architecture (e.g., Clack 2012), buoyancy and water viscosity play a major controlling role in aquatic organisms (Fish 2000). Paedomorphism, as manifested in reduced ossification, is among the most common convergent trends among secondarily-adapted tetrapods at the level of bone histology and external morphology (de Ricqlès 1975; Rieppel 1989a; Houssaye et al. 2016). Aquatic skeletal paedomorphism is a passively selected modular trait caused by the hydrostatic balance provided by the aquatic medium. In contrast to their terrestrially-adapted counterparts, the formation of additional surface area for muscular and tendinous attachment via additional osseous processes is ineffectual in aquatic tetrapods. Aquatic paedomorphism is manifested in several ways, ranging from decreased degree of skeletal ossification in non-plesiosaurian sauropterygians (Rieppel 2000), to osteologically immature bone histology in ichthyosaurs and mosasauroids (De Buffrénil and Mazin 1990; Sheldon and Bell 1998), delayed neurocentral fusion in thalattosuchian crocodyliforms and ichthyosaurs (Seeley 1908; Herrera et al. 2013), overall skull morphology in baleen whales (neobalaenines) (Tsai and Fordyce 2014), reduction of the carapace ossification in sea turtles (Kordikova 2000, 2002), and the reduction of pectoral musculature in the Galápagos cormorants (Livezey 1992). Such disparate patterns result from different aquatic locomotory styles and clade-specific developmental constraints. Among the most thoroughly studied cases of skeletal paedomorphism are the phocoenids (Galatius and Kinze 2003; Galatius et al. 2006; Galatius 2010). These odontocete cetaceans show a retardation of the fusion of the vertebral epiphysis, pectoral girdle elements, and propodial epiphyses (Galatius and Kinze 2003). However, even in porpoises the neurocentral suture is always fused, which is the general condition in mammals. This shows that heterochronic shifts are deeply constrained by the phylogenetic patterns and developmental programmes of the group in question. For instance, not all pelagic secondarily-adapted tetrapods are selected towards increasing paedomorphism through their evolutionary history. Most mysticete whales are notable examples that do not show any particular trend

towards increasing paedomorphism (Tsai and Fordyce 2014). These disparate trends among secondarily-adapted amniotes can be related to phylogenetic incumbency, different life-history patterns, habitual biomechanical demands, or degree of terrestrial dependency. For instance, the degree of cranial sutural closure may vary significantly within pinnipeds with walruses showing nearly complete closure whereas elephant seals show almost no co-ossification (Goswami et al. 2013). Nevertheless, it is clear that sauropterygians, and plesiosaurs in particular, show an overall pattern towards increasing paedomorphism. The proportion of osteologically immature specimens increases significantly through time and this can only be explained by a long-term trend towards delayed or truncated growth. Despite the relatively small size compared to other contemporaneous plesiosaurs, microcleidids seem to be an exception, with most specimens being osteologically mature (Großmann 2006, 2007). The purported 'juvenile' specimens (Großmann 2006, 2007) seem to be true ontogenetically immature individuals. Microcleidids can be viewed as an example where dwarfism is not attained by heterochronic processes, but rather constrained by phylogenetic and ecological factors.

Conclusions

Paedomorphism is a major confounding factor in determining the ontogenetic stage in plesiosaur skeletons, with subsequent taxonomic implications. As a consequence, many ontogenetic stage determinations for different plesiosaur taxa may be mistaken. Although our results suggest that the ontogenetic stage in early plesiosaurs (Early to Middle Jurassic) may be identifiable based on external morphological features, external morphology alone renders interpretation more difficult in later plesiosaurs, because a high proportion of osteologically immature specimens prevail. Nevertheless, even in basal and early plesiosaur clades, such as rhomaleosaurids, morphological features indicative of osteological immaturity are pervasive, such as unfaceted propodials and lightly co-ossified vertebrae and neural arches. To help tackle these issues we propose:

1. To replace the sexual maturity terminology by Brown (1981) used in ontogenetic assessments, with terms that denote external morphology and osteological maturity instead: osteologically immature, partially osteologically mature, and osteologically mature.
2. Ontogenetic assessments remain hypothetical until backed up with paleohistological data.

Acknowledgements

Funding for this project was provided by the Fundação para a Ciência e a Tecnologia postdoctoral fellowship SFRH/BPD/96205/2013, FCT - AGA KHAN Development Network grant number 333206718, National Geographic Society grant number CP-109R-17. We also thank B. Wahl and C. McHenry for some information of specimens. We also thank Chris Klingenberg, Michael Caldwell and Sven Sachs for their comments on the manuscript.

References

Andrews CW (1895) On the development of the shoulder girdle of a plesiosaur (*Cryptoclidus oxoniensis*, Phillips, sp.) from the Oxford Clay. Annals & Magazine of Natural History 6(88): 333–346. https://doi.org/10.1080/00222939508677894

Andrews CW (1910) A descriptive catalogue of the marine reptiles of the Oxford Clay. Part, I, British Museum (Natural History), London. Order of the Trustees of the British Museum, London.

Angielczyk KD, Feldman CR (2013) Are diminutive turtles miniaturized? The ontogeny of plastron shape in emydine turtles. Biological Journal of the Linnean Society. Linnean Society of London 108(4): 727–755. https://doi.org/10.1111/bij.12010

Araújo R, Polcyn MJ, Lindgren J, Jacobs LL, Schulp AS, Mateus O, Gonçalves AO, Morais M (2015) New aristonectine elasmosaurid plesiosaur specimens from the Early Maastrichtian of Angola and comments on paedomorphism in plesiosaurs. Netherlands Journal of Geosciences 94(1): 93–108. https://doi.org/10.1017/njg.2014.43

Bardet N, Fernández M, Garcia-Ramos JC, Suberbiola XP, Piñuela L, Ruiz-Omeñaca JI, Vincent P (2008) A juvenile plesiosaur from the Pliensbachian (Lower Jurassic) of Asturias, Spain. Journal of Vertebrate Paleontology 28(1): 258–263. https://doi.org/10.1671/0272-4634(2008)28[258:AJPFTP]2.0.CO;2

Barnes LG (1985) Evolution, taxonomy and antitropical distributions of the porpoises (Phocoenidae, Mammalia). Marine Mammal Science 1(2): 149–165. https://doi.org/10.1111/j.1748-7692.1985.tb00003.x

Benson RB, Butler RJ (2011) Uncovering the diversification history of marine tetrapods: Ecology influences the effect of geological sampling biases. Geological Society of London, Special Publications 358(1): 191–208. https://doi.org/10.1144/SP358.13

Benson RB, Druckenmiller PS (2014) Faunal turnover of marine tetrapods during the Jurassic–Cretaceous transition. Biological Reviews of the Cambridge Philosophical Society 89(1): 1–23. https://doi.org/10.1111/brv.12038

Benson RB, Butler RJ, Lindgren J, Smith AS (2010) Mesozoic marine tetrapod diversity: Mass extinctions and temporal heterogeneity in geological megabiases affecting vertebrates. Proceedings. Biological Sciences 277(1683): 829–834. https://doi.org/10.1098/rspb.2009.1845

Benson RB, Evans M, Smith AS, Sassoon J, Moore-Faye S, Ketchum HF, Forrest R (2013) A giant pliosaurid skull from the Late Jurassic of England. PLoS ONE 8(5): e65989. https://doi.org/10.1371/journal.pone.0065989

Benson RB, Butler R, Close RA, Saupe E, Rabosky DL (2021) Biodiversity across space and time in the fossil record. Current Biology 31(19): R1225–R1236. https://doi.org/10.1016/j.cub.2021.07.071

Bhullar BAS, Marugán-Lobón J, Racimo F, Bever GS, Rowe TB, Norell MA, Abzhanov A (2012) Birds have paedomorphic dinosaur skulls. Nature 487(7406): 223–226. https://doi.org/10.1038/nature11146

Britz R, Conway KW, Rüber L (2009) Spectacular morphological novelty in a miniature cyprinid fish, *Danionella dracula* n. sp. Proceedings of the Royal Society B, Biological Sciences 276(1665): 2179–2186. https://doi.org/10.1098/rspb.2009.0141

Brown DS (1981) The English Upper Jurassic Plesiosauroidea (Reptilia) and a review of the phylogeny and classification of the Plesiosauria. Bulletin of the British Museum Natural History (Geol.) 35: 253–347.

Buchy MC, Métayer F, Frey E (2005) Osteology of *Manemergus anguirostris* n. gen. et sp., a new plesiosaur (Reptilia, Sauropterygia) from the Upper Cretaceous of Morocco. Palaeontographica. Abteilung A, Paläozoologie, Stratigraphie 272(5–6): 97–120. https://doi.org/10.1127/pala/272/2005/97

Caldwell MW (1997a) Limb osteology and ossification patterns in *Cryptoclidus* (Reptilia: Plesiosauroidea) with a review of sauropterygian limbs. Journal of Vertebrate Paleontology 17(2): 295–307. https://doi.org/10.1080/02724634.1997.10010976

Caldwell MW (1997b) Modified perichondral ossification and the evolution of paddle-like limbs in ichthyosaurs and plesiosaurs. Journal of Vertebrate Paleontology 17(3): 534–547. https://doi.org/10.1080/02724634.1997.10011000

Caldwell MW (2002) From fins to limbs to fins: Limb evolution in fossil marine reptiles. American Journal of Medical Genetics 112(3): 236–249. https://doi.org/10.1002/ajmg.10773

Carpenter K (1996) A review of short-necked plesiosaurs from the Cretaceous of the Western Interior, North America. Neues Jahrbuch für Geologie und Paläontologie, Abhandlungen 201(2): 259–287. https://doi.org/10.1127/njgpa/201/1996/259

Carpenter K (1999) Revision of North American elasmosaurs from the Cretaceous of the Western Interior. Paludicola 2: 148–173.

Carroll RL (1997) Mesozoic marine reptiles as models of long-term, large-scale evolutionary phenomena. In: Callaway JM, Nicholls EL (Eds) Ancient marine reptiles. Academic Press, 467–489. https://doi.org/10.1016/B978-012155210-7/50025-9

Carroll RL, Gaskill P (1985) The nothosaur *Pachypleurosaurus* and the origin of plesiosaurs. Philosophical Transactions of the Royal Society of London, Series B, Biological Sciences 309: 343–393. https://doi.org/10.1098/rstb.1985.0091

Clack JA (2012) Gaining ground: the origin and evolution of tetrapods. Indiana University Press.

Cleveland WS (1979) Robust locally weighted regression and smoothing scatterplots. Journal of the American Statistical Association 74: 829–836. https://doi.org/10.1080/01621459.1979.10481038

Cruickshank AR, Long JA (1997) A new species of pliosaurid reptile from the Early Cretaceous Birdrong Sandstone of Western Australia. Records of the Western Australian Museum 18: 263–276.

de Buffrenil V, Mazin JM (1990) Bone histology of the ichthyosaurs: comparative data and functional interpretation. Paleobiology 16(4): 435–447. https://doi.org/10.1017/S0094837300010174

de Ricqlès A (1975) Recherches paléohistologiques sur les os longs des tétrapodes VII. – Sur la classification, la signification fonctionelle et l'histoire des tissus osseux des tétrapodes. Première partie. Annales de Paléontologie 61: 51–129.

Delfino M, Sánchez-Villagra MR (2010) A survey of the rock record of reptilian ontogeny. Seminars in Cell & Developmental Biology 21(4): 432–440. https://doi.org/10.1016/j.semcdb.2009.11.007

Druckenmiller PS, Russell AP (2008) A phylogeny of Plesiosauria (Sauropterygia) and its bearing on the systematic status of *Leptocleidus* Andrews, 1922. Zootaxa 1863(1): 1–120. https://doi.org/10.11646/zootaxa.1863.1.1

Fischer V, Bardet N, Benson RB, Arkhangelsky MS, Friedman M (2016) Extinction of fish-shaped marine reptiles associated with reduced evolutionary rates and global environmental volatility. Nature Communications 7(1): 1–11. https://doi.org/10.1038/ncomms10825

Fish FE (2000) Biomechanics and energetics in aquatic and semiaquatic mammals: Platypus to whale. Physiological Zoology 73(6): 683–698. https://doi.org/10.1086/318108

Föllmi KB (2012) Early Cretaceous life, climate and anoxia. Cretaceous Research 35: 230–257. https://doi.org/10.1016/j.cretres.2011.12.005

Fordyce RE, Barnes LG (1994) The evolutionary history of whales and dolphins. Annual Review of Earth and Planetary Sciences 22(1): 419–455. https://doi.org/10.1146/annurev.ea.22.050194.002223

Fostowicz-Frelik L, Gaździcki A (2001) Anatomy and histology of plesiosaur bones from the Late Cretaceous of Seymour Island, Antarctic Peninsula. Acta Palaeontologica Polonica 60: 7–32.

Galatius A (2010) Paedomorphosis in two small species of toothed whales (Odontoceti): How and why? Biological Journal of the Linnean Society, Linnean Society of London 99(2): 278–295. https://doi.org/10.1111/j.1095-8312.2009.01357.x

Galatius A, Kinze CC (2003) Ankylosis patterns in the postcranial skeleton and hyoid bones of the harbour porpoise (*Phocoena phocoena*) in the Baltic and North Sea. Canadian Journal of Zoology 81(11): 1851–1861. https://doi.org/10.1139/z03-181

Galatius A, Andersen MBER, Haugan B, Langhoff HE, Jespersen Å (2006) Timing of epiphyseal development in the flipper skeleton of the harbour porpoise (*Phocoena phocoena*) as an indicator of paedomorphosis. Acta Zoologica 87(1): 77–82. https://doi.org/10.1111/j.1463-6395.2006.00223.x

Galatius A, Berta A, Frandsen MS, Goodall RNP (2011) Interspecific variation of ontogeny and skull shape among porpoises (Phocoenidae). Journal of Morphology 272(2): 136–148. https://doi.org/10.1002/jmor.10900

Gasparini Z, Salgado L, Parras A (2007) Late Cretaceous plesiosaurs from northern Patagonia, Argentina. Geological Journal 42(2): 185–202. https://doi.org/10.1002/gj.1079

Godfrey LR, Sutherland MR (1996) Paradox of peramorphic paedomorphosis: Heterochrony and human evolution. American Journal of Physical Anthropology 99(1): 17–42. https://doi.org/10.1002/ajpa.1330990102

Goswami A, Foley L, Weisbecker V (2013) Patterns and implications of extensive heterochrony in carnivoran cranial suture closure. Journal of Evolutionary Biology 26(6): 1294–1306. https://doi.org/10.1111/jeb.12127

Gould SJ (1977) Ontogeny and Phylogeny. Harvard University Press.

Großmann F (2006) Taxonomy, phylogeny and palaeoecology of the plesiosauroids (Sauropterygia, Reptilia) from the Posidonia shale (Toarcian, Lower Jurassic) of Holzmaden, south west Germany. Doctoral dissertation, Tübingen, Univ., Diss., 2006.

Großmann F (2007) The taxonomic and phylogenetic position of the Plesiosauroidea from the Lower Jurassic Posidonia Shale of south-west Germany. Palaeontology 50(3): 545–564. https://doi.org/10.1111/j.1475-4983.2007.00654.x

Guinot G, Cavin L (2015) Contrasting "fish" diversity dynamics between marine and freshwater environments. Current Biology 25(17): 2314–2318. https://doi.org/10.1016/j.cub.2015.07.033

Guinot G, Cavin L (2016) 'Fish' (Actinopterygii and Elasmobranchii) diversification patterns through deep time. Biological Reviews of the Cambridge Philosophical Society 91(4): 950–981. https://doi.org/10.1111/brv.12203

Hampe O (2005) Considerations on a *Brachauchenius* skeleton (Pliosauroidea) from the lower Paja Formation (late Barremian) of Villa de Leyva area (Colombia). Fossil Record (Weinheim) 8(1): 37–51. https://doi.org/10.5194/fr-8-37-2005

Hampe O (2013) The forgotten remains of a leptocleidid plesiosaur (Sauropterygia: Plesiosauroidea) from the Early Cretaceous of Gronau (Münsterland, Westphalia, Germany). Palaontologische Zeitschrift 87(4): 473–491. https://doi.org/10.1007/s12542-013-0175-3

Hay WW, Floegel S (2012) New thoughts about the Cretaceous climate and oceans. Earth-Science Reviews 115(4): 262–272. https://doi.org/10.1016/j.earscirev.2012.09.008

Herrera Y, Gasparini Z, Fernandez MS (2013) A new Patagonian species of *Cricosaurus* (Crocodyliformes, Thalattosuchia): First evidence of *Cricosaurus* in Middle–Upper Tithonian lithographic limestone from Gondwana. Palaeontology 56(3): 663–678. https://doi.org/10.1111/pala.12010

Hiller N, Mannering AA, Jones CM, Cruickshank AR (2005) The nature of *Mauisaurus haasti* Hector, 1874 (Reptilia: Plesiosauria). Journal of Vertebrate Paleontology 25(3): 588–601. https://doi.org/10.1671/0272-4634(2005)025[0588:TNOMHH]2.0.CO;2

Houssaye A (2009) "Pachyostosis" in aquatic amniotes: A review. Integrative Zoology 4(4): 325–340. https://doi.org/10.1111/j.1749-4877.2009.00146.x

Houssaye A, Sander PM, Klein N (2016) Adaptive patterns in aquatic amniote bone microanatomy—More complex than previously thought. Integrative and Comparative Biology 56(6): 1349–1369. https://doi.org/10.1093/icb/icw120

Hu X, Wagreich M, Yilmaz IO (2012) Marine rapid environmental/climatic change in the Cretaceous greenhouse world. Cretaceous Research 38: 1–6. https://doi.org/10.1016/j.cretres.2012.04.012

Hugi J, Scheyer TM, Sander PM, Klein N, Sánchez-Villagra MR (2011) Long bone microstructure gives new insights into the life of pachypleurosaurids from the Middle Triassic of Monte San Giorgio, Switzerland/Italy. Comptes Rendus. Palévol 10(5–6): 413–426. https://doi.org/10.1016/j.crpv.2011.03.009

Kear BP (2005) A new elasmosaurid plesiosaur from the Lower Cretaceous of Queensland, Australia. Journal of Vertebrate Paleontology 25(4): 792–805. https://doi.org/10.1671/0272-4634(2005)025[0792:ANEPFT]2.0.CO;2

Kear BP (2006) Plesiosaur remains from Cretaceous high-latitude non-marine deposits in southeastern Australia. Journal of Vertebrate Paleontology 26(1): 196–199. https://doi.org/10.1671/0272-4634(2006)26[196:PRFCHN]2.0.CO;2

Ketchum HF, Benson RB (2011a) The cranial anatomy and taxonomy of *Peloneustes philarchus* (Sauropterygia, Pliosauridae) from the Peterborough member (Callovian, Middle Jurassic) of the United Kingdom. Palaeontology 54(3): 639–665. https://doi.org/10.1111/j.1475-4983.2011.01050.x

Ketchum HF, Benson RB (2011b) A new pliosaurid (Sauropterygia, Plesiosauria) from the Oxford Clay Formation (Middle Jurassic., Callovian) of England: Evidence for a gracile, longirostrine grade of Early-Middle Jurassic pliosaurids. Special Papers in Palaeontology 86: 109–129.

Kidder DL, Worsley TR (2010) Phanerozoic large igneous provinces (LIPs), HEATT (haline euxinic acidic thermal transgression) episodes, and mass extinctions. Palaeogeography, Palaeoclimatology, Palaeoecology 295(1–2): 162–191. https://doi.org/10.1016/j.palaeo.2010.05.036

Knutsen EM, Druckenmiller PS, Hurum JH (2012) A new species of Pliosaurus (Sauropterygia: Plesiosauria) from the Middle Volgian of central Spitsbergen, Norway. Norwegian Journal of Geology 92: 235–258.

Klein N (2010) Long bone histology of Sauropterygia from the Lower Muschelkalk of the Germanic Basin provides unexpected implications for phylogeny. PLoS ONE 5(7): e11613. https://doi.org/10.1371/journal.pone.0011613

Kordikova EG (2000) Paedomorphosis in the shell of fossil and living turtles. Neues Jahrbuch für Geologie und Paläontologie. Abhandlungen 218(3): 399–446. https://doi.org/10.1127/njgpa/218/2000/399

Kordikova EG (2002) Heterochrony in the evolution of the shell of Chelonia. Part 1: Terminology, Cheloniidae, Dermochelyidae, Trionychidae, Cyclanorbidae and Carettochelyidae. Neues Jahrbuch für Geologie und Paläontologie. Abhandlungen 226(3): 343–417. https://doi.org/10.1127/njgpa/226/2002/343

Larramendi A, Palombo MR (2015) Body Size, Biology and Encephalization Quotient of *Palaeoloxodon* ex gr. *P. falconeri* from Spinagallo Cave (Hyblean plateau, Sicily). Hystrix 26: 102–109.

Lehman J-P (1955) Les stégocéphales du nor-ouest de Madagascar. Comptes Rendus Hebdomadaires des Séances de l'Académie des Sciences 241: 82–84.

Liebe L, Hurum JH (2012) Gross internal structure and microstructure of plesiosaur limb bones from the Late Jurassic, central Spitsbergen. Norwegian Journal of Geology/Norsk Geologisk Forening 92: 285–309.

Livezey BC (1992) Flightlessness in the Galápagos cormorant (*Compsohalieus* [*Nannopterum*] *harrisi*): Heterochrony, giantism and specialization. Zoological Journal of the Linnean Society 105(2): 155–224. https://doi.org/10.1111/j.1096-3642.1992.tb01229.x

McHenry CR (2009) Devourer of gods: the palaeoecology of the Cretaceous pliosaur *Kronosaurus queenslandicus*. Doctoral dissertation, University of Newcastle.

McNamara KJ (1997) Shapes of time: the evolution of growth and development. Johns Hopkins University Press, Baltimore.

Miller PJ (1996) Miniature vertebrates: the implications of small body size. Oxford University Press.

Miller CV, O'Gorman JP, Salisbury SW, Coria RA, Roberts EM, O'Connor PM, Reguero MA, Lamanna MC (2020) A new plesiosaur (Reptilia: Sauropterygia) specimen from the Upper Cretaceous of West Antarctica, with comments on the ontogeny and morphological diversity of the elasmosaurid pelvic girdle. Annals of the Carnegie Museum 86(2): 93–106. https://doi.org/10.2992/007.086.0201

Mitteroecker P, Gunz P, Bernhard M, Schaefer K, Bookstein FL (2004) Comparison of cranial ontogenetic trajectories among great apes and humans. Journal of Human Evolution 46(6): 679–698. https://doi.org/10.1016/j.jhevol.2004.03.006

Moon BC (2019) A new phylogeny of ichthyosaurs (Reptilia: Diapsida). Journal of Systematic Palaeontology 17: 129–155. https://doi.org/10.1080/14772019.2017.1394922

Ogg JG, Ogg G, Gradstein FM (2016) A concise geologic time scale: 2016. Elsevier.

O'Gorman JP, Coria RA (2017) A new elasmosaurid specimen from the upper Maastrichtian of Antarctica: New evidence of a monophyletic group of Weddellian elasmosaurids. Alcheringa. An Australasian Journal of Palaeontology 41(2): 240–249. https://doi.org/10.1080/03115518.2016.1224318

O'Gorman JP, Gasparini Z, Salgado L (2014) Reappraisal of *Tuarangisaurus? cabazai* (Elasmosauridae, Plesiosauria) from the upper Maastrichtian of northern Patagonia, Argentina. Cretaceous Research 47: 39–47. https://doi.org/10.1016/j.cretres.2013.10.003

O'Keefe FR (2002) The evolution of plesiosaur and pliosaur morphotypes in the Plesiosauria (Reptilia: Sauropterygia). Paleobiology 28(1): 101–112. https://doi.org/10.1666/0094-8373(2002)028%3C0101:TEOPAP%3E2.0.CO;2

O'Keefe FR, Chiappe LM (2011) Viviparity and K-selected life history in a Mesozoic marine plesiosaur (Reptilia, Sauropterygia). Science 333(6044): 870–873. https://doi.org/10.1126/science.1205689

O'Keefe FR, Sander PM, Wintrich T, Werning S (2019) Ontogeny of polycotylid long bone microanatomy and histology. Integrative Organismal Biology (Oxford, England) 1(1): oby007. https://doi.org/10.1093/iob/oby007

Oromi N, Pujol-Buxó E, San Sebastián O, Llorente GA, Hammou MA, Sanuy D (2016) Geographical variations in adult body size and reproductive life history traits in an invasive anuran, *Discoglossus pictus*. Zoology (Jena, Germany) 119(3): 216–223. https://doi.org/10.1016/j.zool.2016.02.003

Ősi A, Young MT, Galácz A, Rabi M (2018) A new large-bodied thalattosuchian crocodyliform from the Lower Jurassic (Toarcian) of Hungary, with further evidence of the mosaic acquisition of marine adaptations in Metriorhynchoidea. PeerJ 6: e4668. https://doi.org/10.7717/peerj.4668

Otero RA, Soto-Acuna S, Vargas AO, Rubilar-Rogers D (2014) A new postcranial skeleton of an elasmosaurid plesiosaur from the Upper Cretaceous of central Chile and reassessment of *Cimoliasaurus andium* Deecke. Cretaceous Research 50: 318–331. https://doi.org/10.1016/j.cretres.2014.05.008

Otero RA, O'Gorman JP, Hiller N (2015) Reassessment of the upper Maastrichtian material from Chile referred to *Mauisaurus* Hector, 1874 (Plesiosauroidea: Elasmosauridae) and the taxonomical value of the hemispherical propodial head among austral elasmosaurids. New Zealand Journal of Geology and Geophysics 58(3): 252–261. https://doi.org/10.1080/00288306.2015.1037775

Otero RA, Soto-Acuña S, O'Keefe FR (2018) Osteology of *Aristonectes quiriquinensis* (Elasmosauridae, Aristonectinae) from the upper Maastrichtian of central Chile. Journal of Vertebrate Paleontology 38(1): e1408638. https://doi.org/10.1080/02724634.2017.1408638

Piveteau J, Dechaseaux C (1955) Trematosauria. Traité de Paléontologie 5: 126–135.

Polcyn MJ, Jacobs LL, Araújo R, Schulp AS, Mateus O (2014) Physical drivers of mosasaur evolution. Palaeogeography, Palaeoclimatology, Palaeoecology 400: 17–27. https://doi.org/10.1016/j.palaeo.2013.05.018

Racicot RA, Colbert MW (2013) Morphology and variation in porpoise (Cetacea: Phocoenidae) cranial endocasts. The Anatomical Record 296(6): 979–992. https://doi.org/10.1002/ar.22704

Raff RA (1996) The shape of life. University of Chicago Press. https://doi.org/10.7208/chicago/9780226256573.001.0001

Rieppel O (1989a) *Helveticosaurus zollingeri* Peyer (Reptilia, Diapsida) skeletal paedomorphosis, functional anatomy and systematic affinities. Palaeontographica. Abteilung A, Paläozoologie, Stratigraphie 208: 123–152.

Rieppel O (1989b) A new pachypleurosaur (Reptilia: Sauropterygia) from the Middle Triassic of Monte San Giorgio, Switzerland. Philosophical Transactions of the Royal Society of London, Series B, Biological Sciences 323: 1–73. https://doi.org/10.1098/rstb.1989.0001

Rieppel O (2000) Sauropterygia I: Placodontia, Pachypleurosauria, Nothosauroidea, Pistosauroidea. Encyclopedia of paleoherpetology 12: 1–134.

Sachs S (2004) Redescription of *Woolungasaurus glendowerensis* (Plesiosauria: Elasmosauridae) from the Lower Cretaceous of Northeast Queensland. Memoirs of the Queensland Museum 49: 713–732.

Sames B, Wagreich M, Wendler JE, Haq BU, Conrad CP, Melinte-Dobrinescu MC, Hu X, Wendler I, Wolfgring E, Yilmaz IÖ, Zorina SO (2016) Short-term sea-level changes in a greenhouse world—A view from the Cretaceous. Palaeogeography, Palaeoclimatology, Palaeoecology 441: 393–411. https://doi.org/10.1016/j.palaeo.2015.10.045

Sanchez S, Ahlberg PE, Trinajstic KM, Mirone A, Tafforeau P (2012) Three-dimensional synchrotron virtual paleohistology: A new insight into the world of fossil bone microstructures. Microscopy and Microanalysis 18(5): 1095–1105. https://doi.org/10.1017/S1431927612001079

Sato T, Wu XC (2006) Review of plesiosaurians (Reptilia: Sauropterygia) from the upper cretaceous horseshoe canyon formation in Alberta, Canada. Paludicola 5: 150–169.

Seeley HG (1908) LXVIII. On the extremity of the tail in Ichthyosauria. Annals and Magazine of Natural History 1(5): 436–441. https://doi.org/10.1080/00222930808692428

Sheldon A, Bell Jr GL (1998) Paedomorphosis in Mosasauroidea (Squamata): Evidence from fossil bone microstructure. Paludicola 2: 190–205.

Smith KK (2001) Heterochrony revisited: The evolution of developmental sequences. Biological Journal of the Linnean Society, Linnean Society of London 73(2): 169–186. https://doi.org/10.1111/j.1095-8312.2001.tb01355.x

Smith AS (2007) The back-to-front plesiosaur *Cryptoclidus* (*Apractocleidus*) *aldingeri* from the Kimmeridgian of Milne Land, Greenland. Bulletin of the Geological Society of Denmark 55: 1–7. https://doi.org/10.37570/bgsd-2007-55-01

Sollas WJ (1881) On a new species of *Plesiosaurus* (*P. conybeari*) from the Lower Lias of Charmouth; with observations on *P. megacephalus*, Stutchbury, and *P. brachycephalus*, Owen. Quarterly Journal of the Geological Society 37(1–4): 440–481. https://doi.org/10.1144/GSL.JGS.1881.037.01-04.42

Storrs GW (1995) A juvenile specimen of? *Plesiosaurus* sp. from the Lias (Lower Jurassic, Pliensbachian) near Charmouth, Dorset, England. Proceedings of the Dorset Natural History and Archaeological Society 116: 71–76.

Storrs GW, Arkhangel'skii MS, Efimov V (2000) Mesozoic marine reptiles of Russia and other former Soviet republics. In: Benton MJ, Shishkin MA, Unwin DM, Kurochkin EN (Eds) The age of dinosaurs in Russia and Mongolia. Cambridge University Press, Cambridge, UK, 187–210.

Talevi M, Fernández MS (2015) Remodeling of skeletal tissues bone and structural specialisations in an elasmosaurid (Sauropterygia: Plesiosauroidea) from the Upper Cretaceous of Patagonia, Argentina. Historical Biology 27(1): 60–67. https://doi.org/10.1080/08912963.2013.863882

Tarlo LB (1959) *Stretosaurus* gen. nov., a giant pliosaur from the Kimmeridge Clay. Palaeontology 2: 39–55.

Tsai CH, Fordyce RE (2014) Juvenile morphology in baleen whale phylogeny. Naturwissenschaften 101(9): 765–769. https://doi.org/10.1007/s00114-014-1216-9

Tumarkin-Deratzian AR, Vann DR, Dodson P (2006) Bone surface texture as an ontogenetic indicator in long bones of the Canada goose

Branta canadensis (Anseriformes: Anatidae). Zoological Journal of the Linnean Society 148(2): 133–168. https://doi.org/10.1111/j.1096-3642.2006.00232.x

Vavrek MJ, Wilhelm BC, Maxwell EE, Larsson HC (2014) Arctic plesiosaurs from the Lower Cretaceous of Melville Island, Nunavut, Canada. Cretaceous Research 50: 273–281. https://doi.org/10.1016/j.cretres.2014.04.011

Vincent P (2010) A juvenile plesiosaur specimen from the Lower Jurassic of Holzmaden, Germany. Palaeontographica, Abteilung A, Paläozoologie, Stratigraphie 291(1–3): 45–61. https://doi.org/10.1127/pala/291/2010/45

Welles SP, Gregg DR (1971) Late Cretaceous marine reptiles of New Zealand. Records of the Canterbury Museum 9: 1–111.

Wiffen J, Moisley WL (1986) Late Cretaceous reptiles (Families Elasmosauridae and Pliosauridae) from the Mangahouanga Stream, North Island, New Zealand. New Zealand Journal of Geology and Geophysics 29(2): 205–252. https://doi.org/10.1080/00288306.1986.10427535

Wiffen J, De Buffrénil V, De Ricqlès A, Mazin JM (1995) Ontogenetic evolution of bone structure in Late Cretaceous Plesiosauria from New Zealand. Geobios 28(5): 625–640. https://doi.org/10.1016/S0016-6995(95)80216-9

Wintrich T, Scaal M, Sander PM (2017) Foramina in plesiosaur cervical centra indicate a specialized vascular system. Fossil Record (Weinheim) 20(2): 279–290. https://doi.org/10.5194/fr-20-279-2017

Supplementary material 1

Raw data and analyses

Authors: Ricardo Araújo, Adam S. Smith

Data type: Excel files (in ZIP. archive)

Explanation note: Plesiosaur occurrences, osteological maturity assessment, references and statistical analyses.

Copyright notice: This dataset is made available under the Open Database License (http://opendatacommons.org/licenses/odbl/1.0). The Open Database License (ODbL) is a license agreement intended to allow users to freely share, modify, and use this Dataset while maintaining this same freedom for others, provided that the original source and author(s) are credited.

Link: https://doi.org/10.3897/fr.26.97686.suppl1

Fossil Record 26 (1) 2023, 103–115 | DOI 10.3897/fr.26.102570

Early Jurassic silicified woods from Carapace Nunatak, South Victoria Land, Antarctica

Agathe Toumoulin[1], Anne-Laure Decombeix[2,3], Carla J. Harper[3,4], Rudolph Serbet[3]

1 *Department of Botany and Zoology, Masaryk University, Brno, Czech Republic*
2 *AMAP, Univ Montpellier, CIRAD, CNRS, INRAe, IRD, Montpellier, France*
3 *Division of Paleobotany, Biodiversity Institute, University of Kansas, Lawrence, Kansas, USA*
4 *Botany Department, School of Natural Sciences, Trinity College Dublin, Dublin 2, Ireland*

https://zoobank.org/5213691A-5C25-4E71-A74E-FF2CF82C2C16

Corresponding authors: Agathe Toumoulin (agathe.toumoulin@gmail.com); Anne-Laure Decombeix (anne-laure.decombeix@cirad.fr)

Academic editor: Alexander Schmidt ♦ **Received** 23 February 2023 ♦ **Accepted** 5 May 2023 ♦ **Published** 19 May 2023

Abstract

The Jurassic vegetation of Antarctica remains poorly known and, while there have been several reports of large fossil trees from that time period across the continent, detailed anatomical studies of their wood are extremely scarce. Here we describe new silicified woods of Early Jurassic (probably Toarcian) age from Carapace Nunatak, South Victoria Land. The genera *Agathoxylon* and *Brachyoxylon* are formally recognized for the first time in the Jurassic of Antarctica. The preservation of the woods is imperfect, which is likely explained by the presence in some of the specimens of fungi, whose anatomical structures are described in detail. Combined with previous reports of pollen, leaves, and cones from South and North Victoria Land, these new specimens support the presence of several conifer families in the Early Jurassic floras of the region.

Key Words

Agathoxylon, Araucariaceae, *Brachyoxylon*, conifers, fossil fungi, gymnosperms, Hirmeriellaceae, Mesozoic

Introduction

Abundant fossils indicate that Antarctica was vegetated for most of its history. Permineralized trunks, some of them preserved *in situ*, demonstrate the establishment of forests on the continent from the Permian and their persistence in some areas until the late Miocene (e.g. Cantrill and Poole 2012). Dwarf trees (*Notofagus*) are also documented in the Transantarctic Mountains during the Pliocene (Francis and Hill 1996). Detailed studies of permineralized wood conducted since the early 1900s have provided valuable information on the taxonomic affinities but also on the growth and physiology of these trees (e.g. Kraüsel 1962; Francis 1986; Falcon-Lang and Cantrill 2001; Taylor and Ryberg 2007; Gulbranson et al. 2014; Miller et al. 2016). However, most of these studies have focused on Permian, Triassic, and Cretaceous specimens. Fossil wood and tree trunks are also known from Jurassic deposits of Antarctica, but they have received comparatively less attention and only a small number of specimens have been described to date. The first detailed description was that of Early Jurassic trunks from the Mesa Range region, in Northern Victoria Land, by Jefferson et al. (1983). The trees were engulfed in lava and are preserved in growth position. They reach 1 meter in diameter. Based on their secondary xylem anatomy, they were compared to the morphogenus *Protocupressinoxylon*, a nomenclatural synonym of *Protobrachyoxylon* Holden, 1913 (Philippe 1993), which might belong to the Hirmeriellaceae (or Cheirolepidiaceae, see Paclt 2011; Doweld 2020 for discussion), i.e. an extinct family of conifers. In the Antarctic Peninsula, del Valle et al. (1997) reported the presence of fossil stems and trunks, some of them up to 50 cm in diameter, within volcaniclastic rocks of the Early to Late Jurassic age from Brebbia Nunatak and Ramírez Nunatak. However, they did not

Copyright *Agathe Toumoulin et al.* This is an open access article distributed under the terms of the Creative Commons Attribution License (CC BY 4.0), which permits unrestricted use, distribution, and reproduction in any medium, provided the original author and source are credited.

provide an anatomical description of the specimens. Late Jurassic – early Cretaceous anatomically preserved wood fragments were also reported from Hope Bay (Torres et al. 2000). Large woody axes are also known to occur in Middle Jurassic cherts at Storm Peak, in the Central Transantarctic Mountains (Kellogg and Taylor 2004), but again these specimens have never been formally described. In Northern Victoria Land, new Early Jurassic fossil woods have been collected recently and are under study (Bomfleur et al. 2011; Harper et al. 2012). In Southern Victoria Land, Garland et al. (2007) described an Early Jurassic coniferous stump preserved in a basalt flow at Coombs Hills. The specimen is about 40 cm in diameter and was compared to the Podocarpaceae.

Carapace Nunatak, located about 10 km from Coombs Hills, is known for its well-preserved Early Jurassic fossils plants and animals occurring in lacustrine deposits intercalated between lava flows of the Kirkpatrick Basalt Formation. Various arthropods are present in the deposits, with an abundance of conchostracans and other crustaceans indicating a shallow and/or ephemeral freshwater environment (Ballance and Watters 1971; Ball et al. 1979; Shen 1994). Palynofloras include a relatively high count of *Classopollis* pollen (Bomfleur et al. 2014), which has been related to the Hirmeriellaceae (e.g., Taylor et al. 2009; Thévenard et al. 2022). Plant macrofossils identified to date correspond to fern leaves and rhizomes, isolated ovules, cycadophyte leaves, and conifer foliage and cones. Among the conifers, Townrow (1967a) listed the presence of several fossils of putative podocarpaceous affinities: shoots and seed cones of *Nothodacrium warrenii* and the pollen cone *Masculostrobus warrenii*. He also noted the presence of *Brachyphyllum*- and *Pagiophyllum*-like shoots (Townrow 1967b). More recently, two new pollen cones have been described from Carapace Nunatak: *Classostrobus elliotii*, which has been assigned to the Hirmeriellaceae (Hieger et al. 2015), and *Chimaerostrobus minutus*, with characters reminiscent of both Voltziales and Araucariaceae (Atkinson et al. 2018). Here we describe fossil woods collected at the locality during the austral summer 2014–2015. We discuss their affinities and how they fit within our knowledge of conifer diversity in Antarctica during the Early Jurassic.

Materials and methods

Locality and age of the specimens

The fossil woods described in this study were collected from the moraine located on the E-NE side of Carapace Nunatak, southern Victoria Land, Central Transantarctic Mountains, Antarctica (76°53'S, 159°25'E, elevation 2150 m, Convoy Range Quadrangle; Fig. 1). Two formations outcrop at Carapace Nunatak, the Carapace Sandstone Fm and the overlaying Kirkpatrick Basalt Fm. Radiometric dating and palynological analyses indicate an Early Jurassic age for both formations, with an early Toarcian (ca. 180 Ma) age for the Kirkpatrick Basalt Fm (Elliot 2013 and references therein; Bomfleur et al. 2014). The woods occurred on the moraine together with blocks of silicified chert containing plant material from the lacustrine beds of the Kirkpatrick Basalt Fm. Based on the matrix surrounding some of the specimens, their location on the moraine, and their co-occurrence with blocks of silicified chert, we consider the specimens to be derived from the Kirkpatrick Basalt Fm and thus to be Toarcian in age.

Specimen preparation and imaging

Of the 10 putative wood specimens collected, four (#270, 271, 272, 274) were preserved well enough to observe all the characters important for wood taxonomy. Specimens 273, 275, 276 and 279 are more distorted and, while qualitative characters can be observed, obtaining a significant number of measurements proved more difficult. Finally, specimen 277 is insufficiently preserved to allow its anatomy description and taxonomic analysis. Specimen 278 lacked anatomical preservation: it consisted of a wood impression on a piece of sedimentary rock containing small fusains.

The specimens are heavily silicified and were prepared as thin-sections in the transverse, tangential, and radial planes following the classical technique (Hass and Rowe 1999). Images were taken in reflected light using ArchiMed software (Microvision Instruments, Evry, France) with Sony XCD-U100CR digital cameras attached to an Olympus SZX12 stereomicroscope and to an Olympus BX51 compound microscope, except for Fig. 4A–C, which were taken with a Keyence VHX 7000 digital microscope and the associated imaging software. Plates were composed with Adobe Photoshop version 21.0.1 (Adobe Systems, San José, California, USA). Transformations made in Photoshop included cropping, rotation, and adjustment of exposure, contrast, when needed.

Statistical analyses

Statistical analyses were performed to describe ray height and its variability across the specimens, to better distinguish between wood morphospecies. They were performed using Rstudio software (version 4.0.3; R Core Team 2020, Boston, USA). For each specimen, thirty ray heights were measured on tangential or radial sections. Data normality was tested by a Shapiro-Wilk test and homoscedasticity, with a Levene test (package *car*, version 3.0-10, Fox and Weisberg 2019). Since normality and variance homogeneity hypotheses were most of the time not respected, only non-parametric tests were used to compare ray heights. Differences between specimens were evaluated using Mann-Whitney-Wilcoxon. Kruskal-Wallis and Multiple Comparison Kruskal-Wallis tests (package *agricolae*, version 1.3-3, de Mendiburu 2020) were used to compare specimens (Fig. 5). For the different tests, a significance level, α, of 0.05 was chosen.

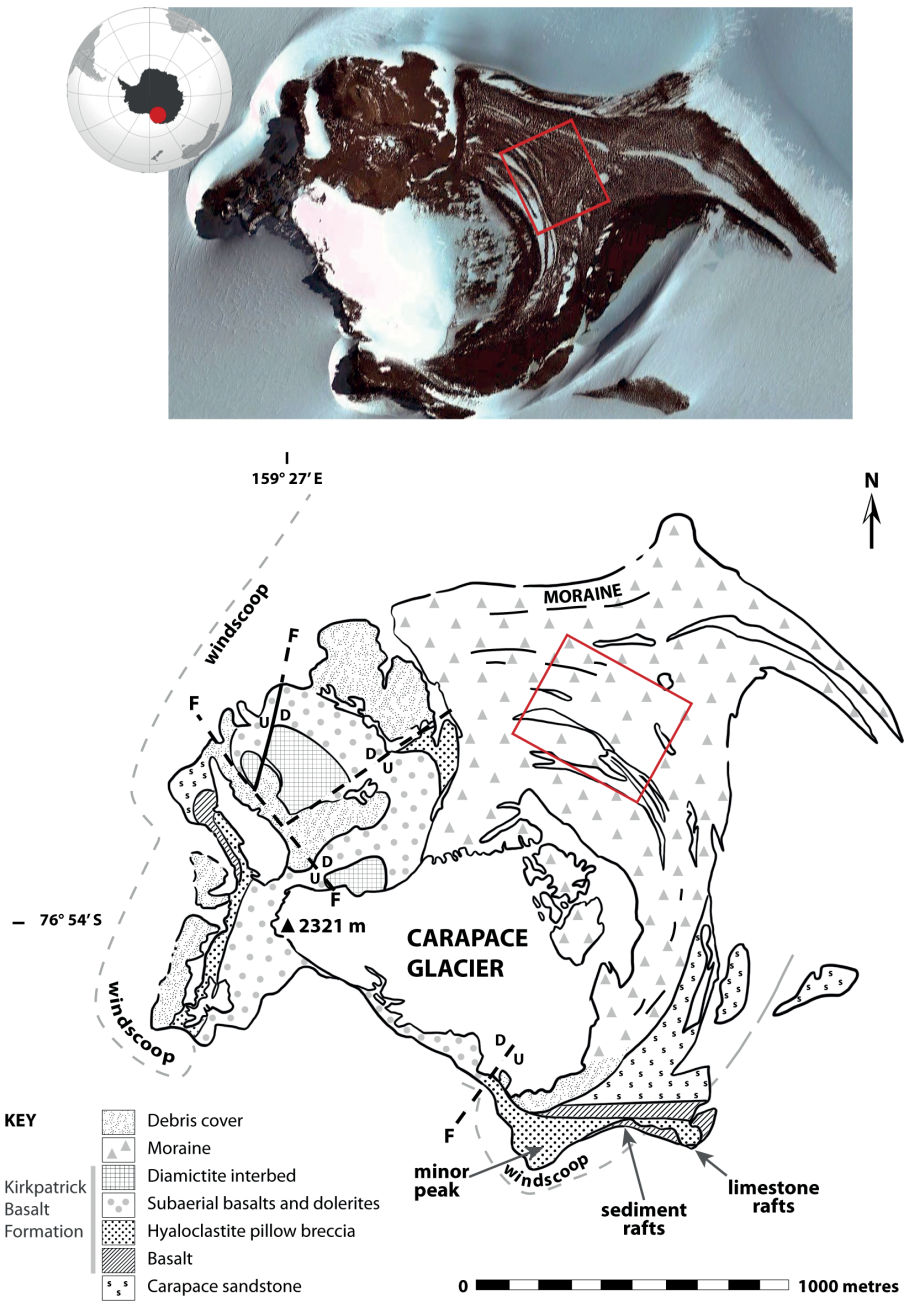

Figure 1. Location of the fossil wood locality. Aerial view of Carapace Nunatak (Source: Google Earth); the red square represents the area where the specimens were collected. Geological map modified after Bradshaw (1987). F: fault, U: up, D: down.

Results

With the exception of specimen 271, which corresponds to a branch about 7 x 5 cm in diameter (Fig. 2A), all the specimens represent pieces of wood with no indication of their origin within the plant. All wood specimens are composed of tracheids and parenchymatous rays. They share a number of characters but differ by ray height and type of radial pitting.

Anatomical characters shared by all samples

Specimen 271 shows several growth rings boundaries (Fig. 2B, C). In all other specimens, the limited extent of non-distorted wood prevents the detection of potential growth rings. The woods typically appear distorted and poorly preserved, often with the rays darker, more conspicuous, than the tracheids both in transverse (Fig. 2E, F) and in tangential (Fig. 2G–I) sections. The average diameter of tracheids range 25–30 µm depending on the specimens (Fig. 2D–F). Rays are uniseriate (Fig. 2D–I), rarely partly biseriate, and a few, i.e. up to 10, cells high (Figs 2G–I, 3). They have thin, straight unperforated cell walls and often have a dark brown to black content. In radial section, the end wall is perpendicular to sub-perpendicular to the ray (e.g. Fig. 3). There are rare instances of axial parenchyma with no particular organization. When preserved, cross-field pitting is araucarioid, i.e. pits are mostly cupressoid, often in groups of 3 or more, organized in a relatively

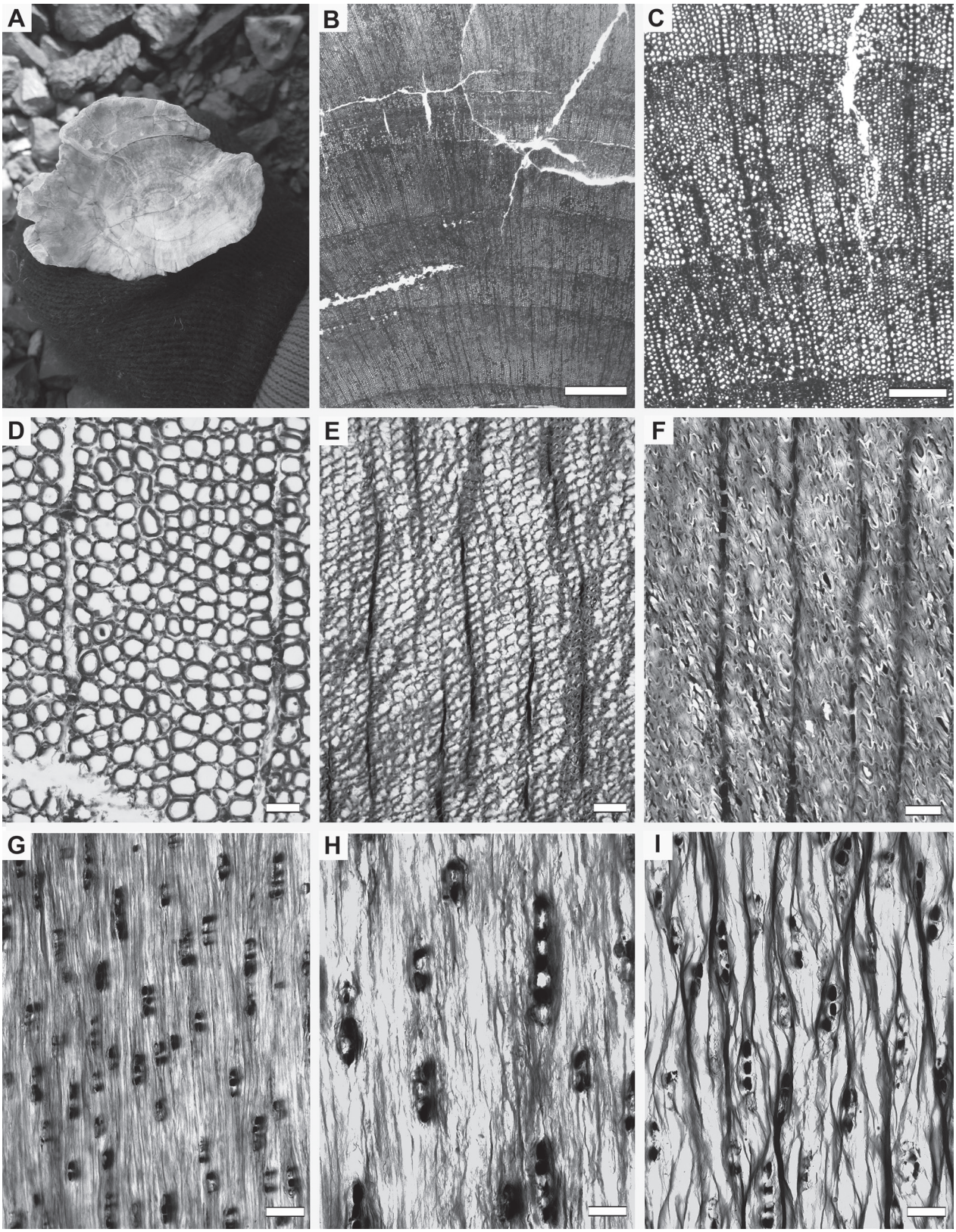

Figure 2. Early Jurassic woods from Carapace Nunatak in transverse and tangential section: **A.** General view of specimen 271 in the field; **B.** Transverse section of the previous specimen showing several growth ring boundaries. Slide 30781; **C.** Detail of two rings with a small amount of late wood. Slide 30,781; **D.** Close up of wood anatomy in transverse section showing tracheids and two uniseriate rays. Slide 30781; **E.** Transverse section of specimen 270 showing poorly preserved tracheids and several uniseriate rays. Slide 30775; **F.** Transverse section of specimen 276 showing extremely distorted tracheids and several uniseriate rays. Slide 35934; **G.** General view of specimen 274 in tangential section showing numerous uniseriate and low rays. Slide 35924; **H.** Detail of rays in 274. Slide 35924; **I.** General view of specimen 276 in tangential section showing numerous uniseriate and low rays. Tracheid walls are almost completely degraded. Slide 35931. Scale bars: 2 mm (**B**); 500 µm (**C**); 50 µm (**D, F, H, I**); 100 µm (**E, G**).

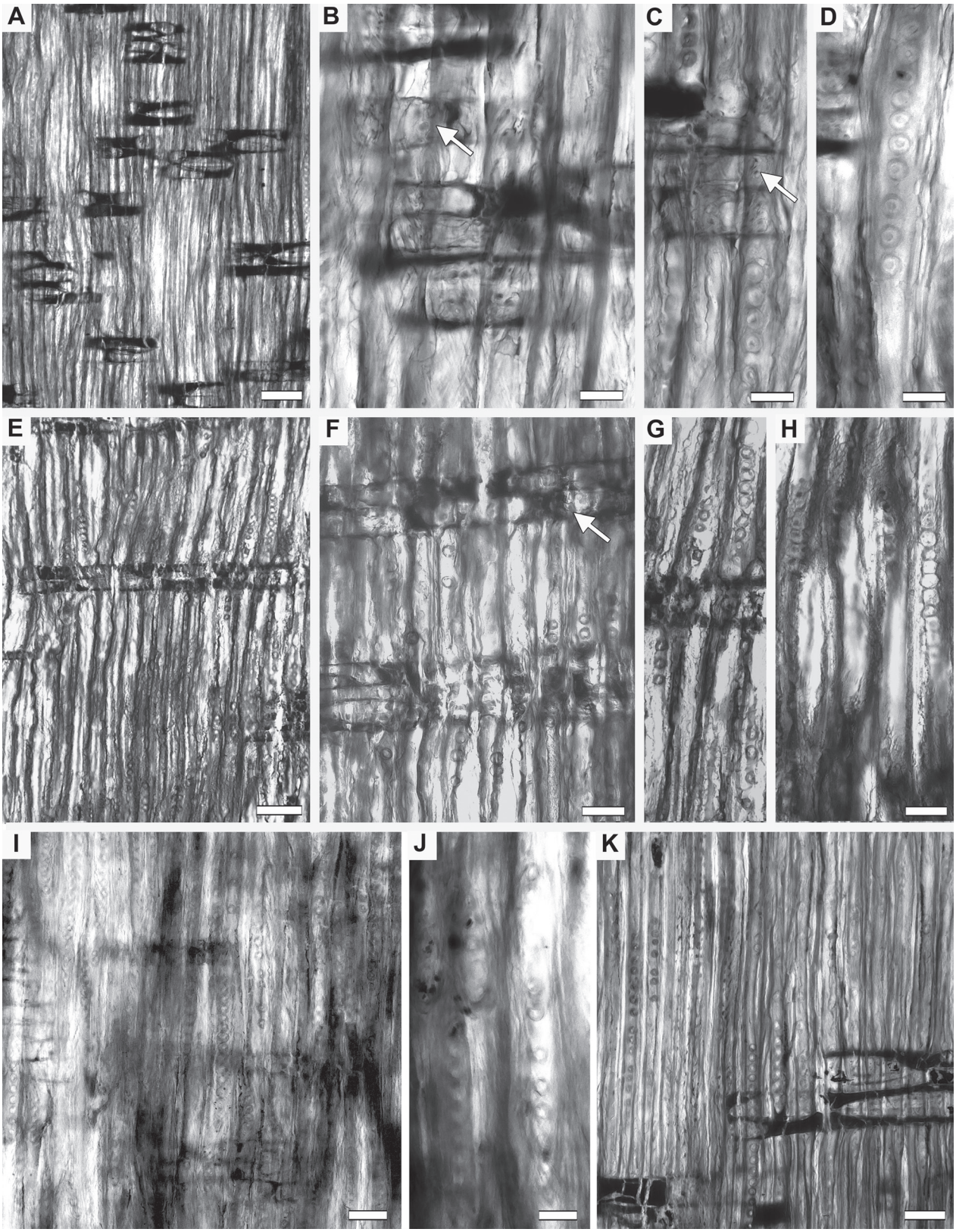

Figure 3. Early Jurassic woods from Carapace Nunatak with mixed pitting in radial section. Specimens 270 (**A–D**), 271 (**E–H**), 272 (**I–J**) and 274 (**K**). **A.** General view of specimen 270 in radial section showing the low rays. Slide 35913; **B.** Cross-field region in specimen 270. Slide 35913; **C.** Other detail showing the cross-field and relatively crowded radial pitting. Slide 35913; **D.** Detail of a tracheid with abietinean pitting. Slide 35913; **E.** General view of specimen 271 in radial section showing the low rays and mixed radial pitting. Slide 30784; **F.** Detail showing the cross-field and radial pitting. Slide 30783; **G.** Detail of E, showing araucarian and abietinean radial pitting. Slide 30784; **H.** Detail showing araucarian radial pitting. Slide 30784; **I.** General view of specimen 272 in radial section showing the low rays and mixed radial pitting. Slide 35915; **J.** Detail of abietiean pitting. Slide 35915; **K.** General view of specimen 274 in radial section showing the low rays and mixed radial pitting. Slide 35925. Scale bars: 100 µm (**A, E**); 25 µm (**B–D, J**); 50 µm (**F, H, I, K**).

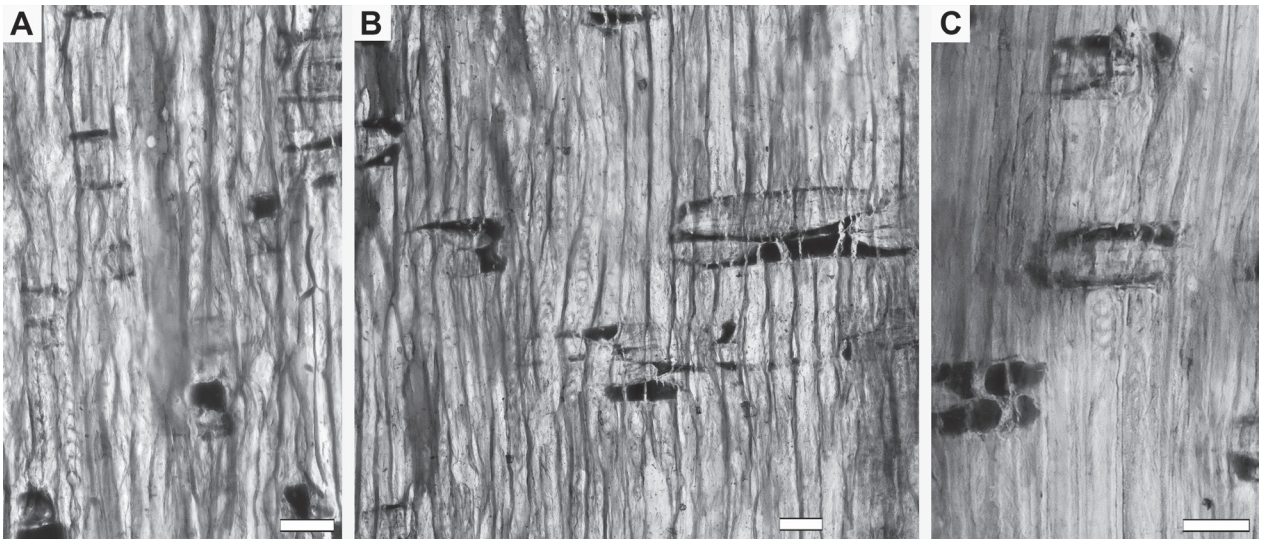

Figure 4. Early Jurassic woods from Carapace Nunatak with only araucarian pitting in radial section. Specimen 276. **A.** Tracheids with araucarian pitting. Slide 35937; **B.** Rays and tracheids with araucarian pitting. Slide 35937; **C.** Rays and tracheids with araucarian pitting. Slide 35938. Scale bars: 50 µm (**A–C**).

crowded alternate fashion (Fig. 3B, C). Resin canals are absent (e.g. Fig. 2B–F).

Radial pitting

Two major morphotypes of wood can be distinguished based on the pitting on the radial wall of their tracheids:

- n°270, 271, 272, and 274 have mixed pitting, with the presence of both araucarian and abietinean pitting (Fig. 3). The proportion is about 55–60% of araucarian pits on the tracheids where pitting is visible. The distribution of the two types of pitting is not homogeneous through the wood, especially in specimen 270.
- n°273, 275, 276, and probably 279 have araucarian pitting (Fig. 4). Pits appear contiguous in 90% of the cases and are often flattened. When multiseriate, pits are always arranged alternately.

Ray height

Ray height typically ranges 1–10 cells (Figs 2G–I, 3A, F, I, Suppl. material 1). Because the number of cells composing a ray was not easy to assess on all the specimens, comparisons were made using ray height in µm. It ranges 25.5–310.6 µm, with average heights of 61.0–166.6 µm (see Fig. 5). Significant height differences are visible between specimens (Kruskal-Wallis test: chi-squared = 71.148, df = 7, p-value = <0.001; Figs 3, 5A). Ray height is on average higher in specimens with mixed radial pitting than with araucarian radial pitting, with mean heights of 85.5 and 107.2 µm respectively (Wilcoxon test: W = 5758, p-value = <0.001; Fig. 5B). However, the important across-specimen variability does not enable the use of this anatomical feature to distinguish between the morphogenera (Fig. 5A).

Fungal remains

One of the possible reasons for the poor preservation of the material is that the woods were already partly decayed when they were silicified. This is supported by the presence of abundant fungal remains in some of them (Fig. 6A–N). Direct evidence of fungal remains occurs in highest concentration in the rays and adjacent cells. Fungi consist of fragmented hyphae that are smooth and narrow (2–5 µm in diameter; Fig. 6A) to wider forms (≥6 µm in diameter; Fig. 6I), both types are connected (Fig. 6I) are sparsely septate (arrow in Fig. 6A; black arrow in Fig. 6E). Hyphae frequently produce perpendicular branching at uneven intervals (white arrow in Fig. 6C). Some hyphae are fractured and disarticulated (Fig. 6B; black arrow in Fig. 6C), which is likely a result of preservation. Clamp connections are rare but present (Fig. 6D). Small ellipsoidal (6–8 µm long by 3–5 µm high) to spherical propagules occur terminally (Fig. 6E) or intercalary (Fig. 6F) on hyphae, which can be dark in color (Fig. 6E) to opaque (Fig. 6F). Similar structures do co-occur, or are connected, with fungal mycelia, but it is possible that they may represent preservational artifacts (arrowheads in Fig. 6G) or possible tyloses (Fig. 6H). Like the host wood, fungal mycelia are poorly preserved and degraded (Fig. 6G, I, J_1–J_2, K), which may have happened before burial or during the taphonomic process. Wide hyphae have a rough, crystalline texture (Fig. 6J_1–J_2); it is possible that the thin, smooth hyphae could have been covered in mineral precipitates during

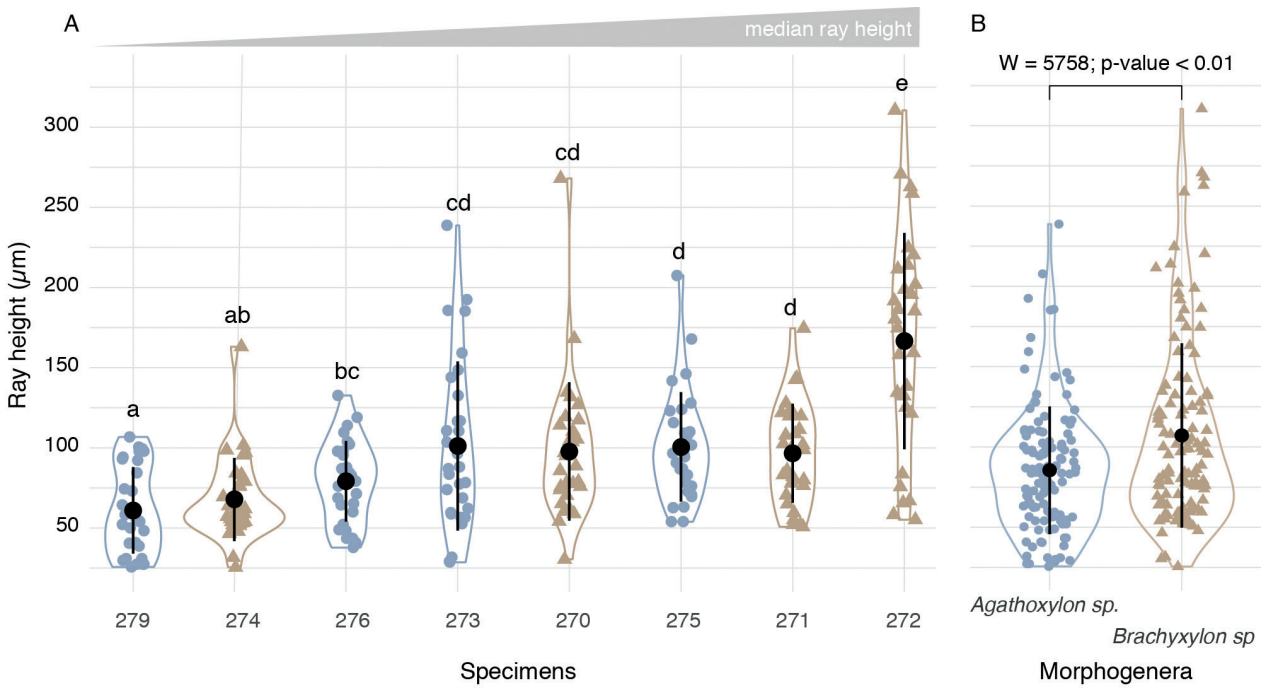

Figure 5. Ray height and pitting type in the specimens from Carapace Nunatak. Ray height across specimens and wood morphogenera (µm). Specimens with mixed (i.e., araucarian and abietinean) and araucarian radial pitting are represented by caffè latte and blue-gray colors respectively. **A.** Size group distinction between specimens based on the Multiple Comparison Kruskal-Wallis test. Groups sharing letters are not characterized by significantly different sizes. Specimens are ordered in ascending order of their median value; **B.** Average ray height within the different wood morphogenera. Significance of the mean ray height was evaluated with a Wilcoxon test. Central black dots and lines indicate means and standard deviation of ray height measurements.

preservation (arrow in Fig. 6J$_2$), and 'wide' hyphae represent a biomimetic structure. Mycelia occur in multiple orientations in radial and tangential sections and traverse from tracheid to adjacent tracheid via the pits (Fig. 6K, arrows in 6L). Indirect evidence of fungi includes areas in transverse sections of wood that are highly degraded with numerous, and large, erosional notches and cavities (Fig. 6M), which gives lumina a 'starburst'-like appearance. At higher magnification, erosional troughs are present in all wall layers in adjacent tracheids (Fig. 6N). Although it is impossible to confidently determine the systematic affinity of the fungus (or fungi because there may be multiple species co-occurring within the wood), based on presence of clamp connections, at least one of the fungi is a basidiomycete. The degradational pattern within the wood is similar to decay by some extant soft rot fungi (Schwarze 2017: see figs 52, 54–55, 62–63, 68, 70), which makes the wood soft and spongy, thus, less conducive to preservational processes and making wood anatomical features difficult to discern.

Taxonomic affinities of the woods

Philippe and Bamford (2008) published a key to Mesozoic conifer-like woods that summarizes the diversity known at that time and the characters considered significant to distinguish the different morphogenera. The new specimens from Carapace Nunatak share the following characters from Philippe and Bamford's key: (1) all rays uniseriate, except for some local biseriation, (2) radial pits never scalariform, (3) axial parenchyma present or absent, neither particularly associated with the rays nor inflated, and (4) all ray cell walls thin and smooth, unpitted. Although ray height is sometimes used to distinguish taxa, this criterion is not included in the key of Philippe and Bamford (2008) and does not seem to carry additional information in the analysis of our specimens. In addition, since the position within the whole plants of the different wood specimens from Carapace Nunatak is unknown, it is very likely that these variations represent at least in part the normal heterogeneity of wood. Differences in radial pitting on the tracheid walls are taxonomically significant and visible. They are used hereafter to distinguish two types of wood. Because of the small number of specimens and their poor and variable preservation, we choose here to only identify them at the generic level.

Specimens with araucarian pitting on radial wall of tracheids: *Agathoxylon* sp.

Within the group with araucarian pitting specimens, 273, 275, and 276 share the following characters:

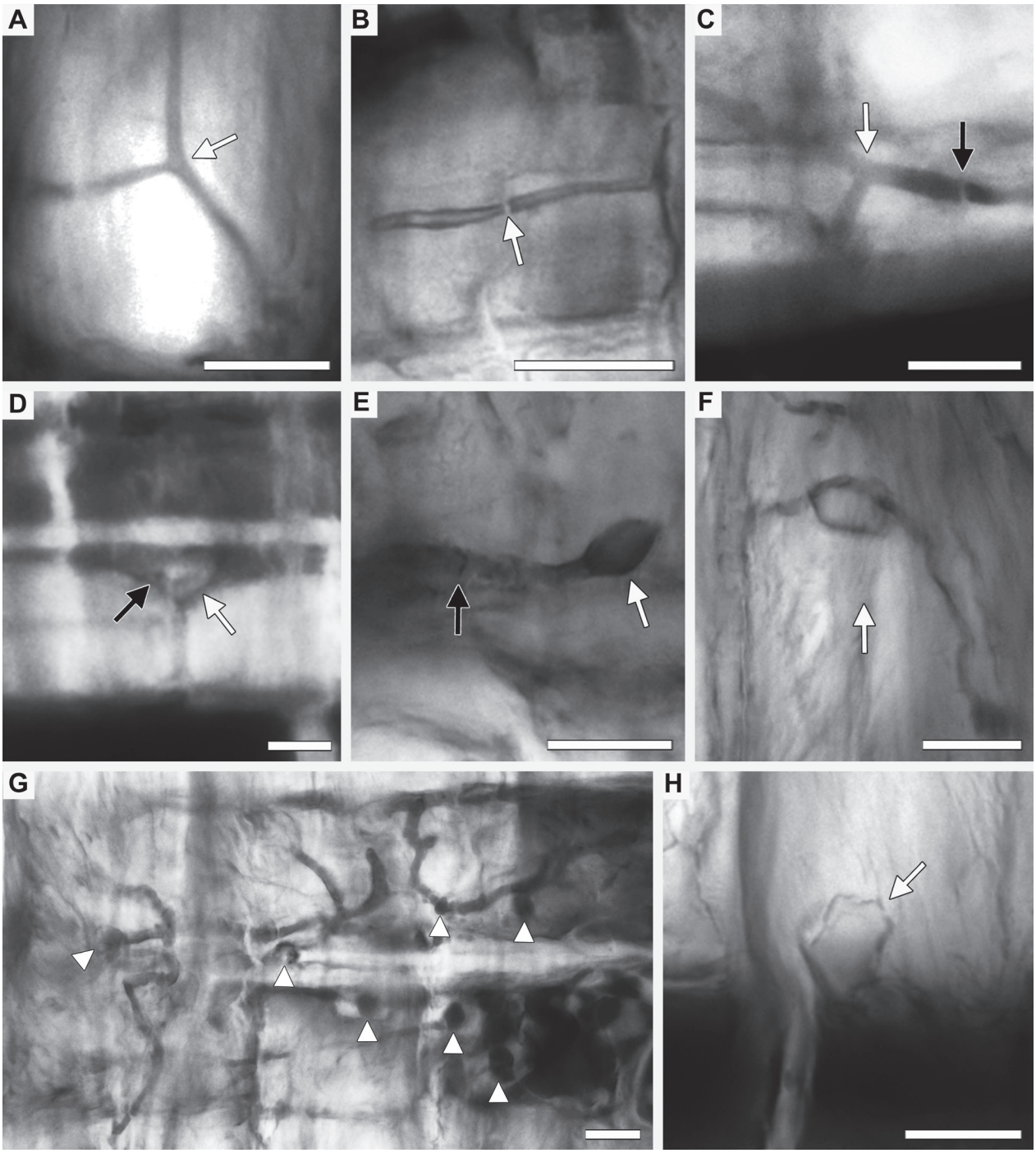

Figure 6. Fungal remains in Early Jurassic woods from Carapace Nunatak. **A.** Perpendicularly branching hyphae with septum (arrow). Slide 30780; **B.** Disarticulated hypha with single fracture. Slide 30780; **C.** Branching hypha (white arrow) with single fracture (black arrow). Slide 35923; **D.** Hypha with clamp connection. Slide 35923; **E.** Septate hypha (black arrow) with terminal propagule (white arrow). Slide 30780; **F.** Intercalary propagule (arrow). Slide 30780; **G.** Multi-branching hyphae with terminal swellings (arrow heads) in rays. Slide 35923; **H.** Ellipsoidal structure, possible tylosis (arrow). Slide 30780. Scale bars: 10 µm (**A–H**).

(1) cross-fields of the araucarian type, i.e. with numerous contiguous unordered cupressoid to taxodioid oculipores, (2) spiral thickening absent, and (3) end wall of ray cells perpendicular or subperpendicular to the ray. They are thus assigned to the genus *Agathoxylon* Hartig, 1848 (Philippe and Bamford 2008; Rößler et al. 2014 and references therein). Specimen 279 also seems to fit this diagnosis but given its poor preservation we assign it to this genus with caution. More than 400 morphospecies of *Agathoxylon* have been reported, dating from the Carboniferous to the present (Rößler et al. 2014), and *Agathoxylon*-type wood has been associated with various taxa, including cordaites, conifers, and several groups of pteridosperms. Although *Agathoxylon* is known to occur in Gondwana during the Jurassic and in Antarctica during the Cretaceous, it is the first time to the extent of our knowledge that the genus is formally reported from the Jurassic of Antarctica.

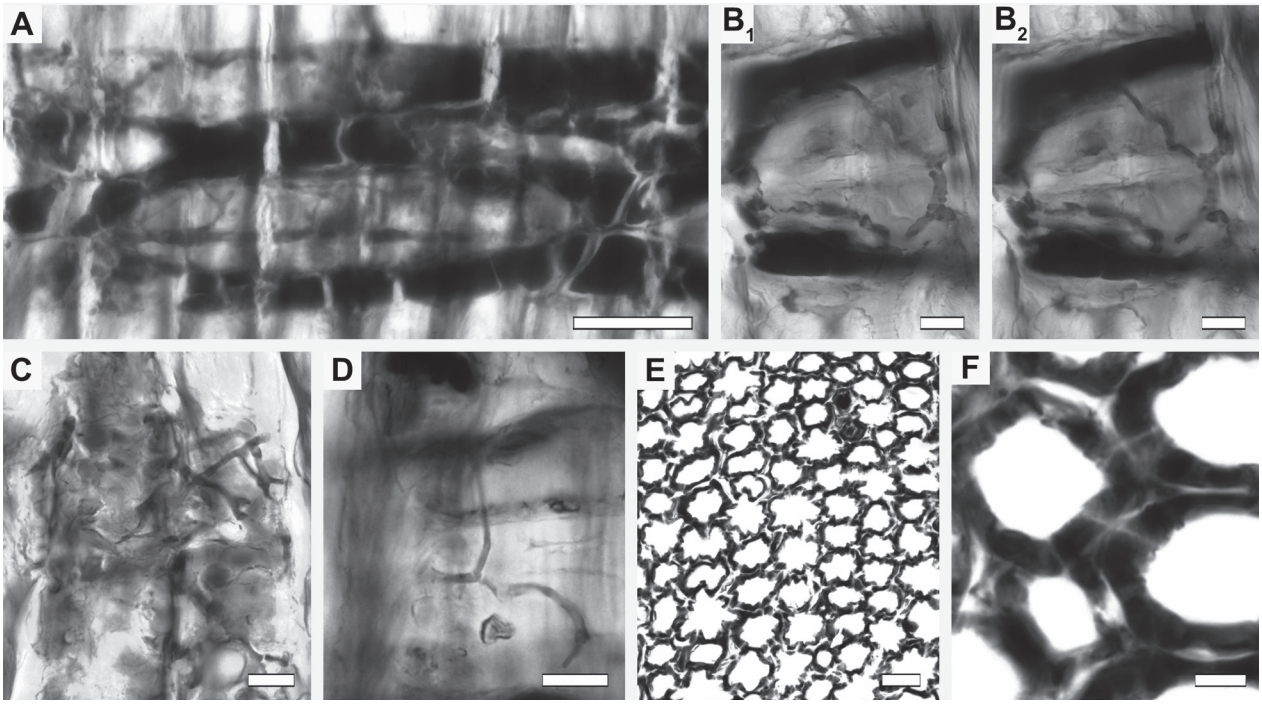

Figure 7. Fungal remains in Early Jurassic woods from Carapace Nunatak. **A.** Wide hypha with branching narrow hyphae (arrow). Slide 274 (radial B1); **B_1, B_2.** Multiple focal planes of wide hyphae; note thin structure inside of wide hypha (arrow). Slide 30780; **C.** Degraded hyphae traversing between two adjacent tracheids with abnormal Y-branch (arrow). Slide 30780; **D.** Hypha traversing through pits (arrows). Slide 30780; **E.** Highly degraded tracheids in transverse section. Note starburst pattern in lumina from multiple, and coalescing, erosional cavities. Pattern is similar to extant soft rot fungi. Slide 30781; **F.** Prominent erosional troughs in adjacent tracheids (arrows). Slide 30781. Scale bars: 50 µm (**A, E**); 10 µm (**B_1, B_2, C, D**).

Specimens with mixed pitting: *Brachyoxylon* sp.

The three specimens with mixed pitting (araucarian and abietinean; n°270, 271, 272, and 274) share the following characters: (1) in the earlywood oculipores always cupressoid, i.e. with an aperture narrower than one margin, and (2) cross-fields of the araucarian type, i.e. with contiguous unordered and often alternate oculipores. They are thus assigned to the genus *Brachyoxylon* Hollick & Jeffrey, 1909 (Philippe and Bamford 2008). *Brachyoxylon* was originally established for Late Cretaceous woods from the USA (Hollick and Jeffrey 1909). It has since been reported in Jurassic and Cretaceous localities of Europe, Asia, South America and North America (Philippe et al. 2004; Tian et al. 2018; Greppi et al. 2021 and references therein). Kurzawe and Merlotti (2010) also reported *Brachyoxylon* from the Permian of Brazil. *Brachyoxylon* wood has been linked to various conifer families, including Araucariaceae, Cupressaceae, and Hirmeriellaceae. It is, however, more frequently associated with Hirmeriellaceae remains (leaves, *Classopolis* pollen, or *Classopolis* producing cones; e.g. Alvin et al. 1981; Alvin 1982; Machhour and Pons 1992; Limarino et al. 2012; Tian et al. 2018). This is the first report of *Brachyoxylon* from the Jurassic of Antarctica. Like *Agathoxylon*, the genus is known elsewhere in Gondwana during the Jurassic (Philippe et al. 2004; Greppi et al. 2021). In Antarctica, it was only reported previously in Early Cretaceous deposits of the South Shetland Islands (Philippe et al. 1995; Torres et al. 1997).

Discussion

Comparisons with previously described Early Jurassic woods from Antarctica

The woods assigned to *Protocupressinoxylon* (= *Protobrachyoxylon* Holden, 1913 (Philippe 1993)) described by Jefferson et al. (1983) from the Mesa Range region in North Victoria Land have a distinct anatomy from the ones of Carapace Nunatak. A major difference is their cross-field pitting, with 3–6 non-contiguous cupressoid pits vs. crowded pits in the new specimens. Rays are also higher in Jefferson specimens (up to 40 cells) and axial parenchyma is absent while it occurs in some of our specimens.

The stump from Coombs Hills, Southern Victoria Land, reported by Garland et al. (2007) shares numerous characters with the woods from Carapace Nunatak, including uniseriate rays, ray cells that are thin-walled with no pits in horizontal walls, and araucarioid cross-fields with up to 9 crowded cupressoid pits (Garland et al. 2007). Radial pitting in the Coombs Hill stump consists of "mainly non-contiguous" bordered pits that are always uniseriate. Tracheid diameter is very small, 11–15 µm. Rays are slightly higher than in the Carapace Nunatak specimens, with a maximum height of 15 cells with an average height of 66 µm, i.e. 990 µm for an average ray. Garland et al. (2007) compared the stump from Comb Hills to Podocarpaceae but without indicating which character(s) they based this affinity on. Given the lack of data on the

frequency of abietinean vs. araucarian pitting on the wall of the tracheids, it is difficult to rule out a similarity with some of the new woods from Carapace Nunatak. The only notable differences are quantitative: ray height and tracheid diameter, which could have been affected by the mode of preservation, the number of rows of radial pits (which is likely linked to tracheid diameter), and the original position of the sample within the log (e.g., inner vs. outer, basal vs. apical, normal vs. reaction wood).

The specimens from Carapace Nunatak described in this paper indicate that at least three distinct wood morphotypes occurred in Victoria Land during the Early Jurassic: *Protocupressinoxylon* (= *Protobrachyoxylon* Holden), *Agathoxylon*, and *Brachioxylon*. The trunk from Coombs Hills reported by Garland might represent additional diversity. Very few wood types are reported from the high latitudes of Gondwana during the Jurassic. The cosmopolitan genus *Agathoxylon* was the only taxa listed by Philippe et al. (2004) in their cold temperate region -which included Antarctica- for the Early Jurassic, based on specimens from Australia. Reports are also extremely scarce for the Middle and Late Jurassic. This low diversity is to be compared with, for example, what is reported in the same region during the Cretaceous, when at least 6 wood morphogenera are present in the high-latitude belt: *Agathoxylon*, *Araucariopitys*, *Circoporoxylon*, *Podocarpoxylon*, *Protocircoporoxylon*, and *Taxodioxylon* (Philippe et al. 2004). The small number of wood morphotaxa in the Jurassic of Antarctica could be caused by a variety of factors, including paleoenvironmental constraints (climate, strong volcanism) and limited sampling. It is indeed important to consider that, while the presence of fossil wood is often mentioned in field reports, it is rarely sampled as extensively as other plant organs for which the presence of various genera can be assessed directly in the field, such as leaves or reproductive structures. In addition, among the sampled specimens, only a few have been the subject of taxonomic studies. The apparent scarcity of Jurassic woods in Antarctica is thus at least in part due to a collecting/study bias, a situation already reported for Triassic woods from this region (Oh et al. 2016).

Early Jurassic conifers in Antarctica

The new woods from Carapace Nunatak supports the evidence provided by other types of plant fossils regarding the presence of several groups of conifers in the Early Jurassic of Antarctica. In North Victoria Land, gymnosperm material occurring in the Early Jurassic Shafer Peak Fm includes conifers' remains with the voltzialean bract-scale complex *Schizolepis* and three types of foliage with preserved cuticle assigned to cf. *Allocladus*, cf. *Elatocladus*, and cf. *Pagiophyllum* (Bomfleur et al. 2011). In South Victoria Land, the presence at Carapace Nunatak of wood assignable to *Brachyoxylon* further supports the presence of the Hirmeriellaceae, already documented by abundant *Classopolis* pollen (e.g. Bomfleur et al. 2014) and the permineralized Hirmeriellaceae pollen cone *Classostrobus elliotii* (Hieger et al. 2015). While *Agathoxylon* is a wood known to occur in a wide range of gymnosperm taxa, it is interesting to note that it is found in Araucariaceae and Voltziales (Philippe, 2011). It is thus possible that the *Agathoxylon* specimens from Carapace Nunatak are linked to the plant that produced *Chimaerostrobus minutus*, a pollen cone with a combination of characters reminiscent of these two groups of conifers (Atkinson et al. 2018).

Conclusions

The scarcity of information available on Early Jurassic environments of Antarctica suggests the presence of a vegetation dominated by conifers belonging to the Araucariaceae, Hirmeriellaceae, and possibly Podocarpaceae, with an understory of ferns and seed plants including Benettitales, Caytoniales and Peltaspermales (Bomfleur et al. 2011). The new fossil woods from Carapace Nunatak constitute, to the extent of our knowledge, the first report of *Agathoxylon* and *Brachyoxylon* in Antarctica and further support the presence of several groups of conifers. This is especially important considering that modern conifer clades including the Podocarpaceae, Cupressaceae, Araucariaceae, and Taxaceae diverged and diversified during the Late Triassic–Early Jurassic period (e.g. Rothwell et al. 2012; Leslie et al. 2018; Contreras et al. 2019 and references in these papers). In addition to a better reconstruction of Early Jurassic floras and environments, new studies of fossil woods from Antarctica will undoubtedly contribute to our understanding of conifer evolution during this key period.

Data availability

The specimens described in this paper and the 65 corresponding thin-sections are part of the Division of Paleobotany collections, Biodiversity Institute, University of Kansas, Lawrence, USA. They are accessible under specimen field numbers 272–279 and slide accession numbers 30,775–30,796 (large slides) and 35,911–35,938 (small slides). See supplements for the detailed slide list with accession numbers and the ray size measurements.

Author contributions

This work was conducted during AT's 1st year of MSc project at UMR AMAP in 2016. AT prepared the specimens and performed the measurements, observations, and systematic comparisons. ALD supervised the project and contributed expertise of fossil wood anatomy and Antarctic floras. CJH contributed expertise on fossil fungi and plant-fungi interactions. RS contributed expertise on fossil conifers and handled specimen access and curation. All authors have provided critical inputs and feedback, contributed significantly to the manuscript, and accepted the final version.

Competing interests

The authors declare that they have no conflict of interest.

Acknowledgements

We warmly thank the other members of the 2014–2015 G-496 team: Drew Brown, Dave Buchanan, Charles Daghlian, Ignacio Escapa, Erik Gulbranson, Lauren Michel, and Ana Zajivciek for their help in the field. This study would not have been possible without the US Antarctic Program pilots and helo techs who flew us to the capricious place that is Carapace Nunatak, and among them we are especially grateful to Rebecca Voltin (Lyons, OR, USA) who also found one of the first and best-preserved specimens presented in this paper. We thank the anonymous reviewer and Alexander Schmidt for their constructive comments, and editorial handling. This work was partially funded by an award from the US National Science Foundation (#1142495) to Edith L. Taylor (Lawrence, KS, USA), who we thank for her mentorship and support. AMAP (botAny and Modelling of Plant Architecture and vegetation) is a joint research unit that associates Montpellier University, CNRS (UMR 5120), CIRAD (UMR51), INRAe (UMR931) and IRD (UR123). Finally, AT thanks Sandrine Escobar and Morgane Ganault for their help on Fig. 2.

References

Alvin KL (1982) Cheirolepidiaceae: Biology, structure and paleoecology. Review of Palaeobotany and Palynology 37: 71–98. https://doi.org/10.1016/0034-6667(82)90038-0

Alvin KL, Fraser CJ, Spicer RA (1981) Anatomy and palaeoecology of *Pseudofrenelopsis* and associated conifers in the English Wealden. Palaeontology 24: 759–778. https://www.palass.org/publications/palaeontology-journal/archive/24/4/article_pp759-778

Atkinson BA, Serbet R, Hieger TJ, Taylor EL (2018) Additional evidence for the Mesozoic diversification of conifers: Pollen cone of *Chimaerostrobus minutus* gen. et sp. nov. (Coniferales), from the Lower Jurassic of Antarctica. Review of Palaeobotany and Palynology 257: 77–84. https://doi.org/10.1016/j.revpalbo.2018.06.013

Ball HW, Borns Jr HW, Hall BA, Brooks HK, Carpenter FM, Delevoryas T (1979) Biota, age, and significance of lake deposits, Carapace Nunatak, Victoria Land, Antarctica. In: Laskar B, Rao CSR (Eds) Fourth International Gondwana Symposium: Papers (Vol. 1). Hindustan Publishing Corporation, New Delhi, 166–175. https://www.coldregions.org/vufind/Record/156115

Ballance PF, Watters WA (1971) The Mawson Diamictite and the Carapace Sandstone, formations of the Ferrar Group at Allan Hills and Carapace Nunatak, Victoria Land, Antarctica. New Zealand Journal of Geology and Geophysics 14: 512–527. https://doi.org/10.1080/00288306.1971.10421945

Bomfleur B, Pott C, Kerp H (2011) Plant assemblages from the Shafer Peak Formation (Lower Jurassic), north Victoria Land, Transantarctic Mountains. Antarctic Science 23: 188–208. https://doi.org/10.1017/S0954102010000866

Bomfleur B, Schöner R, Schneider JW, Viereck L, Kerp H, McKellar JL (2014) From the Transantarctic Basin to the Ferrar Large Igneous Province–New palynostratigraphic age constraints for Triassic–Jurassic sedimentation and magmatism in East Antarctica. Review of Palaeobotany and Palynology 207: 18–37. https://doi.org/10.1016/j.revpalbo.2014.04.002

Bradshaw MA (1987) Additional field interpretation of the Jurassic sequence at Carapace Nunatak and Coombs Hills, south Victoria Land Antarctica. New Zealand Journal of Geology and Geophysics 30: 37–49. https://doi.org/10.1080/00288306.1987.10422192

Cantrill DJ, Poole I (2012) The Vegetation of Antarctica Through Geological Time. Cambridge University Press, Cambridge. https://doi.org/10.1017/CBO9781139024990

Contreras DL, Escapa IH, Iribarren RC, Cúneo NR (2019) Reconstructing the Early Evolution of the Cupressaceae: A Whole-Plant Description of a New *Austrohamia* Species from the Cañadón Asfalto Formation (Early Jurassic), Argentina. International Journal of Plant Sciences 180: 834–868. https://doi.org/10.1086/704831

del Valle RA, Lirio JM, Lusky JC, Morelli JR, Nuñez HJ (1997) Jurassic trees at Jason Peninsula, Antarctica. Antarctic Science 9: 443–444. https://doi.org/10.1017/S0954102097000576

Doweld AB (2020) The controversial nomenclature of the fossil plant names *Cheirolepis*, *Cheirolepidium* and *Hirmeriella* (Cheirolepidaceae/Cheirolepidiaceae/Hirmeriellaceae). Taxon 69: 1092−1098. https://doi.org/10.1002/tax.12287

Elliot DH (2013) The geological and tectonic evolution of the Transantarctic Mountains: a review. Geological Society, London, Special Publications 381: 7–35. https://doi.org/10.1144/SP381.14

Falcon-Lang HJ, Cantrill DJ (2001) Leaf phenology of some mid-Cretaceous polar forests, Alexander Island, Antarctica. Geological Magazine 138: 39–52. https://doi.org/10.1017/S0016756801004927

Francis JE (1986) Growth rings in Cretaceous and Tertiary wood from Antarctica and their palaeoclimatic implications. Paleontology 29: 665–684. https://www.palass.org/publications/palaeontology-journal/archive/29/4/article_pp665-684

Francis JE, Hill RS (1996) Fossil plants from the Pliocene Sirius Group, Transantarctic Mountains: Evidence for climate from growth rings and fossil leaves. Palaios 11: 389–396. https://doi.org/10.2307/3515248

Fox J, Weisberg S (2019) An {R} Companion to Applied Regression, 3rd Edn. Thousand Oaks CA: Sage. https://socialsciences.mcmaster.ca/jfox/Books/Companion

Garland MJ, Bannister JM, Lee DE, White JDL (2007) A coniferous tree stump of late Early Jurassic age from the Ferrar Basalt, Coombs Hills, southern Victoria Land, Antarctica. New Zealand Journal of Geology and Geophysics 50: 263–269. https://doi.org/10.1080/00288300709509836

Greppi CD, Pujana RR, Umazano AM, Bellosi ES (2021) Early Cretaceous *Brachyoxylon* woods from argentinean Patagonia and comments on the Cheirolepidiaceae distribution. Journal of South American Earth Sciences 106: e103050. https://doi.org/10.1016/j.jsames.2020.103050

Gulbranson EL, Ryberg PE, Decombeix A-L, Taylor EL, Taylor TN, Isbell JL (2014) Leaf habit of Late Permian *Glossopteris* trees from high-palaeolatitude forests. Journal of the Geological Society 171: 493–507. https://doi.org/10.1144/jgs2013-127

Harper CJ, Bomfleur B, Decombeix A-L, Taylor EL, Taylor TN, Krings M (2012) Tylosis formation and fungal interactions in an Early Jurassic conifer from northern Victoria Land, Antarctica. Review of Palaeobotany and Palynology 175: 25–31. https://doi.org/10.1016/j.revpalbo.2012.02.006

Hartig T (1848) Beiträge zur Geschichte der Pflanzen und zur Kenntnis der norddeutschen Braunkohlen-Flora. Botanische Zeitung 6: 122–128. [137–141, 166–172 and 185–190.]

Hass H, Rowe NP (1999) Thin sections and wafering. In: Jones TP, Rowe NP (Eds) Fossil Plants and Spores: Modern Techniques. The Geological Society, London, 76–81.

Hieger TJ, Serbet R, Harper CJ, Taylor TN, Taylor EL, Gulbranson EL (2015) Cheirolepidiaceous diversity: an anatomically preserved pollen cone from the Lower Jurassic of southern Victoria Land, Antarctica. Review of Palaeobotany and Palynology 220: 78–87. https://doi.org/10.1016/j.revpalbo.2015.05.003

Holden R (1913) Contributions to the anatomy of Mesozoic conifers. No. I. Jurassic coniferous woods from Yorkshire. Annals of Botany 27: 533–545. https://doi.org/10.1093/oxfordjournals.aob.a089473

Hollick CA, Jeffrey EC (1909) Studies of Cretaceous coniferous remains from Kreischerville, New York. Memoirs of the New York Botanical Garden 3: 1–137. https://doi.org/10.5962/bhl.title.44790

Jefferson TH, Siders MA, Haben MA (1983) Jurassic trees engulfed by lavas of the Kirkpatrick Basalt group, northern Victoria Land. Antarctic Journal of the United States 18: 14–16. https://s3.amazonaws.com/Antarctica/AJUS/AJUSvXVIIIn1.pdf

Kellogg DW, Taylor EL (2004) Evidence of oribatid mite detritivory in Antarctica during the late Paleozoic and Mesozoic. Journal of Paleontology 78: 1146–1153. https://doi.org/10.1666/0022-3360(2004)078<1146:EOOMDI>2.0.CO;2

Kräusel R (1962) Antarctic fossil wood. In: Plumstead EP (Ed.) Fossil floras of Antarctica: 133–140. Transantarctic expedition (1955–1958) scientific reports No. 9. Transantarctic expedition committee, London.

Kurzawe F, Merlotti S (2010) O complexo *Dadoxylon-Araucarioxylon*, Carbonífero e Permiano do Gondwana: estudo taxonômico do gênero *Araucarioxylon*. Pesquisas em Geociências 37: 41–50. https://doi.org/10.22456/1807-9806.17720

Leslie AB, Beaulieu J, Holman G, Campbell CS, Mei W, Raubeson LR, Mathews S (2018) An overview of extant conifer evolution from the perspective of the fossil record. American Journal of Botany 105: 1531–1544. https://doi.org/10.1002/ajb2.1143

Limarino CO, Passalia MG, Llorens M, Vera EI, Loinaze VSP, Césari SN (2012) Depositional environments and vegetation of Aptian sequences affected by volcanism in Patagonia. Palaeogeography, Palaeoclimatology, Palaeoecology 323–325: 22–41. https://doi.org/10.1016/j.palaeo.2012.01.021

Machhour L, Pons D (1992) Bois de coniférales dans l'Albien du synclinal du Beausset (Var, SE France): Signification paléogéographique et paléoclimatique. Geobios 25: 181–193. https://doi.org/10.1016/S0016-6995(06)80394-3

Mendiburu F de (2020) Agricolae: Statistical Procedures for Agricultural Research. R package version 1.3-3. https://CRAN.R-project.org/package=agricolae

Miller MF, Knepprath NE, Cantrill DJ, Francis JE, Isbell JL (2016) Highly productive polar forests from the Permian of Antarctica. Palaeogeography, Palaeoclimatology, Palaeoecology 441: 292–304. https://doi.org/10.1016/j.palaeo.2015.06.016

Oh C, Park T-YS, Woo J, Bomfleur B, Philippe M, Decombeix A-L, Kim Y-HG, Lee JI (2016) Triassic *Kykloxylon* wood (Umkomasiaceae, Gymnospermopsida) from Skinner Ridge, northern Victoria Land, East Antarctica. Review of Palaeobotany and Palynology 233: 104–114. https://doi.org/10.1016/j.revpalbo.2016.07.006

Paclt J (2011) Proposal to conserve the name Cheirolepidaceae (fossil Coniferales). Taxon 60(4): e1219. https://doi.org/10.1002/tax.604031

Philippe M (1993) Nomenclature générique des trachéidoxyles fossiles mésozoïques à champs araucarioïdes. Taxon 42: 74–80. https://doi.org/10.2307/1223305

Philippe M (2011) How many species of *Araucarioxylon*? Comptes Rendus Palevol 10: 201–208. https://doi.org/10.1016/j.crpv.2010.10.010

Philippe M, Bamford MK (2008) A key to morphogenera used for Mesozoic conifer-like woods. Review of Palaeobotany and Palynology 148: 184–207. https://doi.org/10.1016/j.revpalbo.2007.09.004

Philippe M, Bamford M, McLoughlin S, Alves LSR, Falcon-Lang HJ, Gnaedinger S, Ottone EG, Pole M, Rajanikanth A, Shoemaker RE, Torres T, Zamuner A (2004) Biogeographic analysis of Jurassic–Early Cretaceous wood assemblages from Gondwana. Review of Palaeobotany and Palynology 129: 141–173. https://doi.org/10.1016/j.revpalbo.2004.01.005

Philippe M, Torres T, Barale G, Thévenard F (1995) President Head, Snow Island, South Shetland, a key-point for Antarctic Mesozoic palaeobotany. Comptes Rendus de l'Académie des Sciences Paris, série IIa 321: 1055–1061. https://gallica.bnf.fr/ark:/12148/bpt6k64102286/f129.item

R Core Team (2020) R: A language and environment for statistical computing. R Foundation for Statistical Computing, Vienna. https://www.R-project.org/

Rößler R, Philippe M, van Konijnenburg-van Cittert JHA, McLoughlin S, Sakala J, Zijlstra G, Annamraju R, Ash S, Baas P, Bamford M, Bateman R, Booi M, Boonchai N, Brea M, Crisafulli A, Decombeix A-L, Dolezych M, Dutra T, Esteban LG, Falaschi P, Falcon-Lang H, Feng Z, Gnaedinger S, Guerra Sommer M, Harland M, Herbst R, Hilton J, Iamandei E, Iamandei S, Jiang H-H, Jiang Z, Kim K, van Konijnenburg-van Cittert J, Kunzmann L, Kurzawe F, McLoughlin S, Merlotti S, Meyer-Berthaud B, Naugolnykh S, Nishida H, Oh C, Orlova O, Palacios P de, Philippe M, Pole M, Poole I, Pujana R, Rößler R, Ryberg P, Sakala J, Savidge R, Schultka S, Süß H, Taylor E, Terada K, Thévenard F, Torres T, Vera E, Wheeler E, Yang X, Zijlstra G, Zheng S, Zhang W (2014) Which name(s) should be used for *Araucaria*-like fossil wood?–Results of a poll. Taxon 63: 177–184. https://doi.org/10.12705/631.7

Rothwell GW, Mapes G, Stockey RA, Hilton J (2012) The seed cone *Eathiestrobus* gen. nov.: Fossil evidence for a Jurassic origin of Pinaceae. American Journal of Botany 99: 708–720. https://doi.org/10.3732/ajb.1100595

Schwarze FWMR (2017) Wood decay under the microscope. Fungal Biology Reviews 21: 133–170. https://doi.org/10.1016/j.fbr.2007.09.001

Shen Y (1994) Jurassic conchostracans from Carapace Nunatak, southern Victoria Land, Antarctica. Antarctic Science 6: 105–113. https://doi.org/10.1017/S0954102094000131

Taylor EL, Ryberg PE (2007) Tree growth at polar latitudes based on fossil tree ring analysis. Palaeogeography, Palaeoclimatology, Palaeoecology 255: 246–264. https://doi.org/10.1016/j.palaeo.2007.06.013

Taylor TN, Taylor EL, Krings M (2009) Paleobotany. The Biology and Evolution of Fossil Plants. Academic Press, San Diego.

Thévenard F, Chernomorets O, Moreau J-D, Neraudeau D, Philippe M (2022) A review of the Hirmeriellaceae (Cheirolepidiaceae) wood. IAWA Journal 43(4): 428–447. https://doi.org/10.1163/22941932-bja10099

Tian N, Zhu Z-P, Wang Y-D, Wang S-C (2018) Occurrence of *Brachyoxylon* Hollick et Jeffrey from the Lower Cretaceous of Zhejiang Province, southeastern China. Journal of Palaeogeography 7: 1–8. https://doi.org/10.1186/s42501-018-0008-0

Torres T, Barale G, Meon H, Philippe M, Thévenard F (1997) Cretaceous floras from Snow Island (South Shetland Islands, Antarctica) and their biostratigraphic significance. In: Ricci CA (Ed.) The Antarctic Region: Geological Evolution and Processes. Terra Antarctica Publication, Siena, 1023–1028.

Torres T, Galleguillos H, Philippe M (2000) Maderas fosiles en el Monte Flora, Bahia Esperanza, Peninsula Antartica. Actas 9° Congreso geologico chileno, 1-4 agosto, Puerto Varas 2: 386–390.

Townrow JA (1967a) Fossil plants from Allan and Carapace Nunataks, and from the upper Mill and Shackleton Glaciers, Antarctica. New Zealand Journal of Geology and Geophysics 10: 456–473. https://doi.org/10.1080/00288306.1967.10426750

Townrow JA (1967b) Conifer from the Jurassic of east Antarctica. Papers and Proceedings of the Royal Society of Tasmania 101: 137–149. https://eprints.utas.edu.au/14261/

Supplementary material 1

Table with ray height measurments for the different specimens

Authors: Agathe Toumoulin, Anne-Laure Decombeix, Carla J. Harper, Rudolph Serbet

Data type: table (excel file)

Copyright notice: This dataset is made available under the Open Database License (http://opendatacommons.org/licenses/odbl/1.0). The Open Database License (ODbL) is a license agreement intended to allow users to freely share, modify, and use this Dataset while maintaining this same freedom for others, provided that the original source and author(s) are credited.

Link: https://doi.org/10.3897/fr.26.102570.suppl1

Fossil Record 26 (1) 2023, 117–133 | DOI 10.3897/fr.26.102128

The helochelydrid turtle *Helochelydra nopcsai* from the Early Cretaceous (late Barremian – early Aptian) fissure fills of Balve, North Rhine-Westphalia, Germany, including a large sample of granicones

Walter G. Joyce[1], Serjoscha W. Evers[1], Sara Ren[1], Yann Rollot[1], Achim H. Schwermann[2]

1 *Department of Geosciences, University of Fribourg, 1700 Fribourg, Switzerland*
2 *LWL-Museum of Natural History, Westphalian State Museum and Planetarium, 48161 Münster, Germany*

https://zoobank.org/141AAAE3-8F1D-4117-A64B-D240B6BDF660

Corresponding author: Walter G. Joyce (walter.joyce@unifr.ch)

Academic editor: Torsten Scheyer ♦ **Received** 17 February 2023 ♦ **Accepted** 9 May 2023 ♦ **Published** 2 June 2023

Abstract

Early Cretaceous (late Barremian – early Aptian) fissure fill deposits near Balve, North Rhine Westphalia, Germany, have yielded a rich continental vertebrate fauna over the course of the last two decades. More than 250 fragmentary specimens, including more than 150 osteoderms (i.e., granicones), represent the late Early Cretaceous helochelydrid *Helochelydra nopcsai*, which had previously been reported from the UK, France, and Spain. The new material mostly differs from that from the type section by exhibiting a reduced to absent entoplastral scute and by displaying distinct cranial scute sulci, both of which are interpreted as intraspecific variation. Although morphological insights are limited, the new material reveals that the visceral cavity extends anteriorly and posteriorly to the bridge, a relatively novel feature previously reported for an eclectic mix of compsemydids, pleurosternids, and other helochelydrids. The available sample of granicones reveals great shape diversity, but a morphometric analysis concludes that no distinct morphotypes exist.

Key Words

granicones, *Helochelydridae*, *Testudinata*

Introduction

Helochelydra nopcsai is a helochelydrid turtle from the Lower Cretaceous of Europe (Joyce, 2017). The type specimen, NHMUK R171, a fragmented shell and associated girdles from the Early Cretaceous (Barremian) Wessex Formation of the Isle of Wight, England, was originally described by Nopcsa (1928) as a new taxon, but only given the genus name *Helochelydra*. Nopcsa (1928) realized that rare turtles from the Cretaceous of Europe and North America, including the German *Helochelys danubina* Meyer, 1855 and the North American *Naomichelys speciosa*, are unified by a highly unusual shell surface texture consisting of pin-like tubercles, a grouping for which he proposed the name Helochelydrinae. Nopcsa (1928) provided a relatively detailed description of NHMUK R171, but the associated figures insufficiently document the apparent morphology. As the ICZN (1999) demands that all valid genera include at least one named species, Lapparent de Broin and Murelaga (1999) many decades later named the new species *Helochelydra nopcsai*, which is based on NHMUK R171 as well and now serves as the type species of *Helochelydra*.

Joyce et al. (2011) more recently provided description of IWCMS 1998.21, a nearly complete cranium and associated postcranial fragments from the Wessex Formation of the Isle of Wight, England, which they referred to as *Helochelydra nopcsai* based on apparent similarities in shell surface texture and its provenience from the type formation. As fragmentary helochelydrids had been reported from numerous localities across Europe in the previous decades, Joyce et al. (2011) also provided a taxonomic review of

Copyright *Walter G. Joyce et al.* This is an open access article distributed under the terms of the Creative Commons Attribution License (CC BY 4.0), which permits unrestricted use, distribution, and reproduction in any medium, provided the original author and source are credited.

the group that focused on shell surface texture, as this is the only characteristic that can be studied in fragmentary shell material. This review concluded that many specimens are known from across the Cretaceous of Europe that show a surface texture similar to that of *Helochelydra nopcsai*, but also that it is prudent to restrict this taxon to the Early Cretaceous (Barremian) Wessex Formation and its correlates. Following this recommendation, Joyce (2017) attributed fragmentary material from the Early Cretaceous (Hauterivian/Barremian) of France (Néraudeau et al. 2012) and the Early Cretaceous (Barremian) of Spain (Pérez García 2009; Pérez-García et al. 2012, 2013; Scheyer et al. 2015) to *Helochelydra nopcsai*, thereby extending the range of this taxon across western Europe.

The evolutionary relationships of helochelydrids with other turtles are not fully understood. Although early phylogenetic assessments of the group differed with regard to placing helochelydrids as stem-cryptodires (Hirayama et al. 2000) or stem-turtles (Joyce et al. 2011), this was largely due to the variable interpretation of multiple relatively closely related turtle clades with a Mesozoic origination as either crown or stem turtles. Since then, most studies interpret these clades (e.g., meiolaniforms, paracryptodires) as perichelydian stem turtles (e.g., Joyce 2017). Latest studies agree that helochelydrids are placed more crownwardly than meiolaniforms or sichuanchelyids (e.g., Joyce et al. 2016; Rollot et al. 2021, 2022a, b; Tong et al. 2022, 2023), although it is not clear if they represent an evolutionary lineage distinct from other clades (Joyce et al. 2016; Tong et al. 2022, 2023), or if they constitute a subclade of paracryptodires (Rollot et al. 2021, 2022a, b).

In addition to the unusual shell surface texture and several cranial and postcranial characteristics (e.g., Rollot et al. 2022b), at least some helochelydrids are characterized by the presence of textured osteoderms called granicones (Owen, 1878). These elements had initially been collected in isolation from Early Cretaceous (Berriasian) sediments of the English Purbeck Limestone Formation, but their identity as helochelydrid osteoderms had not been established until they were found associated with the near complete skeleton of the North American helochelydrid *Naomichelys speciosa* (Barret et al. 2002; Joyce et al. 2014). A single granicone had previously been reported from the Wessex Formation of the Isle of Wight (Sweetman, 2007), which likely represent *Helochelydra nopcsai* (Joyce et al. 2011; Joyce 2017), but as the turtle fauna from this formation remains poorly known, this association remains tentative for the moment.

In the Busche quarry near Balve-Beckum, North Rhine Westphalia, Germany, mining operations have cut into a cave system whose origin can be traced back to deep hydrothermal karst. The cavities are completely filled with late Early Cretaceous (late Barremian–early Aptian) sediments, which have yielded a rich vertebrate fauna, including turtles, still being excavated and evaluated at present (Schwermann et al. 2018). Only a few larger objects (up to a maximum of 30 cm) have been found to date. Work so far has mainly focused on isolated theropod teeth (Lanser and Heimhofer 2015), salamanders (Skutschas et al, 2020), sauropods (Hornung et al. 2023), and mammals (Martin et al. 2021, 2022). A preliminary analysis of several hundred turtle fragments from this quarry highlights the presence of more than 200 isolated specimens, including more than 150 granicones, that can be attributed to *Helochelydra nopcsai*. The primary goal of this contribution is to describe this material and to discuss its attribution to *Helochelydra nopcsai*. The remainder of the turtle fauna, which preliminarily is thought to include *Chitracephalus dumonii*, *Peltochelys duchastelii*, and a new species of pleurosternid, will be provided elsewhere.

Institutional abbreviations: **IWCMS**, Dinosaur Isle Museum, Sandown, United Kingdom; **NHMUK**, Natural History Museum, London, United Kingdom; **WMNM**, **LWL**-Museum of Natural History, Münster, Germany.

Materials and methods

Geological settings

The Busche Quarry is located just to the northeast of the village of Beckum within the commune of Balve, North Rhine-Westphalia, Germany (Fig. 1). The rock being quarried there is a Devonian limestone, which is punctured by fissures filled with sand rich clays (Lanser and Heimhofer 2015). Palynological evidence suggests that the fissures were filled during the late Barremian to early Aptian (Lanser and Heimhofer 2015). Most of the *Helochelydra nopcsai* remains presented herein were collected over the course of the last 20 years from two distinct fissures, of which the smaller one is a relatively narrow passage no more than 4 m wide, while the large one represents a large cavern that may reach 35 m in diameter. All specimens can therefore be traced back to a spatially confined area. As the turtle fauna appears homogenous across the fossiliferous deposits and as systematic collecting failed to find plausible associations among elements, we here treat the fauna as being homogeneous, while acknowledging that it may be affected by time averaging. Specimens range from black to tan in color, reflecting variation in mineral overgrowth and weathering (Fig. 2).

Visualization

A fragment of a left parietal and a selection of the best-preserved carapace and shell fragments and granicones were subjected to scanning at the CT Image Core Facility of the Department of Geosciences, University of Fribourg, using a microcomputed tomography (µCT) scanner Bruker Skyscan 2211. Three scanning sessions were performed for the granicones. The first scan was performed with a voltage of 110 kV, a current of 475 µA, an exposure of 120 ms, and a titanium filter, resulting in 4279 coronal slices with a voxel size of 12 µm. The second scan was performed with a voltage of 110 kV, a current of 450 µA, an exposure of 120 ms, and a titanium filter, resulting in 4743 coronal slices with a voxel size of 12 µm. The third granicone scan was performed with

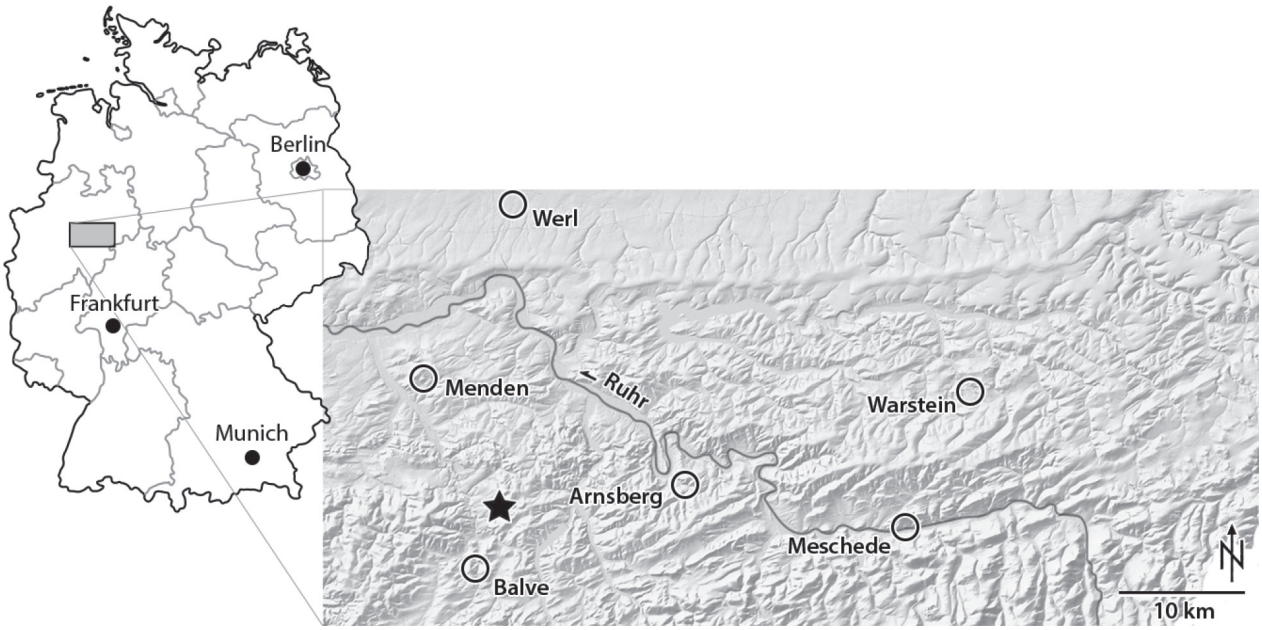

Figure 1. A simplified map of Germany highlighting location of the Busche quarry (black star) near Balve, North Rhine Westphalia, Germany.

a voltage of 110 kV, a current of 450 µA, an exposure of 50 ms, and a titanium filter, resulting in 3750 coronal slices with a voxel size of 12 µm. The scanning of the carapace and shell fragments required 4 scanning sessions. The first scan was performed with a voltage of 190 kV, a current of 210 µA, an exposure of 200 ms, and a molybdenum filter. The second scan was performed with a voltage of 190 kV, a current of 95 µA, an exposure of 180 ms, and a molybdenum filter. The third scan was performed with a voltage of 189 kV, a current of 600 µA, an exposure of 220 ms, and a molybdenum filter. The fourth scan was performed with a voltage of 190 kV, a current of 95 µA, an exposure of 220 ms, and a molybdenum filter. A total of 1997, 2230, 2079, and 3150 coronal slices were obtained, respectively, all with a voxel size of 45 µm. The left parietal fragment was scanned separately, with a voltage of 110 kV, a current of 450 µA, an exposure of 37 ms, and a titanium filter, resulting in 2110 coronal slices with a voxel size of 31 µm.

All specimens were segmented in Amira 3D (2021.2; https://www.fei.com/software) using the magic wand tool. The 3D models were exported as .ply files and visualized in Meshlab (2022.02; https://www.meshlab.net). All models are available at MorphoSource (https://www.morphosource.org/projects/000497160).

Morphometric analysis

A qualitative assessment of all available granicones suggested that three informal morphotypes can be recognized: cone-shaped granicones, hook-shaped granicones with offset apices, and flat, plate-like granicones (see Description below). We used Principal Components Analysis (PCA) to investigate if the pre-assigned morphotypes form separate clusters in morphospace. For this purpose, we took four basic measurements from the 136 best preserved granicones: the maximum length of the base, the minimum width of the base, height of the apex, and offset of the apex relative to the center of the base. All measurements were taken in right angles relative to another using digital calipers with an accuracy to 1/100 of a millimeter (see Suppl. material 1 for data). We conducted a PCA using the prcomp function in R 4.2.2 (R Core Team 2022). Specimens were scaled to have unit variance before analysis. We calculated re-scaled proportions of variance explained for PC2–4 to the exclusion of PC1, as the latter was associated with size.

Systematic paleontology

***Testudinata* Klein, 1760**
***Helochelydridae* Chkhikvadze, 1970**

***Helochelydra nopcsai* Lapparent de Broin & Murelaga, 1999**

Type material. NHMUK R171 (holotype), a fragmentary shell associated with limb and girdle elements (Nopcsa 1928).

Type locality. Isle of Wight, United Kingdom (Nopcsa, 1928).

Type stratum. Wessex Formation, Wealden Group, Barremian, Early Cretaceous (Joyce et al. 2011).

Diagnosis. *Helochelydra nopcsai* can most easily be diagnosed as a helochelydrid by the presence of a secondary pair of occipital tubercles that are formed by the pterygoids, a triangular fossa that is formed by the squamosal at the posterior margin of the skull, a shell covered by a surface texture consisting of distinct tubercles, expansion of the visceral cavity to the front and back of the peripheral series (also present in some compsemydids and pleurosternids), and presence of an entoplastral scute.

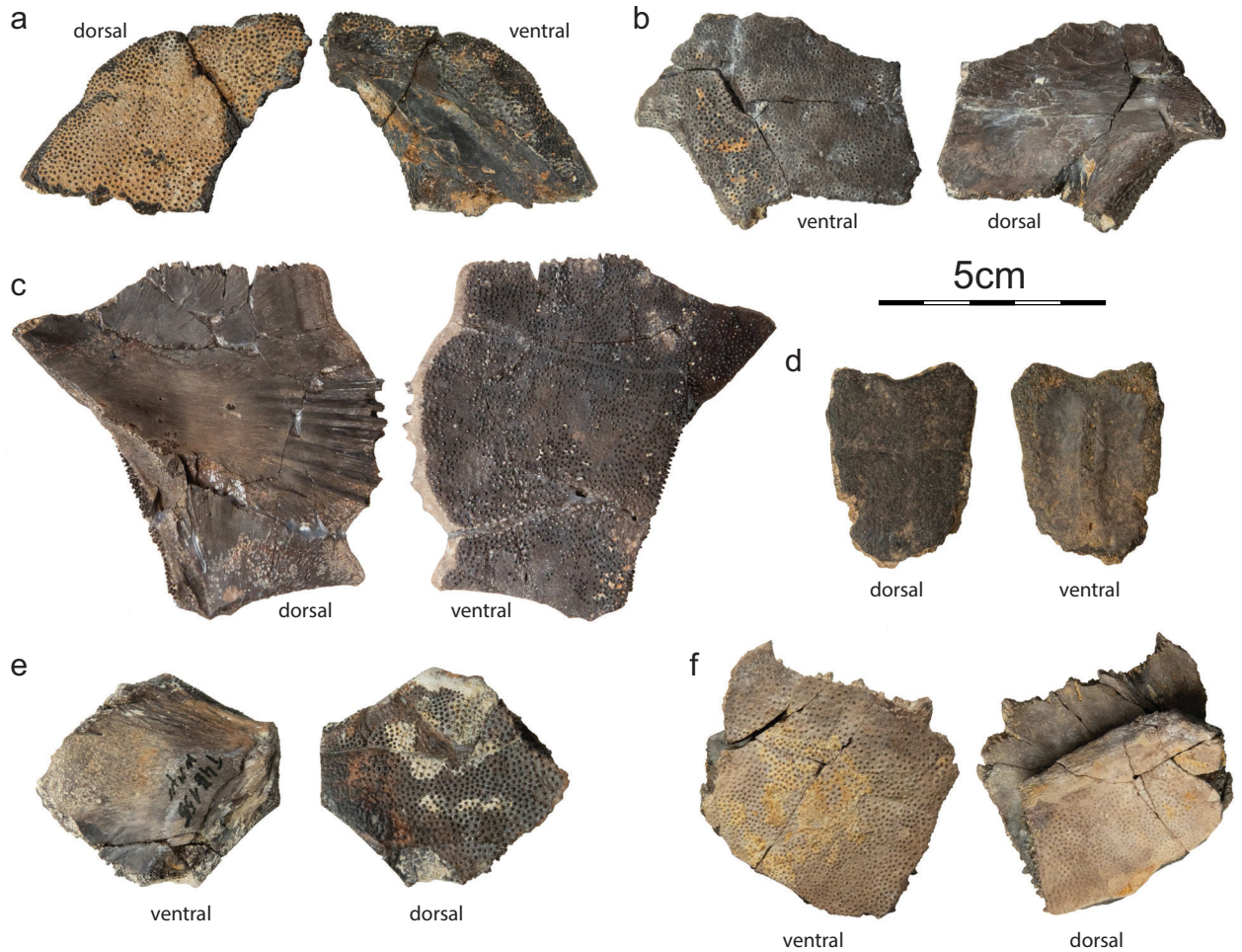

Figure 2. Shell remains of *Helochelydra nopcsai* from the Early Cretaceous (late Barremian – early Aptian) of Balve, North Rhine-Westphalia, Germany. Photographs of select specimens highlighting variation in preservation. (**a**) WMNM P88818, a right epiplastron (also see Fig. 5b); (**b**) WMNM P88824, a right partial hypoplastron (also see Fig. 5k); (**c**) WMNM P88823, a partial left hypo- and xiphiplastron (also see Fig. 5i); (**d**) WMNM P88808, a partial, anterior neural (also see Fig. 3a); (**e**) WMNM P88813, a partial nuchal (also see Fig. 4b); (**f**) WMNM P88816, a partial left peripheral XI (also see Fig. 4h). All specimens are to scale.

Helochelydra nopcsai can be distinguished from other helochelydrids by a shell surface texture consisting of evenly spaced tubercles that easily dislocate (also present in *Helochelys danubina*), cone-, hook-, and plate-shaped osteoderms (also present in *Naomichelys speciosa*), and pterygoids that fully cover the parabasisphenoid ventrally. No other helochelydrid is known to possess compound granicones. *Helochelydra nopcsai* currently cannot be distinguished from *Helochelys danubina* using morphological features, because the latter is poorly known and its holotype lost. Stratigraphic criteria (i.e., an age difference of more than 20 Ma) nevertheless suggest that they represent distinct taxa.

Referred material. Early Cretaceous (Barremian), Wessex Formation, Isle of Wight, United Kingdom (material referred by Lapparent de Broin and Murelaga 1999 and Joyce et al. 2011; Pleurosternidae of Sweetman and Insole 2010); Early Cretaceous (Hauterivian–Barremian), Nouvelle-Aquitaine, France (Solemydidae of Néraudeau et al. 2012); Early Cretaceous (Barremian), Aragon, Castile and León, La Rioja, and Valencia, Spain (Solemydidae of Pérez García 2009; Pérez-García et al. 2012, 2013; Scheyer et al. 2015); Early Cretaceous (late Barremian – early Aptian), Balve, Germany (all material described herein).

Description. Although the available sample consists of more than 250 specimens, including more than 150 granicones, only a small number of specimens provide useful anatomical information. This description is therefore focused on the most informative specimens.

Surface texture. The surface of all available shell material and granicones is evenly covered by distinct tubercles (Figs 2–5). Each tubercle is columnar and clearly separated from neighboring tubercles. The tubercles of the shell easily dislocate at their base, where they leave behind a circular scar, which can easily be recognized under the microscope. Although some variation is apparent across the shell (e.g., tubercles are less densely spaced over the neurals), most are about 0.5 to 1 mm wide, about 0.5 to 1.5 mm tall, and separated from neighboring tubercles by about 1.5 to 2 mm. The tubercles are less distinct on the available cranial fragment and all granicones, but similar in dimensions. In all regards, the surface texture closely approximates to that of *Helochelydra nopcsai* material

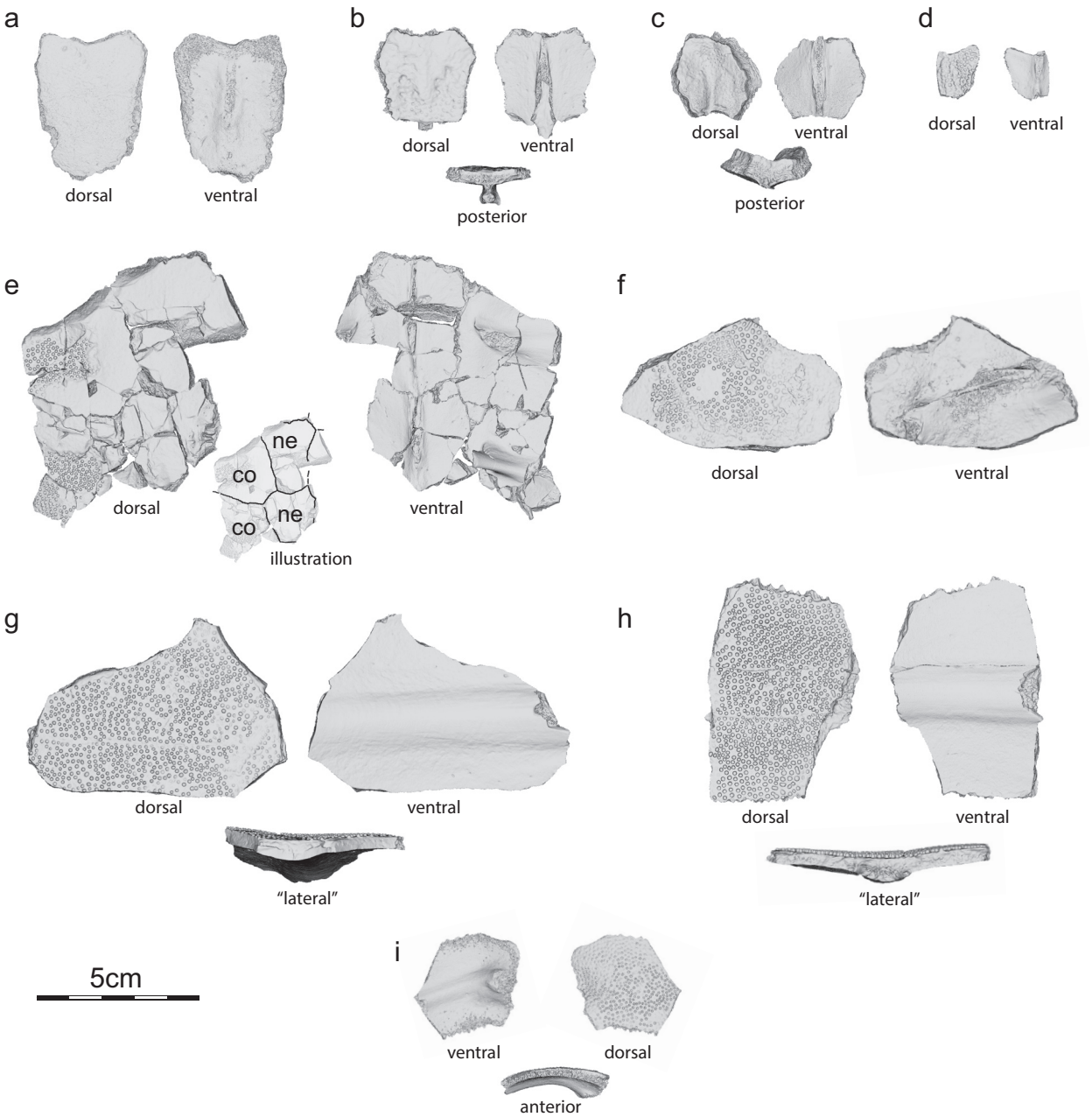

Figure 3. Neural and costal remains of *Helochelydra nopcsai* from the Early Cretaceous (late Barremian – early Aptian) of Balve, North Rhine-Westphalia, Germany. All images were obtained from CT generated 3D models. (**a**) WMNM P88808, a partial, anterior neural; (**b**) WMNM P49476, a partial, posterior neural; (**c**) WMNM P49351, a partial, posterior neural; (**d**) WMNM P88809, a partial, posterior neural; (**e**) WMNM P88807, a carapacial fragment consisting of two neurals and remnants of three adjacent costals; (**f**) WMNM P88810, a partial left costal I; (**g**) WMNM P88812, a partial costal; (**h**) WMNM P88811, a partial costal; (**i**) WMNM P49470, a partial right costal. Anatomical direction are placed in quotes for elements with uncertain orientation. With the exception of the illustrations, all specimens are to scale. *Abbreviations*: co = costal; ne = neural.

from the Wessex Formation of England (NHMUK R171, R5195–5199, R5201, R5205, R5238).

Carapace. The available material (Figs 3, 4) suggests that the carapace had a length of up to 70 cm (see Costals below), a nuchal notch extending laterally up to peripheral II (see Nuchal below), and that deep grooves decorated the neural-costal contacts along the posterior half of the shell (see Costals and Neurals below). The carapace is 5 to 6 mm thin along the peripherals and costals, but thickens to 8 mm at the neurals. All parts of the carapace are evenly covered by distinct tubercles that disarticulate easily (Figs 3, 4).

Neurals. We are able to identify six elements as neurals: WMNM P88808 (Fig. 3a), P49476 (Fig. 3b), P49351 (Fig. 3c), P88809 (Fig. 3h), and P88807 (Fig. 3e). WMNM P88807 is a larger shell fragment that consists of two neural elements in addition to costal remains including two neural elements that are up to 8 mm thick (Fig. 3e). The posteriorly angled orientation of the associated rib heads relative to the neural column suggest that

the elements represent neurals V, VI, or VII. Their outline is hexagonal with short anterolateral sides. The anterior of the two neural shows faint traces of a midline keel, as has also been reported for neurals of *Naomichelys speciosa* (Joyce et al. 2011). WMNM P88808 (Fig. 3a) is the largest available neural, flat, about 5 mm thick, and has a hexagonal outline (i.e., contacts with six surrounding bones are apparent). Its dorsal surface is badly eroded: there are faint traces of an intervertebral sulcus, but only the bases remain of the surface tubercles. The orientation of this element is not clear, but its size suggests that it originates from the anterior half of the shell. WMNM P49351 (Fig. 3c) is only half as long anteroposteriorly as the previous element, but about 7 mm thick. A sharp median depression crosses its surface. WMNM P49476 (Fig. 3b) has similar dimensions to WMNM P49351, but it is only about 4 mm thick and flat. The equilateral, hexagonal outline of the last two elements suggests an origin from the back of the shell. WMNM P88809 (Fig. 3d) is the smallest available neural and only about 2 mm thin. Only the right two thirds are preserved. Its small size and equilateral, hexagonal outline suggest that it originates from the posterior portions of the shell of a juvenile.

Costals. A number of elements can be diagnosed as costals, of which the following seven are the most informative: WMNM P88807 (Fig. 3e), a shell fragment that includes remains of three costals, WMNM P88810, a partial left costal I (Fig. 3f), P88811 (Fig. 3h) and P88812 (Fig. 3g), two large costal fragments, and P49470, the median portion of a midsized costal (Fig. 3i). The dermal portion of these costals is about 4 mm thick. The ribs, when present, are broad, about a quarter of the anteroposterior width of the costal, but only add about 2–3 mm to the thickness of each element. The three costal remains preserved in WMNM P88807 (Fig. 3e) are in articulation with two neurals and, therefore, best document the medial aspect of these elements. The slight posteriorly angled orientation of the ribs suggest that they originate from the mid-posterior part of the shell. All elements have two contacts with the adjacent neurals. The free, medial portion of one costal rib is well preserved. It is relatively narrow, about 2 mm across, and delimits a relatively low costovertebral tunnel. WMNM P88810 (Fig. 3f) can be identified as a partial left costal I by the presence of the articular scar for dorsal rib I. The sulcus between vertebral I and pleural I diagonally traverses the dorsal surface of this element. A rounded anteromedial facet for articulation with the nuchal suggests that the nuchal deeply inserted between the anterior costals. WMNM P88811 (Fig. 3h) is significant, as it possesses intact anterior and posterior margins. The greatest anteroposterior "width" of this element is 56 mm, which is a little greater than the greatest costal width that can be observed for the only known complete skeleton of the helochelydrid *Naomichelys speciosa* (Joyce et al. 2014). Assuming similar proportions, the full carapace may therefore have reached a length of over 70 cm. WMNM P49470 (Fig. 3i) only has an anteroposterior "width" of 3 cm and, therefore, likely originates from the back of the shell of a smaller individual. It is notable for exhibiting a concavity just above the rib head, near its medial articulation with the neurals. Together with the grooved neurals, this suggests some meso-scale sculpturing of the shell surface towards the back of the shell.

Nuchal. Two specimens preserve remains of the nuchal: WMNM P88813, the right half of a large nuchal (Fig. 4a), and WMNM P88814, a smaller nuchal fragment, which remains articulated with remnants of the adjacent right costal I and peripherals I and II (Fig. 4b). The two specimens suggest that a broad nuchal notch was present that was framed by peripherals II, as is typical for helochelydrids (Joyce et al. 2014; Pérez-García et al. 2020a). The oblique anterolateral contact of the nuchal with peripheral I is oriented more to the anterior than the side. There is no evidence for costiform processes. The right portion of a cervical scute is preserved in WMNM P88813 (Fig. 4a). As this specimen broke near the midline, we estimate that the complete cervical was at least twice as wide than long. Lateral to the cervical scute, a sulcus is apparent that delimits the contact between marginal I and vertebral I. There is no evidence for the presence of a prepleural on the nuchal. The skin-scute sulcus runs on the underside of the nuchal just behind the anterior margin of the bone.

Peripherals. A number of peripherals are preserved, of which we present the six most informative. WMNM P88814 includes a nearly complete right peripheral I articulated with remnants of the adjacent element (Fig. 4b). WMNM P88815 is a first peripheral I as well, but lacks much of its dorsal surface (Fig. 4c). These two elements document that peripheral series articulated with the nuchal laterally along an oblique (WMNM P88814) to straight (WMNM P88815) suture, costal I posteriorly, and peripheral II laterally. The scute-skin sulcus runs diagonally across the underside of the peripheral, thereby bridging the location of this sulcus near the margin of the shell at the nuchal with the deep location on the second peripheral. Although damaged, these bones also document that the visceral cavity extends all the way from the bridge region to the medial fifth of peripheral I, as had previously been documented for other helochelydrids (Joyce et al, 2014; Pérez-Garcia et al, 2020a). WMNM P88816 is a relatively large peripheral element that we tentatively interpret as the right peripheral XI, as it displays a small, but elongate facet on its visceral side best interpreted by reference to *Naomichelys speciosa* (Joyce et al. 2014) as the articulation site for thoracic rib IX (Fig. 4h). This element shows faint traces of an intermarginal scute sulcus and documents that the visceral cavity extends posteriorly from the bridge region to reach the pygal. The visceral cavity of *Helochelydra nopcsai*, therefore, extended all the way from the medial fifth of peripheral I to the pygal, much as in *Aragochersis lignitesta* (Pérez-Garcia et al, 2020a), but also *Pleurosternon bullockii* (Joyce et al. 2022). However, three finger-like pockets within the cavity of WMNM P88816 suggests that the visceral cavity is not developed evenly across the

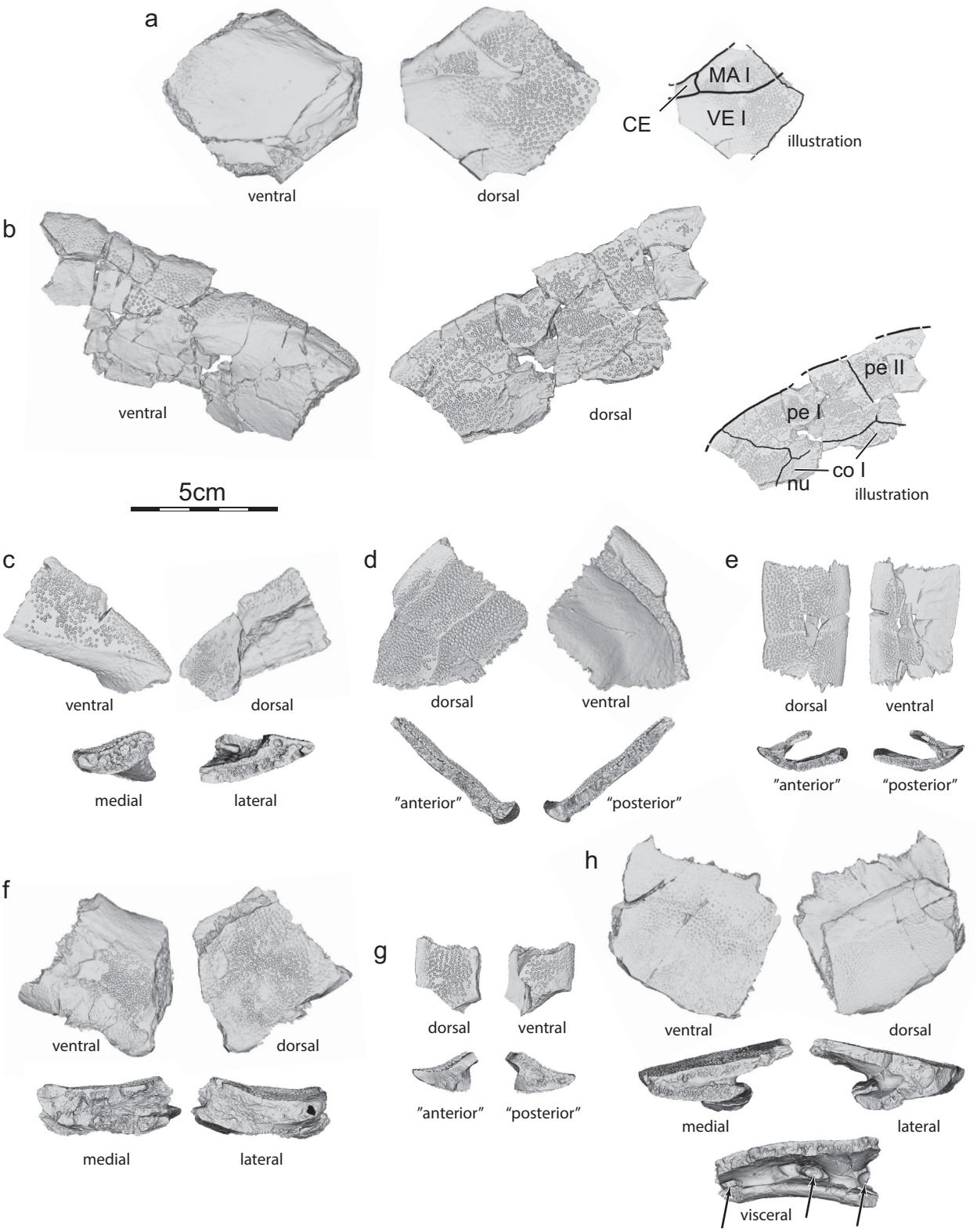

Figure 4. Nuchal and peripheral remains of *Helochelydra nopcsai* from the Early Cretaceous (late Barremian – early Aptian) of Balve, North Rhine-Westphalia, Germany. All images were obtained from CT generated 3D models. (**a**) WMNM P88813, a partial nuchal; (**b**) WMNM P88814, a carapacial fragment consisting of remnants of a nuchal, rights peripheral I, remnants of right peripheral II, and remnants of right costal I; (**c**) WMNM P88815, a partial right peripheral I; (**d**) WMNM P49051, a partial bridge peripheral; (**e**) WMNM P88817, a partial bridge peripheral; (**f**) WMNM P41690, a partial right peripheral XI; (**g**) WMNM P47259, a partial peripheral; (**h**) WMNM P88816, a partial left peripheral XI. Anatomical direction are placed in quotes for elements with uncertain orientation. With the exception of the illustrations, all specimens are to scale. *Abbreviations*: CE = cervical scale; co = costal; MA = marginal scale; nu = nuchal; pe = peripheral; VE = vertebral scale.

shell (see arrows in Fig. 4h). The waning visceral cavity combined with minor asymmetries suggest that WMNM P41690 is a damaged right peripheral X as well (Fig. 4f). As the most anterior and most posterior peripherals show evidence of a visceral cavity, it is not possible to identify the serial identity of the damaged, remaining peripheral elements. Three notable remains, WMNM P47259 (Fig. 4g), P49051 (Fig. 4d), and P88817 (Fig. 4e) nevertheless document variable development of a low gutter. WMNM P49051 and P88817 furthermore highlight that the dorsal and ventral branches that make up each peripheral are thin-walled and meet each other just medial to the edge of the carapace. The peripherals of the bridge region are therefore extremely fragile.

Epiplastron. The only available epiplastron, WMNM P88818, is near complete, but mineral precipitations on the external surface partially conceal its sulci (Fig. 5b). The epiplastron formed the anterior aspects of the transversely oriented anterior plastral lobe. The epiplastron has a convex posteromedial contact with the entoplastron. The epiplastron hereby slightly underlaps the entoplastron, which, as a result, would have appeared smaller in ventral than in dorsal view. An equally broad contact is present posterolaterally with the hyoplastron. Though damaged, deep pockets along the posterolateral margin of the epiplastron suggest that at least two peg-like processes of the hyoplastron inserted into the epiplastron. A short median contact is furthermore apparent with its counterpart. A notch along the anterior margin of the epiplastron signifies the location of the gular-extragular sulcus. A faint trace of this sulcus can be gleaned on the ventral surface that runs posteriorly from the notch (Fig. 5b). A similar notch for the extragular-humeral sulcus is apparent on the lateral margin of the epiplastron (Fig. 5b). On the dorsal side, the extragular-humeral sulcus veers posteriorly to cross the lateral side of the epiplastron (see arrows in Fig. 5b). Its posterior end is not preserved, as this was likely located on the hyoplastron. As a result of this arrangement, the extragular covered only part of the epiplastron in ventral view, but most of it in dorsal view. The dorsal side of the epiplastron is characterized by a thickened epiplastral lip.

Entoplastron. Two partial entoplastra are available, WMNM P48296 (Fig. 5a) and P88819 (Fig. 5c), of which the former is better preserved. The posterior half of the entoplastron is lacking in either specimen, but comparison with *Helochelydra nopcsai* (NHMUK R171) suggests that the entoplastron was slightly longer than wide. The entoplastron slightly overlaps the epiplastron along its slightly convex anterolateral contact. The posterolateral contact, as far as preserved, broadly underlapped the hyoplastron. Traces of the embryonic interclavicle are apparent on the dorsal side of both available elements, much as in other helochelydrids. The gulars only cover a small triangular surface on the ventral side of WMNM P48296, but about a third of the ventral surface of P88819. The extragulars minutely overlapped both elements. Only a minute entoplastral scute is apparent in WMNM P48296. An entoplastral scute seems to be absent in WMNM P88819, in which the humeral-gular junction is just about preserved.

Hyoplastron. Two partial hypoplastral remains can be identified with confidence. WMNM P47721 (Fig. 5d), the more complete of the two, documents the lateral margin of the anterior plastral lobe, just posterior to the articulation of the hyoplastron with the epiplastron, while WMNM P88820 (Fig. 5e) documents a segment slightly further to the back. The two fragments combined indicate that the skin-scute sulcus is barely located on the visceral side of the hyoplastron, but converges with its margin towards the back. Indeed, the sulcus terminates in WMNM P88820 near the margin, which suggests that this element broke at the humeral-pectoral sulcus. The resulting lip is only lightly developed towards the back, as seen in WMNM P88820, but becomes pronounced anteriorly to form a finger-like process that inserted anteromedially into the epiplastron, as seen in WMNM P47721.

Two additional, fragmentary specimens, WMNM P48226 (Fig. 5f) and P88821 (Fig. 5h), exhibit radiating, pin-like tubercles on their visceral sides that are reminiscent of those found on the hyoplastron of *Naomichelys speciosa*, but they may also represent remains of the mesoplastra or hypoplastra. A third fragment, WMNM P88822 (Fig. 5g), is a fragment of the bridge that may similarly represent part of the hyo- or hypoplastron. A rib-like thickening on the visceral side of this fragment is the remnants of a buttress. A series of clearly delineated sulci form the outlines of at least two inframarginals, two marginals, and the neighboring plastral scutes.

Mesoplastron. No mesoplastral remains could be identified as such.

Hypoplastron. We are able to identify at least three remains as hypoplastra, WMNM P88823 (Fig. 5i), P88825 (Fig. 5j), and P88824 (Fig. 5k), all of which preserve the thickened inguinal notch, but can be recognized as hypoplastra by remnants of the xiphiplastral articulation. WMNM P88823, the best of the three preserved elements, documents the transverse contact with the mesoplastron and the slightly oblique posterior contact with the xiphiplastron, which is dorsally stabilized by two xiphiplastral processes that dorsally cover the hypoplastron and a hypoplastral process that dorsally covers the xiphiplastron (Fig. 5i). The relatively intact medial margin suggests that central and posterior plastral fontanelles are present (see arrows in Fig. 5i) and that the hypoplastra only contacted one another along rib-like processes that radiate from the inguinal notch, features otherwise found in *Naomichelys speciosa* (Joyce et al. 2014), but not in the holotype of *Helochelydra nopcsai* (NHMUK R171). The relatively small size of this specimen opens the possibility, however, that these are juvenile features. As preserved, the abdominal/femoral sulcus crosses the hypoplastron diagonally from the inguinal notch to the central plastral fontanelle, but otherwise runs posterior from the notch to meet with the skin-scute sulcus on the dorsal side (Fig. 5i). In this area, the hypoplastron is thickened to nearly 2 cm in

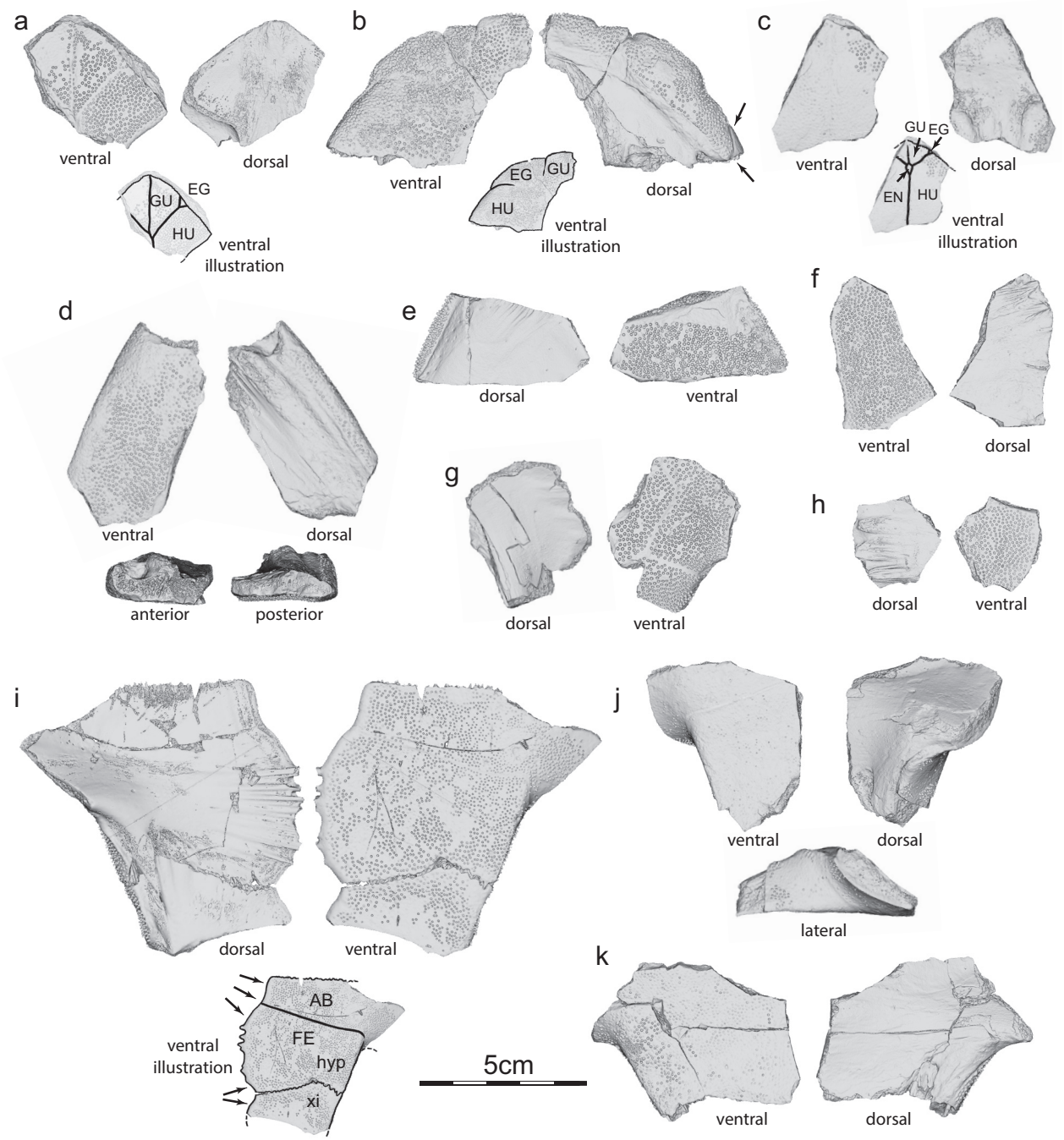

Figure 5. Plastral remains of *Helochelydra nopcsai* from the Early Cretaceous (late Barremian – early Aptian) of Balve, North Rhine-Westphalia, Germany. All images were obtained from CT generated 3D models. (**a**) WMNM P88819, a partial entoplastron; (**b**) WMNM P88818, a right epiplastron; (**c**) WMNM P48296, a partial entoplastron; (**d**) WMNM P47721, a partial right hyoplastron; (**e**) WMNM P88820, a partial left hyoplastron; (**f**) WMNM P48226, a plastral fragment; (**g**) WMNM P88822, a plastral fragment; (**h**) WMNM P88821, a plastral fragment; (**i**) WMNM P88823, a partial left hypo- and xiphiplastron; (**j**) WMNM P88825, a partial right hypoplastron; (**k**) WMNM P88824, a right partial hypoplastron. With exception of the illustrations, all specimens are to scale. *Abbreviations*: AB = abdominal scale; EG = extragular scale; EN = entoplastral scale; FE = femoral scale; GU = gular scale; HU = humeral scale; hyp = hypoplastron; xi = xiphiplastron.

the smallest available specimen (WMNM P88823), but reaches 2.5 cm in the largest (WMNM P88825). In the area of the notch, the skin-scute sulcus runs onto the dorsal side of the hypoplastron to form a semi-lunate lip, but runs near parallel to the margin once it reaches the xiphiplastron (Fig. 5j).

Xiphiplastron. The remnants of a xiphiplastron are preserved in WMNM P88823 attached to the hypoplastron (Fig. 5i). Its contact with the hypoplastron is described above, as is the development of the skin-scute sulcus. A comparison with *Naomichelys speciosa* suggests that the xiphiplastron broke close to the femoral-anal sulcus. The

anal scute, therefore, did not cross the hypoplastra-xiphiplastral suture.

Granicones. More than 150 granicones are available for study (Fig. 6). With few exceptions (see below), all granicones are singular, conical elements that consist of a flat base, which anchored the element into the skin, and an apex, which protruded from the body (Joyce et al. 2014). The external surface of all elements is covered by surface texture that closely mirrors that of the shell. A qualitative assessment suggests that three morphotypes are present: cones (ca. 35%), hooks (ca. 43%), and plates (ca. 22%). As the name implies, cones are conical elements where the apex is situated above the base (e.g., Fig. 6: P88864, P88873). These elements tend to be smaller. Hooks greatly resemble cones, but the apex is offset beyond the surface of the base (e.g., Fig. 6: P88922, P88856). Plates, finally, resemble hooks in that the base is offset from the base, but that are notably flat (e.g., Fig. 6: P88939, P88921). These tend to be the largest available elements. Our morphometric analysis (see below) suggests that these morphotypes do not populate discrete parts of the morphospace, but rather grade into each other. We nonetheless retain this terminology for convenience. As all elements were found in isolation, we do not know which parts of the body they once covered. A complete skeleton of *Naomichelys speciosa* that includes numerous articulated granicones, however, suggests that plates covered the external surfaces of the lower limbs while the spur-like hooks were located on the walking surfaces of the limbs (Joyce et al. 2014).

A total of five elements deviate strongly from the three morphotypes described above (Fig. 6). Two of these (WMNM P88935 and P88940) resemble large hooks by having an apex that is offset relative to the base, but the base in itself is not flat and round, but rather folded along the long axis of the element. We speculate that this type of element may have covered folds on the outside of the limbs. The three other unusual granicones are remnants of compound granicones. WMNM P88974 consists of a single, conical apex, but open sutures on at least one side of its base suggest that it was laterally sutured to at least one more granicone. WMNM P88964 consists of two conical apices that are broadly sutured to one another at their bases. Although the outline of the jointly formed base is somewhat angular, the element appears to be intact. WMNM P88962 also consists of two conical apices, but numerous angularly arranged sutures on both sides of the jointly formed base suggest that it formally articulated with at least two, but likely up to five additional granicones, to form a compound element with at least four to seven apices.

PCA of all measurements indicates that 65.7% of the overall variance can be explained by size or allometric differences between specimens, explained by PC1 (Table 1). No differentiation of morphotypes is apparent based on size differences alone. Our morphospace plot of size-adjusted principal components (Fig. 7) shows that PC2, which explains 71.9% of shape variation after correcting for size, is the only principal component along which separate clusters of specimens may be determined, as plated granicones plot at low PC2 values with minimal overlap of specimens pre-assigned to other morphotypes. Cones and hooks have broad overlap across PC3 (20% of variance; Fig. 7a) and PC4 (8.0% of variance; Fig. 7b). The absence of separation for these morphotypes and the broad spread of values across PC3 can be explained by shape variation within the pre-assigned hook or cone condition. For example, hooks exist that have large basal measurements but low tip height (Table 1), such as WMNM P88873 (Fig. 7a), the positive extreme point on PC3, but simultaneously hooks exist that have high tip heights compared to relatively small bases (e.g., WMNM P88864, which plots at low PC3 values for the hooked morphotype; Fig. 7a). Similarly, cones with strongly asymmetrical bases plot at extreme negative PC3 values (e.g., WMNM P88940), whereas cones with similar tip offset but symmetrical bases plot at extreme positive PC3 values (e.g., WMNM P88921). The relatively close association in morphospace of hooks like WMNM P88873 and cones like WMNM P88921 is thus primarily caused by similar base dimensions paired with low tip heights (Table 1), regardless of their difference in tip offset which is the primary distinction of cones and hooks based on qualitative comparisons.

Table 1. PCA results (n = 136).

	PC1	PC2	PC3	PC4
Eigenvalues	2.628	0.987	0.275	0.110
Proportion of total variance explained	0.657	0.247	0.069	0.028
Proportion of shape variance explained	–	0.719	0.200	0.080
Eigenvector coefficients				
height	0.170	0.963	-0.155	0.140
minimum base	0.575	-0.010	0.551	0.597
maximum base	0.591	0.045	0.229	-0.772
tip offset	0.540	-0.24	-0.788	0.166

Cranium. A three-dimensionally preserved, partial, left parietal (WMNM P88806) is the only skull bone in the sample (Fig. 8). The anterolateral and medial margins of its dorsal plate, which formerly contacted the left postorbital and the right parietal, are intact, but the anterior and posterior margins show signs of damage. Striations on the posteromedial side of the element, contained within the area that constituted the cavum cranii, could plausibly represent the articulation area with the supraoccipital, which is usually overlain by the parietal in this area. A short posterolateral facet may represent the former contact with the left squamosal. A comparison with IWCMS 1998.21, a complete *Helochelydra nopcsai* skull from the Isle of Wight (Joyce et al. 2011), suggests that only the anterior half of the element is preserved. The two specimens likely originated from individuals of the same size, as WMNM P88806 has an anteroposterior length of about 2.7 cm, while the equivalent area measures about 2.8 cm in IWCMS 1998.21. The two skulls differ notably in that WMNM P88806 exhibits clear cranial sulci which outline at least 12 polygonal cranial scutes. Their great number, however, obscures homology

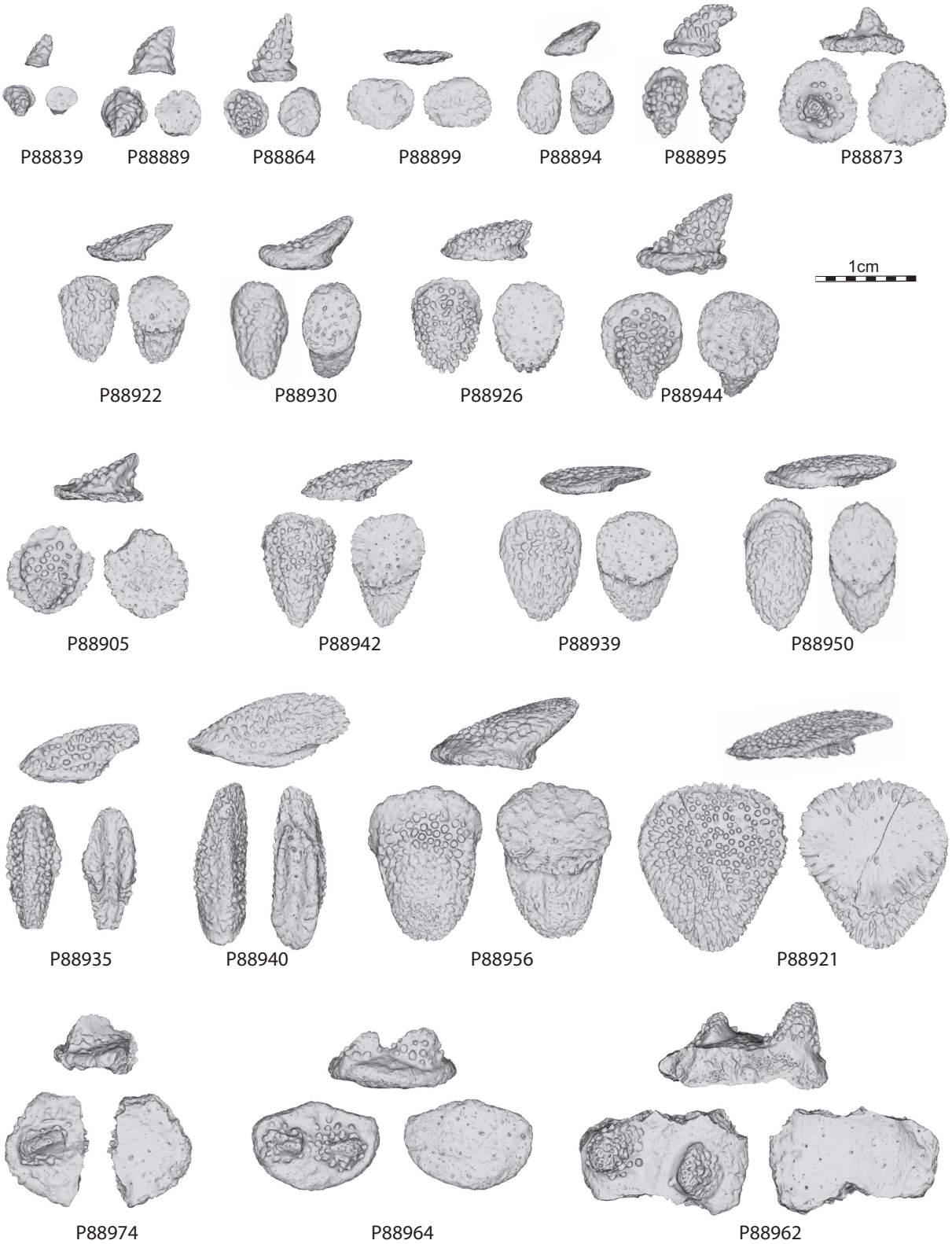

Figure 6. A selection of granicones, *Helochelydra nopcsai* from the Early Cretaceous (late Barremian – early Aptian) of Balve, North Rhine-Westphalia, Germany. All images were obtained from CT generated 3D models. All specimens are shown to scale in lateral (top), apical (bottom left), and basal view (bottom right) and associated with their WMNM catalog number. Specimens were in part chosen to highlight the morphological extremely highlighted by the PC plots (see Fig. 7).

with the cranial scutes of other Cretaceous turtles, as these typically exhibit only four scutes in the equivalent area (Sterli and de la Fuente 2013; Evers et al. 2021). On the ventral side, traces remain of the heavily damaged descending process. What remains is an outwardly convex crest of bone that documents the greatest width of the cavum cranii.

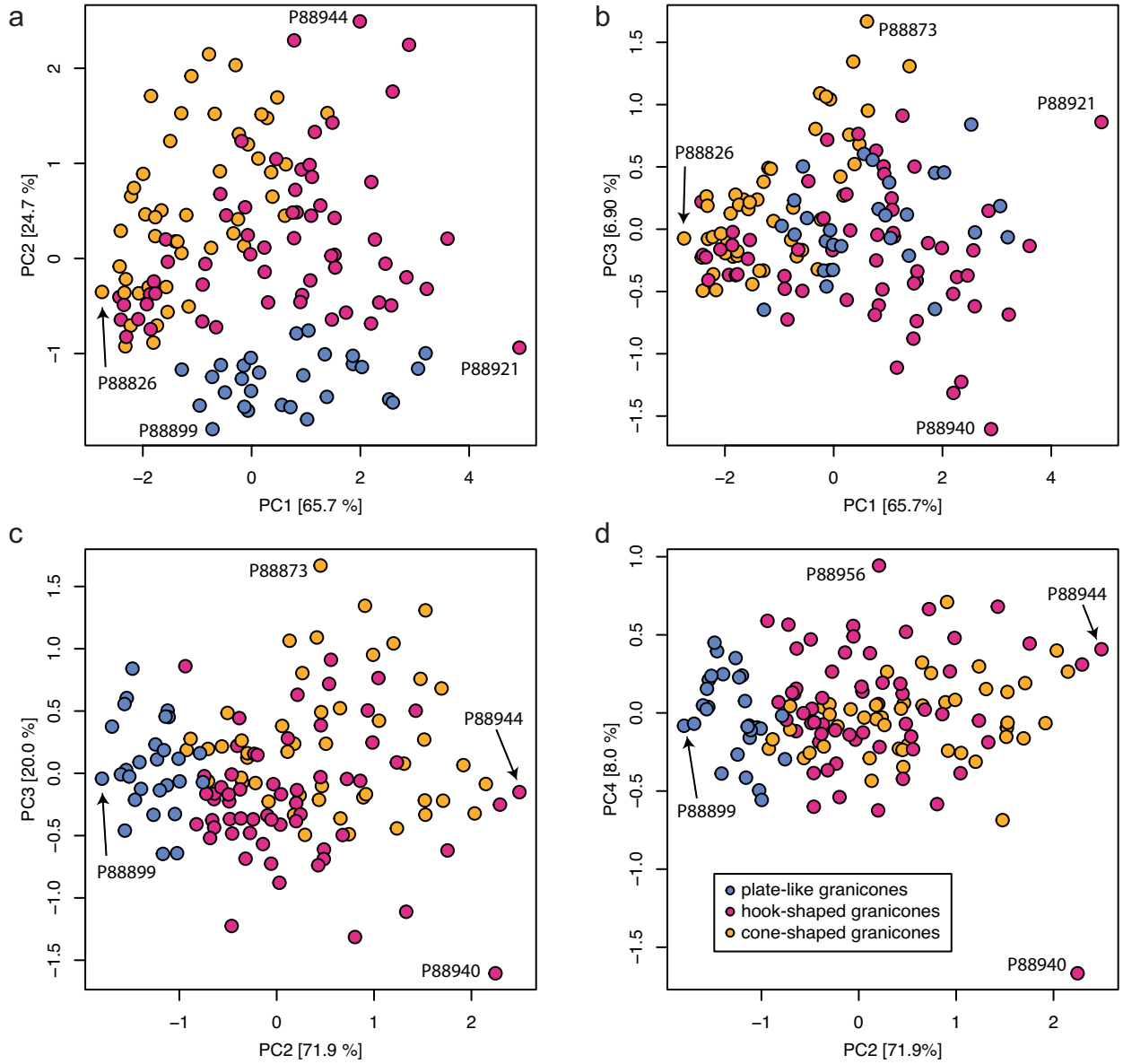

Figure 7. Morphospaces of four granicone measurements from PCA ordination (N = 165). (**a, b**), bivariate morphospaces including size variation. (**c, d**), morphospaces corrected for size and allometry. A, PC1 vs. PC2. B, PC2 vs. PC3. C, PC2 vs. PC3. D, PC2 vs. PC4. The proportion of variance explained by PC axes are indicated in the axis labels, whereby values in **A, B** represent total variance (including size) and values in **B, C** represent shape variance (re-scaled to exclude PC1). An identical plot with unique point labels is provided in Suppl. material 2.

Discussion

Alpha taxonomy

The vast majority of helochelydrid remains cannot be identified rigorously, in part because the true diversity of helochelydrid turtles is not yet understood, but also because fragmentary remains rarely yield diagnostic characters beyond shell surface texture. For these reasons, Joyce et al. (2014) developed a preliminary taxonomy that is focused on shell surface texture, but further recommends assigning material to named taxa based on biogeographic and temporal considerations. Using these criteria, the fossil turtle material presented herein can be assigned to *Helochelydra nopcsai*, as it closely mirrors its shell surface texture consisting of evenly spaced tubercles that easily dislocate, as it originates from sediments broadly coeval with the type stratum (i.e., Barremian–Albian), and because northern Germany and southern England are typically reconstructed to have been part of the same depositional system at that time (e.g., Aguado et al. 2022; Sanjuan et al. 2022).

Although comparisons are limited, we are able to highlight two notable differences between the new material from Balve and previously described postcranial (Nopcsa 1928; Lapparent de Broin and Murelaga 1999) and cranial material (Joyce et al. 2011) from the Wessex Formation of England. First, while the only available entoplastron from the Wessex Formation exhibits are relatively large entoplastral scutes, the two entoplastra

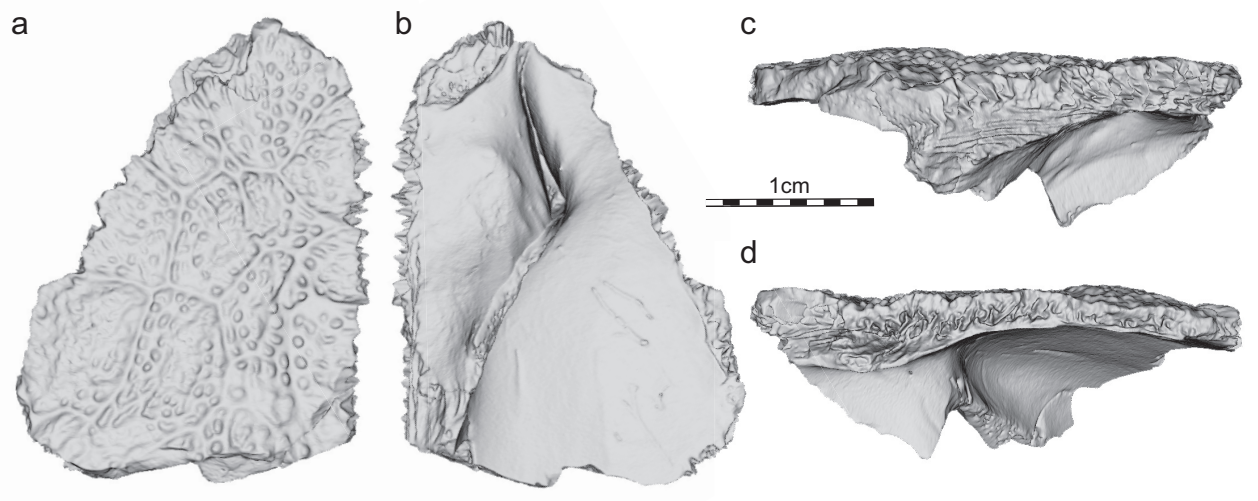

Figure 8. *Helochelydra nopcsai* from the Early Cretaceous (late Barremian – early Aptian) of Balve, North Rhine-Westphalia, Germany. WMNM P88806, a partial parietal in dorsal (**a**), ventral (**b**), medial (**c**), and lateral view (**d**). All images were obtained from CT generated 3D models.

from Balve appear to have no, or only a small entoplastral scute. And second, while the only available skull from the Wessex Formation lacks evidence of cranial scutes, the parietal fragment from Balve is clearly marked by numerous cranial scute sulci.

Large entoplastral scutes have been reported for some helochelydrids, notably *Naomichelys speciosa* and *Solemys* spp. (Hay 1908; Lapparent de Broin and Murelaga 1999; Joyce et al. 2014; Tong et al. 2023), but this scute is relatively small to absent in others, including not only *Aragochersis lignitesta* and *Plastremys rutteri* (Pérez-García et al. 2020a; Joyce 2022) but also *Helochelydra nopcsai*. As the scutes of other turtles are known to vary widely, including the entoplastral scute of specimens referred to *Naomichelys speciosa* (Hay 1908; Ostrom 1970; Joyce et al. 2014), we here attribute the observed differences to intraspecific variation, as we find the difference between a small and very small entoplastral to absent entoplastral scute to be minor.

We are unaware of any studies that explicitly document variation to the development of cranial scute sulci in turtles. We are therefore unable to assess if the difference we observe in the development of cranial scute sulci has taxonomic differences. We suspect nonetheless that cranial scute sulci are developed more distinctly in juvenile material, perhaps suggesting that the parietal from Balve originates from a less mature individual.

Morphology

The type material of *Helochelydra nopcsai* is a partial skeleton that remains poorly described to date. Though fragmentary as well, the new material from Balve yields important new insights regarding the morphology of helochelydrids in general and *Helochelydra nopcsai* specifically. We here focus on two characters: the expansion of the visceral bridge cavity to the front and back of the shell and the presence and development of granicones.

Expansion of the visceral bridge cavity

In the vast majority of turtles, the peripherals are modified into two basic shapes: while the peripherals anterior and posterior to the bridge are flat, as they only connect to the carapacial disk medioventrally, the bridge peripherals are V-shaped in cross section to allow articulating with the carapace dorsolaterally and the plastron ventrolaterally. As a result, the visceral cavity of the shell is laterally defined by the bridge peripherals. Lapparent de Broin and Murelaga (1999) documented for the first time that the visceral cavity of the late Late Cretaceous helochelydrids *Solemys gaudryi* and *Solemys vermiculata* extends from the bridge region to the most lateral aspects of the nuchal. The anterior peripherals therefore exhibit a V-shape: the dorsal branch remains articulated with the carapace while the ventral branch creates a shelf that projects towards the visceral cavity. Joyce et al. (2014) extended this observation to the late Early Cretaceous helochelydrid *Naomichelys speciosa*, highlighting that this feature may be a more general feature of helochelydrids. More recently, Pérez-García et al. (2020a) documented that the visceral cavity not only extends anteriorly, but also posteriorly in the late Early Cretaceous helochelydrid *Aragochersis lignitesta*. The presence of a visceral cavity that extends along the full peripheral margin of the shell, however, was soon after documented as well for the early Cretaceous compsemydids and pleurosternids *Peltochelys duchastelii*, *Pleurosternon bullockii*, and *Tongemys enigmatica* (Joyce et al. 2022). The presence of this character is particularly surprising for *Pleurosternon bullockii*, as this taxon had historically been known from numerous shells, but never been shown to display this feature (e.g., Owen 1853; Lydekker 1889; Milner 2004; Guerrero and Pérez-García 2021). The primary reason for this oversight is because this taxon is typically preserved as complete, but flattened shells. The anterior and posterior peripherals are therefore compressed to obscure the presence of a cavity. The presence of this cavity is nevertheless

clearly revealed in relatively rare disarticulated remains of this taxon, which allow viewing the peripherals in cross section, but also hinted at as a step-like ridge also apparent in compressed individuals (Joyce et al. 2022).

Our limited sample of peripherals from Balve documents that the visceral cavity of *Helochelydra nopcsai* not only extends from the bridge anteriorly to peripheral I, but also posteriorly to peripheral XI. While the anterior extension looks to be continuous, the posterior extension is achieved through a series of pockets best documented for peripheral XI. It is unclear to us if these pockets are developed in other helochelydrids as well.

We here also note that the step-like ridge apparent in many individuals of *Pleurosternon bullockii* is apparent in the posterior peripherals of *Naomichelys speciosa* as well. We therefore speculate that the visceral cavity of this taxon is more extensive than noted by Joyce et al. (2014).

The phylogenetic relevance of this relatively novel character complex has not yet been explored in full, in part as its distribution remains poorly documented, but it provides evidence for the moment for the hypothesis that helochelydrids are a subclade of *Paracryptodira*, perhaps closely linked with pleurosternids (Rollot et al. 2021, 2022a, b). However, the possible presence of similar expansions of the visceral cavity into the anterior or posterior peripherals of Triassic turtles (pers. comm. Tomasz Szczygielski 2023) suggests that this feature may also be plesiomorphic for the group.

Granicones

A preliminary assessment of the turtle fauna from Balve suggests that four turtles are present, in particular the enigmatic *Chitracephalus dumonii*, the small compsemydid *Peltochelys duchastelii*, a new species of pleurosternid, and *Helochelydra nopcsai*, the focus of this study. Our visual inspection of all granicones from Balve concludes that all display the same surface texture, regardless of shape or size, which closely mirrors the shell surface texture of *Helochelydra nopcsai*. We, therefore, conclude with confidence that *Helochelydra nopcsai* is the only taxon at Balve that possessed osteoderms.

To date, helochelydrid granicones (i.e., osteoderms) have only been reported from a relatively small number of localities. A handful of conical elements were initially described during the 19th century from the Early Cretaceous (Berriasian) Purbeck Limestone Formation of England (Owen 1878; Barrett et al. 2002). Despite their greater age, these broadly correspond in their morphology with the cone-shaped granicones we here report from Balve. A single granicone was previously reported from the Early Cretaceous (Barremian) Wessex Formation of England (Sweetman, 2007), which, unsurprisingly, resembles closely the cone-shaped granicones we here report from Balve. This supports its taxonomic assignment to *Helochelydra nopcsai* (Joyce et al. 2011). A large sample of granicones found in articulation with a skeleton of the Early Cretaceous *Naomichelys speciosa* (Barrett et al. 2002; Joyce et al. 2014) also resembles those from Balve by variously consisting of cones, hooks, and plates. This may suggest particularly close phylogenetic relationships between *Helochelydra nopcsai* with *Naomichelys speciosa*.

A small number of additional granicones have been reported from other formations that strongly deviate in their morphology from those from Balve. Lapparent de Broin and Murelaga (1999) referred a single late Late Cretaceous (Maastrichtian) element to *Solemys vermiculata* that resembles the granicones of *H. nopcsai* and *N. speciosa* by being covered by a helochelydrid surface texture, but differs by looking to be a compound element consisting of sutured plates, not cones. Pérez-García et al. (2020b) similarly referred an early Late Cretaceous (Cenomanian) element from Spain to *Plastremys lata*, which differs from the granicones of *H. nopcsai* and *N. speciosa* by having a less distinct surface texture and by looking to be a composite element consisting of two unevenly sized cones. Future finds may prove these differences to have taxonomic significance.

The dearth of material is surprising given that helochelydrids broadly occur from throughout the Cretaceous of North America and Europe. We suspect that three factors may play a role. First and foremost, the notable absence of granicones in the well-preserved skeletons of *Aragochersis lignitesta* (Pérez-García et al. 2020a) suggest that granicones may perhaps not be present in all helochelydrids. Second, we suspect that few continental localities are systematically screen washed for small sized fossils, such as granicones. And, third, even if small sized fossils are systematically collected, we would not be surprised if the granicones either remain unidentified as such or unreported. We hope that the large set of images and 3D models associated with this contribution will ease their identification and comparisons in the future.

Paleoecology

The paleoecology of helochelydrids is generally assumed to be terrestrial because they are mostly found in continental sediments, exhibit shell bone density similar to extant tortoises, and because osteoderms are otherwise only associated with terrestrially adapted turtles, including, among others, the Late Triassic *Proganochelys quenstedtii*, Late Cretaceous nanhsiungchelyid *Basilemys* spp., the Pleistocene meiolaniform *Meiolania platyceps*, and extant testudinids (Lapparent de Broin 1999; Joyce et al. 2011, 2014; Scheyer et al. 2015). Yet, the best preserved helochelydrid skull, that of *Helochelydra nopcsai*, lacks characteristics typical of terrestrial turtles, such as an inflated nasal cavity (Paulina-Carabajal et al. 2017), but instead possesses broad triturating surfaces, which are otherwise mostly associated with aquatic feeding preferences (Foth et al. 2017; Hermanson et al. 2022). Although Joyce et al. (2014) attempted to resolve

this conundrum by suggesting that *H. nopcsai* may have fed on hard terrestrial food items, such as grubs and snails, additional insights are called for to further resolve this question. It should also be noted that osteoderms are ubiquitously known in aquatic non-turtle reptiles, such as phytosaurs, crocodyliforms, or placodonts (Romer, 1956).

The taphonomic setting of the Balve fissure fill deposits is still under investigation. Fissure fills often create taphonomic filters that prefer terrestrial versus aquatic taxa. An informal census of several hundred shell fragments from Balve concludes that less than 1% of finds represent *Chitracephalus dumonii*, about 10% *Peltochelys duchastelii*, about 35% the new species of pleurosternid, and then the remaining 45% *Helochelydra nopcsai*. The remains of *Helochelydra nopcsai* are notable for being particularly fragile, but complete, but this only suggests to us that these remains were not transported, not that this turtle was necessarily terrestrial versus aquatic. The presence of unambiguously aquatic versus terrestrial taxa (Lanser and Heimhofer 2015; Schwermann et al. 2018; Skutschas et al. 2020; Martin et al. 2021, 2022; Hornung et al. 2023) conversely suggests that the fissure fauna at Balve is mixed. We, therefore, conclude that we cannot gain further insights regarding the paleoecology of this animal using taphonomic considerations.

Data availability

All specimens described herein are housed at the LWL-Museum of Natural History, Münster, Germany. 3D mesh models are available at MorphoSource (https://www.morphosource.org/projects/000497160).

Author contributions

WGJ designed the study, CT scanned specimens, illustrated specimens, compiled figures, and wrote a primary draft. SWE performed the morphometric study. SR obtained all measurements of granicones. YR segmented CT data and exported 3D mesh models. AHS organized field work and curated specimens. All authors wrote, read, and approved the manuscript and contributed to editing.

Competing interests

The authors declare that they have no conflicts of interest.

Financial support

This research was supported by grants from the Swiss National Science Foundation (SNF 200021_178780/1) and the German Research Foundation (DFG MA 1643/26-1).

Acknowledgements

We thank the numerous people who have been active in the excavations at Balve-Beckum over the course of the past 20 years. This includes student assistants, student interns, preparation trainees, volunteers, and employees of the LWL-Museum of Natural History. The success of the excavation is continuously promoted by good cooperation with and the support of the Lhoist company. This manuscript profited from careful reading and thoughtful comments from Tomasz Szczygielski and an anonymous reviewer.

References

Aguado R, Company M, O'Dogherty L, Sandoval J, Martinez M (2022) New insights into the Barremian–lower Aptian calcareous nannofossils of the Mediterranean Tethys: chronostratigraphic and paleobiogeographic implications. Marine Micropaleontology 173: 102114. https://doi.org/10.1016/j.marmicro.2022.102114

Barrett PM, Clarke JB, Brinkman DB, Chapman SD, Enson PC (2002) Morphology, histology and identification of the 'granicones' from the Purbeck Limestone Formation (Lower Cretaceous: Berriasian) of Dorset, southern England. Cretaceous Research 23: 279–295. https://doi.org/10.1006/cres.2002.1002

Chkhikvadze VM (1970) [Classification of the subclass Testudinata]. Nauchnaya Sessiya Instituta Paleobiologii, Tezisy Dokladov 14: 7–8. [in Russian]

Evers S, Rollot Y, Joyce WG (2021) New interpretation of the cranial osteology of the Early Cretaceous turtle *Arundelemys dardeni* (Paracryptodira) based on a CT-based re-evaluation of the holotype. PeerJ 9: e11495. https://doi.org/10.7717/peerj.11495

Foth C, Rabi M, Joyce WG (2017) Skull shape variation in recent and fossil *Testudinata* and its relation to habitat and feeding ecology. Acta Zoologica 98: 310–325. https://doi.org/10.1111/azo.12181

Guerrero A, Pérez-García A (2021) Morphological variability and shell characterization of the European uppermost Jurassic to lowermost Cretaceous stem turtle *Pleurosternon bullockii* (Paracryptodira, Pleurosternidae). Cretaceous Research 125: 104872. https://doi.org/10.1016/j.cretres.2021.104872

Hay OP (1908) The Fossil turtles of North America. Carnegie Institution of Washington Publication 75: 1–568.

Hermanson G, Benson RBJ, Farina BM, Ferreira GS, Langer MC, Evers SW (2022) Cranial ecomorphology of turtles and neck retraction as a possible trigger of ecological diversification. Evolution 76(11): 2566–2586. https://doi.org/10.1111/evo.14629

Hirayama R, Brinkman DB, Danilov IG (2000) Distribution and biogeography of non-marine Cretaceous turtles. Russian Journal of Herpetology 7: 181–198.

Hornung JJ, Sachs S, Schwermann AH (2023) The first record of sauropod dinosaurs from a palaeotopographical upland environment and its implications for megaherbivorous dinosaur faunal turnover in the Early Cretaceous of northwestern Europe. Geologie und Paläontologie in Westfalen 97: 3–35.

ICZN [International Commission on Zoological Nomenclature] (1999) International Code of Zoological Nomenclature. 4th edn. London: International Trust for Zoological Nomenclature, 306 pp.

Joyce WG (2017) A review of the fossil record of basal Mesozoic turtles. Bulletin of the Peabody Museum of Natural History 58: 65–113. https://doi.org/10.3374/014.058.0105

Joyce WG (2022) A review of helochelydrid shell material from late Albian to early Cenomanian greensands of Southern England, United Kingdom. Anatomical Record 2023: 1–13. https://doi.org/10.1002/ar.25086

Joyce WG, Bourque JR, Fernandez V, Rollot Y (2022) An alternative interpretation of small bodied turtles from the "Middle Purbeck" of England as a new species of compsemydid turtle. Fossil Record 25: 263–274. https://doi.org/10.3897/fr.25.85334

Joyce WG, Chapman SD, Moody RTJ, Walker CA (2011) The skull of the solemydid turtle *Helochelydra nopcsai* from the Early Cretaceous (Barremian) of the Isle of Wight (UK) and a review of Solemydidae. Special Papers in Paleontology 86: 75–97.

Joyce WG, Sterli J, Chapman SD (2014) The skeletal morphology of the solemydid turtle *Naomichelys speciosa* from the Early Cretaceous of Texas. Journal of Paleontology 88: 1257–1287. https://doi.org/10.1666/14-002

Joyce WG, Rabi M, Clark JM, Xu X (2016) A toothed turtle from the Late Jurassic of China and the global biogeographic history of turtles. BMC Evolutionary Biology 16: 236. https://doi.org/10.1186/s12862-016-0762-5

Klein IT (1760) Klassification und kurze Geschichte der vierfüßigen Thiere (translation by F. D. Behn). Jonas Schmidt.

Lanser K-P, Heimhofer U (2015) Evidence of theropod dinosaurs from a Lower Cretaceous karst filling in the northern Sauerland (Rhenish Massif, Germany). Paläontologische Zeitschrift 89: 79–94. https://doi.org/10.1007/s12542-013-0215-z

Lapparent de Broin F de, Murelaga X (1999) Turtles from the Upper Cretaceous of Laño (Iberian peninsula). Estudios del Museo de Ciencias Naturales de Alava 14: 135–211.

Lydekker R (1889) On certain chelonian remains from the Wealden and Purbeck. Quarterly Journal of the Geological Society of London 45: 511–518. https://doi.org/10.1144/GSL.JGS.1889.045.01-04.34

Martin T, Averianov AO, Schultz JA, Schwermann AH (2021) First multituberculate mammals from the Lower Cretaceous of Germany. Cretaceous Research 119: 104699 https://doi.org/10.1016/j.cretres.2020.104699

Martin T, Averianov AO, Schultz JA, Schellhorn R, Schwermann AH (2022) First spalacotheriid and dryolestid mammals from the Cretaceous of Germany. Acta Palaeontologica Polonica 67: 155–175. https://doi.org/10.4202/app.00914.2021

Meyer H von (1855) *Helochelys danubina* aus dem Grünsande von Kelheim in Bayern. Palaeontographica 4: 96–105.

Milner AR (2004) The turtles of the Purbeck Limestone Group of Dorset, southern England. Palaeontology 47: 1441–1467. https://doi.org/10.1111/j.0031-0239.2004.00418.x

Néraudeau D, Allain R, Ballèvre M, Batten DJ, Buffetaut E, Colin JP, Dabard MP, et al. (2012) The Hauterivian–Barremian lignitic bone bed of Angeac (Charente, south-west France): stratigraphical, palaeobiological and palaeogeographical implications. Cretaceous Research 37: 1–14. https://doi.org/10.1016/j.cretres.2012.01.006

Nopcsa F (1928) Palaeontological notes on reptiles. Geologica Hungarica, Palaeontology Series 1: 1–84.

Ostrom JH (1970) Stratigraphy and paleontology of the Cloverly Formation (Lower Cretaceous) of the Bighorn Basin Area, Wyoming and Montana. Bulletin of the Peabody Museum of Natural History 35: 1–234.

Owen R (1853) Monograph on the fossil Reptilia of the Wealden and Purbeck formations, Part 1, Chelonia. Palaeontographical Society Monograph 7: 1–12. https://doi.org/10.1080/02693445.1853.12113207

Owen R (1878) On the fossils called "granicones"; being a contribution to the histology of the exo-skeleton in "Reptilia." Journal of the Royal Microscopical Society 1: 233–236. https://doi.org/10.1111/j.1365-2818.1878.tb01721.x

Paulina-Carabajal A, Sterli J, Georgi J, Poropat SF, Kear BP (2017) Comparative neuroanatomy of extinct horned turtles (Meiolaniidae) and extant terrestrial turtles (Testudinidae), with comments on the palaeobiological implications of selected endocranial features. Zoological Journal of the Linnean Society 180: 930–950 . https://doi.org/10.1093/zoolinnean/zlw024

Pérez-García A (2009) Revisión histórica y sistemática de las primeras citas de quelonios del Cretácico español. Revista Española de Paleontología 24: 93–104. https://doi.org/10.7203/sjp.24.1.20346

Pérez-García A, Murelaga X, Huerta P, Torcida Fernández-Baldor P (2012) Turtles from the Lower Cretaceous of the Cameros Basin (Iberian Range, Spain). Cretaceous Research 33: 146–158. https://doi.org/10.1016/j.cretres.2011.09.011

Pérez-García A, Scheyer TM, Murelaga X (2013) The turtles from the uppermost Jurassic and Early Cretaceous of Galve (Iberian Range, Spain): anatomical, systematic, biostratigraphic and palaeobiogeographical implications. Cretaceous Research 44: 64–82. https://doi.org/10.1016/j.cretres.2013.03.011

Pérez-García A, Espílez E, Mampel L, Alcalá L (2020a) A new basal turtle represented by the two most complete skeletons of *Helochelydridae* in Europe. Cretaceous Research 107: 104291. https://doi.org/10.1016/j.cretres.2019.104291

Pérez-García A, Bardet N, Fregenal-Martínez MA, Martín-Jiménez M, Mocho P, Narvarez I, Torices A, Vullo R, Ortega F (2020b) Cenomanian vertebrates from Algora (central Spain): new data on the establishment of the European Upper Cretaceous continental faunas. Cretaceous Research 115: 104566. https://doi.org/10.1016/j.cretres.2020.104566

Rollot Y, Evers S, Joyce WG (2021) A redescription of the Late Jurassic turtle *Uluops uluops* and a new phylogenetic hypothesis of Paracryptodira. Swiss Journal of Paleontology 140: 23. https://doi.org/10.1186/s13358-021-00234-y

Rollot Y, Evers SW, Cifelli RL, Joyce WG (2022) New insights into the cranial osteology of the Early Cretaceous paracryptodiran turtle *Lakotemys australodakotensis*. PeerJ 10: e13230. https://doi.org/10.7717/peerj.13230

Rollot Y, Evers SW, Pierce SE, Joyce WG (2022) Cranial osteology, taxonomic reassessment, and phylogenetic relationships of the Early Cretaceous (Aptian-Albian) turtle *Trinitichelys hiatti* (Paracryptodira). PeerJ 10: e14138. https://doi.org/10.7717/peerj.14138

Romer A (1956) Osteology of Reptiles. Chicago: University of Chicago Press, 772 pp.

Sanjuan J, Vicente A, Pérez-Cano J, Stoica M, Martín-Closas C (2022) Early Cretaceous charophytes from south Dobrogea (Romania). Biostratigraphy and palaeobiogeography. Cretaceous Research 122: 104762. https://doi.org/10.1016/j.cretres.2021.104762

Scheyer TM, Pérez-García A, Murelaga X (2015) Shell bone histology of solemydid turtles (stem Testudines): palaeoecological implications. Organisms Diversity and Evolution 15: 199–212. https://doi.org/10.1007/s13127-014-0188-0

Schwermann AH, Schöllmann L, Pott C (2018) Vertebrate fauna of a fissure filling from the Lower Cretaceous (Barremian–Aptian) of Balve, Westphalia, Germany. Abstracts, 13th Symposium on Mesozoic Terrestrial Ecosystems and Biota, 111–112.

Skutschas PP, Kolchanov VV, Schwermann AH (2020) First salamander from the Lower Cretaceous of Germany. Cretaceous Research 116: 104606 https://doi.org/10.1016/j.cretres.2020.104606

Sterli J, de la Fuente MS (2013) New evidence from the Palaeocene of Patagonia (Argentina) on the evolution and palaeo-biogeography of Meiolaniformes (*Testudinata*, new taxon name). Journal of Systematic Palaeontology 11: 835–852. https://doi.org/10.1080/14772019.2012.708674

Sweetman SC (2007) Aspects of the microvertebrate fauna of the Early Cretaceous (Barremian) of the Early Cretaceous (Barremian) Wessex Formation of the Isle of Wight, Southern England. Ph.D. Thesis, University of Portsmouth, 1–360.

Tong H, Tortosa T, Bufferaut, E, dutour Y, Turini E, Claude J (2022) A compsemydid turtle from the Upper Cretaceous of Var, southern France. Annales de Paléontologie 108: 102536 https://doi.org/10.1016/j.annpal.2022.102536

Tong H, Buffetaut E, Méchin P, Méchin-Salessy A, Claude JA (2023) A *Solemys* skull from the Late Cretaceous of Southern France. Diversity 15: 58. https://doi.org/10.3390/d15010058

Supplementary material 1

Granicone measurements taken as part of this study

Authors: Walter G. Joyce, Serjoscha W. Evers, Sara Ren, Yann Rollot, Achim H. Schwermann

Data type: table (excel file)

Copyright notice: This dataset is made available under the Open Database License (http://opendatacommons.org/licenses/odbl/1.0). The Open Database License (ODbL) is a license agreement intended to allow users to freely share, modify, and use this Dataset while maintaining this same freedom for others, provided that the original source and author(s) are credited.

Link: https://doi.org/10.3897/fr.26.102128.suppl1

Supplementary material 2

Morphospaces of four granicone measurements from PCA ordination

Authors: Walter G. Joyce, Serjoscha W. Evers, Sara Ren, Yann Rollot, Achim H. Schwermann

Data type: figure (pdf file)

Explanation note: Morphospaces of four granicone measurements from PCA ordination (N = 165). A–B, bivariate morphospaces including size variation. C–D, morphospaces corrected for size and allometry. A, PC1 vs. PC2. B, PC2 vs. PC3. C, PC2 vs. PC3. D, PC2 vs. PC4. The proportion of variance explained by PC axes are indicated in the axis labels, whereby values in A–B represent total variance (including size) and values in B–C represent shape variance (re-scaled to exclude PC1). In contrast to fig. 5, specimen labels are provided for all datapoints.

Copyright notice: This dataset is made available under the Open Database License (http://opendatacommons.org/licenses/odbl/1.0). The Open Database License (ODbL) is a license agreement intended to allow users to freely share, modify, and use this Dataset while maintaining this same freedom for others, provided that the original source and author(s) are credited.

Link: https://doi.org/10.3897/fr.26.102128.suppl2

Fossil Record 26 (1) 2023, 135–149 | DOI 10.3897/fr.26.99096

New findings of *Prototherium ausetanum* (Mammalia, Pan-Sirenia) from paving stones in Girona (Catalonia, Spain)?

Manja Voss[1,2], Oliver Hampe[1,3], Kristin Mahlow[1], Joan C. Vilanova[4]

1 *Museum für Naturkunde Berlin, Leibniz-Institut für Evolutions- und Biodiversitätsforschung, Invalidenstraße 43, 10115 Berlin, Germany*
2 *Leibniz-Institut zur Analyse des Biodiversitätswandels, LIB, Martin-Luther-King-Platz 3, 20146 Hamburg, Germany*
3 *Institut für Geologische Wissenschaften, Fachrichtung Paläontologie, Freie Universität Berlin, Malteserstr. 74-100, 12249 Berlin, Germany*
4 *Department of Radiology, Clínica Girona, Institute of Diagnostic Imaging (IDI)-Girona, Faculty of Medicine, University of Girona, Girona, Spain*

https://zoobank.org/9DBCF75B-FCBC-47F1-B6EC-24FC9991B4BF

Corresponding author: Oliver Hampe (oliver.hampe@mfn.berlin)

Academic editor: Torsten Scheyer ♦ **Received** 21 December 2022 ♦ **Accepted** 24 May 2023 ♦ **Published** 20 June 2023

Abstract

Taxonomic and morphological approaches on Eocene sirenians from Catalonia (Spain) benefit from a newly discovered specimen found in a quite unusual locality, the pedestrian zone in the city of Girona. Two fossil-bearing limestone slabs from middle Eocene (Bartonian) layers of a quarry in the wider surrounding area north-west of Barcelona, were CT-scanned in the Clínica Girona to enhance more detailed investigations. Post-processing of the scans and, as far as possible, 3D-reconstruction of the preserved elements in the slabs was performed at Museum für Naturkunde Berlin. Thereby, a skull of a *Dugong* specimen was used as a reference point. Based on the combined analysis of macroscopic and CT-data, the specimen most likely represents *Prototherium ausetanum* Balaguer & Alba, 2016 and complements the available information of the holotype and hitherto only known specimen of that species. The Girona specimen is an adult, but small individual that corroborates *P. ausetanum* as a generally small-sized species compared to other known *Prototherium* taxa.

Key Words

3D-visualisation, CT-scanning, Eocene, morphology, taxonomy, urban fossil

Introduction

In a preceding study (Voss et al. 2019), one of the oldest sirenian remains in Europe found under peculiar circumstances was introduced to the scientific community and the wider audience of citizen scientists and the general public interested in geological heritage and geotourism.

Two limestone slabs from the late middle Eocene of Sant Vicenç de Castellet (Catalonia, NE Spain, Fig. 1) were once processed in a pedestrian pavement in the city of Girona and were recently detected to contain remains of an extinct sirenian, a large, herbivorous marine mammal. Based on macroscopic investigations and first CT-data, the fossil find could be confirmed as belonging to a single specimen (Voss et al. 2019). As such, it is a particularly lucky circumstance that the two fossil-bearing slabs have been placed precisely next to each other. Furthermore, Voss et al. (2019) could limit the relative age of the specimen and its taxonomic identity. Mainly judging from the dental formula, this sea cow material represents a young adult belonging to the genus *Prototherium*.

The objective of this follow-up article is to verify the preliminary results from Voss et al. (2019) by resolving other still outstanding issues. The latter refers especially to the taxonomic assignment on the species level. For the time being, the Girona sea cow is tentatively assigned to *P. ausetanum* considering the palaeobiogeographic and stratigraphic background. If this can be confirmed, this specimen would complement the available information of the holotype, and hitherto only known specimen, of *P. ausetanum* described by Balaguer and Alba (2016). Based on CT-data and subsequent 3D-reconstruction of

Copyright *Manja Voss et al.* This is an open access article distributed under the terms of the Creative Commons Attribution License (CC BY 4.0), which permits unrestricted use, distribution, and reproduction in any medium, provided the original author and source are credited.

Figure 1. Panoramic view of the SW side of the limestone quarry southeast of Sant Vicenç de Castellet showing the massive blocks of Bartonian carbonates bound by micritic matrix, and containing besides macroforaminifers, such as nummulites and discocyclinids, bryozoans, corals, and bivalves vertebrate remains (here described: MAC GIR-042375).

the preserved sea cow remains, the identification of additional diagnostic features referring to the snout region, the dentition, and the basicranium is uncovered. As a consequence, this allows a more accurate morphological and taxonomic interpretation of the Girona specimen. In light of the wider picture, this study will help to better understand the evolutionary history and diversity especially of Eocene sirenians.

Material and methods

For this subsequent and complementing article on fossil remains of a sea cow found in two slabs in the pedestrian zone in the city of Girona, CT-scans made at the Clínica Girona were analyzed in detail as best as possible. The CT used here was a GE light speed Optima CT520 (General Electric Company, GE Healthcare, Chalfont St Giles/UK) and was utilized under the following protocol parameters: slice thickness 0.625 mm; space 0.31 mm; pitch 0.56 mm; single collimation width 0.625 mm; pixel spacing 0.4 × 0.4; matrix 512 × 512; field of view 250 mm; convolution kernel: Boneplus; tube voltage and stabilizer 120 kVp, 140 mA. Post-processing of the scanned slabs, i.e., segmentation of the individual bones and the combination of the separate section planes in 3D, is hampered by inclusions of iron-rich minerals and by the characteristic thick and dense sirenian bones itself keeping the contrast between bone and surrounding limestone relatively low. Nevertheless, the individual bones could be segmented and combined in 3D allowing further morphological examination of the skull. Analysis and visualization of the CT-data were performed with VGStudio MAX 2.2.

The taxonomic-morphological comparisons of the Girona specimen MAC GIR-042375 are based almost solely on personal investigations of the taxa for comparison. This refers to *P. veronense* De Zigno, 1875 and *P. intermedium* Bizzotto, 1983 from the Bartonian and Priabonian of North Italy, respectively, stored at MGPD (MV). In each case, the holotype and associated specimens were investigated as is provided by Voss (2013: appendix 2). One of the results of Voss' (2013) study is a phylogeny of Sirenia based on a revised character-taxon matrix. This implies that the character coding of all considered sirenian taxa, including *P. veronense* and *P. intermedium*, was verified and, if necessary due to personal observations, adjusted. Morphological characters that are relevant here and scored contrary to other studies (e.g., Domning 1994; Díaz-Berenguer et al. 2018, 2022) are also stressed in the comparative Description chapter. Moreover, the holotypes, and hitherto only known specimens, of *P. montserratense* and *P. solei* Pilleri et al., 1989 were personally examined at MGSB (MV, OH). The holotype MGSB 44892 of *P. montserratense* from Castellbell i el Vilar (Catalonia, Spain) is

embedded in the surrounding sediment, but still reveals a number of cranial and postcranial elements that represent "probably a complete animal" (Pilleri et al. 1989: 37). Reference to selected material is provided in the chapters Description and Discussion when relevant for comparison. The holotype MGSB 48657 of *P. solei* from Tona (Catalonia, Spain) represents a partially preserved specimen. Thereof, the following elements were investigated: a skullcap including the frontal, parietal, supraoccipital, and the left zygomatic process of the squamosal (MGSB 48657-1), the left mandibular ramus with M_{1-3} (MGSB 48657-2), a premaxillary fragment (MGSB 48657-3), the partially preserved maxilla with molars (MGSB 48657-4), and the left humerus (MGSB 48657-8). Comparisons with *Prototherium ausetanum* are based on the morphological descriptions from Balaguer and Alba (2016).

Institutional abbreviations

MAC, Museu d'Arqueologia de Catalunya, Girona, Spain; **MGPD,** Museo di Geologia e Paleontologia, Padova, Italy; **MGSB,** Museu Geològic del Seminari de Barcelona, Spain; **RGHP**, Réserve géologique de haute Provence, Digne-les-Bains, France; **ZMB**, Museum für Naturkunde Berlin, Zoological Collection, Germany

Systematic palaeontology

Class Mammalia Linnaeus, 1758
Afrotheria Stanhope et al., 1998
Tethytheria McKenna, 1975
Pan-Sirenia O'Leary et al., 2013
Genus *Prototherium* de Zigno, 1887

***Prototherium* cf. *ausetanum* Balaguer & Alba, 2016**

Nomenclatural remark. The present systematic palaeontology considers the quite recently established clade Pan-Sirenia, O'Leary et al., 2013. Thereby, O'Leary et al. (2013: supplementary material, table 4) apply the total group concept (Jefferies 1979) and distinguish between Pan-Sirenia as representing the total clade of Sirenia Illiger, 1811, whereas Sirenia is redefined and restricted to the node-based crown group as the least inclusive clade containing all living sirenians, their last common ancestor, and all of its descendants. The same concept is introduced later again by Vélez-Juarbe and Wood (2018). Therefore, priority, and hence reference for Pan-Sirenia, is given here to O'Leary et al. (2013).

Material. MAC GIR-042375, partial skull and rib remains documented in urban paving stones of Girona, Catalonia, Spain.

Locality. Limestone quarry south of Sant Vicenç de Castellet, central Catalonia, Spain.

Stratigraphic position. Late Bartonian, middle Eocene. The age of the find is corrected from early Bartonian (Voss et al. 2019) to late Bartonian (Galindo et al. 2003).

Description

The sirenian remains are embedded in a shallow carbonate platform sediment consisting of an alternation of biomicritic limestones, lutites and bluish-grey claystones (Figs 1, 2), and are distributed on two slabs, each measuring 2 cm in thickness. The preserved elements mainly belong to the skull of a single specimen and include parts of the rostrum (premaxilla and maxilla), frontal, vomer, basicranium, and fragments of the zygomatic arch (jugal and squamosal). From the teeth, the upper molars M^1-M^3 including crowns and roots are preserved. Otherwise, the dentition is indicated by the presence of alveoli. In addition to the macroscopic analysis, CT-scanning and post-processing allow more detailed morphological examination of the preserved skull parts. As already performed in Voss et al. (2019), the slab preserving a relative upper region of the skull roof and snout is designated as slab 1, the other representing a relatively deeper level within the skull is designated as slab 2 (Fig. 3).

The first new observation refers to the orientation of the single fossil-bearing slabs. With the help of an adult skull of the extant dugong (*Dugong dugon*, ZMB_MAM 69306), the partial skull was aligned in an anatomically correct position mainly considering the slope of both, the jugal and the rostrum. As a result, each slab shows oblique angles in the transversal plane, hence do not lie one-to-one at that specific level. For slab 1, the angles are 28.22° in lateral view, and 4.3° in frontal view; for slab 2, the angles are 28.22° in lateral view, and 6.0° in frontal view, respectively (Fig. 3a, b). This explains, amongst others, why each slab preserves skull elements from a vertically higher level on the right side and from a somewhat lower level on the left side. The same applies to the antero-posterior orientation of the slabs, which accordingly show skull elements from a lower level anteriorly and cranial parts from a higher level posteriorly. As it will be outlined below, the oblique orientation sometimes impedes the correlation of specific structures between the slabs, which resulted in amendments as to some observations made in Voss et al. (2019).

The distance between both slabs could be ascertained to be 11.4 mm (Fig. 3). As such, a total of 50 mm, i.e., 40 mm fossil-bearing stone plus circa 10 mm non-preserved interspace, is the basis for this study. This equals about 50% to 77% of the height of a typical Eocene-Oligocene sirenian skull (Voss 2013: appendix 3, Measurements of crania: top of supraoccipital to ventral sides of occipital condyles (de)).

Furthermore, the preliminary results by Voss et al. (2019) on the individual age and the taxonomic assignment of the Girona find can be verified.

Voss et al. (2019) determine the Girona specimen as representing at least a young adult based on the advanced

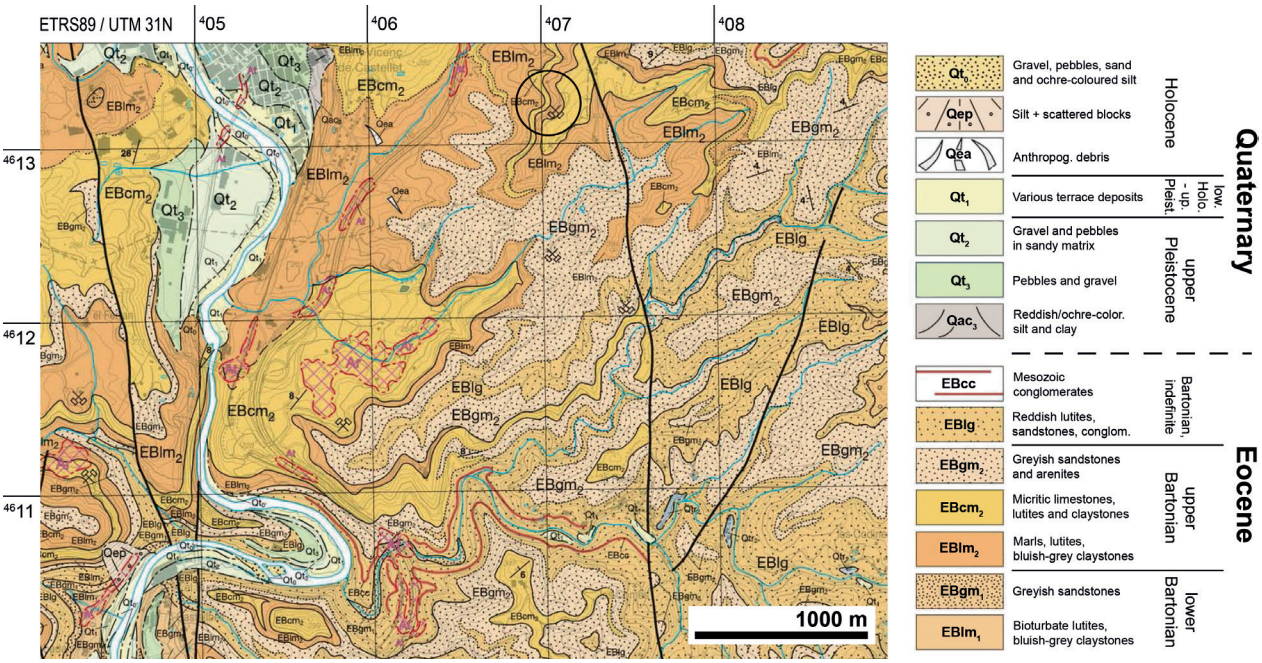

Figure 2. Modified extract from the geological map (Mapa geològic de Catalunya 1:25 000, Monistrol de Montserrat 392-1-1 (71-29)) showing the position of the limestone quarry (circle: SE Sant Vicenç de Castellet, E of Llobregat river) from which the pavement slabs containing the MAC GIR-042375 *Prototherium* cf. *ausetanum* remains came from. All sediments from this area are dated to the late Bartonian.

state of wear of the M^3 and its position at the level of the posterior margin of the zygomatic orbital bridge (Mitchell 1973). At this point, an amendment to the preceding description in Voss et al. (2019) is necessary. While the position of the M^3 is confirmed in macroscopic view and in the CT-scans (Voss et al. 2019: fig. 6b, c), the position of M^{1-2} as shown in slab 1 (Voss et al. 2019: fig. 6a) has to be adjusted. The two visible alveoli in the latter figure belong most certainly to P^4-P^3 considering the higher anatomical level of slab 1 combined with the transversally non-planar cut of the slabs (Fig. 4a).

For relative age determination, it is also highly indicative whether sutures between certain bones are open, fused or even obliterated (Pocock 1940; Mitchell 1973). The contact between the basisphenoid and basioccipital is especially important for the identification of adulthood. Elements of the basicranium are clearly and best visible on the unpolished bottom side of slab 1 (Fig. 4a) showing parts of the basisphenoid, the spheno-occipital eminences, and the basioccipital that is mainly preserved with its left extension. The anterior ends of the spheno-occipital eminences mark the approximate contact between basisphenoid and basioccipital. Both bones are considered as being firmly fused, since there is no indication of a suture. This is also confirmed in the respective CT-Scan (Fig. 4b) despite interferences that reduce the scan quality. Consequently, the Girona specimen definitively belongs to an adult individual.

With respect to the taxonomic assignment, Voss et al. (2019) identified the Girona sea cow as a representative of the Eocene genus *Prototherium* (and finally *P. ausetanum*) based on the antemolar dental formula. This is corroborated also in this study and observable in slab 2 (Fig. 5). Thereby, Fig. 4a reflects mainly alveoli in macroscopic dorsal view of slab 2 and Fig. 4b shows the corresponding CT-scan with teeth in ventral view of slab 2. As a result, four alveoli for single-rooted premolars (P^{1-4}) can be unambiguously ascertained (Fig. 5a). The complete number of premolars reflects plesiomorphic conditions and is characteristic for Eocene sirenians (e.g., Voss 2013). The most important feature is the absence of a persistent DP^5, a molariform upper deciduous fifth premolar, which is a peculiarity in the dental formula of *Prototherium* (e.g., Domning 1994; Bizzotto 2005; Balaguer and Alba 2016). While also the lack of DP^5 can be deduced directly from the preserved maxillary parts on the slabs, the presence and absence of alveoli is hardly observable in the corresponding CT-Scan even after careful post-processing and evaluation of the ventral side of the slab (Fig. 5b). This is primarily based on the fact that the contrast between sirenian bone and surrounding matrix is relatively low. Additionally, inclusions of iron-rich minerals cause harmful interferences.

Nevertheless, the present results support the Girona specimen as belonging to the genus *Prototherium*. As such, its identification on the species level focusses on comparisons with three *Prototherium* species generally considered valid: *P. veronense* De Zigno, 1875 from the late middle Eocene (Bartonian) of Verona (Italy), *P. intermedium* Bizzotto, 1983 from the late Eocene (Priabonian) of Possagno (north-east from Verona, Italy), and the recently established *P. ausetanum* Balaguer & Alba, 2016 from the Bartonian of Tona (Catalonia, Spain). Additionally, the taxonomic-morphological comparisons are complemented by two further

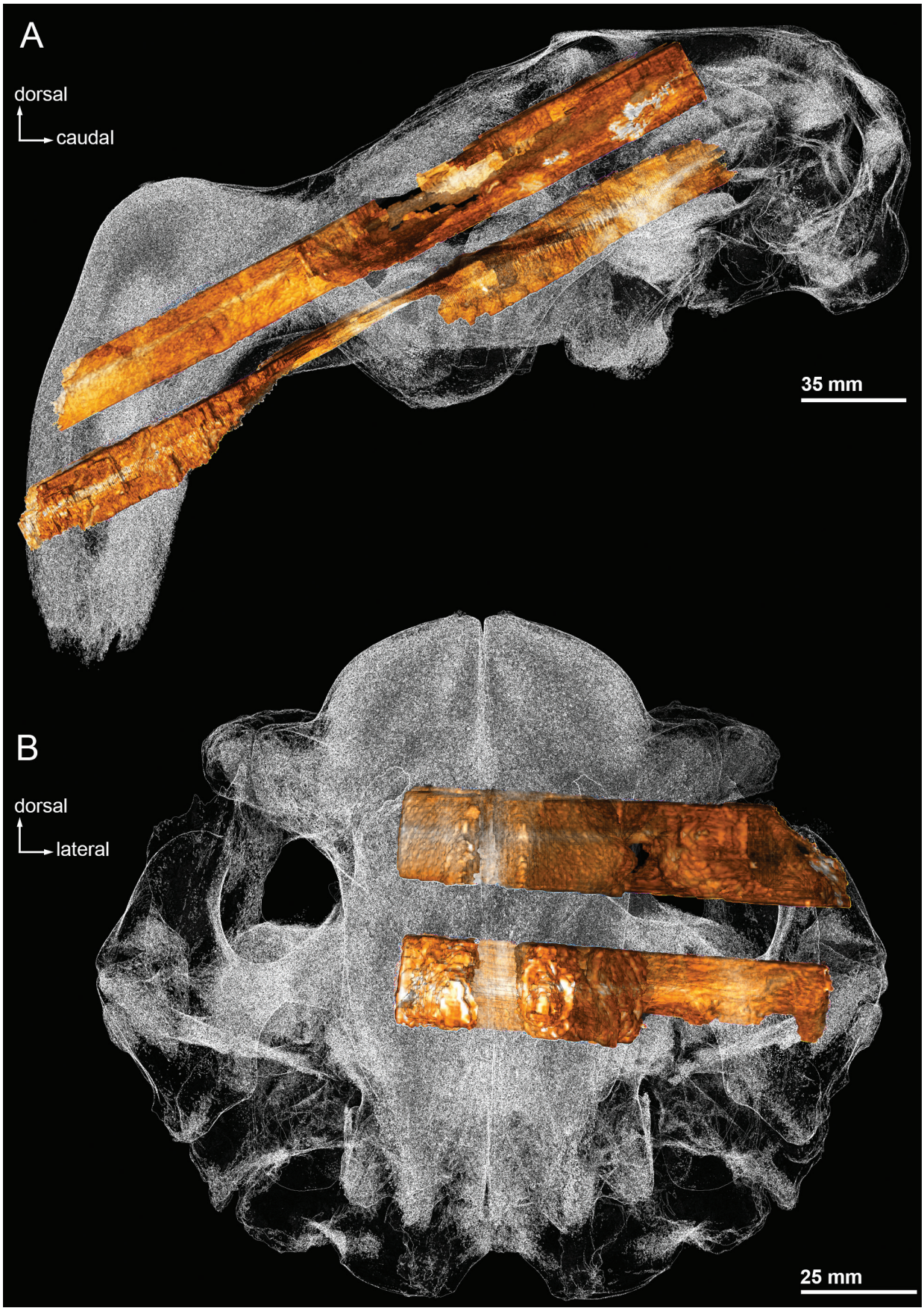

Figure 3. Spatial orientation of the fossil-bearing slabs in **A.** Lateral view; **B.** Frontal view. CT-scans of the upper slab 1 and the lower slab 2 (both in color) are aligned in an anatomically correct position using the extant dugong as reference (grey-scaled CT-scan of *Dugong dugon* ZMB_MAM 69306).

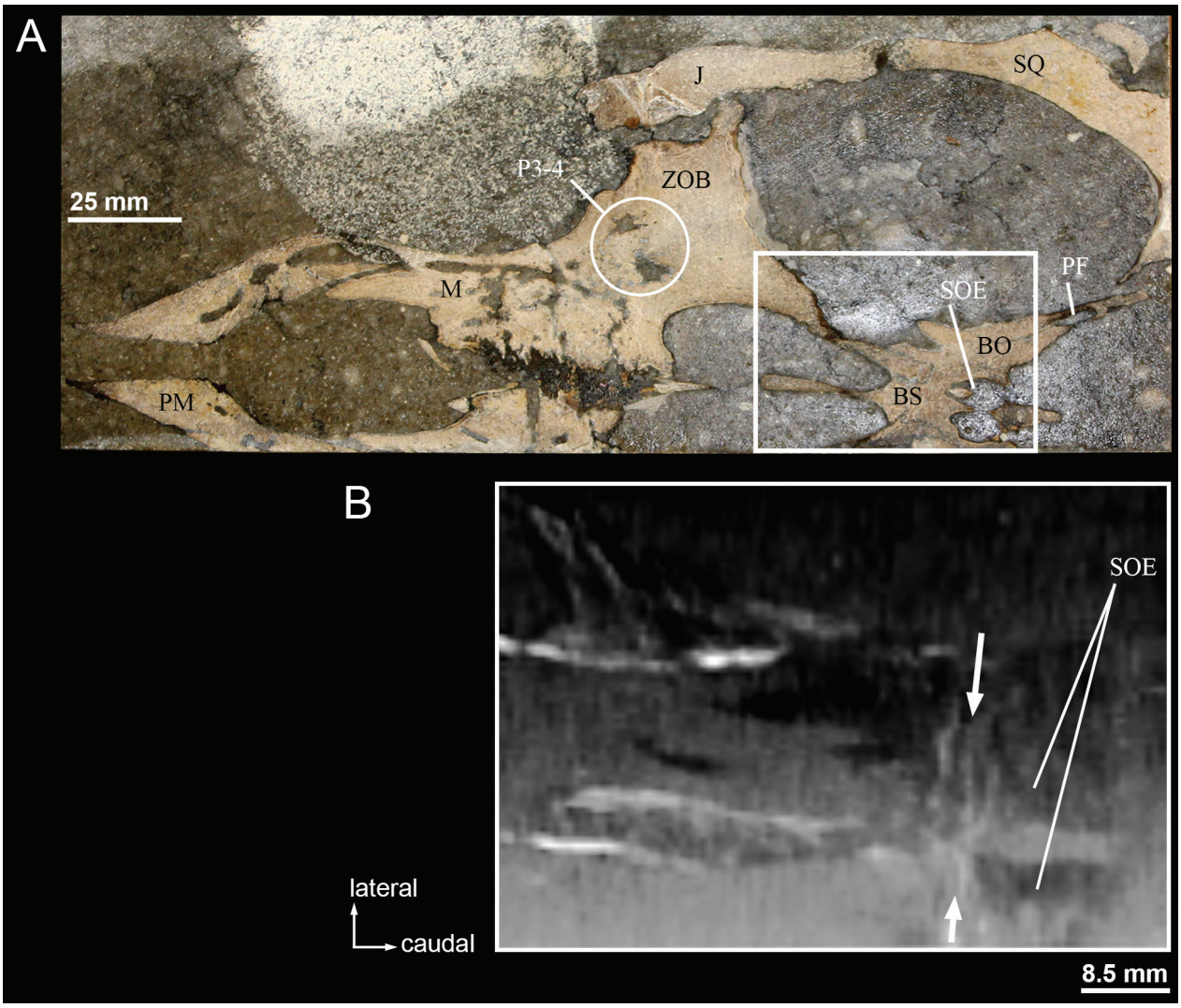

Figure 4. *Prototherium* cf. *ausetanum*, MAC GIR-042375. **A.** Photograph; **B.** Corresponding CT-scan of slab 1 with focus on the basicranium. The unpolished bottom side of slab 1 (**A**) shows parts of the basisphenoid, the spheno-occipital eminences, and the basioccipital, all of which being firmly fused indicating adulthood. The CT-Scan of the basicranium (**B**) shows interferences, however, the suture between basisphenoid and basioccipital is unequivocally obliterated and estimated to be more or less level with the vertical interference (indicated by arrows). Abbreviations: BO, basioccipital; BS, basisphenoid; J, jugal; M, maxilla; PF, pharyngeal fossa; PM, premaxilla; P^{3-4}, third and fourth upper permanent premolars; SOE, spheno-occipital eminences; ZOB, zygomatic-orbital bridge of maxilla.

Prototherium species from the Bartonian of Catalonia, *P. solei* Pilleri et al., 1989 and *P. montserratense* Pilleri et al., 1989. As it will be discussed later, their status and affinities are uncertain (e.g., Domning 1996; Bizzotto 2005; Balaguer and Alba 2016). However, the geographic and stratigraphic occurrence of both species raise particular relevance for the comparison with specimen MAC GIR-042375 from Girona.

The subsequent new results on the morphology and taxonomy of the Girona specimen include additional data on the premaxilla, the maxilla (zygomatic-orbital bridge), the basicranium, and the dentition. All comparative descriptions rely on the preserved features only.

For the premaxilla, plesiomorphic conditions of the dental formula have been assumed by Voss et al. (2019). However, analyses of the CT-scans do not allow drawing further conclusions on this. While one pair of upper incisor tusks (I^1) is clearly indicated by distinct alveoli and verified by both, macroscopic and CT-data (Fig. 5a, b), further alveoli, i.e., for a second and third upper incisor (I^{2-3}), cannot be ascertained from the CT-scans. Although the premaxillary dental formula is known to be complete in *P. veronense* and *P. intermedium* and hence would not provide a distinctive feature on species level here, the morphological information of the Girona specimen remains limited in this regard. As such, the available data of the holotype of *P. ausetanum* cannot be complemented assuming that the Girona sea cow is a representative of that species. The same applies to *P. solei* and *P. montserratense*. While *P. solei* shows an incomplete premaxilla that does not reveal informative characters relevant here, the premaxilla of *P. montserratense* is temporarily not accessible, because the holotype specimen is still embedded in sediment.

Further preserved diagnostic features of the premaxilla refer to the length of the alveolus for the first upper incisor

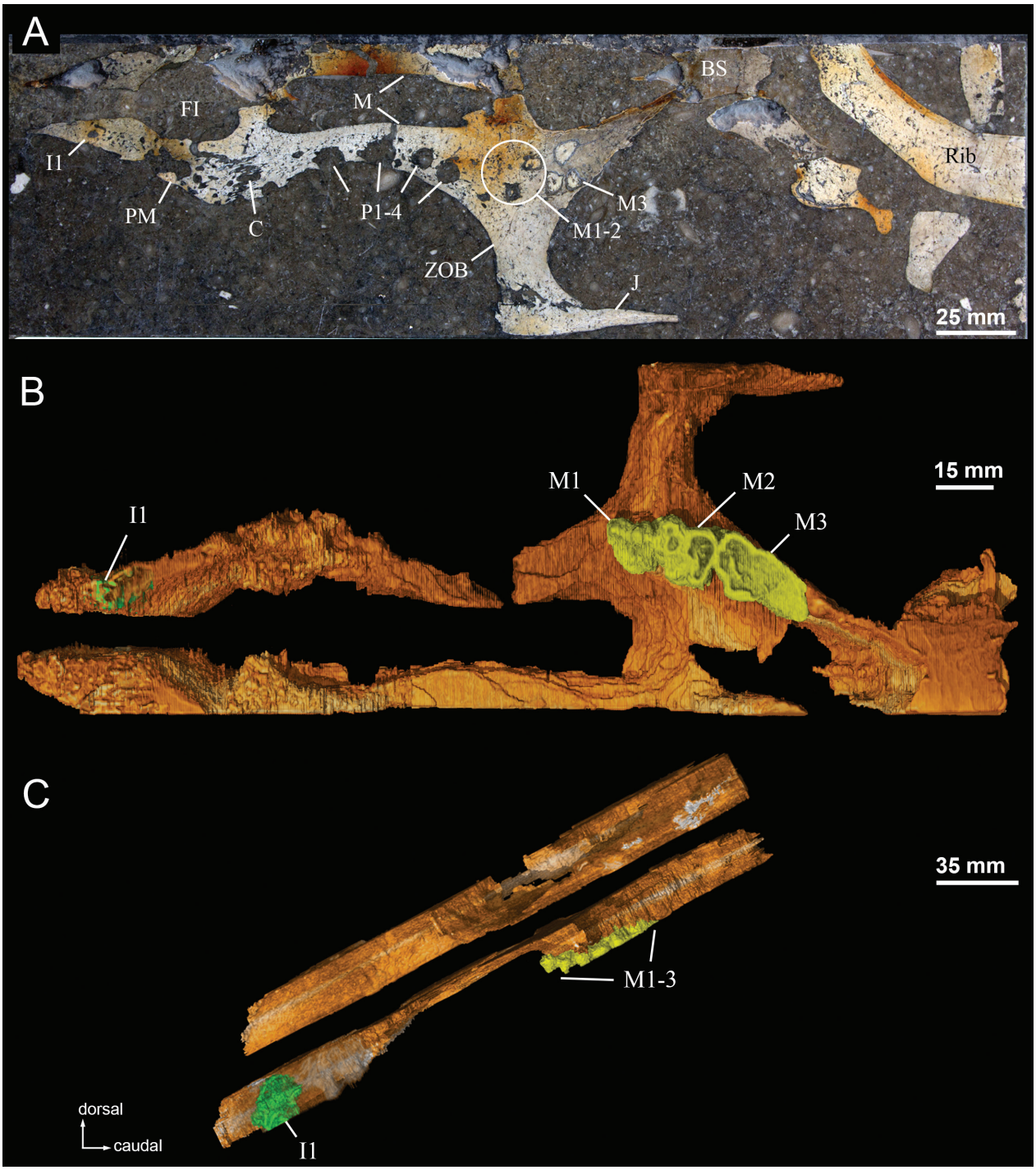

Figure 5. *Prototherium* cf. *ausetanum*, MAC GIR-042375. **A.** Photograph showing the dorsal side of slab 2; **B.** Corresponding CT-scan showing the ventral side of slab 2 focusing on the dentition; **C.** CT-scans of anatomically correct combined slab 1 and 2 in lateral view. The CT-scan of the lower side of slab 2 (**B**) reveals the crowns of the upper molars 1–3 (M^{1-3}) with the M^3 fully erupted and clearly in wear. Abbreviations: BS, basisphenoid; C, upper canine; FI, foramen incisivum; I1, first upper incisor; J, jugal; M, maxilla; M^{1-3}, first to third upper molars; P^{1-4}, first to fourth permanent upper premolars; PM, premaxilla; ZOB, zygomatic-orbital bridge of maxilla.

(I^1). Slab 2 reveals the alveoli of both I^1 (Fig. 5a, b). While the alveolus on the right side is distorted by inclusions, the one on the left side is already shown to be tapered dorsally indicating the uppermost part of the alveolus (Fig. 5c). Slab 2 represents the lower 2 cm of the preserved partial skull with the left side reflecting a more ventral level than the right side. Hence, it is plausible to conclude that the left I^1 alveolus definitively did not exceed half the length of the premaxillary symphysis considering slab 1 and the interspace between slab 1 and 2, both commencing at least 3 cm (Fig. 5c). Moreover, it is likely that the I^1 alveolus extends even less than half the length of the symphysis similar to *P. veronense* and *P. intermedium* (re-scored by Voss 2013: character 157), even though it is not exactly

clear how much of the dorsalmost and ventralmost parts of the premaxilla are missing in MAC GIR-042375.

Another morphological feature with diagnostic value is related to the position of the zygomatic-orbital bridge of the maxilla with respect to the palate (e.g., Domning 1994: character 11; Voss 2013: character 21; Springer et al. 2015). According to Balaguer and Alba (2016), it is more or less level with the alveolar plane in *P. ausetanum* (about 6 mm above the tooth arcade). This is also the case with the Girona specimen as can be inferred from the CT-Scan shown in Fig. 4c. In fact, the zygomatic-orbital bridge in MAC GIR-042375 is even on the same level with the tooth arcade. While this condition is also observable in *P. solei*, this is a strong contrast compared to *P. veronense* and, according to personal observations also to *P. intermedium*, where the zygomatic-orbital bridge is elevated above the palate, with its ventral surface lying more than 15 mm above the alveolar margin (Voss 2013). In *P. montserratense*, the zygomatic-orbital bridge is not accessible.

The morphology of the basicranium may have very likely diagnostic value. As stated above, the basisphenoidal-basioccipital region is preserved, which is best visible in macroscopic view of slab 1 (Fig. 4a). Amongst sirenians, the shape of the spheno-occipital eminences varies in either being concave or convex, and therefore, may provide differences at species level (Voss 2013). While these are convex in *P. veronense* and *P. montserratense*, they are concave in *P. intermedium*. This is a similarity with the Girona sea cow MAC GIR-042375. The postulated concavities at this level in macroscopic view are supported by the respective CT-scan (Fig. 4b). In *P. ausetanum*, this character cannot be assessed, because the respective area is incomplete, covered by sediment and deformed insofar that bony material from the right side overlay the posteroventral region of the skull (Jordi Balaguer 2023, pers. comm.). In *P. solei*, the basicranium is not preserved.

At this point also a correction as to the presence of a hypoglossal foramen is made (Voss et al. 2019: fig. 6a). CT-scanning and post-processing do not confirm a hypoglossal foramen on the left side of the basioccipital. Instead, the visible "foramen" in Fig. 4 is either the result of an inclusion or it could be a ventral excavation in the basioccipital, a pharyngeal fossa (PF). However, a hypoglossal foramen, if present in that species, would be positioned more caudad within the basioccipital.

Moreover, our examination of the preserved M^{1-3} crowns in deeper levels of slab 2 further helps to substantiate the taxonomic identity of the Girona specimen (Fig. 5a). Compared with the species of *Prototherium*, it shows differences in the mesiodistal length of the molars (Table 1). The M^1 in MAC GIR-042375 is generally smaller than in the three *Prototherium* taxa hitherto considered valid with a deviation of about 16% and 21% in *P. veronense* and *P. intermedium*, respectively, but only 2% in *P. ausetanum* if the M^1 from the left side is compared. The M^2 is also distinctly smaller than in *P. veronense* and *P. intermedium* having a difference of 18% and 9.5%, respectively, but it is about 5% larger than in *P. ausetanum*. With the exception of *P. intermedium*, which lacks respective information (presumably, because both M^3 in the holotype are not fully measurable according to personal observations), the mesiodistal length of the M^3 in the Girona sea cow is 11% and 5% smaller than in *P. veronense* and *P. ausetanum*, respectively.

Extending the comparisons upon the preserved M^{2-3} in *P. solei* and *P. montserratense* from Spain unveils interesting results. The M^{2-3} in MAC GIR-042375 (and in *P. ausetanum*) is about 13% and 12% larger than in *P. solei*, respectively, making the latter species the smallest in terms of the molar dimensions. However, compared with *P. montserratense*, the M^{2-3} are almost as large as in MAC GIR-042375 (Table 1). Taken together, these measurements point to a sirenian that is rather small compared with the *Prototherium* taxa from Italy, but that is very similar in size compared with *P. ausetanum* and *P. montserratense* from Spain.

Table 1. Mesiodistal length of molars M^{1-3} of the "Girona specimen" MAC GIR-042375 compared to other *Prototherium* species: data for *P. veronense* and *P. intermedium* are taken from Pilleri et al. (1989: table VII), and data for *P. ausetanum* are from Balaguer and Alba (2016: table 2). Measurements for *P. solei* and *P. montserratense* were taken personally and are similar or correspond, respectively, to Pilleri et al. (1989: table on page 19 and table XIII). l and r correspond to measurements from the left and right side, respectively.

	mesiodistal length in mm		
	M^1	M^2	M^3
P. veronense (cast of holotype)	16	21	23
P. intermedium (holotype)	17	19	/
P. ausetanum (holotype)	13.8 l / 15.5 r	16.3 l / 16.6 r	21.6 l / 21.4 r
Girona specimen (MAC GIR-042375)	13.5	17.2	20.5
P. montserratense (holotype)	/	17	21
P. solei (holotype)	/	15	18

Another molar feature to distinguish MAC GIR-042375 refers to the shape of the M^{2-3}. Except for *P. ausetanum*, all taxa for comparison show a trapezoid M^2, with the protoloph each wider than the metaloph, whereas in both, MAC GIR-042375 (Fig. 5b) and *P. ausetanum* (Balaguer and Alba 2016: fig. 4), the proportions of the lophs are similar resulting in a rather rectangular outline of the M^2. Similarly, the M^3 is trapezoid in all *Prototherium* species from Italy and Spain, but not in MAC GIR-042375 (Fig. 5b) and *P. ausetanum* (Balaguer and Alba 2016: fig. 4) where the M^3 is rather oval and tapering distad.

In the following, the description of specimen MAC GIR-042375 is complemented with regard to the preserved morphology visible in slab 1 (Fig. 6) in order to provide overall insights to the reader.

The CT-scan of the slab represents a relatively deep level of the upper part of the skull (Fig. 6b).

After post-processing, the nasal area could be made well visible by reconstructing the extension of the vomer. The vomer is a mediolaterally thin element and triangular

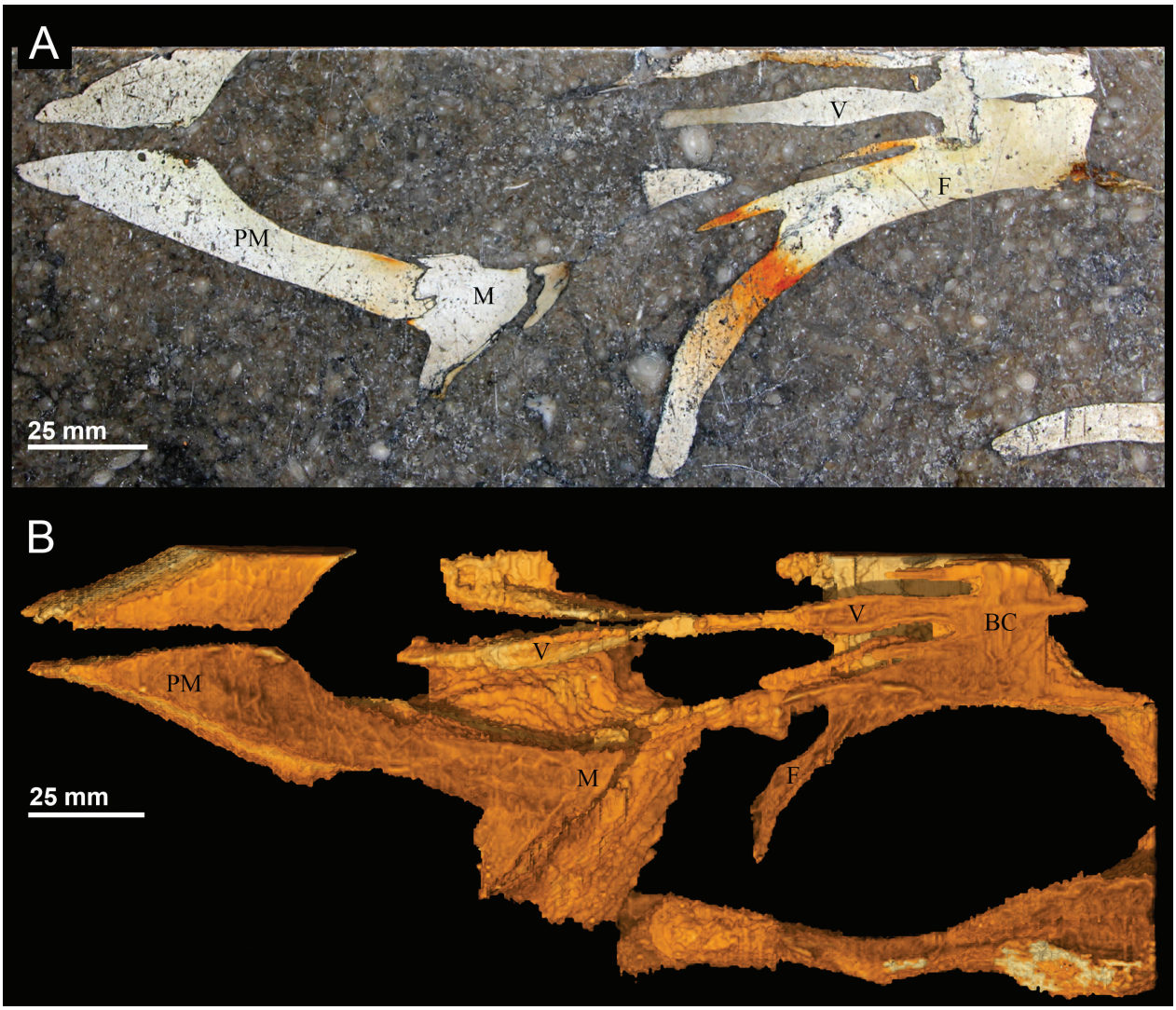

Figure 6. *Prototherium* cf. *ausetanum*, MAC GIR-042375. **A.** Photograph; **B.** Corresponding CT-scan of slab 1 providing data on the overall morphology of the specimen. Abbreviations: BC, basicranium; F, frontal; M, maxilla; PM, premaxilla; V, vomer.

in cross section as in other sirenians. It passes through most of the internal narial passage, contacts the maxilla laterally (and most likely the palatine, that, however, cannot be distinguished here) and extends in a longitudinal groove on the dorsal surface of the maxilla slightly forward into the mesorostral fossa (external nasal opening). Anteriorly, the vomer builds up the nasal septum. Posteriorly, the vomer runs indistinctly out into the basicranium.

On the left side, parts of the frontal are visible with the slightly downturned supraorbital process. A complex of remnants of the left jugal anteriorly and the left zygomatic process posteriorly indicate the zygomatic arch of the squamosal.

Discussion

The analysis of the CT-Scans resulted in a genuine added value in terms of supplemented morphological data that allow for a more coherent taxonomic assignment of the Girona sea cow.

First of all, this specimen is undoubtedly considered as representing a *Prototherium* species. As mentioned above, the key characteristic for the genus *Prototherium* is the lack of a persistent DP^5/ DP_5 (e.g., Domning 1994; Bizzotto 2005; Balaguer and Alba 2016) that is also supported in this study.

Taking into account observations in more derived sea cows, i.e. members of the Dugonginae that show mesial drift of their molars and, as a consequence, lose preceding teeth in lifetime, one can argue that there may have been an unreplaced DP^5 that was worn out and shed given the advanced age of the Girona specimen. The gap between P^4 and M^1 would then have been closed by mesial drift. Although this is an interesting perspective, it is likewise a difficult one. For example, there are two specimens known from Eocene strata representing adults of "*Halitherium*" *taulannense* that show irregular resorption of DP^5/DP_5 (holotype skull RGHP D040 and paratype mandible RGHP E.7.096a (Voss 2013)). The respective specimens reveal traces of resorption in so far that the area between P^4/P_4 and M^1/M_1 is roughened and spongy,

but still retracing the former alveoli. Mesial drift however is not indicated in those specimens.

Traces of resorption are commonly present in specimens that are known to have lost teeth due to mesial drift, especially amongst members of the subfamily Dugonginae that are characterized by the reduction of the antemolar dentition (e.g., Domning 1989). According to Luckett (1993), resorption can take place in different degrees. For example, this is observable in the maxilla of *Dioplotherium manigaulti* Cope, 1883 in which the antemolar area is characterised by bone-filled, degenerated alveoli indicating the former presence of deciduous premolars; the only distinct socket remaining in this roughened area is for the lingual root of the originally three-rooted DP^5 (Domning 1989). Exactly such traces of resorption are missing in the Girona specimen. Instead, the area between P^4 and M^1 appears to be unsuspicious as are the roots of the preserved molars that do not indicate mesial drift (Fig. 5a, b). Consequently, the lack of a persistent DP^5/DP_5 as a generic distinguishing feature for *Prototherium* is not questioned here.

Although the data basis remains limited not at least due to the lack of material between and in each of the two fossil-bearing slabs, the present study provides a combination of characters that argues with the utmost probability for the Girona specimen as being a representative of *P. ausetanum*. Two characters corroborate that hypothesis on the species level and refer to the shape of the M^2 and M^3. As outlined above, only MAC GIR-042375 and *P. ausetanum* share a rectangular M^2 as well as an oval M^3. Three further characters that do not argue unambiguously for a taxonomic assignment to *P. ausetanum*, but can be put into perspective, refer to the mesiodistal length of the molar crowns, the position of the zygomatic-orbital bridge, and the shape of the spheno-occipital eminences. Of all taxa for comparison, the mesiodistal length especially of M^{2-3} is most similar between MAC GIR-042375, *P. ausetanum*, and *P. montserratense*. A zygomatic-orbital bridge nearly level with the alveolar margin is congruent only in MAC GIR-042375, *P. ausetanum*, and *P. solei*. While *P. montserratense* differs from MAC GIR-042375 in having convex spheno-occipital eminences (a morphological feature that is also present in *P. veronense*), personal observations of the holotype specimen also reveal that it is not fully grown. This is indicated by the non-obliterated spheno-occipital suture and the only slightly worn M^3. As such, the subadult age may qualify the current results on the mesiodistal length of M^{2-3} in *P. montserratense*. The material basis of *P. solei* does not provide further morphological characters that can be compared here. However, three differing dental characters as mentioned above versus one shared cranial character, i.e. the level of the zygomatic-orbital bridge, question a taxonomic assignment of MAC GIR-042375 to *P. solei*. Against that background, the feature of concave spheno-occipital eminences in the Girona specimen may potentially supplement the morphological information of the holotype of *P. ausetanum*, which lacks respective data. In fact, these eminences are likewise concave in *P. intermedium*, but the latter differs from MAC GIR-042375 in the dental features outlined above and in that the zygomatic-orbital bridge is clearly elevated above the alveolar margin. As such, the fossil sea cow remains from Girona resp. Sant Vicenç de Castellet contribute to more and new information that enhance and supplement our knowledge on the morphology and, considering the similar age and area, distribution of *P. ausetanum*.

In addition to the morphology, the stratigraphy and palaeogeography implicate, at least in part, new hypotheses on the taxonomic identity of the species for comparison, which, conversely, support the assignment of MAC GIR-042375 to *P. ausetanum*. In the Bartonian, potentially four *Prototherium* taxa are present in southern Europe: *P. ausetanum* (including MAC GIR-042375), *P. montserratense* and *P. solei*, each from Spain, and *P. veronense* from Italy. For the latter species, different and sometimes contradictory information on its geological age exist throughout the literature, and therefore, this issue shall be clarified first. Apart from Bizzotto (1983: 106) and Balgauer and Alba (2016), for example, who provided a Bartonian age for *P. veronense*, it is also indicated as coming from late Eocene (Priabonian) strata (Domning 1994, 1996; Zalmout and Gingerich 2012: table 1). Meanwhile, the age of the find locality of *P. veronense*, Monte Duello in the Italian Province of Verona, is considered to pertain to the middle Eocene, i.e. Bartonian (Zorzin et al. 2012; Zorzin and Frisone 2013), making this taxon synchronous with the sirenians from Spain. The only *Prototherium* species coming from stratigraphically younger sediments, i.e. Priabonian, is *P. intermedium* from Italy (Bizzotto 1983; Domning 1996). Interestingly, the stratigraphically older and palaeogeographically more distant species, *P. montserratense* and *P. solei* (Pilleri et al. 1989), are considered synonymous with *P. intermedium*, either both (Domning 1996) or only *P. solei* (Sagne 2001; Balgauer and Alba 2016). New hypotheses about the validity of the synonymously treated species are discussed as follows.

As outlined above, the present study provides morphological information from the not yet fully prepared holotype of *P. montserratense* that is even now valuable for comparison. For the time being, the morphological characters of it presented here argue for a species distinct from *P. intermedium*, hence, neither supporting a synonymy (Domning 1996: 388) nor the status of a subspecies (Bizzotto 2005) with the latter taxon. While Sagne (2001) already refuted the synonymy of *P. montserratense* with *P. intermedium* on a morphological basis, the distinction of both is also reinforced by their stratigraphic and palaeogeographic data. Moreover, *P. montserratense* is not considered a *nomen dubium* (Balguer and Alba 2016) though this treatment is well noted as being only provisional pending further investigations. Instead, similarities with *P. veronense* (and differences with *P. intermedium*) like convex spheno-occipital eminences, may argue for the hypothesis that *P. montserratense* is a subadult representative of the

former, hence potentially synonymous with *P. veronense*. Such synonymy that was also pondered by Balaguer and Alba (2016) would be additionally in accordance with the stratigraphic occurrence of both and the consideration of sirenians as migrating species. This hypothesis finds support through a number of other morphological features that are, however, not present in the object of this study. Taking into account that a taxonomic revision of the genus *Prototherium* is not the scope of the present study, this shall nevertheless be shortly outlined here. For example, *P. veronense* and *P. montserratense* show a ventral border of the horizontal mandibular ramus that is tangent to the angle as well as a posterior border of the mandible that has a distinct steplike process below the condyle, both character states contrasting with *P. intermedium* (Voss 2013: appendix 4). Therefore, it shall be emphasized here that it is highly relevant to examine the holotype specimen of *P. montserratense* completely in order to clarify its status, either as a distinct, and hence valid species, or a synonym of *P. veronense*.

Similarly, *P. solei* is questioned here to be either a junior synonym (Domning 1996; Sagne 2001; Balaguer and Alba 2016) or a subspecies (Bizzotto 2005) of *P. intermedium*. On the one hand, the stratigraphic and palaeogeographic data provide arguments for a distinction of both species. On the other hand, morphological differences like the position of the zygomatic orbital bridge argue against an assignment of *P. solei* to *P. intermedium*. Considering again characters beyond those preserved in the object of this study, the mandibular morphology in *P. solei* reveals an interesting combination of characters. The course of the ventral border of the horizontal ramus that is most likely tangent with the angle resembles that in *P. montserratense* and *P. veronense*, whereas the posterior border of the mandible seems to lack a distinct process below the condyle similar to *P. intermedium*. In summary, *P. solei* demonstrates similarities and, at the same time, differences with all taxa for comparison, including *P. ausetanum* (and MAC GIR-042375). These incongruences illustrate that *P. solei* needs to be carefully reinvestigated in consideration of the other *Prototherium* species aiming at a thorough revision of the genus in total. As such, and for the time being, *P. solei* is provisionally treated as a distinct species according to Pilleri et al (1989).

Further studies could also help to fix the issue of the controversially discussed interrelationships of the genus *Prototherium*, which is shown as para- and polyphyletic in Balaguer and Alba (2016) as well as in the first (Domning 1994) and the most recent (Díaz-Berenguer et al. 2022; Heritage and Seiffert 2022) cladistic analyses of sirenians. In Vélez-Juarbe and Wood (2018), the interrelationships of Eocene sirenians, including *Prototherium*, are not resolved at all, showing a large polytomy. Domning (1996: 388) already assumed that *P. intermedium* is probably generically distinct from *P. veronense*, a hypothesis that has not further developed until to date. Therefore, this issue should be rather addressed after a thorough taxonomic-morphological revision of the genus, including the clarification of the status and affinities of *P. solei* and *P. montserratense* as outlined above.

This approach is particularly suggested in light of an alternative phylogenetic hypothesis that supports the monophyly of *Prototherium* by showing a sister group relationship between *P. veronense* and *P. intermedium* (Voss 2013). This sister grouping is confirmed by a unique combination of homoplasies and a good agreement between the phylogeny and stratigraphy (Voss 2013: fig. 75). Except character 21 referring to the level of the zygomatic-orbital bridge (Voss 2013), none of the features supporting the sister grouping are preserved in MAC GIR-042375. Therefore, Voss' (2013) data set and cladistic analysis shall be updated and tested for stability first before further conclusions on the phylogenetic interrelationships are drawn.

Considering the bigger picture, better-resolved intra- and intergeneric relationships based on new informative fossils such as MAC GIR-042375 have the potential to contribute to a better understanding of the interrelationships of Eocene taxa and sirenians in total. Although this task is beyond the scope of this paper, it shall be outlined here that the classification of Sirenia has long been controversial. In other words: the traditional classification concept of Sirenia, which distinguishes four families (e.g., Domning 1996), is incongruent with the results of phylogenetic analyses of the order. This refers especially to the Dugongidae, the family that *P. ausetanum* is traditionally referred to according to Balaguer and Alba (2016). While only two dugongid groups are consistently revealed as monophyletic, the derived Dugonginae and Hydrodamalinae, Eocene dugongids are conspicuously paraphyletic as well as most of the genera (e.g., Domning 1994; Springer et al. 2015). Additionally, some approaches (e.g. Vélez-Juarbe et al. 2012; Springer et al. 2015) reveal Dugongidae as a clade, whereas other studies, including one of the latest (Domning 1994; Voss 2013; Díaz-Berenguer et al. 2018), do not affirm this hypothesis. Consequently, Eocene sirenians, and Eocene dugongids from the traditional point of view, represent one of the most controversially discussed taxa.

In order to solve this drastic paraphyly problem, Voss (2013) proposed the total group concept (Jefferies 1979) and distinguishes a stem group, which, by definition, is consistently paraphyletic, and a monophyletic crown group within the clade Sirenia, hence setting aside the traditional classification concept of four sirenian families. In the same year, and as already outlined in the Systematic palaeontology chapter, O'Leary et al. (2013) introduced Pan-Sirenia as the most inclusive group comprising all species more closely related to crown-Sirenia than to any other living species. This finds also consideration in the very latest and total evidence phylogenetic analysis by Heritage and Seiffert (2022). As such, Eocene dugongids in the traditional sense (compare previous studies cited above) fall into the stem group of Pan-Sirenia. Most of the more derived dugongids are part of crown-Sirenia and form the more exclusive, but monophyletic Dugongidae

as defined by Heritage and Seiffert (2022). In terms of *P. ausetanum*, this species has to be considered now as a stem-group representative, i.e., a pan-sirenian that falls outside crown-Sirenia.

Palaeobiogeographic overview

Fig. 7 shows a comprehensive selection of Eocene pan-sirenian findings from Central and South Europe, and North Africa, providing an overview on the distribution of that group in this region and time frame.

There is a rough SW-NE direction or tendency of distribution regarding the geological ages of the records. In the southwestern Tethyan area, ear bones from the early Eocene (Ypresian) of Tunisia represent the oldest sea cow remains (Benoit et al. 2013). Although the taxonomic identity of these periotics remains unclear, the morphology of these is even more primitive compared to those from the hitherto earliest known prorastomids (*Prorastomus* and *Pezosiren*), and pan-sirenians at all, from Jamaica (Benoit et al. 2013). There are also stratigraphically old pan-sirenians known from the early middle Eocene (Lutetian) of the Pyrenean Basin with taxonomically not further defined postcrania from Navarre (late Lutetian of Spain; Astibia et al. 2010) as well as the recently established and even older species *Sobrarbesiren cardieli* from Huesca (middle Lutetian of northeastern Spain; Díaz-Berenguer et al. 2018). The latter is especially interesting since it represents the first adequately known quadrupedal sea cow from Eurasia, including several skulls and diverse postcranial elements (Díaz-Berenguer et al. 2020). In the deepest embayment of the Pyrenean Basin, *P. ausetanum* is documented from younger middle Eocene sediments, i.e., Bartonian. This refers to the likely representative from Girona described by Voss et al. (2019) and reviewed herein, and the holotype specimen from Tona (Balaguer and Alba 2016). These records are followed up northeastwards by on trend younger fossils such as several skulls, mandibles and postcranial material of *Eotheroides* sp. (late Lutetian to Priabonian) and "*Halitherium*" *taulannense* (Priabonian), both from Taulanne (Alpes-de-Haute-Provence, France; Domning et al. 1982; Sagne 2001), and the Bartonian *P. veronense* (de Zigno 1875) and the Priabonian *P. intermedium* (Bizzotto 1983), both from within the Helvetian trough of North Italy. The known pan-sirenian fossils from the Eocene of Hungary still show a stratigraphic range. While the partial skull and mandibular fragment of *Sirenavus hungaricus* (Kretzoi 1941) as well

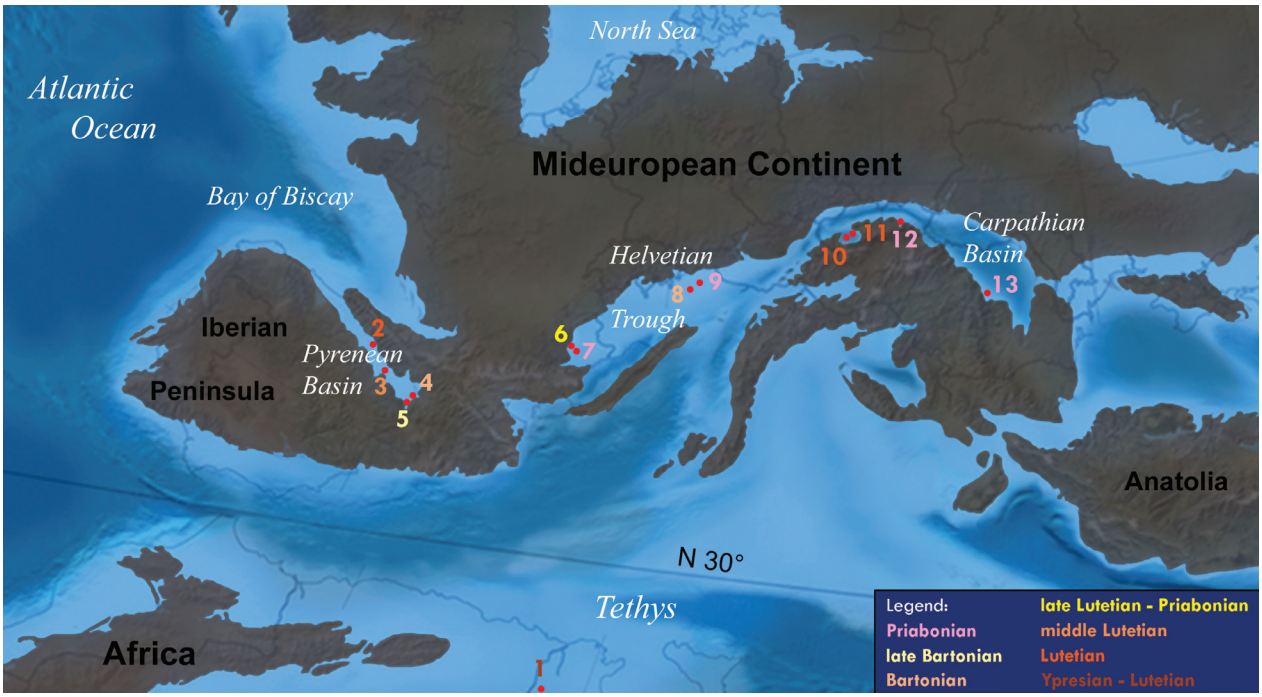

Figure 7. Palaeogeographic map of Europe during the Eocene based on templates of Ron Blakey (2020) showing relevant sirenian findings. **1**, Pan-Sirenia indet., Ypresian-Lutetian of Jebel Chambi, Tunisia (Benoit et al. 2013); **2**, ?Dugongidae indet. (according to the traditional classification concept – but most likely Pan-Sirenia indet.), Lutetian of Navarre, Western Pyrenees, Spain (Astibia et al. 2010); **3**, *Sobrarbesiren cardieli*, middle Lutetian of Castejón de Sobrarbe, Huesca, Spain (Díaz-Berenguer et al. 2018); **4**, *Prototherium ausetanum*, Bartonian of Tona, Catalonia, Spain (Balaguer and Alba 2016); **5**, *Prototherium* cf. *ausetanum*, late Bartonian of Sant Vicenç de Castellet, Catalonia, Spain (this paper); **6**, *Eotheroides* sp., late Lutetian-Priabonian of Taulanne, Alpes-de-Haute-Provence, France (Domning et al. 1982); **7**, "*Halitherium*" *taulannense*, Priabonian of Catellane, Alpes-de-Haute-Provence, France (Sagne 2001); **8**, *Prototherium veronense*, Bartonian of Monte Duello, N Italy (De Zigno, 1875); **9**, *Prototherium intermedium*, Priabonian of Possagno, N Italy (Bizzotto 1983); **10**, *Sirenavus hungaricus*, Lutetian of Felsőgalla, Hungary (Kretzoi 1941); **11**, *Anisosiren pannonica*, Lutetian of Oroszlány, Hungary (Kordos 1979); **12**, *Paralitherium tarkanyense*, Priabonian of Felsőtarkány, Hungary (Kordos 1977); **13**, Sirenia indet. (most likely Pan-Sirenia, see Discussion), Priabonian of Cluj-Napoca, Romania (Fuchs 1970).

as the maxilla of *Anisosiren pannonica* (Kordos 1979) are recorded from the Lutetian, the mandibles of *Paralitherium tarkanyense* (Kordos 1977) are Priabonian in age. Apart from that, a single cranial roof documents a Priabonian occurrence in the northeast-most European Tethyan realm of the Carpathian Basin and is determined as Sirenia indet. from Romania (Fuchs 1970).

In light of this stratigraphic and taxonomic background, the hypothesis on a Tethyan origin of sea cows is reinforced. Pan-Sirenia form a well-substantiated clade called Tethytheria together with their extant sister group Proboscidea (McKenna 1975; McKenna and Bell 1997). While the origin of the latter is well-recorded in Africa, the earliest pan-sirenians have long been only known from the Eocene of Jamaica (Savage et al. 1994; Domning 2001a, b). The periotics from the late Ypresian-early Lutetian (late early-early middle Eocene) of Tunisia do not only represent the oldest sea cow remains from Africa (Benoit et al. 2013), but can be now also considered to predate *Prorastomus sirenoides* from Jamaica according to Heritage and Seiffert (2022). Additionally, the morphology of the ear bones reflects more plesiomorphic conditions than those of *P. sirenoides* (Benoit et al. 2013), which is also shown by Heritage and Seiffert (2022), who phylogenetically identify the Tunisian find as the basal-most pan-sirenian. Thus, the morphological, stratigraphic and biogeographic evidence corroborates a North African origin of Pan-Sirenia that, in turn, contributes to a better understanding of the Tethytheria hypothesis (e.g., Tassy and Shoshani 1988; Murphy et al. 2001).

Although a fast dispersal remains a solid hypothesis in the evolutionary history of stem pan-sirenians (e.g., Domning 1994), this no longer includes the Jamaican prorastomids alone, but also a number of European fossils and taxa from the early middle Eocene (Lutetian) as mentioned above. Especially the Pyrenean Basin appears to be a kind of hot spot that yielded a number of stem sea cows limited to the middle Eocene. On the one hand, *Sobrarbesiren cardieli* is the hitherto oldest record of western Europe and the only quadrupedal form of Eurasia (Díaz-Berenguer et al. 2018), hence providing one of the rare examples for dispersal amongst early pan-sirenians that probably had an already fully aquatic lifestyle (Díaz-Berenguer et al. 2020: 672). On the other hand, the Bartonian *P. ausetanum* including the Girona specimen (Balaguer and Alba 2016; Voss et al. 2019) indicates further diversification in this area. With emphasis on the North African – Eurasian Tethyan realm considered here (Fig. 7), the southwestern Tethys is hypothesized as the evolutionary center for Eocene Pan-Sirenia, from where they dispersed westwards through the Atlantic (Benoit et al. 2013; Heritage and Seiffert 2022) as well as northwards through the Tethyan Ocean.

Conclusions

The present study incorporates the non-invasive analysis of CT-scans and macroscopic data generated from a sirenian find embedded in two paving slabs. On the basis of these data, and supplementing the results from Voss et al. (2019), the Girona sea cow MAC GIR-042375 belongs to the genus *Prototherium* and most likely represents *P. ausetanum* Balaguer & Alba, 2016 from the middle Eocene of Catalonia (Spain). Morphological results on the maxilla, the basicranium, and the dentition confirm and complement the available information of the holotype of that species. Against the background that MAC GIR-042375 is determined as adult, it is especially the mesiodistal length of the molar crowns that outline *P. ausetanum* as a small-sized species in general, hence distinct from other *Prototherium* taxa.

Considering the distribution of stem pan-sirenians across Eurasia in total, the records not only reflect a rough southwest-northeast oriented trend towards younger geological ages, but also mark the Pyrenean Basin as one of the centers of abundant and well-preserved pan-sirenians, including nearly complete skulls and skeletons even of a plesiomorphic evolutionary stage like *Sobrarbesiren cardieli* (Díaz-Berenguer et al. 2018).

Data availability

The paving stones containing the fossil sea cow remains are being exhibited in the Museu d'Arqueologia de Catalunya (Archaeology Museum) in Girona and have the collection number MAC GIR-042375.

All CT images of this sirenian are archived in the Museum für Naturkunde and accessible through the Department of Science Data Management under https://doi.org/10.7479/c65w-cj22 (Voss et al. 2022; Cranial CT-data of Eocene *Prototherium ausetanum* from Catalonia compared to a *Dugong* skull [Dataset], shared under a CreativeCommons CC-BY license).

Author contribution

MV and OH conceived the research, processed the morphological analyses and wrote the manuscript. JCV run the CT analyses at the Clínica Girona. KM finalised segmentation of the CT data and provided the 3D reconstruction. MV prepared Figs 3 to 6. OH produced Figs 1, 2 and 7. All authors edited the final version of the manuscript.

Competing interest

The authors declare that they have no conflict of interest.

Acknowledgments

We are deeply thankful to Roger Mata Lleonart (Caldes de Malavella, Spain), Jordi Ferrer Lopez and Marta Picó (both Girona, Spain) – without whose kind assistance, this

work could not have been realised. We are indebted to the Mayor of the City of Girona, Maria Madrenas who warmly welcomed us and supported our research operation. We are grateful to Daryl P. Domning (Washington, D.C.) who provided valuable comments that were considered in the discussion on the dentition. Jan Philipp Kundt (Berlin, Germany) prepared initial CT segmentations, David M. Alba and Jordi Balaguer Bruguera (both Barcelona, Spain) kindly helped with the interpretation of the basicranium of the holotype of *P. ausetanum*. Finally, we deliver our thanks to the two reviewers, Iyad Zalmout (Jeddah, Saudi Arabia) and one anonymous, who provided very constructive comments that significantly improved our article.

References

Astibia H, Bardet N, Pereda-Suberbiola X, Payros A, de Buffrénil V, Elorza J, Tosquella J, Berreteaga A, Badiola A (2010) New fossils of Sirenia from the middle Eocene of Navarre (Western Pyrenees): the oldest West European sea cow record. Geological Magazine 147(5): 665–673. https://doi.org/10.1017/S0016756810000130

Balaguer J, Alba DM (2016) A new dugong species (Sirenia, Dugongidae) from the Eocene of Catalonia (NE Iberian Peninsula). Comptes Rendus Palevol 15(5): 489–500. https://doi.org/10.1016/j.crpv.2015.10.002

Benoit J, Adnet S, Mabrouk EE, Khayati H, Haj Ali MB, Marivaux L, Merzeraud G, Merigeaud S, Vianey-Liaud M, Tabuce R (2013) Cranial remain from Tunisia provides new clues for the origin and evolution of Sirenia (Mammalia, Afrotheria) in Africa. PLoS ONE 8(1): e54307. https://doi.org/10.1371/journal.pone.0054307

Bizzotto B (1983) *Prototherium intermedium* n. sp. (Sirenia) dell'Eocene Superiore di Possagno e proposta di revisione sistematica del taxon *Eotheroides* Palmer 1899. Memorie degli Istituti di Geologia e Mineralogia dell'Universita di Padova 36: 95–116.

Bizzotto B (2005) La struttura cranica di *Prototherium intermedium* (Mammalia: Sirenia) dell' Eocene superiore Veneto. Nuovi Contributi alla sua Anatomica e Sistematica. Lavori Societá Veneziana di Scienze Naturali 30: 107–125.

Blakey RC (2020) Deep Time Maps. https://deeptimemaps.com

Cope ED (1883) On a new extinct genus of Sirenia from South Carolina. Proceedings of the Academy of Natural Sciences of Philadelphia 35: 52–54.

De Zigno A (1875) Sirenii fossili trovati nel Veneto. Memorie del Reale Instituto veneto di scienze, lettere ed arti 18: 427–456.

De Zigno A (1887) Quelques observations sur les siréniens fossiles. Bulletin de la Société Geologique de France 15: 728–732.

Díaz-Berenguer E, Badiola A, Moreno-Azanza M, Canudo JI (2018) First adequately-known quadrupedal sirenian from Eurasia (Eocene, Bay of Biscay, Huesca, northeastern Spain). Scientific Reports 8(1): 1–13. https://doi.org/10.1038/s41598-018-23355-w

Díaz-Berenguer E, Houssaye A, Badiola A, Canudo JI (2020) The hind limbs of *Sobrarbesiren cardieli* (Eocene, Northeastern Spain) and new insights into the locomotion capabilities of the quadrupedal sirenians. Journal of Mammalian Evolution 27(4): 649–675. https://doi.org/10.1007/s10914-019-09482-9

Díaz-Berenguer E, Moreno-Azanza M, Badiola A, Canudo JI (2022) Neurocranial bones are key to untangling the sea cow evolutionary tree: osteology of the skull of *Sobrarbesiren cardieli* (Mammalia: Pan-Sirenia). Zoological Journal of the Linnean Society 196(4): 1671–1703. https://doi.org/10.1093/zoolinnean/zlac021

Domning DP (1989) Fossil Sirenia of the West Atlantic and Caribbean region. II. *Dioplotherium manigaulti* Cope, 1883. Journal of Vertebrate Paleontology 9(4): 415–428. https://doi.org/10.1080/02724634.1989.10011774

Domning DP (1994) A phylogenetic analysis of the Sirenia. In: Berta A, Deméré TA (Eds) Contributions in marine mammal paleontology honoring Frank C. Whitmore Jr. Proceedings of the San Diego Society of Natural History 29: 177–189.

Domning DP (1996) Bibliography and index of the Sirenia and Desmostylia. Smithsonian Contributions to Paleobiology 80: 1–611. https://doi.org/10.5479/si.00810266.80.1

Domning DP (2001a) Evolution of the Sirenia and Desmostylia. In: Mazin JM, de Buffrénil V (Eds) Secondary adaptation of tetrapods to life in water. Proceedings of the international meeting Poitiers, 1996. Verlag Dr. Friedrich Pfeil, Munich, 151–168.

Domning DP (2001b) The earliest known fully quadrupedal sirenian. Nature 413: 625–627. https://doi.org/10.1038/35098072

Domning DP, Morgan GS, Ray CE (1982) North American Eocene sea cows (Mammalia: Sirenia). Smithsonian Contributions to Paleobiology 52: 1–69. https://doi.org/10.5479/si.00810266.52.1

Fuchs H (1970) Schädelfragment einer Sirene aus dem Eozan von Cluj, SR Rumanien. Geologie 19(10): 1185–1191.

Galindo J, Florensa RM, Puig C, López Blance M, Piña Iglesias J, Picart J (2003) Monistrol de Montserrat 392-1-1 (71-29). Mapa geològic de Catalunya 1:25000, Barcelona, Institut Cartogràfic de Catalunya.

Heritage S, Seiffert ER (2022) Total evidence time-scaled phylogenetic and biogeographic models for the evolution of sea cows (Sirenia, Afrotheria). PeerJ 10: e13886. https://doi.org/10.7717/peerj.13886

Illiger JKW (1811) Prodomus systematis mammalium et avium: additis terminis zographicis utriusque classis eorumque versione Germanica. Salfeld, Berlin, 301 pp. https://doi.org/10.5962/bhl.title.106965

Jefferies RPS (1979) The origin of the chordates – a methodological essay. In: House MR (Ed.) The origin of major invertebrate groups. Systematics Association Special Volume 12: 443–477.

Kretzoi M (1941) *Sirenavus hungaricus* n. g., n. sp. Ein neuer Prorastomide aus dem Mittleozän (Lutetium) von Felsőgalla in Ungarn. Annales historico-naturales Musei Nationalis Hungarici, Pars Mineralogica, Geologica et Palaeontologica 34: 146–156.

Kordos L (1977) Új felső-eocén sziréna (*Paralitherium tarkanyense*) n.g. n.sp. Felsőtárkánybál. A Magyar Állami Földtani Intézet évi jelentése 1975: 349–367.

Kordos L (1979) Major finds of scattered fossils in the palaeovertebrate collection of the Hungarian Geological Institute. A Magyar Állami Földtani Intézet évi jelentése 1977: 313–326.

Linnaeus C (1758) Systema naturae per Regna tria naturae, secundum Classes, Ordines, Genera, Species, cum Characteribus, Differentiis, Synonymis, Locis. Tomus I. Editio Decima, Reformata. Laurentii Salvii, Stockholm, 824 pp. https://doi.org/10.5962/bhl.title.542

Luckett WP (1993) An ontogenetic assessment of dental homologies in therian mammals. In: Szalay FS, Novacek MJ, McKenna MC (Eds) Mammal Phylogeny: Mesozoic Differentiation, Multituberculates, Monotremes, Early Therians, and Marsupials. Springer, New York, 182–204. https://doi.org/10.1007/978-1-4613-9249-1_13

McKenna MC (1975) Toward a phylogenetic classification of the Mammalia. In: Luckett WP, Szalay FS (Eds) Phylogeny of the Primates. Springer, Boston, 21–46. https://doi.org/10.1007/978-1-4684-2166-8_2

McKenna MC, Bell SK (1997) Classification of mammals above the species level. Columbia University Press, New York, 640 pp.

Mitchell J (1973) Determination of relative age in the dugong *Dugong dugon* (Müller) from a study of skulls and teeth. Zoological Journal of the Linnean Society 53(1): 1–23. https://doi.org/10.1111/j.1096-3642.1973.tb01409.x

Murphy WJ, Eizirik E, Johnson WE, Zhang YP, Ryder OA, O'Brien SJ (2001) Molecular phylogenetics and the origins of placental mammals. Nature 409: 614–618. https://doi.org/10.1038/35054550

O'Leary MA, Bloch JI, Flynn JJ, Gaudin TJ, Giallombardo A, Giannini NP, Goldberg SL, Kraatz BP, Luo Z-X, Meng J, Ni X, Novacek MJ, Perini FA, Randall ZS, Rougier GW, Sargis EJ, Silcox MT, Simmons NB, Spaulding M, Velazco PM, Weksler M, Wible JR, Cirranello AL (2013) The placental mammal ancestor and the post-K-Pg radiation of placentals. Science 339: 662–667. https://doi.org/10.1126/science.1229237

Pilleri G, Biosca J, Via L (1989) The Tertiary Sirenia of Catalonia. Brain Anatomy Institute, Ostermundigen, Switzerland, 98 pp.

Pocock RI (1940) Some notes on the dugong. Annals and Magazine of Natural History 5(28): 329–345. https://doi.org/10.1080/00222934008527109

Sagne C (2001) *Halitherium taulannense*, nouveau sirénien (Sirenia, Mammalia) de l'Éocène supérieur provenant du domaine Nord-Téthysien (Alpes-de-Haute-Provence, France). Comptes rendus de l'Académie des Sciences de la Terre et des Planètes 333: 471–476. https://doi.org/10.1016/S1251-8050(01)01661-5

Savage RJG, Domning DP, Thewissen JGM (1994) Fossil Sirenia of the West Atlantic and Caribbean region. V. The most primitive known sirenian, *Prorastomus sirenoides* Owen, 1855. Journal of Vertebrate Paleontology 14(3): 427–449. https://doi.org/10.1080/02724634.1994.10011569

Springer MS, Signore AV, Paijmans JLA, Vélez-Juarbe J, Domning DP, Bauer CE, He K, Crerar L, Campos PF, Murphy WJ, Meredith RW, Gatesy J, Willerslev E, MacPhee RDE, Hofreiter M, Campbell KL (2015) Interordinal gene capture, the phylogenetic position of Steller's sea cow based on molecular and morphological data, and the macroevolutionary history of Sirenia. Molecular Phylogenetics and Evolution 91: 178–193. https://doi.org/10.1016/j.ympev.2015.05.022

Stanhope MJ, Waddell VG, Madsen O, de Jong W, Hedges SB, Cleven GC, Kao D, Springer MS (1998) Molecular evidence for multiple origins of the Insectivora and for a new order of endemic African insectivore mammals. Proceedings of the National Academy of Sciences 95: 9967–9972. https://doi.org/10.1073/pnas.95.17.9967

Tassy P, Shoshani J (1988) The Tethytheria: elephants and their relatives. In: Benton MJ (Ed.) The phylogeny and classification of the tetrapods. Vol. 2 Mammals. Systematics Association Special Volume 35B: 283–315.

Vélez-Juarbe J, Domning DP, Pyenson ND (2012) Iterative evolution of sympatric seacow (Dugongidae, Sirenia) assemblages during the past ~ 26 million years. PLoS ONE 7(2): e31294. https://doi.org/10.1371/journal.pone.0031294

Vélez-Juarbe J, Wood AR (2018) An early Miocene dugongine (Sirenia: Dugongidae) from Panama. Journal of Vertebrate Paleontology, 38(5): e1511799. https://doi.org/10.1080/02724634.2018.1511799

Voss M (2013) Revision of the *Halitherium*-species complex (Mammalia, Sirenia) from the late Eocene to early Miocene of Central Europe and North America. PhD Thesis, Humboldt-Universität zu Berlin, Berlin.

Voss M, Hampe O, Mata Lleonart R, Ferrer Lopez J (2019) Fossil sea cow remains (Mammalia: Sirenia) on paving stones in the City of Girona (Catalonia, Spain). Geoheritage 11(4): 1981–1987. https://doi.org/10.1007/s12371-019-00419-5

Zalmout IS, Gingerich PD (2012) Late Eocene sea cows (Mammalia, Sirenia) from Wadi al Hitan in the western desert of Fayum, Egypt. University of Michigan Papers on Paleontology 37: 1–158.

Zorzin R, Castellani S, Frisone V, Quaggiotto E (2012) Le campagne di scavo del Museo Paleontologico di Roncà in località Monte Duello (Comune di Montecchia di Crosara) e Valle della Chiesa (Comune di Roncà), nei Monti Lessini veronesi (Italia settentrionale): primi risultati. Bollettino del Museo Civico di Storia Naturale di Verona (Geologia Paleontologia Preistoria) 36: 53–62.

Zorzin R, Frisone V (2013) Montecchia di Crosara, Monte Duello. Il giacimento ricco di spicole di spugna: indagini 2011–2013. Notizie di Archeologia del Veneto 2: 99–103.